MEMOIRS
OF THE
RAMAN RESEARCH INSTITUTE

Vol. VI
(Nos. 95 to 109)

BANGALORE
1958

CONNEMARA PUBLIC LIBRARY
4 JAN 1965
MADRAS

MEMOIRS
OF THE
RAMAN RESEARCH INSTITUTE

Volume VI. Nos. 95 to 109

95. Optical properties and unit cell parameters of nickel nitrate hexahydrate — A. JAYARAMAN

96. The specific heats of crystals and the fallacy of the theories of Debye and Born .. .. C. V. RAMAN

97. Generalised theory of interference and its applications. Part III. Interference figures in transparent crystals .. .. .. S. PANCHARATNAM

98. Generalised theory of interference and its applications. Part IV. Interference figures in absorbing biaxial crystals .. .. .. S. PANCHARATNAM

99. The theory of the anharmonic oscillator .. .. K. S. VISWANATHAN

100. The Raman spectrum of calcite and its interpretation .. .. D. KRISHNAMURTI

101. The specific heats of crystalline solids: Parts I and II .. .. C. V. RAMAN

102. Light propagation in absorbing crystals possessing optical activity .. S. PANCHARATNAM

103. The heat capacity of diamond between 0 and 1,000° K. .. .. C. V. RAMAN

104. The tetrahedral carbon atom and the structure of diamond .. .. C. V. RAMAN

105. Anharmonicity of vibration in molecules .. .. K. S. VISWANATHAN

106. Reciprocal lattice photography; Unit cell parameters, space-group and optical properties of cobalt nitrate hexahydrate .. A. JAYARAMAN

107. The optic interference figures of amethystine quartz—Parts I & II .. S. PANCHARATNAM

108. The Raman spectrum of quartz and its interpretation .. .. D. KRISHNAMURTI

109. The diffraction of X-rays in diamond: Parts I–III .. .. .. C. V. RAMAN

4 JAN 1965

Reprinted from "The Proceedings of the Indian Academy of Sciences",
Vol. XLV, No. 4, Sec. A, 1957

OPTICAL PROPERTIES AND UNIT CELL PARAMETERS OF NICKEL NITRATE HEXAHYDRATE

BY A. JAYARAMAN, F.A.SC.
(*Memoir No. 95 of the Raman Research Institute, Bangalore-6*)

Received March 30, 1957

1. INTRODUCTION

NICKEL nitrate is known to form three hydrates with three, six and nine molecules of water at 55° C., – 16° C. and – 27° C. respectively. Very little is known regarding the structure and physical properties of these hydrates. Groth in his *Chemische Crystallographie* reports some measurements of interfacial angles, axial ratios, density and melting point of nickel nitrate hexahydrate. The hexahydrate is reported to occur as green deliquescent crystals having a density of 2·05 gm./c.c. in the monoclinic prismatic class with axial ratios $a:b:c = 1{\cdot}164:1:1{\cdot}905$ and $\beta = 101°\,26'$. In the literature as far as the author could find, the structure and optical properties of this substance has not been reported. Further it would be of particular interest to study the magnetic properties of single crystals of this substance. It should however be borne in mind that the material is of a highly hygroscopic nature and hence needs special technique of study. It was with a view to understand the structure and optical properties of this substance, that the present investigation was undertaken and the results of study are reported in the present communication. It would be in place to mention here that the crystals of hexahydrate obtained by the author could only be placed in the triclinic system as the optical and X-ray investigations unequivocally show this to be the case. This is in contrast to the previous report quoted earlier.

2. EXPERIMENTAL STUDY

Crystals of nickel nitrate hexahydrate for both optical and X-ray work were grown from a purified commercially available sample. The solubility of this substance is very high in water and is considerable in many organic compounds, particularly alcohol and acetone. A saturated solution in water of the substance was kept inside an airtight bell jar in a crystallising dish along with a small quantity of P_2O_5 or anhydrous calcium chloride in a separate container which served to absorb water. It was observed that crystals of

large size could be grown by this method. Since the crystals are extremely deliquescent, they were taken out of the mother liquor and transferred promptly to a bottle containing kerosene after the adhering solution was removed between blotting papers.

Needle-shaped crystals were obtained by rapid crystallisation while large elongated plates were obtained by slower crystallisation. The crystals were of a beautiful emerald green in colour and well developed crystallographic faces could be observed in it. Visual examination of the morphological characters revealed that the crystals did not possess any element of symmetry and the form was suggestive of a triclinic pinacoidal type. In very well developed crystals, many other faces could be discerned. However an optical goniometric study was not attempted as this would necessitate special immersion methods.

3. Cell Parameters

Rotation and zero-layer Weissenberg X-ray photographs were taken with thin rods cut parallel to the three observed edges of the crystal form. Considerable difficulty was experienced in handling the specimens, cutting them parallel to the chosen edges, and shaping them to correct thickness owing to the extreme hygroscopic nature of the material. The rod-shaped specimen was placed in a thin-walled pyrex capillary tube, sealed at one end while the other open end was closed with wax and mounted on the goniometer head. Cu Kα radiation was employed to record the X-ray patterns. The following linear dimensions of the unit cell and its angular constants were obtained from the three single crystal and the three zero-layer Weissenberg photographs. With these six photographs cross checks of the data were possible.

$$a = 5\cdot 79 \text{ Å.U.} \qquad \alpha = 106°\cdot 38'$$

$$b = 7\cdot 69 \text{ Å.U.} \qquad \beta = 80°\cdot 32'$$

$$c = 11\cdot 89 \text{ Å.U.} \qquad \gamma = 101°\cdot 27'$$

$$a : b : c = 0\cdot 753 : 1 : 1\cdot 546$$

The density of the material was found to be about 2 gm./c.c. and the number of molecules per unit cell when calculated came out very close to 2, revealing thereby that there are two molecules per unit cell.

In the convergent light figure observed with the cleavage plate of the crystal the brush is quite dark and very distinct while crossing the eyes, thereby indicating that the crystal is not optically active. Further, when copper radiation is used for recording the X-ray patterns, one is working very close

to the absorption edge of nickel, a favourable circumstance for the breakdown of Friedel's law if there were no centre of symmetry. No such breakdown was noticeable in the X-ray photographs and therefore it is highly probable that the crystal belongs to the centro-symmetric class of the triclinic system, the corresponding space group symobl being C_i^1 or $P\bar{1}$.

It should be remarked here that the crystal exhibits a very perfect (001) cleavage. The needle axis is found to be 5·79 A.U. while the *c*-axis is 11·89 A.U.

4. Optical Properties

The optical properties of the crystal were determined with the help of a polarising microscope. The habit plane of the crystal which is found to be the (010) face by X-ray methods exhibits straight extinction. The cleavage plate which is found to be parallel to the (001) face gives an inclined extinction, the vibration direction making an angle of 11° with the straight edge of the crystal which is parallel to the *a*-axis (100).

The convergent light figure is observed on the (001) face that is the cleavage plate and the β vibration direction lies on this. The optic axial angle was determined by adopting the undermentioned procedure which was found to be very convenient. The cleavage plate was mounted between a glass plate and a cover slip with a suitable immersion liquid and this was placed on a Federov stage. The stage was fixed on to a polarising microscope and a glass hemisphere belonging to the Federov stage was attached to the stage of the microscope in the aperture admitting light. This acted as a converging lens and with a low power objective and the Betrand lens one could easily observe the interference figure. The crystal could easily be set by proper adjustment of the stage such that the axial plane is brought parallel to one of the cross wires. Having obtained this setting, the axial angle is easily determinable and two principal refractive indices could also be obtained. For obtaining the latter, parallel light is needed which can be got by removing the hemispherical glass condenser and lowering the substage, while leaving the desired setting of the crystal undisturbed.

The axial angle and the two refractive indices β and γ were obtained by following the above procedure and using immersion methods to measure the refractive index. The third principal refractive index (α) was measured on the (010) face by suitably tilting the stage to get the vibration direction parallel to the cross wire. The following are the values obtained for sodium light.

$$\alpha = 1\cdot422$$
$$\beta = 1\cdot555 \qquad 2\,V = 41°\cdot12'$$
$$\gamma = 1\cdot577$$

A diagram is reproduced below to show the orientation of the optic elements with respect to the crystallographic elements observed in the crystal. The acute bisectrix is the (α) vibration direction and the crystal is therefore biaxial negative.

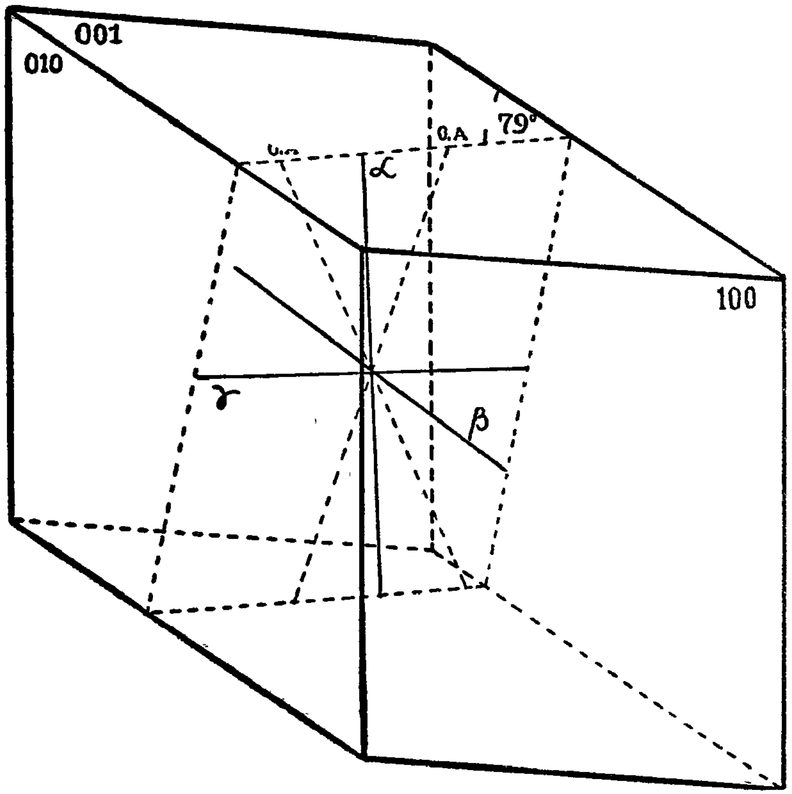

FIG. 1

As already remarked, crystals of Ni $(NO_3)_2$ $6H_2O$ are emerald green in colour and exhibit pleochroism in polarised light. Pleochroism is very striking on the (010) face. For a vibration parallel to (α) the colour is bluish green while it is yellowish green for a vibration parallel to the (β) vibration direction. Pleochroism is not marked on the cleavage face and the difference in absorption is not observable for a vibration parallel to β and γ vibration directions.

5. SOME REMARKS

A study of the optical properties in relation to the observed morphological characters of the crystal by itself revealed that the crystal can only

be placed in the triclinic system. The straight extinction observed can only be an accident the possibility of which is not totally excluded for a cyrstal belonging to the triclinic system. Otherwise, the optical properties bear no symmetric relationship to the crystal edges and faces.

It would be seen from an examination of refractive index data that the maximum refractive index lies very close to the cleavage plane and the minimum index is nearly normal to it. The difference between the two indices, *i.e.*, the birefringence, is fairly high. The perfect cleavage of the (001) plane and the refractive properties indicate that the planar nitrate ions lie very close to the cleavage plane.

A complete determination of the structure and other physical properties is under progress and the results will be reported in due course.

In conclusion the author wishes to express his thanks to Sir C. V. Raman, F.R.S., N.L., for his kind interest in the work and to Dr. S. Ramaseshan for helpful criticisms.

Summary

The unit cell parameters and optical properties of nickel nitrate hexahydrate are reported. It is found that the crystal belongs to the centro-symmetric class in the triclinic system. The refractive properties and the very perfect cleavage of the (001) indicate that the planar nitrate ions lie very close to the (001) face.

Reprinted from "The Proceedings of the Indian Academy of Sciences", Vol. XLV, No. 5, Sec. A, 1957

THE SPECIFIC HEATS OF CRYSTALS AND THE FALLACY OF THE THEORIES OF DEBYE AND BORN

BY SIR C. V. RAMAN

(*Memoir No. 96 of the Raman Research Institute, Bangalore 6*)

Received May 9, 1957

1. INTRODUCTION

THE first step in any attempt at a theoretical evaluation of the specific heats of crystals is to determine the nature of the disturbance in their structure produced by the thermal agitation. In an earlier publication[1] and more fully again in the address to the Conference of Nobel Laureates held at Lindau in June 1956 which was printed in these *Proceedings*,[2] this problem was discussed. A general theory of the specific heats of crystals embodying the ideas expressed in those memoirs has since been formulated and published.[3] The theory leads to a determination of the spectroscopic behaviour of crystals and simultaneously with it to an expression for their specific heats as a function of the temperature. The success of the theory in achieving these aims has been demonstrated by a series of fully worked-out examples and a comparison with the facts of experiment.[4]

The principles on which the present approach to specific heat theory is based may be briefly sketched here. While the classical mechanics is made use of in the theory, stress is laid on the necessity of paying due regard at the same time to the basic principles of thermodynamics and to the fundamental notions of the quantum theory. With these requirements in view, the crystal is regarded as an assembly in thermodynamic equilibrium of sets of *similar* oscillators in great number, the energies of vibration of which are *individually* quantised. The identification and enumeration of these oscillators and the determination of their modes and frequencies of vibration is accomplished by taking note of the three-dimensional periodicity of structure characteristic of crystals and applying to the elements of that structure essentially the same methods as those which are so successful in the field of molecular spectroscopy. The determination of the thermal energy of the crystal as a function of the temperature is then effected by the same procedure as that indicated by Einstein in his fundamental paper[5] of 1907 introducing the quantum theory of specific heats.

The present approach to specific heat theory rejects completely the ideas regarding the subject embodied in Debye's well-known paper[6] and also those set out by Born and his school in numerous publications.[7] As the present generation of physicists and chemists has been brought up to believe in these latter theories, it would not be superfluous to explain in some detail why their rejection is necessary. That indeed is the purpose of the present memoir, which is sought to be achieved by a searching examination of the premises underlying the theories of Debye and Born and of the consequences to which those theories lead. It emerges from the examination that those premises are untenable and that the conclusions derived from them are false.

2. THE HYPOTHESIS OF JEANS

The parent of the specific heat theories of Debye and Born and also of other similar theories was a publication[8] by J. H. Jeans which appeared in the *Philosophical Magazine* in the year 1909. Though the title of that paper indicated temperature radiation as its subject, actually it was devoted for the most part to a discussion of the thermal behaviour of material bodies on the basis of classical mechanics. It put forward and sought to establish a proposition which may be stated as follows:—*the thermal energy of material bodies is identifiable with the sum of the potential and kinetic energies of regular trains of waves traversing them and forming stationary wave-patterns filling their volume.* The reader familiar with Debye's specific heat theory will immediately recognise this as the thesis which Debye accepted and elaborated in his attempt to explain the experimental results for the specific heats of elementary solids at low temperatures. It is not surprising in these circumstances that Jeans became an enthusiastic supporter of Debye's theory and by his advocacy helped to promote a general belief in the validity of the thesis on which that theory was based.

The waves considered by Debye in his paper were the longitudinal and transversal waves in an isotropic solid contemplated by the classical theory of elasticity. The formulæ set out in the paper were based on an analysis of the modes of vibration of an elastic solid sphere whose external surface was assumed to be rigidly fixed, followed by their enumeration in terms of their frequencies of vibration. Debye restricted himself for the most part to a consideration of the cases of monatomic solids exhibiting cubic symmetry. No such restriction is contemplated in the theory put forward and developed by Born and his school, which claims to be valid for all crystals. While Debye considered it to be adequate for his purpose to regard the vibrating solid as a continuum, the Born theory claims to take account of the discrete

lattice structure of the crystal. The waves considered in it are also of a more general kind than those recognised by Debye. Nevertheless, the theory of Born, like that of Debye, is based on an acceptance of the same thesis, *viz.*, the hypothesis of Jeans.

3. The Fallacy of the Hypothesis

Simple considerations of a general character suffice to show that the hypothesis of Jeans is a wholly misconceived idea. We have only to remark that the specific heat of a solid is an atomistic property, since its value at any given temperature is completely determined by two quantities, one of which is the number of atoms comprised in unit mass of the substance, and the other is the effective average frequency of vibration of the atoms at that temperature. Any attempt to explain this situation theoretically has, of necessity, to base itself on an atomistic approach to the problem. In other words, we have to consider the individual atoms in the crystal and investigate their dynamic behaviour. *Per contra,* wave-motions and the stationary wave-patterns resulting from the presence of an external boundary limiting their travel are macroscopic concepts, which, it should be emphasised, do not require us to take any notice of the atomicity of structure of the material traversed by the waves. In these circumstances, it is obvious that the attempt to build a theory of specific heats on the assumption that the thermal agitation is identifiable with wave-motions is an illogical and illusory proceeding.

We may usefully enlarge upon the foregoing remarks. The specific heat theories based on the hypothesis of Jeans concern themselves with the enumeration of the stationary wave-patterns assumed to exist within the volume of the solid. But, since the atomicity of structure of the material need not at all be considered in the description and enumeration of the wave-patterns, it remains completely outside the problem. The identification of the thermal energy of the solids with the sum of the kinetic and potential energies of the wave-patterns is therefore incapable of leading us to any determination of their specific heats. The difficulty which arises here is one of pure logic and is fundamental. In the theories now under discussion, the difficulty is sought to be circumvented by introducing an additional assumption, *viz.*, that the total number of wave-patterns is equal to thrice the number of atoms comprised in the crystal. While this assumption may appear plausible, it cannot be pretended that such a fixation of the number of wave-patterns is a necessary consequence or concomitant of the wave hypothesis. Actually, of course, it is introduced in order "to make the theory work", in other words, in order that the results of the theory

might bear some resemblance to the experimental facts. In logic, such a proceeding would be described as *petitio principii,* or begging the question.

4. Thermodynamics and the Theory of Specific Heats

It can be readily shown that the notions underlying the theories of Debye and Born are irreconcilable with the statistical concept of the nature of thermal energy which lies at the very base of the science of thermodynamics. A crystal is an assembly of an immense number of individual atoms which are capable of moving from their positions of equilibrium. Hence, the state of the system can only be described in terms of the values of a very large number of independent variables. No doubt, the atoms are held together by their mutual interactions to form the ordered assemblage which we call a crystal and which can be regarded as a unit in the macroscopic sense. But the statistical concept of thermal energy forbids us from regarding the entire assembly as a single unit in the thermodynamic sense. We cannot, for example, identify the thermal energy of the crystal with the energy of stationary wave-patterns of any sort. Indeed, the constancy of amplitude and coherence of phase relationship over extended regions of space and large periods of time which the formation of such wave-patterns presupposes are excluded by reason of the very nature of thermal energy. *Per contra,* it is to be expected that the thermal energy of a solid exhibits fluctuations in space and in time which preclude any definitive description of it except for domains of space and periods of time which are very small in comparison with macroscopic standards.

5. Classical Mechanics and the Theory of Specific Heats

That the theories of Debye and Born are untenable becomes evident also when we examine them from the standpoint of classical mechanics. For, specific heat theory starts from the well-known theorem that all the possible vibrations of a system of connected particles are superpositions of a set of normal modes in each of which the particles oscillate with the same frequency and in the same or opposite phases. The particles in the present problem are the individual atoms in the crystal and hence we are here concerned with the determination of the normal modes of vibration of *the atoms* in the sense of the theorem just stated. Instead of considering this question, the theories of Debye and Born concern themselves with an entirely different and indeed irrelevant subject, *viz.,* the normal modes of vibration of a macroscopic solid as determined by the form of its external boundary. Their treatment of specific heat theory thus stands revealed as a purely fanciful approach devoid of any validity or significance.

A straightforward application of the standard methods of classical dynamics enables us to determine the characteristic modes and frequencies with which the atoms in a three-dimensionally periodic array can oscillate about their positions of equilibrium. It emerges from the investigation that these characteristic modes can be enumerated and that they are related in a precisely definable manner to the structure and symmetry properties of the atomic groupings in the crystal. In the theories of Debye and Born, on the other hand, which assume that the modes of vibration are determined by the external boundary conditions and further, that the total number of wave-patterns is equal to thrice the number of atoms included in the crystal, we encounter results of an altogether different character. According to these theories, the great majority of the stationary wave-patterns which they contemplate have "wave-lengths" of the same order of magnitude as the lattice-spacings of the crystal. But these wave-lengths are all different and represent different frequencies of vibration. As a consequence, the "cells" of the wave-pattern in which the phase of vibration alternates bear no relation whatever to the structure of the crystal, while the wave-patterns themselves appear in immense numbers and are all different from each other. Such a description of the dynamical behaviour of the atoms linked with one another in the geometrically ordered structure of a crystal is, on the face of it, a fantastic misrepresentation. It is, in effect, a *reductio ad absurdum* of the theories which lead up to it.

6. The Quantum Theory of Specific Heats

The ideas which connect the hypothesis of energy quanta with the theory of specific heats were very clearly expounded in Einstein's classic paper[5] of 1907. If it be assumed that radiation is emitted or absorbed in energy-quanta proportional to the frequency, it follows as a necessary consequence that the mechanical energy of the oscillator which thus emits or absorbs would itself diminish or increase respectively by finite steps of the same amount. Generalising this result, Einstein postulated that the energy of any elementary structure capable of mechanical vibration would likewise obey the quantum rule. He then coupled this with the concept of thermodynamic probability embodied in Boltzmann's principle and showed that the relative probabilities of the oscillator being in different energy states could be determined with the aid of the principle. The next step is the evaluation of the average energy of an oscillator in an assembly consisting of a great number of such oscillators having a common frequency of vibration. This leads at once to the evaluation of the thermal energy of the whole assembly. The basic ideas of the quantum theory were further clarified and illumined by

Einstein in the famous paper[9] of 1917 in which he showed that the exchange of energy between a radiation field and the oscillators located in it can properly be described only in terms of statistical concepts. The probability of the oscillator being in any given state appears in the paper as the product of two factors, one of which is the thermodynamic probability factor given by the Boltzmann formula and the other is the intrinsic statistical weight of that state.

The foregoing remarks are made to emphasise that the quantum theory of specific heats rests on thermodynamic-statistical concepts which are wholly alien to the determinism of macroscopic physics. In other words, the theory of energy-quanta possesses a meaning and significance only in relation to the behaviour of the ultimate units of which matter is composed; *per contra* it is wholly out of place in any considerations regarding the behaviour of matter in bulk. For example, we can speak of the energy states of rotation or vibration of a molecule of benzene, but it would be nonsensical to discuss the problem of quantising the vibrations of a tuning fork or the rotations of a fly-wheel.

It will be clear from the foregoing remarks that Debye and Born fell grievously into error when they rejected the basic ideas of Einstein's theory and sought to build a theory of the specific heats of crystals on the behaviour of macroscopic solids. In doing this, not only did they ignore all considerations of logic as well as the physical principles bearing on the subject, but they also sought to impose on the quantum theory a fantastic and altogether meaningless interpretation.

7. THE SPECTROSCOPIC BEHAVIOUR OF CRYSTALS

The specific heats of crystals and their spectroscopic behaviour are intimately related properties since they are both determined by the frequencies of vibration of the atoms about their positions of equilibrium. This relationship is conveyed more precisely by the statement that the elementary oscillators in the crystal which are the carriers of its heat energy are also the oscillators capable of absorbing, emitting or scattering the radiations incident on it. It follows that any valid specific heat theory contains within itself a complete description of the vibration spectrum of a crystal: *vice versa*, a theory of the spectroscopic behaviour of crystals which correctly describes the facts of observation in that field necessarily contains within itself all the data needed for the evaluation of the specific heat as a function of the temperature.

From the foregoing remarks, it follows that the theories of Debye and Born which are based on erroneous assumptions regarding the carriers of the thermal energy in crystals also lead to a false picture of their vibration spectra. That is actually the case, for the assumptions made in these theories lead to the conclusion that the vibration frequencies of a crystal are immensely numerous and are all different from each other and hence that the vibration spectrum exhibits a continuous band of frequencies stretching over the entire range. *Per contra*, the atomistic theory of specific heats shows that the vibration spectrum of a crystal consists of a finite number of discrete monochromatic frequencies accompanied by a residual spectrum with a relatively small statistical weight which may be considered as continuous and which goes down to very low frequencies.

Spectroscopy is an exact science, and the vibration spectra of crystals are accessible to precise study and investigation by several different techniques and with a great variety of materials. In every case, the experimental results support and confirm the results of the atomistic theory in an unequivocal fashion. They are therefore also an objective demonstration of the falsity of the Debye and Born theories.

8. Summary

It is shown that the hypothesis, originally proposed by Jeans and adopted in the theories of Debye and Born, that the thermal energy of a solid is identifiable with the energy of wave-motions in its interior is not logically sustainable as a basis for a theory of their specific heats. The constancy of amplitude and of phase-relationships in extended volumes and periods of time demanded by the hypothesis is irreconcilable with the statistical-thermodynamical concept of the nature of thermal energy, and the idea that the theory of specific heats can be treated as a boundary-value problem in the physics of macroscopic solids is therefore misconceived. It is shown that such an approach is repugnant both to classical mechanics and to the principles of the quantum theory. It must therefore give place to a purely atomistic approach which gives us a wholly different picture of the nature of the thermal agitation in the solid and of its vibration spectrum.

9. References

1. Raman, C. V. .. Memoir No. 77 of the Raman Research Institute, *Proc. Ind. Acad. Sci.*, 1955, **42 A**, 163.
2. ———— .. Memoir No. 85 of the Raman Research Institute, *Ibid.*, .. 1956, **43 A**, 327.

3. Raman, C. V. .. Memoir No. 87 of the Raman Research Institute, *Proc. Ind. Acad. Sci.*, 1956, **44 A**, 153.

4. ——— .. Memoirs 86, 87, 91 and 93 of the Raman Research Institute, *Ibid.*, 1956, **44 A**, 99, 160 and 367; 1957, **45 A**, 1, 7, 59 and 139.

5. Einstein, A. .. *Ann. Der. Physik.*, 1907, **22**, 180.

6. Debye, P. .. *Ibid.*, 1912, **39**, 789.

7. Born and Karman .. *Physik., Zeits.*, 1912, **13**, 297.

8. Jeans, J. H. .. *Phil. Mag.*, 1909, **17**, 229.

9. Einstein, A. .. *Physik. Zeits.*, 1917, **18**, 121.

Reprinted from "The Proceedings of the Indian Academy of Sciences", Vol. XLV, No. 6, Sec. A, 1957

GENERALISED THEORY OF INTERFERENCE AND ITS APPLICATIONS

Part III. Interference Figures in Transparent Crystals

By S. Pancharatnam

(*Memoir No.* 97 *from the Raman Research Institute, Bangalore*-6)

Received April 11, 1957
(Communicated by Sir C. V. Raman)

§ 1. Introduction

Among the most beautiful and interesting phenomena in crystal optics are the interference figures displayed by crystalline plates in convergent light. Figures of the most diverse descriptions are met with even in the realm of transparent crystals, and this is not a matter for surprise: for, firstly the crystal may possess optical activity—in which case the two waves propagated along any direction in the medium are in general elliptically polarised; and secondly the state of polarisation of the incident light as well as that of the light for which the analysing arrangement is completely transparent may be adjusted to be linear, circular or elliptic in form. By the use of the Poincaré sphere, the varied phenomena which fall under this head may be brought under a general method of analysis, which—without complicating the explanation of the simpler phenomena—helps in the understanding of more complex phenomena.

As specific applications of the method we shall consider some of the interference figures displayed by the optically active crystal, quartz. Using a single basal section, an interference figure consisting of two spirals coiled around each other may be obtained with a circular polariser and a linear analyser. This case has been theoretically discussed in the treatises of Walker,[1] Pockels[2] and Szivessy[3] (though, due to certain minor errors, the final description of the spirals given in these treatises differ as regards the handedness and orientation of the spirals). When a usual polarising microscope is used, the quarter-wave plate has be to inserted just prior to the analysing nicol, and hence the spirals have to be observed under an arrangement slightly different from that considered in the above-mentioned references. The spirals thus observed with a linear polariser and a 'circular analyser' are discussed in the treatise of Mascart.[4] The sense of description of the spirals is reversed when the quarter-wave plate is transferred from a position behind the quartz plate to a position in front of it (though Mascart states that the same results are obtained under both arrangements).

We shall also discuss from a novel point of view, the *Airy's spirals* observed when two basal sections of quartz of equal thickness and of opposite sign are superposed, and the combination observed between crossed nicols in convergent light.

§ 2. Discussion of the General Case

As is well known, each point in a convergent light figure is the focal point of a particular bundle of *parallel* rays emerging from the plate, of which each pair of rays which have been derived by the splitting of a common incident ray, can (after passing through the analysing arrangement) interfere at the focal point. Hence our first step is to discuss the interference effects presented in *parallel light* at normal incidence by an arbitrarily cut plate of any transparent material when examined between an elliptic polariser C_1 and an elliptic analyser C_2.† The crystal being transparent, the two waves propagated through it must necessarily be in two oppositely polarised states A and A′ as indicated in Fig. 1 (since only then will the intensity of the emerging beam be independant of the phase retardation introduced by the plate [Part I,[5] §2]).

When the incident light (of unit intensity) in the state of polarisation C_1 is split into two beams of opposite polarisation A and A′, these component beams will have the intensities $\cos^2 \frac{1}{2}a_1'$ and $\sin^2 \frac{1}{2}a_1'$ respectively, where a_1' is the angular distance between the states C_1 and A on the Poincaré sphere (Part I, §2). The analyser C_2 transmits the fractions $\cos^2 \frac{1}{2}a_2'$ and $\sin^2 \frac{1}{2}a_2'$ of these beams, since it transmits only the corresponding resolved components[5,6] of these beams in the state of polarisation C_2; here a_2' is the angular separation between the states C_2 and A on the Poincaré sphere. Taking the state of relative phase of the two oppositely polarised beams at the point of entry in the medium as the zero or standard, their phase difference at the point of emergence from the crystal will be equal to δ (which is the path retardation suffered by the slower beam of polarisation A′ relative to the other). The phase difference between the corresponding resolved components transmitted by the analyser will however be smaller than this value by an angle $\hat{A}$; according to Part I, eq. 9, $\hat{A}$ denotes now half the area of the lune $AC_1A'C_2A$, or $\hat{A} = \angle C_2AC_1 = \angle C_1A'C_2$. (The angles are measured with the usual sign convention, being reckoned positive in a counter-clockwise sense [see Fig. 1]).

† An elliptic analyser C_2 appears completely transparent for light of *elliptic* polarisation C_2; a quarter-wave plate followed by a linear analyser together form a simple elliptic analyser (Part I §8).

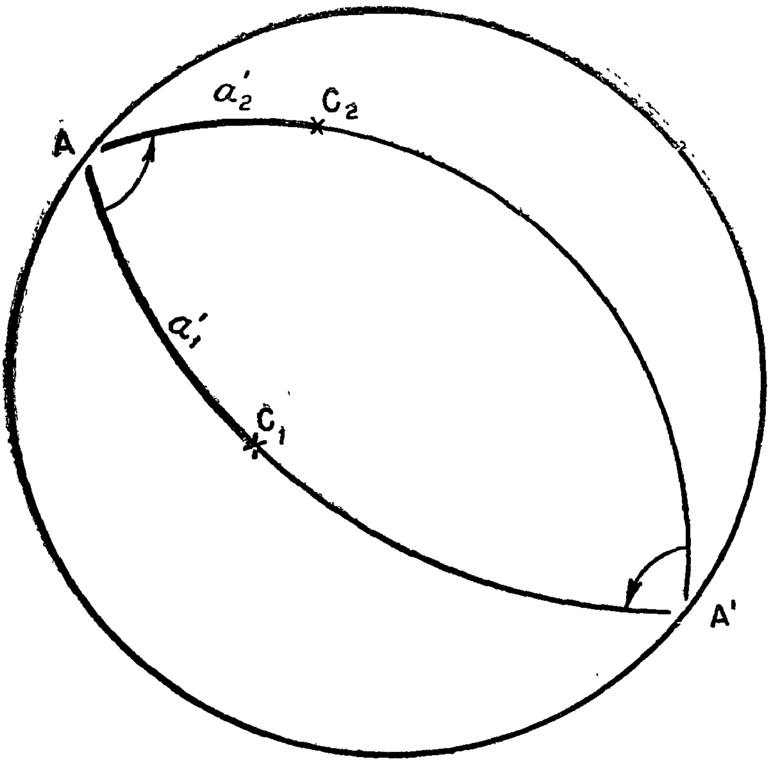

FIG. 1.

Thus the analyser C_2 transmits two beams having intensities I_1 and I_2 and phase difference $\triangle$ given by

$$\left.\begin{aligned} I_1 &= \cos^2 \tfrac{1}{2}a_1' \cos^2 \tfrac{1}{2}a_2'; \quad I_2 = \sin^2 \tfrac{1}{2}a_1' \sin^2 \tfrac{1}{2}a_2' \\ \triangle &= \delta - \hat{A} \end{aligned}\right\} \qquad (1)$$

These beams being in the same state of polarisation, the final intensity I transmitted by the analyser will be given by the usual interference formula

$$I = I_1 + I_2 + 2\sqrt{I_1 I_2} \cos \triangle \qquad (2)$$

The expression for the intensity I can also be written as the difference of two terms, the first of which is the intensity $\cos^2 \frac{1}{2} \widehat{C_1C_2}$ which would be transmitted if the plate were absent ($\delta = 0$), the second term giving rise to subtraction colours in white light.

Equations (1) and (2) are the basic equations on which the further discussion of all interference phenomena shown by transparent crystals are based. Though they have been derived for the most general case they are practically identical with those customarily used[7] for the simplest case, *viz.*, when the plate possesses only linear birefringence, and the polarising and

analysing elements are nicols—in which case $\hat{A}$ is equal to zero or π. In discussing any specific case, the values of the angles a_1', a_2' and A which obtain in that case have to be used; but their explicit values need be introduced not in the general expression (2), but only in certain subsidiary expressions determining those particular aspects of the phenomena which are to be investigated.

The variation of I with the direction of propagation may be observed in convergent light, using a plate cut normal to an optic axis—each *point* in the convergent light figure corresponding to a definite *direction* of propagation. For a plate of moderate thickness the retardation δ introduced by the plate increases rapidly as we proceed outwards along directions normal to the curves of constant retardation. The rate of variation of I as we proceed outwards from the optic axis is therefore taken to be predominantly due to the change in $\triangle$. We should therefore expect the appearance of interference rings, the curves of minimum intensity occurring along directions for which the pairs of pencils transmitted by the analyser ' destructively ' interfere, *i.e.*, along the curves where $\triangle = (2n + 1)\pi$. These do not however coincide with the curves where the retardation of the plate is an odd multiple of π. The physical reason for this is that the final phase difference $\triangle$ between the interfering pencils transmitted by the analyser is not identical with the retardation introduced by the plate but exceeds it by an amount $(-\hat{A})$; this latter may be correctly described as the contribution to the phase difference arising from the processes of dissolution and analysation, and it depends on the mutual relation between the state of incident polarisation C_1, the states of polarisation A and A′ of the beams into which it is split, and the analysing state C_2. The curves of minimum intensity are thus given by

$$\delta = (2n + 1)\pi + \hat{A} \tag{3}$$

and from what has been said above, *these curves of minimum intensity do not in general follow the curves of constant retardation*, $\delta =$ const., because the angle A is not constant but is itself a function of the direction of propagation (since the states A and A′ vary with the direction of propagation). A fairly accurate method of plotting the curves of minimum intensity (for a uniaxial crystal or a biaxial crystal of not too small an axial angle) is obviously the following; the circular curve $\delta = (2n + 1)\pi$ is first drawn and the radii vectors of this curve are increased by amounts which vary with the azimuth and which correspond to an additional retardation of $\hat{A}$. In this manner it can be shown that the interference rings exhibited by a basal

section of quartz between inclined nicols take the form of squares with rounded corners.

The intensity at any point on a curve of minimum intensity may be obtained by substituting $\triangle = \pi$ in (2) and is given by

$$I_{min} = \cos^2 \tfrac{1}{2} (a_1' + a_2') \tag{4}$$

This is not constant along a curve of minimum intensity, since the states A and A′ vary with direction, and hence the rings appear darkest along particular zones which have to be determined for each specific case.

§ 3. SPIRAL FIGURES DUE TO A SINGLE BASAL SECTION OF QUARTZ

In discussing the convergent light figures of quartz we will have to keep in mind the following features regarding the propagation of light near the optic axial direction. Referring to Fig. 2 *a*, consider any point P in the convergent light figure, whose polar co-ordinates are *r*, *θ* (the origin O re-

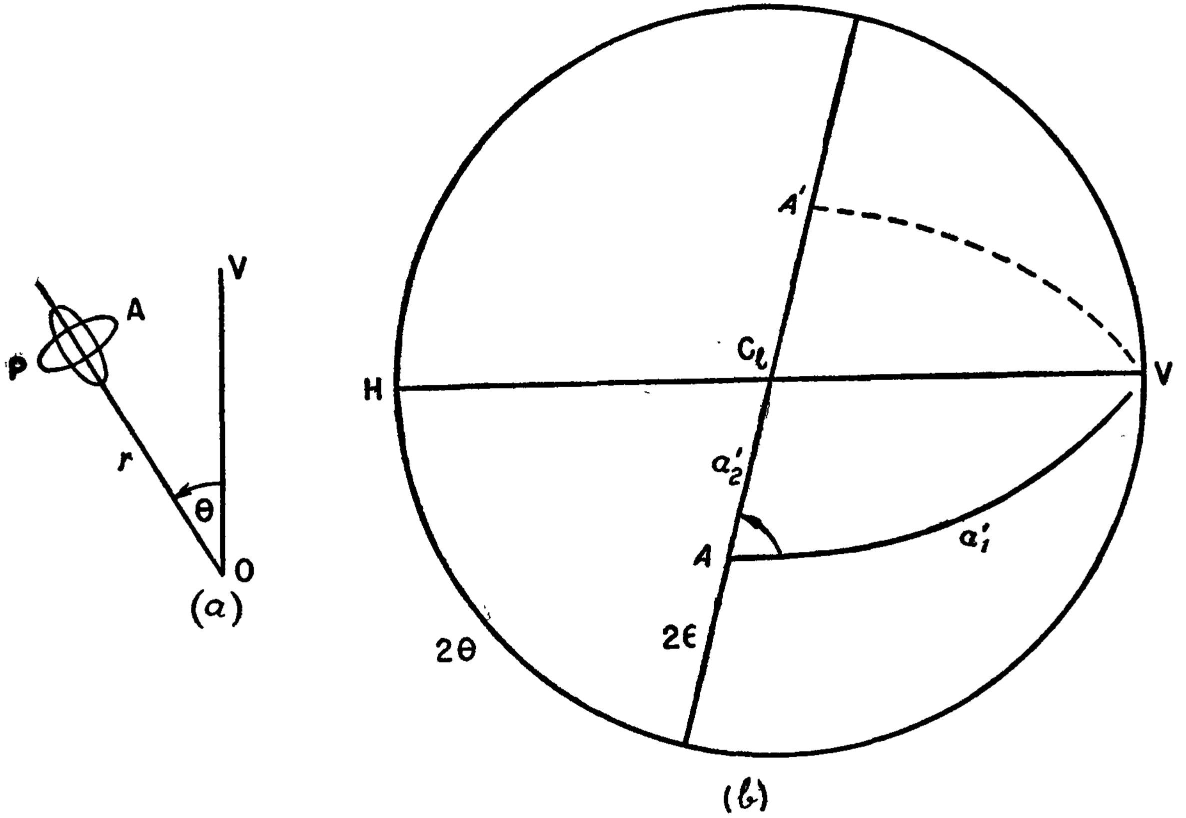

FIG. 2.

presenting the optic axial direction, and OV being a vertical line). Along the direction represented by P are propagated two crossed elliptic vibrations; and since quartz is a positive crystal, the major axis of the *slower*

vibration coincides with the plane of the radius vector OP itself (so that θ is the azimuth of the major axis of the faster vibration A with respect to the horizontal). Hence if ϵ be the ellipticity of the faster wave, its state of polarisation will be represented on the Poincaré sphere (Fig. 2 *b*), by the point A of longitude 2θ and latitude 2ϵ, ϵ being positive or negative according as the crystal is optically left or right handed. The numerical value of the ellipticity decreases rapidly as the angular distance r from the optic axis increases, ($\tan 2\epsilon = 2\rho/\mathrm{A}r^2$), being a maximum along the optic axial direction where opposite circular vibrations are propagated. In what follows the main fact to remember is that for all points P on a circle of radius r, the ellipticity is constant—so that the latitude 2ϵ of the point A is constant, only the longitude 2θ being altered.

We shall first discuss the interference figure presented by a left-rotating basal section when a left-circular analyser (represented by the pole C_l in Fig. 2 *b*) is used, the vibration direction of the incident *plane* polarised light being vertical (represented by the point V). In this case we have $\hat{\mathrm{A}} = \angle C_l\mathrm{AV}$. It is seen immediately from Fig. 2 *b* that (keeping 2ϵ constant) as 2θ increases from $0 \to \frac{1}{2}\pi \to \pi \to 3\pi/2 \to 2\pi$, the $\angle C_l\mathrm{AV}$ also increases continuously and goes through the same range of values $0 \to \frac{1}{2}\pi \to \pi$; $-\pi \to -\frac{1}{2}\pi \to 0$. This means that along the circle $\delta = (2n+1)\pi$, the phase difference $\triangle$ between the interfering pencils transmitted by the analyser falls short of $(2n+1)\pi$ (condition for destructive interference) by an angle $C_l\mathrm{AV}$ which increases continuously with the azimuth θ — and which in fact becomes exactly equal to *twice* the azimuth at $\theta = m\pi/4$. It follows immediately (see Section 2) that the curves of minimum intensity consist of two mutually enwrapping *left-handed* spirals which are related to one another by a rotation of 180°. From the triangle $\mathrm{VA}C_l$ we have

$$\tan \angle C_l\mathrm{AV} = \tan 2\theta/\sin 2\epsilon \qquad (5)$$

In the usual treatment[4] equations (3) and (5) are derived by a more lengthy procedure, and these equations may be used to discuss the form of the spirals in more detail. Close to the optic axial direction we have $\angle C_l\mathrm{AV} \simeq 2\theta$, so that the spirals are given by:

$$\delta = \sqrt{(\mathrm{A}r^2 + 4\rho^2)} = (2n+1)\pi + 2\theta$$

If the two arms of the spiral be extrapolated to the origin (where they actually fade away) the common tangent at the origin will be at an azimuth $(\frac{1}{2}\pi + \rho)$ with respect to the vertical—where ρ is the total optical rotation along the optic axis. Towards the border the figure must approximate to the non-spiral form shown by inactive crystals. The transition occurs by

way of the non-uniform rate of increase of the arm of the spiral—which manifests itself as kinks, which in turn assume the proportion of discontinuities towards the border of the figure (see Pockels, Plate VI, Figs. 3 and 4).

The zones along which the successive arcs of the spiral appear darkest may be determined with sufficient accuracy by studying the variation of (4) along a circle described about the optic axis ($a_2' =$ constant). Referring to Fig. 2 *b*, the arc a_1' acquires its maximum value of $(\pi - 2\epsilon)$ at $2\theta = 0$, and its minimum value of 2ϵ at $2\theta = \pi$. Along directions close to the optic axis (where $2\epsilon > \pi/4$) the sum $(a_1' + a_2')$ lies between the limits $\frac{1}{2}\pi$ to π. Hence the arcs of the spiral appear darkest along the vertical radius of the field of view. This result has also been derived in the usual presentation. We must emphasize however, that for a plate of moderate thickness (say 3 mm.) the above result holds only for points on the first convolution of the spiral, since at greater angular distances $2\epsilon < \pi/4$ (see Pockels, Plate VI, Figs. 3 and 4).

When the analysing state C_2 is changed to its opposite state C_2', the result (as is seen from Fig. 1) is to diminish the value of $\hat{A}$ by π and to change the length of the arc a_2' to its supplement. The same alteration in the expression (2) may be produced if the polarising state C_1 is changed to its orthogonal state. Hence, when a right-circular analyser is used, the entire spiral figure is rotated around by a right angle compared to the previous case (when a left-circular analyser was used).

We may obviously summarise the above results in a form applicable to both right and left-rotating basal sections. The handedness of the double spirals exhibited with a linear polariser and circular analyser is always the same as the handedness of the quartz. When the handedness of the circular analyser is opposite to that of the quartz, the tangent to the spiral at the origin coincides with the vibration direction of the light *emerging* along the optic axial direction; and, close to the optic axis, the spirals appear darkest along the diameter perpendicular to the plane of vibration of the incident light. A change in the handedness of the circular analyser causes a rotation of the entire figure, as such, through a right angle.

We see from Fig. 1 that when the state of polarisation of the incident light, and the state of polarisation C_2 of the light for which the analyser is transparent are interchanged, the sign of $\hat{A}$ is reversed, but the remaining factors in (1) remain unchanged. In Fig. 2 *b* the same result is obtained by change of the sign of 2θ. Hence *the entire spiral figure exhibited with a circular polariser and linear analyser is merely the reflection about the plane of vibration of the analyser, of the figure obtained when the polariser and*

analyser are interchanged. This statement holds with regard to all the details of the figure, and hence we need not discuss this case further.

The results of this section were qualitatively verified using a plate of right-quartz. The general arguments may be applied *mutatis mutandis* for discussing the spiral figures in negative uniaxial crystals and in biaxial crystals. In the latter case only a *single* spiral is formed because, as the polar angle of the point P increases, the azimuth of the major axis of the faster elliptic vibration increases at only *half* the rate.

§ 4. Airy's Spirals Due to Two Superposed Basal Sections

Our general treatment can also be applied to the case of superposed transparent plates which often exhibit curious interference figures (see *e.g.*, Walker, *loc. cit.*, p. 293). For this purpose it is necessary to replace the effect of the passage through a succession of plates by a passage through a single 'equivalent plate'. This can be done by combining successive rotations of the Poincaré sphere.

As an example, let us suppose that a left-handed and a right-handed section of quartz (both of the same thickness and cut at the same angle to the optic axis) are superposed (in that order) such that the corresponding principal planes of the two plates are in coincidence, the combination being then viewed in parallel light at normal incidence.

Referring to Fig. 3, let the point A_1 of latitude 2ϵ represent the state of polarisation of the faster elliptic vibration (of ellipticity ϵ) propagated in the first plate; the state of the faster elliptic vibration of ellipticity $(-\epsilon)$ propagated in the second plate is then represented by a point A_2 of the same longitude as A_1, but of latitude (-2ϵ). Let us construct an isosceles triangle $A_1 X A_2$ as indicated, such that the base angles A_2A_1X and XA_2A_1 are both equal to $\delta/2$ where δ is the retardation of each plate.

The action of the first plate is equivalent to an anti-clockwise rotation of the sphere about A_1 through twice the internal angle at A_1, while the action of the second plate is equivalent to an anti-clockwise rotation about A_2 through twice the internal angle at A_2 (see *e.g.*, Part I, § 6). By a well-known theorem for compounding rotations,[8] the two successive rotations are equivalent to a single rotation about the equatorial diameter through X, through twice the external angle at X. We have thus proved that the *combination is equivalent to a single optically inactive birefringent plate* of retardation Δ, the faster vibration direction of which makes an angle $-a$ with the common principal plane of the two quartz plates (which corres-

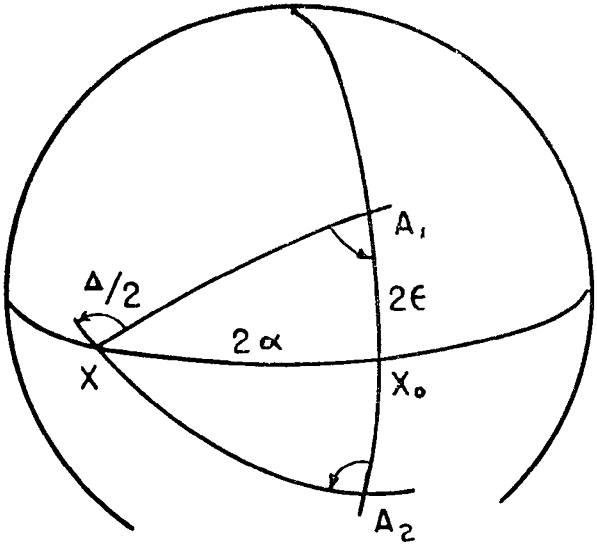

FIG. 3.

ponds to the major axis of the faster ellipse). Here α and $\triangle$ have the values indicated in Fig. 3. From the spherical triangle A_1XX_0 we have

$$\tan 2\alpha = \tan \tfrac{1}{2}\delta \sin 2\epsilon \tag{6}$$

Since the equivalent plate does not possess optical activity we should expect the appearance of ' isogyres ' when two equal basal sections of left- and right-quartz are superposed, and the combination observed between crossed nicols. The ' isogyres ' should occur along the directions where the ' equivalent ' principal planes of the combination coincide with the vibration directions of the polariser and analyser. Since, as we have seen, the equivalent principal planes for any direction of propagation do not coincide with the principal planes of the individual plates the 'isogyres' will *not* take the form of a uniaxial cross. If θ be the azimuth of a point in the field of view with respect to the plane of the polariser, the dark 'isogyres' obviously occur where θ is equal to α or $(\frac{1}{2}\pi + \alpha)$, where α is given by (6). This equation has been derived by an entirely different method of analysis in the usual presentation (Walker,[1] p. 368, eq. 39). According to this equation it may be shown by following the usual treatment that the dark ' isogyres ' take the form of four mutually enwrapping left-handed spirals known as Airy's spirals. Besides these spirals we will have dark curves, where the retardation $\triangle$ of the equivalent plate is a whole multiple of 2π, and from Fig. 3 these occur along the circles $\delta = 2n\pi$.

The sense of description of Airy's spirals is reversed when the right-handed plate is placed first because the sign of α is then changed.

5. Summary

The geometric method of specifying states of polarisation by points on the Poincaré sphere is used for giving a unified and physically intelligible approach to the interference phenomena displayed by crystalline plates in parallel or convergent light—under general conditions when the polarising and analysing states are linear, circular or elliptic in form. Examples discussed are the spiral figures exhibited in convergent light (*a*) by a basal section of quartz between a circular polariser and linear analyser (or *vice-versa*), and (*b*) by two superposed basal sections of left- and right-quartz between crossed nicols. The Airy's spirals observed in the latter case are interpreted as the 'isogyres' of the optically inactive plate to which the combination is equivalent.

6. References

1. Walker .. *Analytical Theory of Light*, Cambridge, 1904, 361 *et seq.*
2. Pockels .. *Lehrbuch der Kristalloptik*, Teubner, 1906, 336 *et seq.*
3. Szivessy .. *Handbuch der Physik*, Springer, 1928, Kap 11, 810 *et seq.*
4. Mascart .. *Traite d'Optique*, 1889, Tome 1, 240; 1891, Tome 2, 301, 317.
5. Pancharatnam .. *Proc. Ind. Acad. Sci.*, 1956, **54 A**, 247.
6. Ramachandran and Ramaseshan *J. Opt. Soc. Am.*, 1952, **42**, 49.
7. Ditchburn .. *Light*, Blackie and Sons, 1952, 385.
8. Ames and Murnaghan .. *Theoretical Mechanics*, Ginn and Co., 1929, 83.

Reprinted from "The Proceedings of the Indian Academy of Sciences"
Vol. XLV, No. 1, Sec. A, 1957

GENERALISED THEORY OF INTERFERENCE AND ITS APPLICATIONS

Part IV. Interference Figures in Absorbing Biaxial Crystals

BY S. PANCHARATNAM
(*Memoir No. 98 of the Raman Research Institute, Bangalore-6*)

Received April 22, 1957
(Communicated by Sir C. V. Raman)

§ 1. INTRODUCTION

THE interference figures displayed by absorbing biaxial crystals are of some general interest—quite apart from the light they throw on the optics of such media (Voigt, 1902 *a*; Boguslowski, 1914; Pancharatnam, 1955 *b*). The appearance of idiophanic interference rings with no analyser, or with no polariser, or with neither polariser nor analyser, finds no parallel in the field of transparent crystals; these peculiarities arise mainly from the fact that the two waves propagated along any particular direction are in *non-orthogonal* states of elliptic polarisation. Attention has already been directed in the introductions to Parts I and II (Pancharatnam, 1956 *a*, *b*) to some of of these phenomena and their broad explanation. It is sufficient therefore to remark that here we meet with practical instances of some of the most general cases of dissolution, composition, etc., which were theoretically envisaged in those papers on completely and partially coherent pencils. The physical concepts developed there enable us to give a comparatively intelligible explanation to otherwise complex phenomena, and the fruitfulness of these ideas is evidenced by the discovery of certain new phenomena in this field, *e.g.*, the formation of spiral interference figures even with optically inactive crystals (§ 8 *b*).

The general theoretical approach is outlined in Sections 2 and 6 which deal respectively with the two classes of interference phenomena into which the subject may be broadly divided, *viz.*, those exhibited respectively *without* and *with* the aid of an analyser behind the plate—the incident light being either completely polarised, partially polarised or even unpolarised. The concept of partially coherent beams discussed in Part II, apart from giving physical insight into the interference phenomena exhibited when the incident light is unpolarised (§§ 4 and 7), also explains certain new phenomena observed when the incident light is partially polarised (§§ 5 and 8 *b*).

§ 2. GENERAL DISCUSSION OF INTERFERENCE PHENOMENA OBSERVED WITHOUT ANY ANALYSER

In the succeeding sections we shall discuss the interference phenomena exhibited by a plate of an absorbing biaxial crystal without the use of an analyser, when the incident light is either completely polarised (§ 3), unpolarised (§ 4) or partially polarised (§ 5). When a *parallel* beam of unit intensity falls on such a plate it is split into two elliptically polarised streams in the states of polarisation A and B that are propagated without change of form in that direction. Let I_1 and I_2 be the intensities of the component beams, ϕ_1 their initial 'phase difference' at the point of entry into the medium, and γ their mutual degree of coherence (which will be equal to unity only in the case when the incident light is completely polarised). The streams travel through the crystal with different velocities and coefficients of absorption. Emerging from the crystal plate, we therefore have two beams (in states of polarisation A and B) whose intensities are now I_1' and I_2', the 'phase advance' of the first beam over the second being now Δ', where

$$\left.\begin{array}{l} I_1' = I_1 e_a{}^2; \quad I_2' = I_2 e_b{}^2 \\ \Delta' = \delta + \phi_1 \end{array}\right\} \qquad (1)$$

the phase retardation introduced by the plate being denoted by δ. These beams can directly interfere with one another, since in general they are in non-orthogonal states of polarisation and are not incoherent. The intensity I obtained on compounding the pencils is given by the general interference formula for beams in different states of polarisation (Part II, eq. 13).

$$I = I_1' + I_2' + 2\gamma\sqrt{I_1' I_2'} \cos \tfrac{1}{2} c \cos \Delta' \qquad (2)$$

where c is the angular separation of the states A and B when represented on the Poincaré sphere.

The variation of I with the direction of propagation may be observed in *convergent* light, using a plate cut normal to an optic axis, each *point* P in the convergent light figure corresponding to a definite *direction* of propagation. For a plate of moderate thickness the retardation δ introduced by the plate increases rapidly as we proceed outwards along directions normal to the curves of constant retardation. The rate of variation of I as we proceed outwards from regions near the optic axis can therefore be taken to be predominantly due to the change in Δ' (for most regions of the convergent light figure). Hence we should in general expect the appearance of idiophanic interference rings. From what has been said above the curves

of minimum intensity occur along directions where the emerging beams destructively interfere, that is, along the curves

$$\Delta' = (2n + 1)\,\pi$$

or

$$\delta = (2n + 1)\,\pi - \phi_1 \tag{3}$$

and a measure of the 'visibility' of the fringes (in the sense defined by Michelson) at any point in the convergent light figure is given by

$$V = \gamma \cos \tfrac{1}{2} c \frac{2\sqrt{I_1' I_2'}}{I_1' + I_2'} \tag{4}$$

From (3) we see that the curves of minimum intensity do not occur at the same position as those obtained between crossed polaroids (which occur at $\delta = 2n\pi$); in fact they do not even follow the curves of constant retardation $\delta =$ const., because the initial phase difference ϕ_1 itself varies with direction (since the states A and B vary with direction). In the case of non-active crystals, as we shall see the idiophanic rings in plane polarised light exhibit clearly the first effect but not the second—which may, however, be strikingly seen with the use of circularly polarised light.

Since all the factors in (4) vary *along* a curve $\Delta' =$ const., we should expect the visibility of the rings to be maximum along some particular zone in the field of view—the determination of which is in general very complex since it depends not only on the state of polarisation of the incident light, but also on the thickness of the plate.

The explanation of the appearance of idiophanic rings (in completely polarised, unpolarised or partially polarised light), and of some of their broad characteristics is thus immediately obvious in the present treatment and applies equally well to absorbing biaxial crystals possessing *optical activity*—where the non-orthogonal elliptic vibrations A and B bear no simple relation to one another (Pancharatnam, to be published).

§ 3. Phenomena in Absorbing Biaxial Crystals Using a Polariser Alone

(*a*) *General discussion.*—If completely polarised light be incident on the plate, the component beams into which it is split will be completely coherent. Their intensities I_1 and I_2, and their initial phase difference ϕ_1, may be expressed (see Part I, eqns. 3 and 5 *b*) in terms of the sides of the spherical triangle ABC_1 on the Poincaré sphere—where C_1 represents the state of polarisation of the incident elliptic vibration, and A and B the states of the beams into which it is split.

$$\left.\begin{array}{l} \mathrm{I}_1 = \dfrac{\sin^2 \frac{1}{2} a_1}{\sin^2 \frac{1}{2} c}\ ; \quad \mathrm{I}_2 = \dfrac{\sin^2 \frac{1}{2} b_1}{\sin^2 \frac{1}{2} c} \\ \phi_1 = \pi - \frac{1}{2} \mathrm{E}' \end{array}\right\} \qquad (5)$$

Here E′ is the area of the triangle $C_1'BA$ (measured with the usual sign convention) C_1' being the point opposite to the incident state C_1 (see Fig. 1, text).

The intensity I at the corresponding point in the field of view is obtained by substituting in (2):

$$\mathrm{I} = \mathrm{cosec}^2 \tfrac{1}{2} c \,\{e_a{}^2 \sin^2 \tfrac{1}{2} a_1 + e_b{}^2 \sin^2 \tfrac{1}{2} b_1 - 2e_a e_b \sin \tfrac{1}{2} a_1 \sin \tfrac{1}{2} b_1 \cos \tfrac{1}{2} c \cos (\delta - \tfrac{1}{2} \mathrm{E}')\} \qquad (6)$$

(*b*) *Phenomena in non-active crystals.*—In order to illustrate that our general method of analysis is capable of handling specific cases we shall briefly consider some of the phenomena exhibited by a plate (cut normal to an optic axis) of the optically inactive orthorhombic mineral iolite. We shall refer to the photographs of the different phenomena exhibited by this mineral published in this paper and in a previous paper (Pancharatnam, 1955 *b*, hereafter referred to as P. 2). The idiophanic rings are always absent along the directions where the waves are orthogonally polarised ($\cos \frac{1}{2} c = 0$)—*i.e.*, along the trace of the axial plane. (The axial plane is kept horizontal in all the photographs).

Voigt (*loc. cit.*) has shown that in non-active absorbing biaxial crystals the two elliptically polarised waves A and B propagated along any one direction, have their major axes crossed and have the same ellipticity ϵ (which, according to the usual sign convention, means that they are also described in the *same* sense). Hence on the Poincaré sphere the longitudes of the points A and B differ by π, but their latitudes are both equal to 2ϵ, as drawn in Fig. 2. [See also Pancharatnam, 1955 *a*.] Accordingly we have to substitute $\frac{1}{2} c = \frac{1}{2} \pi - |2\epsilon|$ in (6), for all the cases discussed below.

If the incident light is, say, *left-circularly polarised,* so that the point C_1 now coincides with the upper pole C_l, then we have to substitute in (6): $a_1 = b_1 = \frac{1}{2} \pi - 2\epsilon$; and $\frac{1}{2} \mathrm{E}'$ equal to π or zero, according as ϵ is positive or negative. Hence the intensity at any point in the field of view is,

$$\mathrm{I} = \frac{1}{2(1 + \sin 2\epsilon)} (e_a{}^2 + e_b{}^2 + 2e_a e_b \sin 2\epsilon \cos \delta). \qquad (7)$$

The *asymmetry* of the idiophanic rings with respect to the axial plane, which is observable in Fig. 3, Plate I (taken with left-circularly polarised light)

is now readily explicable. In the upper half of the figure where the sense of rotation of the ellipses propagated is opposite to that of the incident circularly polarised light, ϵ is negative and hence the minima occur at $\delta = 2\pi$, 4π, etc. (This is verified from the fact that they occur in the same position as in Fig. 1, Plate I, which is obtained when a circular analyser which can cross out the incident light is also introduced.) In the lower half of the figure where ϵ is positive, the minima occur at $\delta = \pi$, 3π, etc. (which is verified from the fact that the fringes are shifted down by half a fringe width relative to those appearing in the upper half of the figure). The expression for I becomes indeterminate at $\epsilon = -\pi/4$, *i.e.*, at the singular axis where *only* a right circular vibration can be propagated *unchanged.* That the emergent intensity is larger than at the other singular axis where the incident light is propagated unchanged, is clearly shown by referring to Fig. 3. This remarkable phenomenon has been theoretically discussed elsewhere (Pancharatnam, 1955 *a*, *b*). When right circularly polarised light is used, the sign of the third term in (7) has to be changed, and the asymmetry about the axial plane will be reversed (see P. 2, Figs. 13 and 14).

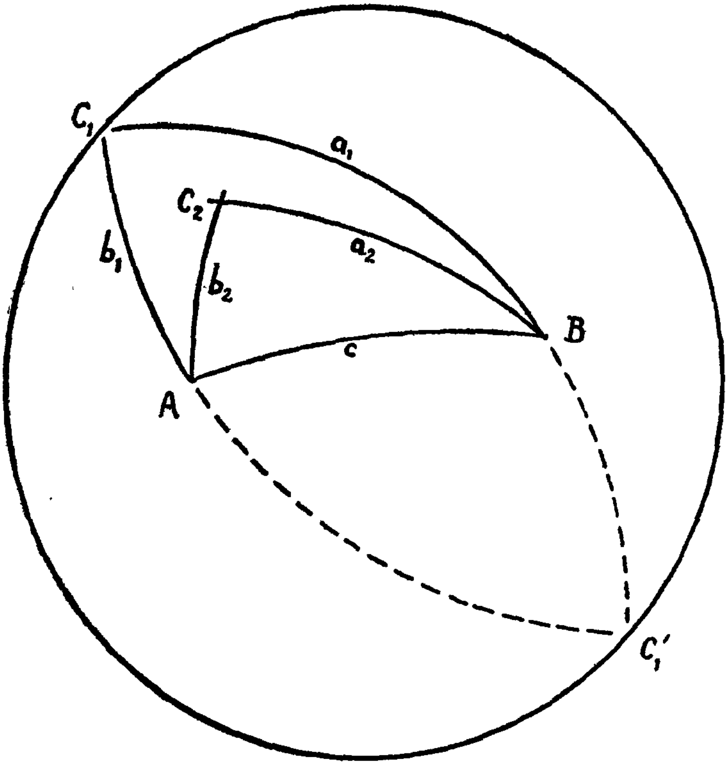

FIG. 1

If the incident light is *plane polarised,* the point C_1 lies on the equator as is drawn in Fig. 2, text. From the figure we see that $b_1 = (\pi - a_1)$ and $E' = - \angle AC_1B$ (since the area E' of the triangle $C_1'BA$ is numerically half the area of the lune of $\angle AC_1B = \hat{C}_1$). Substituting these values in (4), we have

$$I = \operatorname{cosec}^2 \tfrac{1}{2} c \{e_a{}^2 \sin^2 \tfrac{1}{2} a_1 + e_b{}^2 \cos^2 \tfrac{1}{2} a_1 - 2e_a e_b \sin \tfrac{1}{2} a_1 \cos \tfrac{1}{2} a_1 \cdot \cos \tfrac{1}{2} c \cos (\delta + \tfrac{1}{2} \hat{C}_1)\} \tag{8}$$

Let $-\nu$ be the azimuth of the major axis of the faster elliptic vibration with respect to the vibration-direction of the incident light. In directions where the ellipticity is small (so that the points A and B lie near the equator), an approximate formula may be obtained by substitutions $\sin^2 \frac{1}{2} a_1 \simeq \cos^2 \nu$; $\cos^2 \frac{1}{2} a_1 \simeq \sin^2 \nu$; $\sin^2 \frac{1}{2} c \simeq 1$; $\cos \frac{1}{2} c \simeq |2\epsilon|$; and $|\hat{C}_1| = \pi$. We then obtain the approximate formula that is customarily used (Pockels, 1906, p. 423, eq. 9).

$$I = e_a{}^2 \cos^2 \nu + e_b{}^2 \sin^2 \nu + 2\epsilon \sin 2\nu\, e_a e_b \sin \delta \tag{9}$$

Figure 2 of the text shows qualitatively that the last substitution $|\hat{C}_1| = \pi$ will be justified except for directions of propagation where $\nu \simeq 0$, where in any case the interference effects [depending on the last term in (9)], vanish by virtue of the first substitutions. The maxima and minima are thus shifted by *quarter* of a fringe width compared to those obtained between crossed polaroids (see P. 2, Figs. 2 and 9).

To obtain the exact formula for the intensity at any point in the field, we have to use in (8) the exact values of a_1, c and $\hat{C}_1$ which are obtained by spherical trigonometry, from the right-angled triangle AXC_1:

$$\tan \tfrac{1}{2} \hat{C}_1 = \sin 2\nu / \tan 2\epsilon; \quad \cos a_1 = - \cos 2\epsilon \cos 2\nu;$$

$$\sin a_1 \cos \tfrac{1}{2} c = \frac{\cos 2\epsilon \sin 2\nu}{\sin \tfrac{1}{2} \hat{C}_1} \cdot \sin 2\epsilon.$$

It can thus be shown that the approximate formula (9) neglects only the squares and higher powers of the ellipticity ϵ. [Strictly speaking, the idiophanic rings on each side of the axial plane will take the form of the arcs of a spiral (see § 8 *b*) when the polariser is inclined to the axial plane.] It can also be shown that the exact formula deduced by Voigt can be put in the same form as that obtained by the above substitutions.

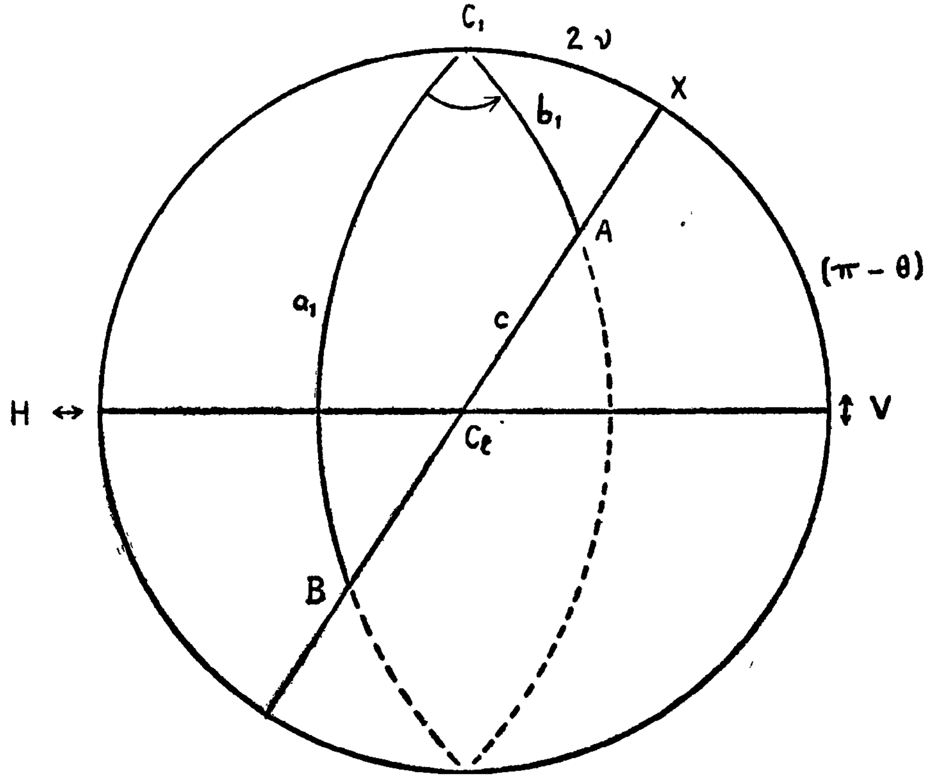

FIG. 2

§ 4. INTERFERENCE PHENOMENA IN ABSORBING BIAXIAL CRYSTALS IN UNPOLARISED LIGHT

It was shown in Part II, § 7, that when unpolarised light is split into two non-orthogonally polarised beams (in the states of polarisation A and B), the component beams are *partially* coherent with one another. The intensities I_1 and I_2 of the component beams, their initial phase difference ϕ_1, and their mutual degree of coherence γ are given by

$$I_1 = I_2 = \tfrac{1}{2}\operatorname{cosec}^2 \tfrac{1}{2}c; \quad \gamma = \cos \tfrac{1}{2}c; \quad \phi_1 = \pi. \tag{10}$$

The intensity I at any point in the field of view, is given by substituting in (2)

$$I = \tfrac{1}{2}\operatorname{cosec}^2 \tfrac{1}{2}\, c\, \{e_a{}^2 + e_b{}^2 - 2e_a e_b \cos^2 \tfrac{1}{2}\, c \cos \delta\} \tag{11}$$

The interference effects observed (Fig. 5, Plate I) are extremely feeble since they depend on the *square* of the factor $\cos \frac{1}{2}c$, which becomes appreciable only in immediate neighbourhood of the singular axes. What is actually seen—both in the optically active crystal amethyst and in the inactive crystal iolite—is the occurrence of the first minimum on either side of the optic axis as two dark spots at the terminii of the Brewster's brushes. These

minima should occur at $\delta = 2\pi$; and in the case of iolite (Fig. 5, Plate I), this is confirmed by the fact that they occur at the same position as the first minima obtained between crossed polaroids (Fig. 6, Plate I)—as may be verified by measurement (see also § 5 *b*).

§ 5. Interference Phenomena in Partially Polarised Light

(*a*) *Incident light partially circularly polarised.*—Just as the addition of two incoherent *non-orthogonally* polarised beams results in a partially polarised beam, so also when a partially polarised beam is split into two non-orthogonally polarised beams it is possible under certain circumstances for the component beams to be completely incoherent with one another. Hence with partially polarised light incident on a plate of an absorbing biaxial crystal, it should be possible under certain conditions for the interference fringes to completely vanish near some particular regions in the convergent light figure (observed with or without an analyser).

Fig. 7, Plate II of this paper shows a photograph of this curious phenomenon as exhibited by a plate of iolite when the incident light is partially circularly polarised. An analysing polaroid was set behind the plate with its vibration direction perpendicular to the axial plane. The partially left-circularly polarised light was obtained by passing partially plane polarised light—emerging from a pile of plates—through a quarter-wave plate.

For analysing the phenomenon we shall use the representation discussed in Part II whereby any beam (completely or partially polarised) is characterised by its total intensity and by a 'Stokes vector' drawn from the centre of the Poincaré sphere; the length of the vector and its orientation (*i.e.*, point of intersection with the sphere) give respectively the intensity and state of polarisation, of the 'polarised fraction' of the beam. Let us denote by $\mathbf{S}$ the vector representing the incident partially left-circularly polarised light (of unit intensity and degree of polarisation p); and let $\mathbf{S}_1$ and $\mathbf{S}_2$ be the Stokes vectors representing the component beams—completely polarised in states A and B—into which the incident light is split. Then obviously

$$\mathbf{S} = p\mathbf{C}_l;\ \mathbf{S}_1 = \mathrm{I}_1\mathbf{A};\ \mathbf{S}_2 = \mathrm{I}_2\mathbf{B} \tag{12}$$

where $\mathbf{C}_l$, $\mathbf{A}$, $\mathbf{B}$ are unit vectors directed towards the points C_l, A and B respectively (see Fig. 3, text). The intensities I_1 and I_2 of the component beams must be equal to one another, since the states A and B are symmetrically situated with respect to the pole C_l, for a non-active crystal; they are given by eq. 21 of Part II,

$$\mathbf{I}_2 = \mathbf{I}_1 = \tfrac{1}{2}(1 - \mathbf{S} \cdot \mathbf{B}) \operatorname{cosec}^2 \tfrac{1}{2}c$$
$$= \tfrac{1}{2}(1 - p \sin 2\epsilon)/\cos^2 2\epsilon \tag{13}$$

It was shown in Part II, § 6, that when two completely polarised beams $\mathbf{S}_1$ and $\mathbf{S}_2$ are combined to give a resultant beam $\mathbf{S}$, then

$$\mathbf{S} = \mathbf{S}_1 + \mathbf{S}_2 + \mathbf{S}_{12}$$

where $\mathbf{S}_{12}$ is a vector arising from the interference of the component beams, and by determining which we can in the present case calculate the degree of coherence γ and the effective phase difference ϕ_1 between the component beams. Substituting from (12) and referring to Fig. 3, text, we have

$$\mathbf{S}_{12} = (p - 2\mathbf{I}_1 \sin 2\epsilon)\, \mathbf{C}_l$$

or from (13)

$$\mathbf{S}_{12} = 2\mathbf{I}_1 \cdot \frac{p - \sin 2\epsilon}{1 - p \sin 2\epsilon}\, \mathbf{C}_l \tag{14}$$

Since $\mathbf{S}_{12}$ is coplanar with $\mathbf{S}_1$ and $\mathbf{S}_2$ it follows from the geometric construction for $\mathbf{S}_{12}$ given in Part II, Fig. 2, that (*a*) the length of the vector $\mathbf{S}_{12}$ is equal to $2\gamma\sqrt{\mathbf{I}_1\mathbf{I}_2}$, and (*b*) the effective phase difference between the component beams is zero or π according as $\mathbf{S}_{12}$ bisects the interior or exterior angle between $\mathbf{S}_1$ and $\mathbf{S}_2$.

The appearance of the figure presented (either without any analyser or with an analyser set along or perpendicular to the axial plane) may now be understood in terms of the variation of the ellipticity of the waves over the region covered by the convergent light figure. (See Voigt, 1902 *a*; also P. 2, Fig. 1.)

In the lower half of the figure where ϵ is negative (because of the manner in which the plate was set), we see from (14) that the degree of coherence never vanishes and the initial phase difference is π. On the other hand, in the region above the trace of the axial plane the degree of coherence vanishes where $\mathbf{S}_{12} = 0$, *i.e.*, where $\sin 2\epsilon$ is equal to the degree of polarisation p. Towards the interior of this region the ellipticity ϵ becomes greater and the initial phase difference ϕ_1 between the component beams is π; while towards the exterior of this region $\sin 2\epsilon < p$ and accordingly the initial phase difference jumps to zero. Thus in Fig. 7, Plate II, as we proceed upwards from the optic axis, the first ring is clearly seen (appearing at the same distance as that in the lower half of the figure); further on *the rings disappear* and then reappear with *a shift of half a fringe width* compared ot those in the lower half of the figure—thus confirming our theoretical

deductions. The use of an analyser behind the crystal plate increases the clarity of the interference phenomena by resolving the beams into the same state of polarisation before making them interfere. This does not affect the main conclusions of our discussion.

(*b*) *Incident light partially plane polarised.*—When a partially polarised beam is decomposed into two non-orthogonally polarised beams, it may be shown that the effective phase difference between the component beams is *not* independant of the degree of polarisation. Let us suppose that the incident light of degree of polarisation p is partially *plane* polarised in any state C_1 (Fig. 2, text). It would then be represented by a vector **S** of length p directed towards C_1. The initial phase difference ϕ_1 between the component beams in the states of polarisation A and B is given by Part II, eqns. 22 *a* and 23 *a*:

$$\tan \phi_1 = V'/U', \quad (\tfrac{1}{2}\pi \leq \phi_1 \leq 3\pi/2)$$

where

$$V' = S_z \operatorname{cosec} \tfrac{1}{2} c; \quad U' = - \cos \tfrac{1}{2} c \operatorname{cosec}^2 \tfrac{1}{2} c$$

and where the positive z direction is in the direction of the vector $\mathbf{A} \times \mathbf{B}$. Considering the case when the beam is incident on an optically inactive absorbing crystal (*e.g.*, iolite) we will have (see Fig. 2, text)

$$\tan \phi_1 = p \sin 2\nu/\tan 2\epsilon = p \tan \tfrac{1}{2} \hat{C}_1 \tag{15}$$

where the symbols have the same meaning as previously (§ 3 *b*). Thus as the degree of polarisation is increased from zero the initial phase difference ϕ_1 alters continuously from π to $(\pi + \tfrac{1}{2}\hat{C}_1)$.

This was experimentally demonstrated by partially polarising the incident light with its vibration parallel to the axial plane of iolite by the use of a pile of plates, and observing the convergent light figure without the use of an analyser. Starting with the light more or less completely polarised (P. 2, Fig. 6), the degree of polarisation was gradually decreased to zero (by turning the pile of plates about an axis perpendicular to the axial plane). It was then observed that not only did the rings become less distinct at the border of the figure, but at the same time they moved slightly *outwards*, till finally when the light was unpolarised what was left were the minima in the Brewster's brushes.

Incidentally the above experiment demonstrates clearly a fact which follows from the theoretical discussion of §§ 3 and 4, namely, that the minima in the Brewster's brushes do not exactly coincide with those observed when

the light is polarised parallel to the axial plane. This fact was not realized in a previous paper (P. 2), though a measurement on the photographs (Figs. 5 and 6) published in that very paper confirms the above result.

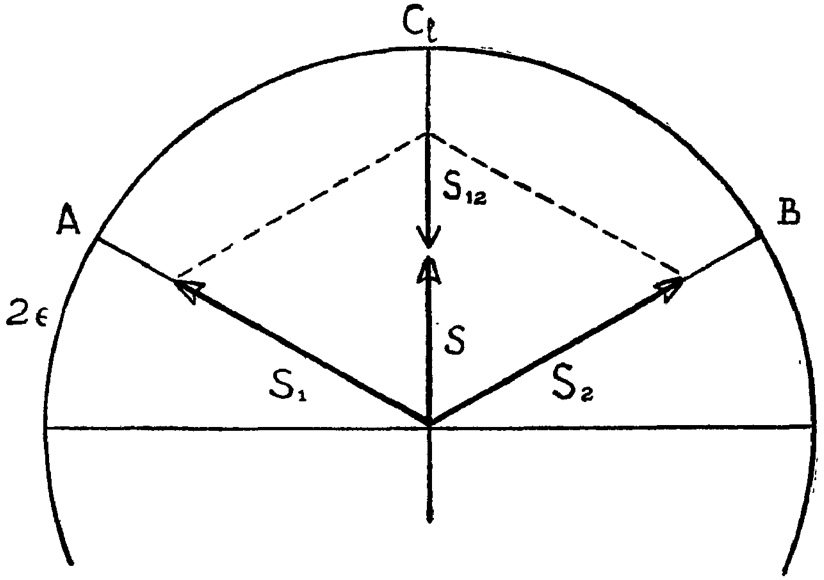

FIG. 3

§ 6. GENERAL DISCUSSION OF INTERFERENCE PHENOMENA INVOLVING USE OF AN ANALYSER

In the succeeding sections we shall discuss the interference phenomena exhibited in convergent light by a crystal plate when an analyser C_2 (which transmits light of elliptic polarisation C_2) is used behind the crystal plate—the incident light being either unpolarised (§ 7), or completely or partially polarised (§§ 8, 9). As before let I_1' and I_2' be the intensities of the two pencils (in the states of polarisation A and B respectively) which emerge from the crystal plate along any particular direction, their degree of coherence being γ, and the effective phase advance of the first beam over the second being Δ'. The analyser transmits the resolved components of these beams in the state of polarisation C_2, and these components can interfere with one another. Let the intensities of the resolved components be I_1'' and I_2'', their effective phase difference being Δ''. These may be written down in terms of the spherical triangle ABC_2 (Fig. 1, text) using the results of Part I, § 8, and Part II, § 4.

Writing $\Delta'' = \Delta' + \phi_2$, we have

$$\left. \begin{aligned} I_1'' &= I_1' \cos^2 \tfrac{1}{2}b_2; \quad I_2'' = I_2' \cos^2 \tfrac{1}{2}\, a_2; \\ \phi_2 &= -\tfrac{1}{2} E_2 \end{aligned} \right\} \tag{16}$$

where E_2 is the area of the triangle ABC_2. The phase diffrence Δ'' between the two finally interfering beams is thus the sum of three terms:

$$\Delta'' = \phi_1 + \delta + \phi_2 \quad (17)$$

where ϕ_1 is the initial phase difference—'introduced in the process of decomposition'—between the pencils at the first surface of the plate, δ is the phase retardation introduced by the plate, and ϕ_2 may be called the phase difference introduced in the process of analysation.

The resultant intensity I transmitted by the analyser is given by the formula for the interference of two beams in the same state of polarisation, having a degree of coherence γ.

$$I = I_1'' + I_2'' + 2\gamma \sqrt{I_1'' I_2''} \cos \Delta'' \quad (18)$$

The general arguments following eq. 2 may be applied *mutatis mutandis* in the present case. The appearance of interference figures with an analyser is therefore to be expected whether the incident light is unpolarised or completely or partially polarised. The curves of minimal intensity follow the curves where $\Delta'' = (2n + 1)\pi$. Since Δ'' is given by (17) these curves will not in general follow the curves of constant retardation $\delta = \text{const.}$; this is because *the sum of the phase differences* ϕ_1 *and* ϕ_2 (which are introduced by the processes of resolution and analysation respectively) *is not constant, but is itself a function of the direction of propagation.* This is the true physical reason why the interference figures in quartz, and, as we shall see, also in iolite, can under suitable conditions even take the form of spirals.

§ 7. Idiophanic Rings with an Analyser Alone

The idiophanic rings in the present case (with the incident light unpolarised) are of the same clarity as those obtained with a polariser *alone* in front of the plate. In the present case, however, the intensity I at any point in the field of view is obtained by substituting the values given by (10) in (18):

$$I = \tfrac{1}{2} \operatorname{cosec}^2 \tfrac{1}{2} c \,\{e_a{}^2 \cos^2 \tfrac{1}{2} b_2 + e_b{}^2 \cos^2 \tfrac{1}{2} a_2 - 2e_a e_b \cos \tfrac{1}{2} a_2 \cos \tfrac{1}{2} b_2 \cos \tfrac{1}{2} c \cos (\delta - \tfrac{1}{2} E_2)\} \quad (19)$$

In view of the fact that this expression differs from (6), an explanation is required as to why the idiophanic rings seen with the polaroid set either before or after the plate do *not* differ in the case of non-active absorbing crystals like iolite (compare Figs. 8 and 10 of P. 2). This equivalence is not a general result but a consequence of the peculiar fact that in non-active

crystals the two ellipses propagated along any direction have their major axes crossed and their ellipticities equal. In such a case (see Fig. 2, text) we have $a = (\pi - b)$ and $E = E'$, so that the expressions (6) and (19) become equal. However in the case of optically active absorbing crystals it can be shown that the states A and B do not bear this simple relation to one another (work to be published), and in such a case the idiophanous figure presented with a polaroid set in front of the crystal should not be the same as that obtained with the polaroid set behind the plate in the same position. This difference has been observed in the case of amethyst.

That the effects presented with a polariser C alone are *in general* not the same as those obtained with an analyser C alone, may be confirmed even in the case of inactive absorbing biaxial crystals if C represents a state of elliptic polarisation. Thus the idiophanic rings with a left-circular analyser (Fig. 4, Plate I) are not the same as with a left-circular polariser (Fig. 3, Plate I), but should be the same as the figure seen with a *right*-circular polariser (as may be shown by comparing eqns. 6 and 19]). This latter proposition has also been confirmed experimentally in iolite.

§ 8. Interference Figures in Absorbing Biaxial Crystals Between Polariser and Analyser

(*a*) *General discussion.*—When *completely* polarised light of unit intensity in the state of polarisation C_1 is incident on a plate of an absorbing biaxial plate, and an analyser C_2 is used behind the plate, the intensities I_1'' and I_2'' and the difference in phase Δ'' of the two pencils transmitted by the analyser along any particular direction are given by substituting in (16) from (5) and (1):

$$I_1'' = \frac{\sin^2 \frac{1}{2} a_1 \cos^2 \frac{1}{2} b_2}{\sin^2 \frac{1}{2} c} \cdot e_a^2; \quad I_2'' = \frac{\sin^2 \frac{1}{2} b_2 \cos^2 \frac{1}{2} a_2}{\sin^2 \frac{1}{2} c} e_b^2$$

$$\Delta'' = \delta + \pi - \tfrac{1}{2}(E_1' + E_2)$$

where, it may be noted, $(E_1' + E_2)$ is the area of the spherical quadrilateral $C_1'BC_2A$ (see Fig. 1, text).

The resultant intensity I_2 transmitted by the analyser is given by the formula (18) for the interference of two completely coherent pencils in the same state of polarisation. Hence

$$I = \operatorname{cosec}^2 \tfrac{1}{2} c \, [e_a^2 \sin^2 \tfrac{1}{2} a_1 \cos^2 \tfrac{1}{2} b_2 + e_b^2 \sin^2 \tfrac{1}{2} b_1 \cos^2 \tfrac{1}{2} a_2 - 2 e_a e_b \sin \tfrac{1}{2} a_1 \sin \tfrac{1}{2} b_1 \cos \tfrac{1}{2} a_2 \cos \tfrac{1}{2} b_2 \cos \{\delta - \tfrac{1}{2}(E_1' + E_2)\}] \quad (20)$$

The equation for the case of transparent crystals (Part III), is obviously a particular case of the above.

For the particular case when polariser and analyser are crossed we have $a_1 = \pi - a_2$; $b_1 = \pi - b_2$ and $(E_1' + E_2) = 0$. Hence

$$I = \frac{\sin^2 \frac{1}{2} a_1 \sin^2 \frac{1}{2} b_1}{\sin^2 \frac{1}{2} c} (e_a{}^2 + e_b{}^2 - 2e_a e_b \cos \delta) \tag{21}$$

We see therefore that—independant of the orientation of the crossed states C_1 and C_1'—the minima of the ring system occur at $\delta = 2\pi$, 4π, etc., and that the rings are seen most clearly along the zone where the absorption coefficients of the two waves are equal, or $e_a = e_b$ (see Figs. 1, 2 and 6, Plate I).

We can now easily show that the interference figures exhibited between crossed nicols by a plate of an absorbing biaxial crystal *not* possessing optical activity, will be unaltered if the polariser and analyser are interchanged. In such a medium (as we have seen at the end of § 3 *b*) the states of polarisation A and B of the waves propagated in any direction are such that when the incident light is *linearly* polarised we will have $a_1 = \pi - b_1$ (see Fig. 2, text). The effect of interchanging analyser and polariser is then got by changing a_1 to $\pi - a_1$ and b_1 to $\pi - b_1$ and such a change will leave the expression (21) for the emergent intensity unaltered.

It is to be noted however that such an interchange of the crossed nicols could alter the expression for the emergent intensity, if the points A and B are any two general points on the sphere—a situation which occurs in optically active absorbing crystals; the alteration of the observed interference figure on interchanging the crossed nicols has been observed in the case of amethyst (work to be published). That the interchange of the crossed polariser and analyser will in general alter the interference figure may be observed even in the *non*-active crystal iolite provided the incident light is not linearly polarised. This may be seen from the photographs (1) and (2) in which one has been taken between a left-circular polariser and a right-circular analyser, while the other has been taken between a right-circular polariser and a left-circular analyser; the difference between the two figures is small but striking and is mainly in the shift in the position of the eccentric spot from the upper to the lower singular axis.

(*b*) *Spiral figures in inactive absorbing crystals.*—It was observed that when the incident light is plane polarised at an angle of, say, 45° to the axial plane, and a circular analyser is used behind the crystal plate, the interference figure takes a spiral form in the centre of the field of view (Figs. 10 and 11, Plate II). If the incident light is only *partially* plane polarised, the kinks occurring along the vertical line of the field of view

become less marked, and several convolutions of the spiral can be clearly traced (Figs. 8 and 9, Plate II).

On the Poincaré sphere (Fig. 2, text) let the horizontal direction (which is also the trace of the axial plane) be represented by H. We shall first treat the case when the analyser is a left-circular analyser C_l, and the state of maximum polarisation of the incident partially plane polarised light is inclined at an angle of $-45°$ to the axial plane and hence represented by the point C_1 on the Poincaré sphere. Any point P in the field of view may be specified by its polar co-ordinates (r, θ) with respect to a horizontal line, and corresponds to a particular direction of propagation in the crystal. Except for points very close to the optic axis, we may take $\frac{1}{2}\theta$ and $(\frac{1}{2}\pi - \frac{1}{2}\theta)$ as the aximuths with respect to the axial plane of the major axes of the faster and slower elliptic vibrations (A and B) propagated in the direction P, their common ellipticity ϵ being given by

$$\epsilon = (K/2\delta) \sin \theta \tag{22}$$

where K is proportional to the dichroism along the optic axis (see Pockels, *loc. cit.*, p. 425, eq. 13). On the Poincaré sphere, A and B will then have the common latitude 2ϵ and longitudes θ and $(\pi - \theta)$ respectively as indicated in Fig. 2, text. According to (17), the phase difference Δ'' between the resolved components transmitted by the analyser in the direction $P(r, \theta)$ exceeds the retardation δ introduced by the plate by an angle ϕ,

$$\Delta'' = \delta + \phi, \tag{23}$$

and we have to show that the locus of the direction for which these beams destructively interfere $[\Delta'' = (2n + 1)\pi]$, forms a spiral. The retardation δ of the plate is proportional to the radius vector r, $(\delta = \beta r)$, for regions not too close to the optic axis, and it remains to express ϕ as a function of the direction of propagation. From (16) we have,

$$\phi = \phi_1 - \tfrac{1}{2} E_2 \tag{24}$$

Since E_2 is the area of the triangle ABC_l we have $\frac{1}{2} E_2 = \pi$ for points above the axial plane, and $\frac{1}{2} E_2 = 0$ for points below. The value of the initial phase difference ϕ_1 is given by (15):

$$\tan \phi_1 = -p \cos \theta / \tan 2\epsilon; \qquad (\pi/2 \leq \phi_1 \leq 3\pi/2) \tag{25}$$

Substituting from (22), we have, on neglecting the squares and higher powers of ϵ,

$$\tan \phi_1 = (p/K)\, \delta \cot \theta \tag{26}$$

From a consideration of equations 26, 23 and 24 we easily obtain the following result. As we proceed along the circle $\delta = (2n + \frac{1}{2}\pi)$ described about the optic axis, the phase retardation Δ'' between the interfering pencils (transmitted by the analyser) falls short of the value $(2n + 1)\pi$ by an angle which *increases continually* with the aximuth θ, and which in fact becomes equal to θ at $\theta = m\pi/2$. In order therefore to plot the curve $\Delta'' = (2n + 1)\pi$ (condition for destructive interference), we have to increase the radii vectors of the circular curve $\delta = (2n + \frac{1}{2})\pi$ by amounts which increase continuously with the polar angle θ, the radius vector of this curve at the plolar angles $\theta = m\pi/2$ taking the values corresponding to $\delta = (2n + \frac{1}{2})\pi + \frac{1}{2}m\pi$. The curves of minimum intensity thus obtained form a continuous spiral which is described in an anticlockwise or left-handed sense (Fig. 8, Plate II). It may be easily shown that the curve of minimum intensity is wrapped round the curve of maximum intensity, the one being obtained from the other by a rotation of 180° about an axis normal to the plane of the figure.

Fig. 10, Plate II, illustrates that a left-handed spiral is still obtained even when a *right*-circular analyser is used, the plane of maximum polarisation of the incident light being the same as in Fig. 8 (though the incident light is now completely polarised). This is not really surprising, because when a right-circular analyser is used, the only difference is that the value of $(-\frac{1}{2}E_2)$—the phase retardation introduced by the process of analysation—differs by π from the corresponding value when a left-circular analyser is used; so that what was a curve of maximum intensity with a left-circular analyser becomes now a curve of minimum intensity.

If, however, the incident light has its plane of maximum polarisation turned through 90°, so that it is inclined at + 45° to the axial plane, it may be shown, by going through the theoretical explanation of the spiral figure, that the sense of description of the spirals will be reversed (being obtained by reflection about a plane perpendicular to the axial plane). Figs. 9 and 11 show the right-handed spirals thus obtained with the incident light respectively partially and completely polarised—the former figure being obtained with a left-circular analyser and the latter with a right-circular analyser.

Along the spiral we have $d\Delta'' = 0$, so that the spiral will be given by

$$\frac{dr}{d\theta} = -\frac{\partial\Delta''}{\partial\theta}\bigg/\frac{\partial\Delta''}{\partial r}$$

Writing $\delta = \beta r$ and $(p/\mathrm{K}) = \alpha$, it may be shown by using (23), (24) and (26) that

$$\frac{dr}{d\theta} = \frac{\alpha r}{\sin^2 \theta + \alpha^2 \beta^2 r^2 \cos^2 \theta + \alpha \sin \theta \cos \theta}$$

so that at $\theta = 0$,

$$\left(\frac{dr}{d\theta}\right)_1 = \frac{\mathrm{K}}{p\beta^2 r}$$

and at $\theta = \frac{1}{2}\pi$,

$$\left(\frac{dr}{d\theta}\right)_2 \doteq \frac{pr}{\mathrm{K}}.$$

Thus as the arm of the spiral turns from a horizontal to a vertical position the increase in its length from $r = (2n + \frac{1}{2})\,\pi/\beta$ to $r = (2n + 1)\,\pi/\beta$ does not take place uniformly. Along the horizontal diameter of the figure the increase in the arm of the spiral per unit increase of the polar angle is inversely proportional to the radius of the spiral and *to the degree of polarisation,* while along the vertical diameter it is directly proportional to the same factors. We have thus explained the fact that as the degree of polarisation is raised, the successive arcs of the spiral approximate more and more towards circular arcs along the horizontal diameter while they become more and more kinked along the vertical zone.

The author owes a debt of gratitude to Prof. Sir C. V. Raman, F.R.S., N.L., but for whose encouragement the present work could not have been undertaken.

§ 9. Summary

Phenomena—involving the interference of polarised light—displayed by crystalline plates (in parallel or convergent light) may be given a general method of analysis, using the physical concepts developed in Parts I and II. The subject is discussed under two main heads: the interference phenomena exhibited *without* and *with* the aid of an elliptic analyser behind the crystal plate—the former involving the interference of beams in different non-orthogonal states of elliptic polarisation. The cases when the incident light is either unpolarised, partially polarised, or completely polarised are all discussed—the concept of partially coherent beams finding fruitful applications in the first two cases.

Illustrative photographs of the interference figures in convergent light shown by the optically inactive mineral iolite accompany the paper. Parti-

cular mention may be made of the interference figure with the incident light partially circularly polarised—showing the fading away of the ring system (due to incoherence) at a particular region in the figure; also of the *spiral* interference figures which are observed between a plane polariser and a circular analyser—even though the crystal is optically inactive.

REFERENCES

Boguslowski, S.	.. *Ann. der Physik.*, 1914, **44**, 1084.
Pancharatnam. S.	.. *Proc. Ind. Acad. Sci.*, 1955 *a, b*, **42 A**, 86, 235.
————	.. *Ibid.*, 1956 *a, b*, **54 A**, 247, 398.
Pockels	.. *Lehrbuch der Kristalloptik*, Teubner, 1906.
Voigt	.. *Ann. Phys.*, 1902 *a*, **9**, 367.
————	.. *Phil. Mag.*, 1902 *b*, **4**, 90.

DESCRIPTION OF PLATES

All the photographs show the optic axial interference figures exhibited in convergent light by the absorbing biaxial mineral, iolite, the axial plane being horizontal. Figures 5, 6 and 7 were taken with a much denser specimen than that used for the other photographs.

FIG. 1. Left-circular polariser and right-circular analyser: lower singular axis extinguished.

FIG. 2. Right-circular polariser and left-circular analyser: upper singular axis extinguished.

FIG. 3. Left-circular polariser *alone*: dark rings in lower half of the figure correspond to bright rings in upper half, and the lower singular axis appears darker than the other.

FIG. 4. Left-circular analyser *alone*: asymmetry with respect to the axial plane is reversed, compared to Fig. 3.

FIG. 5. Brewster's brushes with neither polariser nor analyser: minima at tip of brushes are at the same distance as first dark ring in Fig. 6.

FIG. 6. Crossed polaroids: vibration directions along and perpendicular to axial plane.

FIG. 7. Incident light partially left-circularly polarised, and linear analyser with vibration-direction vertical: in the upper half of the figure, the ring system fades away near second and third rings, and reappears further out with a shift of half a fringe width.

FIGS. 8–9. Left-circular analyser, incident light *partially* plane polarised with vibration at $-45°$ and $+45°$ respectively, with respect to axial plane: note the difference in the handedness of the spiral in the two cases

FIGS. 10–11. Right-circular analyser, incident light *completely* plane polarised, with vibration at $-45°$ and $+45°$ respectively, with respect to axial plane: kinks along the vertical diameter are conspicuous compared to Figs. 8 and 9.

CONNEMARA PUBLIC LIBRARY
4 JAN 1965
MADRAS

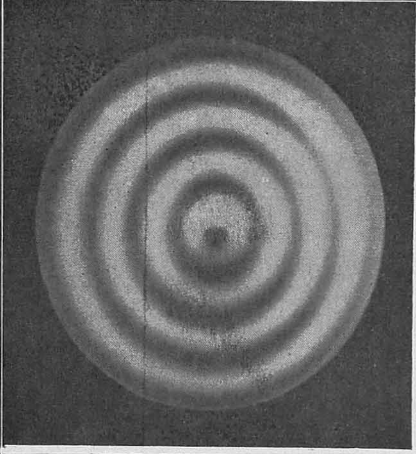

FIG. 1

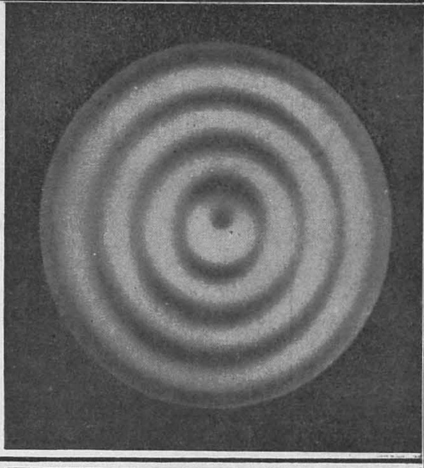

FIG. 2

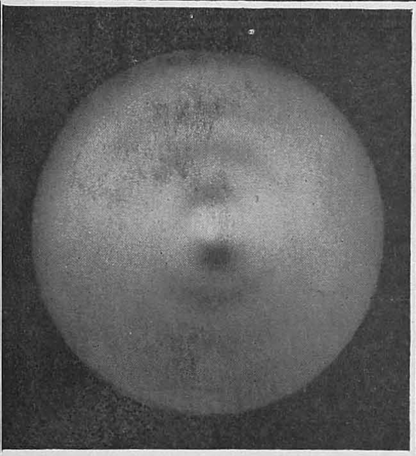

FIG. 3

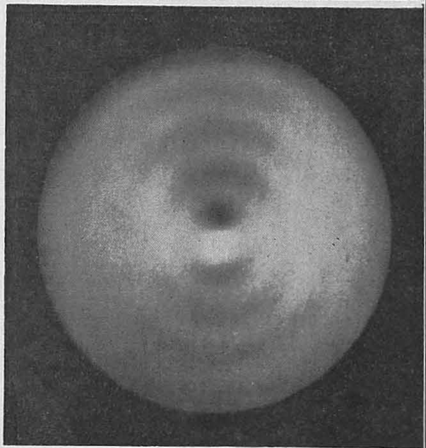

FIG. 4

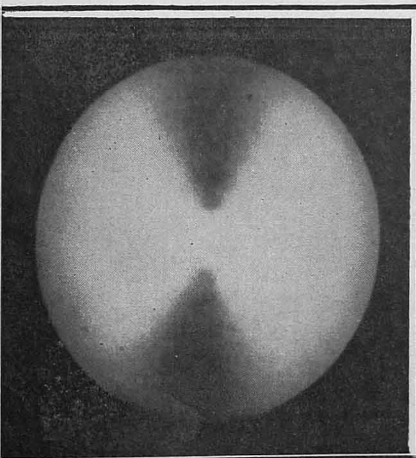

FIG. 5

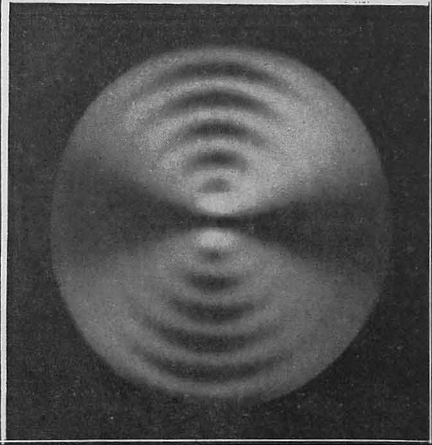

FIG. 6

FIG. 7

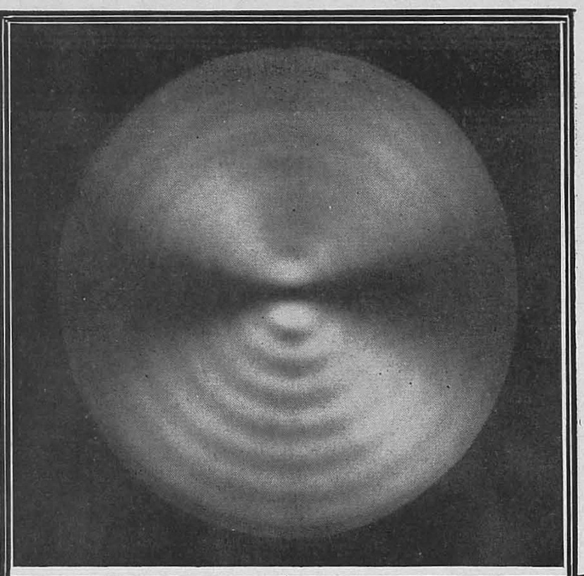

FIG. 8

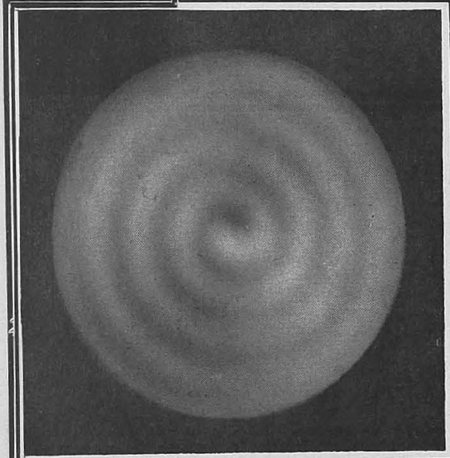

FIG. 9

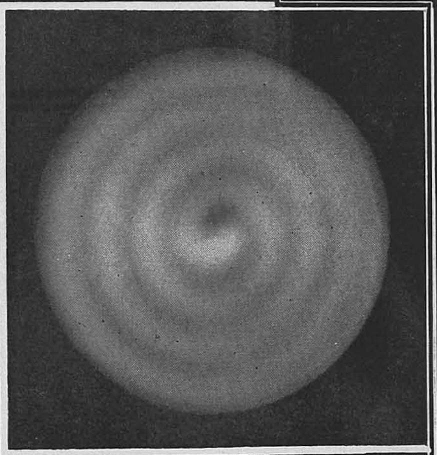

FIG. 10

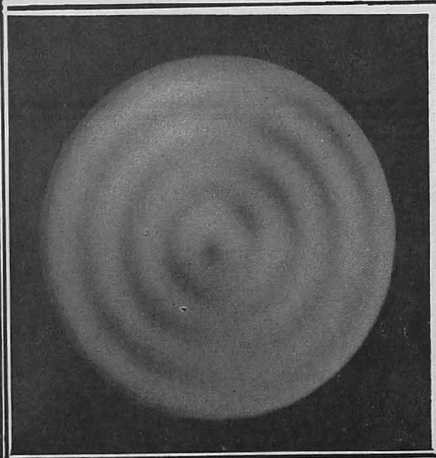

FIG. 11

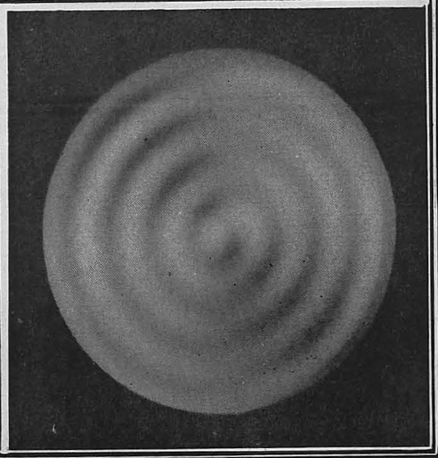

Reprinted from "The Proceedings of the Indian Academy of Sciences",
Vol. XLVI, No. 3, Sec. A, 1957

THE THEORY OF THE ANHARMONIC OSCILLATOR

BY K. S. VISWANATHAN, F.A.SC.
(*Memoir No. 99 of the Raman Research Institute, Bangalore-6*)

Received May 22, 1957

1. INTRODUCTION

ANHARMONICITY of vibration plays an important role in several branches of physics. Its importance was first recognised in acoustics[1]; the presence of overtones of the fundamental mode of a tuning fork and the alteration of its pitch with intensity changes were successfully accounted for as the effects of the anharmonicity of the oscillator. More recently, the subject has acquired a fresh interest in relation to the subject of molecular spectroscopy.[2] The thermal expansion[3] of crystals also owes its origin to the anharmonic nature of the vibrations inside a crystal lattice.

It is the object of the present note to give an exact treatment of the classical problem of the anharmonic oscillator and also to draw attention to certain of its features which by an appeal to the Correspondence Principle lead to the results of wave mechanics. In Section 2, exact expressions have been given for the shift in the mean position of the oscillator from the origin, its frequency and the amplitudes of the different harmonics. In section 4, the eigenvalues of the oscillator are determined by using the W.K.B. method. It is shown that these are the solutions of a transcendental equation involving elliptic functions and that the first correction to any energy level of the system from its harmonic oscillator value is identical with the one obtained from the perturbation theory.

2. THE CLASSICAL PROBLEM

Let m denote the mass of the oscillator and x be its displacement. The potential energy of the system may be expressed as

$$V = \tfrac{1}{2}k_1x^2 + \frac{1}{3!}k_2x^3. \tag{1}$$

We stop with the cubic term of the expansion since this is sufficient to explain most of the observed features of the spectra of diatomic molecules. Further, we take the constant k_2 to be negative in accordance with the conventions of molecular spectroscopy.

The equation of conservation of energy for the oscillator is

$$\tfrac{1}{2} m\dot{x}^2 + \tfrac{1}{2} k_1 x^2 + \tfrac{1}{6} k_2 x^3 = \bar{h} \tag{2}$$

where $\bar{h}$ is the energy of the system.

Or,

$$\frac{dx}{dt} = (A - \omega^2 x^2 + 4\alpha x^3)^{\frac{1}{2}} \tag{3}$$

where

$$A = \frac{2\bar{h}}{m}; \qquad \omega^2 = \frac{k_1}{m} \quad \text{and} \quad 4\alpha = -\frac{k_2}{3m}.$$

Before proceeding further, we consider the roots of the expression

$$f(x) = (4\alpha x^3 - \omega^2 x^2 + A) \tag{4}$$

which define the regions wherein the right-hand side of (3) is real. The discriminant of the cubic, namely $(G^2 + 4H^3)$, is equal to

$$64A\alpha^2\left(4A\alpha^2 - \frac{\omega^6}{27}\right)$$

and this will be negative as long as

$$\frac{A\alpha^2}{\omega^6} \angle \frac{1}{108}. \tag{5}$$

When this condition is satisfied all the three roots of $f(x) = 0$ are real, and two of them will be positive and the remaining one negative. Denoting these roots by x_1, x_2 and x_3 where $x_1 > x_2 > x_3$, we have

$$f(x) = 4\alpha(x - x_1)(x - x_2)(x - x_3). \tag{6}$$

Now $\{f(x)\}^{\frac{1}{2}}$ is real in two cases, *viz.*, (i) when $x > x_1$, or (ii) when x lies in the region $x_2 \geqslant x \geqslant x_3$.

For $x > x_1$,* the force acting on the molecule becomes repulsive and it increases with increasing distance of the oscillator from the origin. The vibrations in this case are unstable and the oscillator flies off to infinity within

---

* The solution in this case is given by $x = x_2 + (x_1 - x_2)\, nc^2\,(u, k)$. Since $cn\,(u, k)$ has zeros at points $u = (2n + 1)\,K$, where n is an integer, the displacement is infinite at these points. Thus within a period $t = \pi/\bar{\omega}$ after crossing the point x_1, the molecule dissociates.

a short period after crossing the point x_1. In other words, when the inter-nuclear distance of a diatomic molecule exceeds its equilibrium value by an amount x_1, the molecule will dissociate.

The vibrations in the region $x_2 \geqslant x \geqslant x_3$ are stable and retain in a measure the characteristics of a harmonic oscillator. Writing

$$\tau = \frac{A^{\frac{1}{2}}\alpha}{\omega^3},$$

the roots of $f(x) = 0$ are approximately

$$x_1 = \frac{\omega^2}{4\alpha}(1 - 16\tau^2 - 512\tau^4)$$

$$x_2 = \frac{\sqrt{A}}{\omega}(1 + 2\tau + 10\tau^2 + 64\tau^3 + 224\tau^4)$$

$$x_3 = -\frac{\sqrt{A}}{\omega}(1 - 2\tau + 10\tau^2 - 64\tau^3 + 224\tau^4). \quad (7)$$

The above relations were derived by using the bionomial expansion in the expressions for the roots of the cubic, assuming that τ is small. One can however easily verify by substitution that they satisfy the equation $f(x) = 0$ upto terms of the order of ω^{-9}. Equation (3) can now be written as

$$t = \frac{1}{2\sqrt{\alpha}} \int_{x_3}^{x} \frac{dx}{\{(x - x_1)(x - x_2)(x - x_3)\}^{\frac{1}{2}}}. \quad (8)$$

The right-hand side of the above equation is an elliptic integral and its value[4] is

$$\frac{1}{2\sqrt{\alpha}} \times \frac{2}{\sqrt{x_1 - x_3}}\, sn^{-1}\left(\sqrt{\frac{x - x_3}{x_2 - x_3}}, \sqrt{\frac{x_2 - x_3}{x_1 - x_3}}\right).$$

Hence writing $u = \sqrt{\alpha(x_1 - x_3)}\, t$ and

$$k^2 = \frac{(x_2 - x_3)}{(x_1 - x_3)},$$

we get the wellknown solution

$$x = x_3 + (x_2 - x_3)\, sn^2(u, k). \quad (9)$$

Given the energy of the oscillator, the above equation determines its complete course in time.

In view of their periodicity properties, the Jacobian elliptic functions admit of expansions as Fourier series. For the function $sn^2(u, k)$, we have the following expansion[5] (see Whittaker and Watson, p. 520, example 5):

$$sn^2(u,k) = \left(\frac{\pi}{kK}\right)^2 \left\{\frac{K(K-E)}{\pi^2} - 2\sum_{n=1}^{\infty} \frac{nq^n}{(1-q^{2n})} \cos 2ny\right\} \tag{10}$$

where

$$y = \frac{\pi}{2K} u; \tag{11}$$

K and E are the complete elliptic integrals of the first and second type which in terms of hyper-geometric functions are defined by

$$K = \frac{\pi}{2} F\left(\tfrac{1}{2}, \tfrac{1}{2}, 1;\ k^2\right)$$

$$E = \frac{\pi}{2} F\left(-\tfrac{1}{2}, \tfrac{1}{2}, 1;\ k^2\right) \tag{12}$$

and q is a parameter which is related to the modulus k of the elliptic function by means of the formula

$$q = \epsilon + 2\epsilon^5 + 15\epsilon^9 + 150\epsilon^{13} + 0(\epsilon^{17}) \tag{13}$$

where again

$$2\epsilon = \frac{1 - \sqrt{k^1}}{1 + \sqrt{k^1}}$$

and

$$k^1 = (1 - k^2)^{\frac{1}{2}}.$$

Substituting (10) in (9) we get

$$x = x_3 + \frac{(x_2 - x_3)}{(Kk)^2}\left[K(K-E) - 2\pi^2 \sum_{n=1}^{\infty} \frac{nq^n}{(1-q^{2n})} \cos 2ny\right]. \tag{14}$$

Equation (14) shows that the displacement of the oscillator is no longer a simple sinusoidal function, but contains a constant term and harmonics of the fundamental mode. The coefficient of t in $2y$ namely $(\pi/K)\sqrt{a(x_1 - x_3)}$

gives the circular frequency of the system. Denoting this by ϖ, we have therefore

$$\varpi = \frac{\pi}{K}\sqrt{a\,(x_1 - x_3)} \tag{15}$$

The shift $\langle x \rangle$ in the mean position of the oscillator is given by the constant term of the expansion (14) and is equal to

$$x_3 + \frac{(x_2 - x_3)\,(K - E)}{Kk^2} \tag{16}$$

The amplitude of the nth harmonic is proportional to

$$\frac{nq^n}{(1 - q^{2n})}. \tag{17}$$

In particular the intensities of the first three harmonics are in the ratio

$$\frac{q^2}{(1 - q^2)^2} : \frac{4q^4}{(1 - q^4)^2} : \frac{9q^6}{(1 - q^6)^2}. \tag{17a}$$

Equations (15) and (16) express the frequency of the oscillator and its mean shift as functions involving elliptic integrals. We shall now obtain approximations for these which are useful for appreciating their physical magnitudes as well as for comparison with earlier work.

The following expansions now hold good for k^2, K, (K − E) and $\sqrt{a\,(x_1 - x_3)}$ when $\tau \ll 1$:

$$\begin{aligned} k^2 &= 8\tau\,(1 - 4\tau + 50\tau^2 - 336\tau^3 + 3694\tau^4) \\ K &= \frac{\pi}{2}\,(1 + 2\tau + \tau^2 + 78\tau^3) \\ \sqrt{a\,(x_1 - x_3)} &= \frac{\omega}{2}\,(1 + 2\tau - 14\tau^2 + 48\tau^3) \\ (K - E) &= 2\pi\tau\,(1 - \tau + 41\tau^2 - 80{\cdot}5\tau^3). \end{aligned} \tag{18}$$

Substituting (7) and (18) in (15) and (16), one finds after some simplification that the change in frequency of the oscillator and its mean displacement from the origin are approximately given by

$$(\varpi - \omega) = \frac{-15Aa^2}{\omega^5} \tag{19}$$

$$\langle x \rangle = \frac{3Aa}{\omega^4} + \frac{225}{2}\,\frac{A^2a^3}{\omega^{10}} \tag{20}$$

respectively. The reader can easily see these to be the same as the expressions given in books on acoustics.

3. SOME REMARKS

We shall now consider how the frequency and mean shift of the oscillator get modified when the energy of the system is altered. Remembering that the quantity A occurring in equations (19, 20) is a constant multiple $(2/m)$ of the energy $\bar{h}$ of the system, we get on differentiation of (19) with respect to $\bar{h}$ that

$$\frac{d\tilde{v}}{d\bar{h}} = \frac{-15a^2}{\pi m\omega^5} \tag{21}$$

where

$$\tilde{v} = \frac{\tilde{\omega}}{2\pi}.$$

Thus to an approximation which ignores terms of the order of τ^4, we see that the frequency of the oscillator is a decreasing function of the energy, the rate of decrease being a constant characteristic of the oscillator.

From (21) it follows that the change in the frequency of the system as its energy is increased from ϵ_1 to ϵ_2 is

$$\frac{-15a^2}{\pi m\omega^5}(\epsilon_2 - \epsilon_1).$$

Writing $\epsilon_2 = (v + 3/2)\, h\nu$ and $\epsilon_1 = (v + \frac{1}{2})\, h\nu$, we see that this is equal to

$$\frac{-15a^2}{\pi m\omega^5}\, h\nu$$

or

$$\frac{-5}{48}\,\frac{k_2{}^2 h\nu}{\pi\,(mk_1{}^5)^{\frac{1}{2}}}$$

which is the value given by the perturbation theory.[6] Hence in this case even a semi-classical theory is able to give the correct results yielded by wave-mechanics.

Differentiating now (20) with respect to $\bar{h}$, one finds that

$$\frac{d\langle x\rangle}{d\bar{h}} = \frac{6a}{m\omega^4} + \frac{900a^3}{(m\omega^5)^2}\,\bar{h} \tag{22}$$

which shows that the mean shift of the oscillator increases with rise in the energy of the system.

As before, the magnitude of the shift in the vth state may be obtained by writing $\epsilon_v = (v + \frac{1}{2})\, h\nu$ in (20). We have

$$\langle x \rangle_v = \frac{3ah}{\pi m \omega^3}(v + \tfrac{1}{2}) + \frac{225}{2}\frac{h^2 a^3}{\pi^2 m^2 \omega^8}(v + \tfrac{1}{2})^2. \tag{23}$$

From the above, it is possible to obtain the stretch (or contraction) in the bond-length of a diatomic molecule during a transition between two different quantum states specified by the numbers v and v' respectively. This is given by

$$\frac{3ah}{\pi m \omega^3}(v' - v) + \frac{225}{2}\frac{h^2 a^3}{\pi^2 m^2 \omega^8}(v' - v)(v' + v + 1) \tag{24}$$

4. The Energy Levels

The Schrodinger equation for the oscillator is given by

$$\frac{d^2 u}{dx^2} + \frac{8\pi^2 m}{h^2}(\epsilon - \mathrm{V})\, u = 0 \tag{25}$$

where V has the form given in (1). A method for determining the eigenvalues of an equation of the above type was developed by Wentzel, Kramers and Brillouin, and this was later refined by Langer.[7] According to the latter, if x_3 and x_2 are two consecutive simple zeroes of $\epsilon - \mathrm{V}(x)$ such that $\epsilon > \mathrm{V}$ for $x > x_3$, and $\epsilon < \mathrm{V}$ for $x > x_2$, the eigenvalues of (25) are determined by

$$(n + \tfrac{1}{2})\,\pi = \int_{x_3}^{x_2} \left\{\frac{8\pi^2 m}{h^2}(\epsilon - \mathrm{V})\right\}^{\frac{1}{2}} dx. \tag{26}$$

Writing $\mathrm{A} = 2\epsilon/m$, the above equation becomes

$$(n + \tfrac{1}{2})\,\pi = \frac{2\pi m}{h}\,\mathrm{I} \tag{27}$$

where

$$\mathrm{I} = \int_{x_3}^{x_2} (4ax^3 - \omega^2 x^2 + \mathrm{A})^{\frac{1}{2}}\, dx.$$

The integral I has been evaluated in Appendix I and substituting the value given for it there in (27), one gets

$$(n + \tfrac{1}{2})\, h = \frac{8m}{15}\sqrt{a\eta_2}\,\{-(\mathrm{K} - \mathrm{E})\,[\Sigma(x_2 - x_3)^2] + \eta_1(\eta_1 + \eta_2)\,\mathrm{K}\} \tag{28}$$

where $\eta_1 = (x_2 - x_3)$ and $\eta_2 = (x_1 - x_3)$,

The quantities occurring on the right-hand side of the above equation are all functions of ϵ and hence by solving this transcendental equation for different integral values of n, the eigenvalues $\epsilon_1, \epsilon_2, \ldots\ldots \epsilon_n$ of the oscillator may be determined.

In practice, equation (28) can be solved by expressing the right-hand side as a power series in the parameter τ which will result in a series expansion in ϵ and then inverting the series. For example, by making use of the expansions (7) and (18) and further of the following relations

$$\Sigma (x_2 - x_3)^2 = \frac{\omega^4}{8a^2}; \tag{29}$$

$$\eta_1 (\eta_1 + \eta_2) = \frac{\sqrt{A}\omega}{2a} (1 + 12\tau - 14\tau^2 + 240\tau^3)$$

it can be seen that (28) is equivalent to

$$(n + \tfrac{1}{2}) h = 2m \cdot \frac{\pi A}{2\omega} \left(1 + \frac{15}{2} \tau^2 + 0 (\tau^4)\right). \tag{30}$$

Or, writing $a = - k_2/12m$, $\omega = 2\pi\nu$ and $A = 2\epsilon/m$ we have

$$(n + \tfrac{1}{2}) h\nu = \epsilon + \frac{5}{96\pi\nu} \frac{k_2^2}{(mk_1^5)^{\frac{1}{2}}} \epsilon^2.$$

Hence

$$\epsilon = (n + \tfrac{1}{2}) h\nu - \frac{5}{96} \frac{k_2^2 h^2 \nu}{\pi (mk_1^5)^{\frac{1}{2}}} (n + \tfrac{1}{2})^2 \tag{31}$$

which is the eigenvalue of the oscillator as obtained from the perturbation theory correct to the second order. By expanding (25) still further than in (27), one can obtain higher order corrections.

The author's grateful thanks are due to Professor Sir C. V. Raman for his kind interest in this work.

SUMMARY

Exact expressions have been obtained for the frequency of an anharmonic oscillator, the shift in its equilibrium position from the origin and for the amplitudes of its different harmonics. It is shown that the frequency of the oscillator is a decreasing function of the energy and that some of the results of wave-mechanics can be obtained from the classical theory by substituting in the classical energy of the oscillator the different energy values of a harmonic oscillator. The eigenvalues of the oscillator are determined by using the W.K.B. method. The classical theory of a Morse oscillator has similarly been worked out in Appendix II.

References

1. Lord Rayleigh .. *Theory of Sound*, 1948, pp. 76–78.
2. Herzberg, G. .. *Spectra of Diatomic Molecules*, Second Edition, pp. 90–102.
3. Fermi, E. .. *Moleküle und Kristalle*, p. 140.
4. Magnus, W. and Oberhettinger *Formulas and Theorems for the Special Functions of Mathematical Physics*, 1949, 108.
5. Whittaker and Watson .. *Modern Analysis*, Fourth Edition (Chapters XXI and XXII).
6. Ta-You-Wu .. *Vibrational Spectra and Structure of Polyatomic Molecules*, 1939, 48.
7. Langer, R. E. .. *Phys. Rev.*, 1937, **51**, 669.
8. Morse, P. M. .. *Ibid.*, 1929, **34**, 57.

APPENDIX 1

Evaluation of the integral $I = \int_{x_3}^{x_2} \sqrt{4ax^3 - \omega^2x^2 + A}\, dx$

Obviously we have

$$I = \int_{x_3}^{x_2} \frac{(4ax^3 - \omega^2x^2 + A)}{2\sqrt{a}\{(x - x_1)(x - x_2)(x - x_3)\}^{\frac{1}{2}}}\, dx. \tag{1}$$

If we substitute $(x - x_3) = y^2$ in the above equation and denote by Q_m the integral

$$\int_0^{\sqrt{\eta_1}} \frac{x^m dx}{\sqrt{(x^2 - \eta_1)(x^2 - \eta_2)}}$$

where $\eta_1 = (x_2 - x_3)$ and $\eta_2 = (x_1 - x_3)$, equation (1) takes the form

$$I = (pQ_6 + qQ_4 + rQ_2 + sQ_0) \tag{2}$$

where

$$p = 4\sqrt{a}\,;$$

$$q = \sqrt{a}\left(12x_3 - \frac{\omega^2}{a}\right);$$

$$r = \sqrt{a}\left(12x_3^2 - \frac{2\omega^2x_3}{a}\right); \quad \text{and}$$

$$s = \frac{1}{\sqrt{a}}(4ax_3^3 - \omega^2x_3^2 + A).$$

Since x_3 is a root of $f(x) = 0$, the constant s in the above is equal to zero.

The integrals Q_m can be evaluated by reduction formulæ. For example,

$$\frac{d}{dx}\{x^3\sqrt{Q}\} = \frac{3x^2Q}{\sqrt{Q}} + \frac{x^3Q'}{2\sqrt{Q}}$$

where

$$Q = \sqrt{(x^2 - \eta_1)(x^2 - \eta_2)}.$$

If we integrate this equation between 0 and $\eta_1^{\frac{1}{2}}$, the left-hand side vanishes and we get

$$Q_6 = \frac{1}{5}(4aQ_4 - 3bQ_2) \tag{3}$$

where

$$a = (\eta_1 + \eta_2) \qquad \text{and} \qquad b = \eta_1\eta_2.$$

Similarly

$$Q_4 = \tfrac{1}{3}(2aQ_2 - bQ_0). \tag{4}$$

Substituting (3) and (4) in (2) we get after some reduction that

$$I = -\frac{4}{15}\sqrt{a}\,\{2Q_2(x_1^2 + x_2^2 + x_3^2) - abQ_0\}. \tag{5}$$

Now

$$Q_0 = \int\limits_0^{\sqrt{\eta_1}} \frac{dx}{\sqrt{Q}} = \frac{K}{\sqrt{\eta_2}}. \tag{6}$$

Next by the substitution $x = z\sqrt{\eta_1}$, we find that

$$Q_2 = \frac{\eta_1}{\sqrt{\eta_2}} \int\limits_0^1 \frac{z^2 dz}{\{(1 - z^2)(1 - k^2z^2)\}^{\frac{1}{2}}}$$

where

$$k^2 = \frac{\eta_1}{\eta_2}$$

$$\text{Or } Q_2 = \frac{\eta_1}{\sqrt{\eta_2}} \int\limits_0^K sn^2(u, k)\,du = \sqrt{\eta_2}\,(K - E). \tag{7}$$

Substituting (6) and (7) in (5), one gets

$$I = \frac{4}{15}\sqrt{a\eta_2}\,\{-\Sigma(x_2 - x_3)^2(K - E) + \eta_1(\eta_1 + \eta_2)\,K\} \tag{8}$$

APPENDIX II

The potential (1, Section 2) is valid, when the vibrations are small but nevertheless depart from harmonicity. Apart from its applications in acoustics, it is useful in studying anharmonicity in complex molecules when one splits their vibrations into those of an assembly of anharmonic oscillators. For diatomic molecules however Morse[8] suggested a potential given by

$$V = D\,(1 - e^{-\beta x})^2 \tag{1}$$

where D is the dissociation energy of the molecule and β is a constant, which holds good approximately upto the dissociation range. The quantum mechanical energy values of an oscillator moving in a potential field of the type (1) was given by Morse. We give below the classical theory of such an oscillator which merits attention in view of its extreme simplicity and for purposes of comparison with the quantum theory.

The equation of energy for the Morse oscillator is

$$\tfrac{1}{2}\, m\dot{x}^2 + D\,(1 - e^{-\beta x})^2 = \bar{h} \tag{2}$$

where as before $\bar{h}$ denotes the energy of the system. Hence

$$\dot{x}^2 = c + by + ay^2 \tag{3}$$

where

$$c = \frac{2}{m}(\bar{h} - D)\,; \quad b = \frac{4D}{m}\,; \quad a = \frac{-2D}{m}$$

and $\qquad y = e^{-\beta x}.$ (4)

c can immediately be seen to be negative.

The turning points for the oscillator in its course are $-1/\beta \log\,(1 + \sqrt{\bar{h}/D})$ and $-1/\beta \log.\,(1 - \sqrt{\bar{h}/D})$. We shall measure time from the instant the oscillator is at its extremity in the left.

From (3) and (4) we get

$$t = -\frac{1}{\beta}\int \frac{dy}{y\sqrt{ay^2 + by + c}} \tag{5}$$

or

$$\beta t = \frac{1}{\sqrt{-c}}\,\cos^{-1}\frac{by + 2c}{y\sqrt{b^2 - 4ac}}, \tag{6}$$

Hence we have

$$x = \frac{1}{\beta}\log\frac{D}{(D-\bar{h})} + \frac{1}{\beta}\log\left\{1 - \sqrt{\frac{\bar{h}}{D}}\cos\beta t\sqrt{\frac{2}{m}(D-\bar{h})}\right\} \tag{7}$$

The above equation determines the course of the oscillator with time.

From (7) it is immediately obvious that the frequency of the gravest mode is given by

$$\tilde{\nu} = \frac{\beta}{2\pi}\sqrt{\frac{2}{m}(D-\bar{h})} \tag{8 a}$$

$$= \nu\left(1 - \frac{\bar{h}}{D}\right)^{\frac{1}{2}} \tag{8 b}$$

where

$$\nu = \frac{\beta}{2\pi}\sqrt{\frac{2D}{m}};$$

ν will be the (harmonic oscillator) frequency of the system when the anharmonic terms in the expansion of (1) as a power series in x are neglected.

The eigenvalues of a Morse oscillator are

$$E_n = (n+\tfrac{1}{2})h\nu - z(n+\tfrac{1}{2})^2 h\nu \tag{9}$$

where

$$z = \frac{\beta^2 h}{8\pi^2 m\nu} = \frac{h\nu}{4D}. \tag{10}$$

The frequency of emission of the oscillator during a transition from the nth state to the one immediately below it is given by

$$\nu_{n,n-1} = \nu_n{}^{em} = \nu(1-2nz)$$

$$= \nu\left\{z + \sqrt{\frac{1-4zE_n}{h\nu}}\right\}$$

$$= \nu\left\{z + \sqrt{1-\frac{E_n}{D}}\right\} \tag{11 a}$$

from (10).

Similarly the frequency of absorption from the nth state is given by

$$\nu_n{}^{ab} = \nu_{n+1,n} = \nu\left\{-z + \sqrt{1-\frac{E_n}{D}}\right\}. \tag{11 b}$$

Equation (8 *b*) shows that the frequency of the classical oscillator is a decreasing function of its energy. The dependence of the frequencies of

emission or absorption on the transitional energy levels is likewise described by (11 *a*) and (11 *b*). Apart from the first term which is a consequence of the quantum phenonmenon that has no classical analogue, namely, that the molecule possesses a zero-point energy and on the non-linear dependence of the energy levels on the quantum numbers, the formulæ (11) possess a striking resemblance to the classical formula (8 *b*). In fact $(\nu_n{}^{ab} + \nu_n{}^{em})/2$ depends on the energy of the *n*th level in the same way as the classical frequency does with the energy of the system. When the energy equals its dissociation value the discrete spectrum stops for the oscillator.[8] Classically its frequency then vanishes.

In order to find out the shift in the mean position of the oscillator and the amplitudes of the different harmonics, we express x as a Fourier cosine series in the form

$$x = a_0 + \sum_{n=1}^{\infty} a_n \cos nu \tag{12}$$

where $u = 2\pi \bar{\nu} t$. Then

$$\begin{aligned} a_0 &= \frac{1}{\beta} \log \frac{\mathrm{D}}{(\mathrm{D} - \bar{h})} + \frac{1}{2\pi\beta} \int_{-\pi}^{+\pi} \log \left(1 - \sqrt{\frac{\bar{h}}{\mathrm{D}}} \cos u\right) du \\ &= \frac{1}{\beta} \log \frac{\mathrm{D}}{(\mathrm{D} - \bar{h})} + \frac{1}{\beta} \log \tfrac{1}{2} \left\{1 + \sqrt{1 - \frac{\bar{h}}{\mathrm{D}}}\right\} \\ &= \frac{1}{\beta} \log \tfrac{1}{2} \left\{\frac{1 + \sqrt{1 - \frac{\bar{h}}{\mathrm{D}}}}{1 - \frac{\bar{h}}{\mathrm{D}}}\right\}. \end{aligned} \tag{13}$$

From the above it follows that the shift in the mean position of the oscillator increases with the energy of the system and tends logarithmically to infinity when the energy approaches its dissociation value.

Next we have

$$a_n = \frac{1}{\pi\beta} \int_{-\pi}^{\pi} \log \left(1 - \sqrt{\frac{\bar{h}}{\mathrm{D}}} \cos u\right) \cos nu \, du. \tag{14}$$

The integral may be evaluated by expanding the logarithmic function as a power series, and integrating term by term the resulting series which can be seen to be uniformly convergent for all values of u in $(-\pi, \pi)$. Thus one gets

$$a_n = -\frac{1}{\beta}\sum_{s=n/2}^{\infty}\left(\frac{\bar{h}}{D}\right)^{s}\frac{1}{2s2^{2s-1}}\binom{2s}{\frac{2s-n}{2}} \tag{15 a}$$

for even values of n and

$$a_n = -\frac{1}{\beta}\sum_{s=n-1/2}^{\infty}\left(\frac{\bar{h}}{D}\right)^{2s+1/2}\frac{1}{(2s+1)\,2^{2s}}\binom{2s+1}{\frac{2s+1-n}{2}} \tag{15 b}$$

for odd values of n.

The above formulæ give the law of dependence of the amplitudes of the various harmonics on the energy of the oscillator. One notices that the amplitude of the nth harmonic is of the order of $(\bar{h}/D)^{n/2}$.

Reprinted from "The Proceedings of the Indian Academy of Sciences", Vol. XLVI, No. 3. Sec. A, 1957

THE RAMAN SPECTRUM OF CALCITE AND ITS INTERPRETATION

BY D. KRISHNAMURTI

(*Memoir No.* 100 *from the Raman Research Institute, Bangalore-*6)

Received July 26, 1957

(Communicated by Sir C. V. Raman)

1. INTRODUCTION

THE present memoir embodies the results of experimental studies undertaken in the newly built spectroscopic laboratory of the Raman Research Institute. It is also the first report on the results of a programme of research on the Raman spectra of crystals undertaken with a view to obtain a fuller experimental knowledge as well as a deeper theoretical understanding of the phenomena which present themselves in this field. The present memoir concerns itself with the case of calcite. This was, quite naturally, one of the crystals to be investigated by the earliest workers in the field. An extensive literature has therefore accumulated which deals with the Raman spectrum of calcite and its theoretical interpretation. Nevertheless, the present investigation has brought to light several new facts with important theoretical implications.

It appears appropriate in the present memoir to begin with a brief description of the special features of the new laboratory which was designed and built with a view to carrying out investigations in this field of research. It also appears appropriate to give some details of the experimental techniques adopted in the present investigation which have enabled the results described in it to be achieved.

2. THE NEW SPECTROSCOPIC LABORATORY

The Raman effect being inherently a phenomenon of low intensity, its study usually requires the employment of fast spectrographs and of powerful sources of monochromatic illumination. Even so, it is necessary to give long exposures in order to record the fainter details of the spectra with satisfactory intensity. A serious difficulty in such work is the blurring of the spectral lines noticed with prolonged exposures, arising mainly because of the variations in the temperature of the spectrographs and of the dispersing prisms contained in them. The new laboratory and its equipment were

designed with the special aim of eliminating this difficulty as completely as possible.

The new laboratory is a massive structure of granite which faces north and south without any doors or windows on the eastern and western walls. The building contains two large spectrographic rooms, each 30 feet square and 18 feet high, these being separated from each other by a small hall through which they can be entered, by a photometer room and by a dark room for photographic work; entry into the latter can be made through labyrinths connecting them with the spectrographic rooms on either side. Each of the latter is provided with a false roof of thermally insulating material containing apertures which permit of a low-draught ventilation upwards. The windows of the spectrographic rooms face north and south and are set in such a position that no sunlight ever falls on them. Each of the windows is double, the outer one being of glass and the inner of wood. The admission of light and air into the rooms can thus be strictly controlled. With these arrangements, the diurnal variation of temperature within the laboratory was kept at a minimum and the continued operation of mercury lamps within the laboratory did not result in any noticeable fluctuations in temperature.

It was found of advantage to use two spectrographs in the present investigation, both of them being Hilger instruments with quartz prisms and lenses; one of them was the well-known medium size spectrograph of the ordinary or direct type and the other was a large automatic spectrograph of the Littrow type. The smaller instrument was some twenty times as fast as the larger instrument and was therefore to be preferred when the object was to record the fainter details of the spectrum as completely as possible. The larger instrument had a greater resolving power and was therefore more suitable for exhibiting the finer details of the spectrum. However, it suffers from the disadvantage of the so-called "Littrow fog" which sets the limit to the length of exposures which could usefully be given with it. Each spectrograph was placed on a massive teakwood table inside a double-walled box enclosing the instrument completely, the inner walls of the box being of insulating boards and the outer walls of compressed fibre boards impervious to air; the two walls are separated by an air gap. The small aperture through which the slit of the spectrograph was illuminated was closed by a polished plate of quartz. This arrangement successfully prevented any changes in the temperature of the air of the room penetrating through the enclosures into the instrument, so much so that single exposures could be continued as long as desired over several days or even weeks without any blurring of the spectral lines.

3. The Experimental Arrangements

The monochromatic illumination used was the λ 2536·5 resonance radiation of a water-cooled magnet controlled mercury arc in silica, the current being kept well below two amperes. A heavy inductance was introduced in series with the arc to make it stable. It was found much preferable to use, instead of a completely sealed arc, one that was continuously evacuated. It was however necessary to employ an efficient high-speed pump and to run the arc for a sufficient time for the lines due to oxygen and nitrogen of the air to be eliminated before starting an exposure. The water-cooling of the arc was effected internally and only at the mercury pool electrodes, the arrangement being similar to that adopted in the Toronto type of mercury lamps. The most successful type of electrode was one with parallel strands of fine molybdenum wire sealed up by pressure in a narrow tubule of silica and finally closed up by molten lead. The current was led in by copper wires fixed in the lead.

The crystal was illuminated by placing it quite close to the arc, a current of air from a fan being directed against it continuously to prevent it from warming up. The scattered radiations were focussed on the slit of the spectrograph with a quartz lens, suitable apertures being introduced in the path of both incident and scattered radiations to minimise parasitic illumination. Dishes of mercury inside the spectrograph provided enough mercury vapour to filter out the resonance radiation from the scattered light before it reaches the photographic plate. A comparison spectrum of the light of the mercury arc was recorded in each case on the same plate with an exposure sufficient to bring out even the faintest lines.

It should be mentioned that not all crystals of calcite are equally transparent to the λ 2536·5 resonance radiation. The best of the specimens available in the museum of this Institute were used in the present investigation. One of them was a large, flawless and transparent rhomb 3″×2″×2″ purchased some years ago in New York. A smaller specimen presented by Prof. A. Neuhaus of the Mineralogical Institute of Bonn proved to be of excellent quality and was also used in the research. The advantage of using such clear crystals is that the lines of the mercury arc other than the λ 2536·5 appear only feebly and some of them not at all even in strongly exposed spectrograms. Such of the lines as do appear are readily identified by reference to the comparison spectrum of the mercury arc. The possibility of a mercury arc line being mistaken for a Raman shift or *vice versa* is thereby rendered negligible. The distribution of intensity in the Raman lines along their length is usually different from that of the mercury lines and this is a

further clue which enables them to be distinguished from each other. The analysis of the spectrograms is further facilitated by the extraordinary intensity of the λ 2536·5 radiation in comparison with that of the other lines of the mercury arc run under the conditions employed in the present investigation. Even with the very long exposures given in order to record the faintest Raman shifts, the other lines of the mercury arc do not give observable Raman shifts except in a very few cases. In particular, it has been noticed that the triplet of mercury lines λ 2652·04, λ 2653·68 and λ 2655·13 as well as the line λ 2576·29 do excite the strongest Raman lines observably. As the positions of these lines are exactly calculable, it is easy to locate and eliminate them.

4. General Description of the Results

Five frequency shifts which expressed in wave-numbers are respectively 155, 282, 712, 1086 and 1436 are the most conspicuous features in the Raman spectrum of calcite and were recognized by the earliest investigators, notably Cabannes, Nisi and Rasetti. The three larger frequency shifts arise from the internal vibrations of the CO_3 groups contained in the crystal, while the two smaller frequency shifts arise from the external vibrations of the CO_3 groups which involve translatory and rotatory oscillations of those groups.

We are concerned in the present paper with the study of the various features which make their appearance in the spectra when the exposures are sufficiently prolonged. These changes are most conveniently exhibited in reproductions by recording the spectra with the maximum exposures practicable and then printing them to different depths. The deeper prints exhibit only the most conspicuous features, while in the lighter prints the fainter details are by comparison strongly emphasized. It is found that the reproductions thus obtained represent approximately the effect of varying the original period of exposure of the spectrogram.

Figure 1 (*a*) in Plate IV is a reproduction of a deep print of a spectrogram recorded with our larger instrument by giving an exposure of 100 hours and using a slit-width of 0·05 mm. Fig. 1 (*b*) in the same Plate is a comparison spectrum of the mercury arc. The five principal Raman lines referred to above and their anti-Stokes components are immediately recognized by comparing the two photographs. Fig. 1 (*c*) in the same Plate is a light print of the same spectrogram. It shows various additional features to which we shall return later. A microphotometer record on the scale 1 : 4 of the same spectrogram is reproduced as Fig. 2 in Plate V.

Figure 3 (*a*) and Fig. 3 (*c*) are respectively deep and light prints of a spectrogram recorded with the smaller instrument giving an exposure of

60 hours and using a slit-width 0·04 mm. Taking into account the greater speed of the smaller instrument, this exposure is roughly ten times greater than that used in recording Figs. 1 (*a*) and 1 (*c*) in Plate IV. Under the conditions of the experiment, an exposure of five minutes was found to be sufficient to record all the five Raman lines. Thus, the spectrum reproduced in the Plate represents an exposure 720 times greater than that needed to record what is ordinarily regarded as the Raman spectrum of calcite. Comparing Fig. 1 (*a*) in Plate IV with Fig. 3 (*c*) in Plate VI, it seems almost incredible that they represent one and the same phenomenon. The heavy exposure and the light printing adopted for Fig. 3 (*c*) have evidently resulted in enormously emphasizing the fainter features of the spectrum, while in Fig. 1 (*a*) they are not observable at all. The transition from one extreme to the other can be traced in the sequence from Fig. 1 (*a*) to Fig. 1 (*c*) in Plate IV and then from Fig. 3 (*a*) to Fig. 3 (*c*) in Plate VI. A microphotometer record of the heavily exposed spectrum on the scale 1 : 8 is reproduced as Fig. 4 in Plate VII.

Amongst the phenomena with which we are concerned in the present paper is one of great interest which appears to have been passed over by the earlier investigators without notice, *viz.*, the transformation of the principal Raman shifts from more or less sharply defined lines as recorded with the minimum exposures into bands covering an appreciable range of wavelengths in the strongly exposed spectra. This feature is clearly noticeable in the spectrograms and microphotometer records reproduced in Plates IV, V, VI and VII. The phenomenon is *not* of instrumental origin or due to photographic halation. This is clear from the fact that it is not exhibited by the mercury arc lines of comparable intensity simultaneously recorded in the spectra. The latter do indeed show the well-known photographic spread resulting from prolonged exposures. But this is relatively small and the edges of the lines remain quite sharp. The difference in the behaviour of the lines of the mercury arc and of the principal Raman shifts can be seen very readily by comparing them in the series of four spectra reproduced in Plates IV and VI. It is also evident from a comparison of the microphotometer records reproduced as Fig. 2 in Plate V and Fig. 4 in Plate VII. While there is hardly any difference in the aspect of the mercury arc lines in these two records, there is an enormous difference in the behaviour of the Raman shifts. Fig. 4 in Plate VII exhibits several features which are scarcely, if at all, noticeable in Fig. 2 of Plate V. These, of course, are the fainter features which are recorded in the spectrum only when long exposures are given. The principal Raman shifts which appear in both records also present very different aspects in them. In the record

of the strongly exposed spectrogram they appear broadened out unsymmetrically. This effect is shown by all the five principal Raman shifts but to very different extents. It is only with difficulty observable in the case of the 712 cm.$^{-1}$ shift which might indeed be mistaken for a mercury arc line in this respect. On the other hand, the 1436 cm.$^{-1}$ shift exhibits it very conspicuously. Its unsymmetrical broadening is noticeable even in Fig. 2 of Plate V as will be apparent on comparing its profile with those of the mercury arc lines and is very conspicuous in Fig. 4 of Plate VII. The principal Raman shift of 1086 cm.$^{-1}$ shows the effect conspicuously. It is also exhibited by the low-frequency shifts 155 cm.$^{-1}$ and 282 cm.$^{-1}$; the unsymmetrical broadening of these two lines is evident even in the weakly exposed spectrum and in its photometer record, while in the strongly exposed spectra, the broadening is so large that these two frequency shifts as well as their anti-Stokes components seem to run into each other and form an apparently continuous band of illumination.

We may interpret these phenomena by describing them as due to satellite radiations which accompany the principal Raman lines and represent shifts of frequency differing from them by relatively small amounts. The unsymmetrical character of the broadening indicates that the frequency shifts of the satellite radiations are for the most part smaller than those of the Raman lines which they accompany. The intensity of the satellite radiations is of course very small and this is indicated by the very long exposures needed to record them.

5. THE PRINCIPAL RAMAN SHIFT WITH ITS SATELLITES AND OVERTONES

Light is thrown on the nature and origin of the phenomenon referred to above by a critical study of the principal Raman frequency shift of 1086 cm.$^{-1}$ arising from the totally symmetric internal vibrations of the CO_3 ion and the accompaniments of that line. Rasetti in his investigation made with an instrument similar to our smaller spectrograph, observed and reported that the principal frequency shift of 1086 cm.$^{-1}$ is accompanied by a frequency shift of 1067 cm.$^{-1}$ to which he assigned an intensity zero as compared with an intensity fifty for the main line. In the present investigation, it has been noted that the spectrogram recorded with the smaller instrument and a fine slit exhibits, besides the frequency shift of 1067 cm.$^{-1}$ recorded by Rasetti, another and much fainter line clearly resolved from it and further removed from the principal frequency shift. This component has been proved by exact measurement to be the 1086 cm.$^{-1}$ shift excited by radiation of wave-length λ 2534·8 which appears as a companion of the resonance radiation of wave-length λ 2536·5. The features referred to above are

indicated by inflexions in the microphotometer record on the scale 1 : 8 reproduced as Fig. 4 in Plate VII. But they are seen much more clearly in the microphotometer record on the much larger scale of 1 : 50 reproduced as Fig. 6 in Plate IX. The unsymmetrical broadening of the principal Raman shift is very conspicuously exhibited by that record.

The greater dispersion and resolution of the larger spectrograph used in the present investigation has proved itself invaluable in revealing the true characters of the phenomenon now under consideration. In the spectrogram, obtained with that instrument and reproduced as Fig. 1 (*c*) in Plate IV the features mentioned above are both recognizable. They are however shown far more clearly in the greatly enlarged picture of a part of the same spectrogram reproduced as Fig. 5 (*b*) in Plate VIII. The extreme sharpness and discrete character of the 1067 cm.$^{-1}$ shift is clearly shown in that reproduction. The sharpness of the 1086 cm.$^{-1}$ shift given by the radiation λ 2534·8 of the mercury arc also seen in that picture is noteworthy as it serves to emphasize the real monochromatism of the Raman shift given by crystals as recorded with small exposures. The microphotometer record on the scale 1 : 4 of the same spectrogram reproduced as Fig. 2 exhibits these features recognizably. But a microphotometer record on a much larger scale is needed to disclose the finer features of the phenomenon. Such a record on the scale 1 : 50 is reproduced as Fig. 1 in the text.

The principal peak corresponding to the frequency shift of 1086 cm.$^{-1}$ and the clearly separated subsidiary peak with a shift of 1067 cm.$^{-1}$ are both conspicuous features in the record. Intermediately between these peaks, the photometer curve exhibits two inflexions in its course which correspond to frequency shifts of 1072 cm.$^{-1}$ and 1075 cm.$^{-1}$ respectively. The reality of these inflexions has been confirmed by taking microphotometer records at different points along the same spectral line and also with spectrograms recorded with different exposures.

The results of the investigation may thus be stated as follows: The principal Raman frequency shift of 1086 cm.$^{-1}$ is accompanied by *three* satellites having frequency shifts of 1067 cm.$^{-1}$, 1072 cm.$^{-1}$ and 1075 cm.$^{-1}$ respectively. The reason why the two latter are less conspicuous than the first is evidently because that they are closer to the principal shift recorded with much greater intensity and are therefore less clearly resolved from it than the component differing from it in frequency to the greatest extent. Taking the observed facts at their face value, we may explain the appearance of these three satellites as due to independent discrete normal modes of vibration of the structure of the crystal, which, though Raman-inactive in the first

approximation, are rendered feebly active by reason of their proximity in frequency to the strongly active mode of frequency 1086 cm.$^{-1}$ and presumably also by reason of their possessing certain features of resemblance to it in their respective modes of vibration.

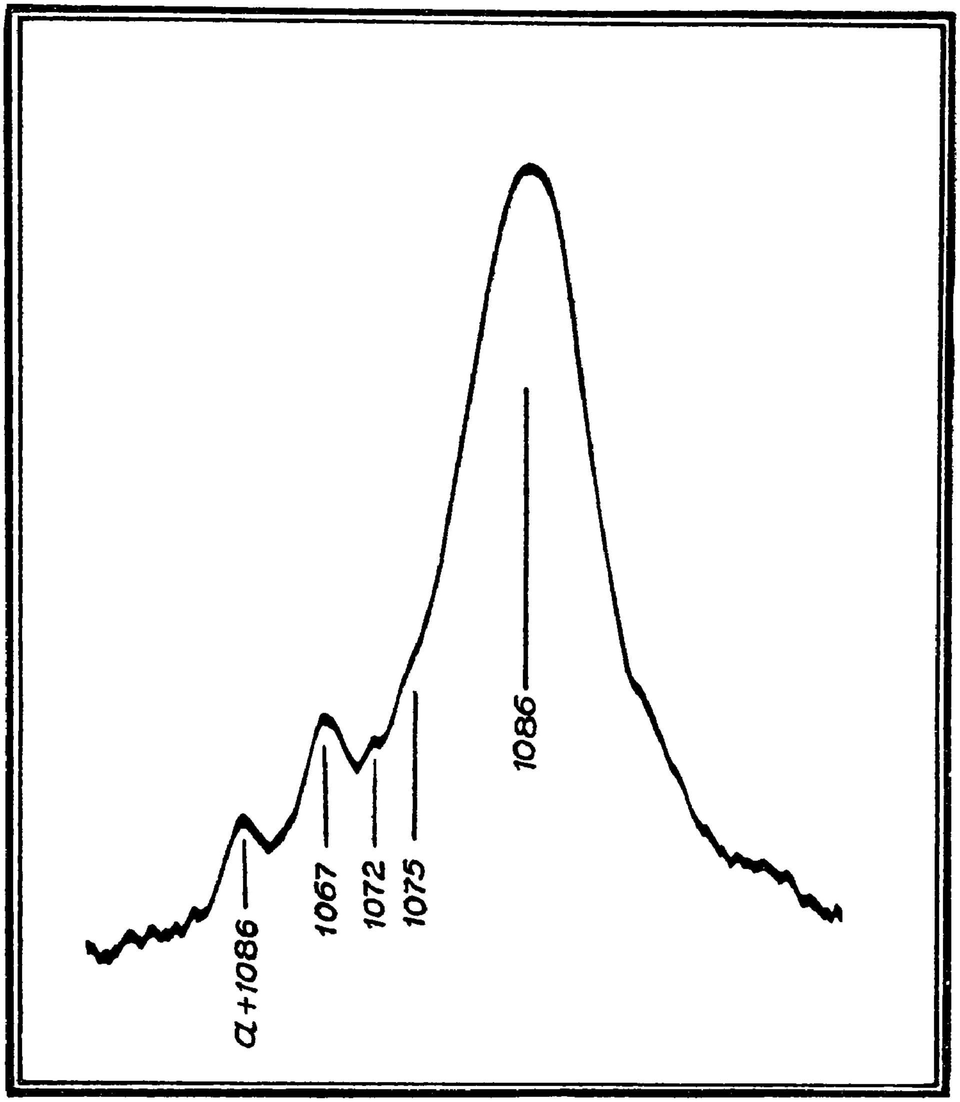

FIG. 1. Enlarged microphotometer record showing the 1086 cm.$^{-1}$ line and its satellites.

The foregoing conclusions receive striking support in the features observable in the strongly exposed Raman spectra in the vicinity of double the frequency shifts under consideration, *viz.*, in the region displaced from the exciting radiation by shifts lying between the range 2172 cm.$^{-1}$ and 2134 cm.$^{-1}$ Shifts of this magnitude would be recorded near the end of the reproduced spectrograms furthest from the exciting radiation. They can

be seen very clearly not far from the last mercury line in Fig. 3 (*a*) in Plate VI. We observe a *sharply defined line* with a frequency shift of 2173 cm.$^{-1}$; and separated from this by a dark region appears a diffuse line of comparable intensity having its peak of intensity at 2148 cm.$^{-1}$ These features are also shown in the spectrum as recorded with the larger instrument and reproduced as Fig. 1 (*c*) in Plate IV. The frequency shift of 2173 cm.$^{-1}$ here appears as a needle-sharp line in striking contrast with the diffuseness of the line clearly separated from it and having its maximum of intensity at a frequency shift of 2148 cm.$^{-1}$ The microphotometer records reproduced as Fig. 2 in Plate V and Fig. 4 in Plate VII exhibit these features quite clearly. The differences in the character of the two microphotometer records arise from the great difference in the photographic exposures and of the resolving powers of the two instruments employed. A microphotometer record on the greatly enlarged scale of 1: 50 showing these features is reproduced in the text as Fig. 2.

The sharp line with a frequency shift of 2173 cm.$^{-1}$ is clearly the octave of the principal Raman frequency shift of 1086 cm.$^{-1}$ The diffuse line with its peak at 2148 cm.$^{-1}$ is explicable as arising from the superposition of the octaves of a number of discrete normal modes whose frequencies are *less* than 1086 cm.$^{-1}$, the lowest of them being 1067 cm.$^{-1}$ and the two others having higher values. These normal modes, being inactive, manifest themselves only very weakly as fundamentals. But theory indicates they would be Raman-active as octaves to the same extent as the active fundamental of 1086 cm.$^{-1}$ The fact that the band centred at 2148 cm.$^{-1}$ is of comparable intensity with the line at 2173 cm.$^{-1}$ thus receives a natural explanation.

6. The Origin of the Satellite Radiations

The frequency shifts observed in the Raman effect arise from the excitation of the normal modes of vibration of the atoms in the structure of the crystal about their positions of equilibrium by the incident radiation. In the determination of these modes and their frequencies, it is usual to consider those modes which can be regarded as characteristic of the groups of atoms included in the unit cells of the crystal structure. If the unit cell contains p atoms, the number of such normal modes of vibration would evidently be $(3p - 3)$, the three excluded degrees of freedom representing the three translations of unit cell. But this way of dealing with the matter is obviously not complete or satisfactory. If we define a normal mode as one in which the atoms in a crystal vibrate with the same frequency and in the same or opposite phases, it can be readily shown to be a consequence of its three-dimensional periodicity of structure, that a crystal has $(24p - 3)$ normal

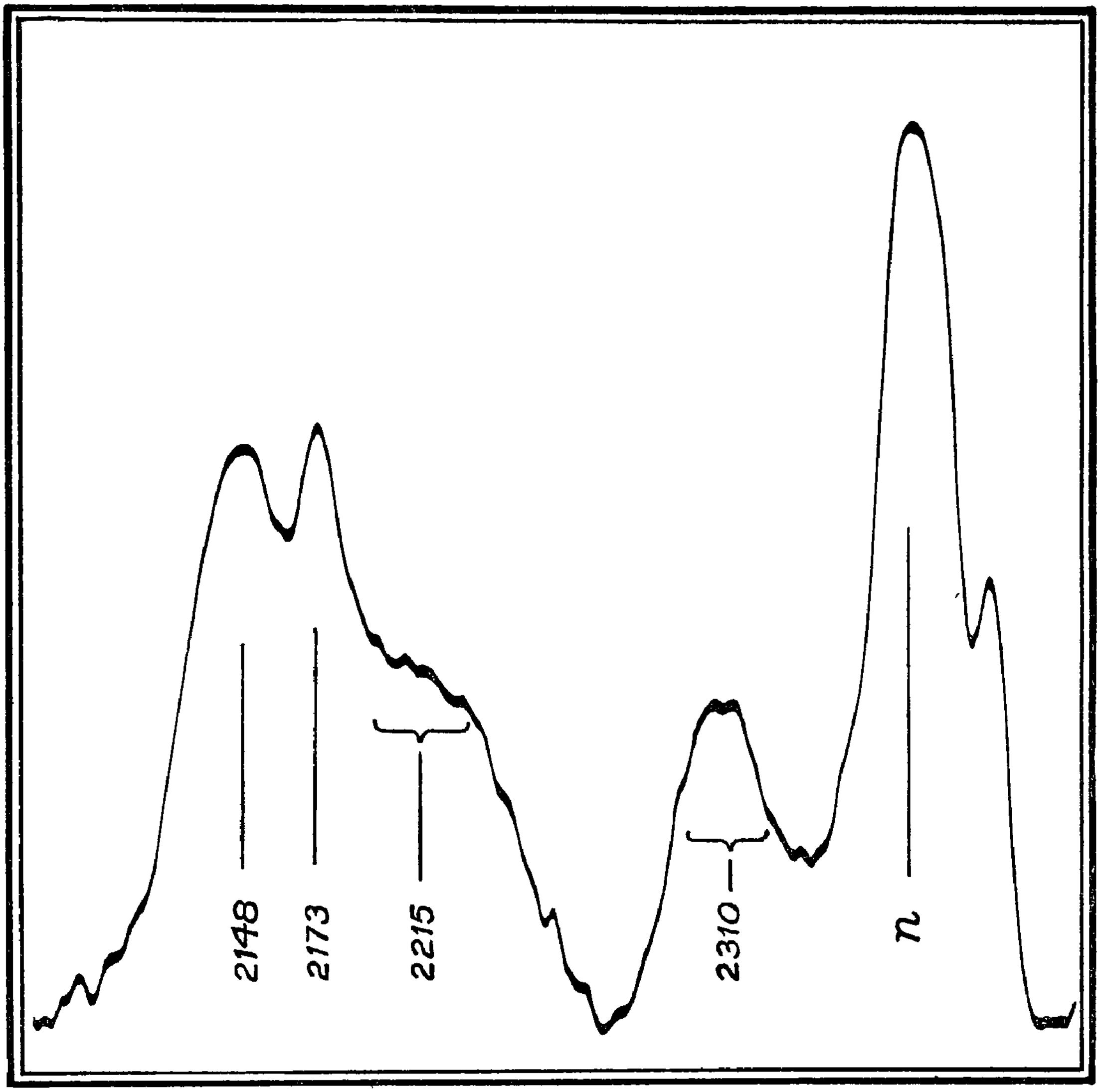

FIG. 2. Enlarged microphotometer record showing the overtone of the principal Raman shift and other features.

modes of vibration, each of which is characterised by a definite monochromatic frequency. In $(3p - 3)$ of these normal modes, equivalent atoms in adjacent cells of the structure have the same amplitude and the same phase of vibration, while in the remaining $21p$ modes they have the same amplitudes of vibration but their phases are opposite along one, two or all the three axes of the crystal structure. The latter may be briefly designated as the superlattice vibrations.

We may proceed to consider the consequences of the foregoing proposition in the case of calcite. We shall confine our attention at first to the modes involving the totally symmetric internal vibrations of the CO_3 group. Each

unit cell of the crystal structure contains two such groups which are non-equivalent, the phases of vibration of which in any normal mode may be either the same or opposite. There are eight different situations regarding the relative phases of vibration in the unit cells of the crystal adjoining each other along the three axes of the structure. Thus, in all, there are 8×2 or sixteen possible kinds of normal modes involving the totally symmetric vibration of the CO_3 groups. The rhombohedral symmetry of the crystal however makes the two axes perpendicular to the trigonal axis equivalent to each other, thereby reducing the number of distinct normal modes from sixteen to eight only. A further simplification becomes possible when we note that the equivalent CO_3 groups located along the trigonal axes are remote from each other in comparison with their relative distances along the two other axes of the crystal. Hence, we may ignore the additional possibilities arising from the reversal of phase of their vibrations along the trigonal axis. The number of *effectively* different normal modes is reduced thereby from eight to four. The mode that is Raman-active would obviously be the one in which any one CO_3 group has the same phase of vibration as all the other groups in its neighbourhood. In each of the three other normal modes, half the number of CO_3 groups vibrate in one phase and the other half in the opposite phase and hence they would be Raman-inactive in the first approximation.

It is evident also that the frequencies of the four normal modes indicated by the foregoing considerations would not be identical. For, these frequencies which are principally determined by the internal forces arising within each group would also be influenced by the interactions between similar groups vibrating with the same frequency in the neighbourhood and such interactions would be altered by a reversal of their relative phases. The order of magnitude of the differences in frequency arising in this manner is indicated by the well-known fact that while the frequency shift as observed in the crystal is 1086 cm.$^{-1}$, a similar vibration in solutions containing CO_3 ions gives a frequency shift of only 1065 cm.$^{-1}$

As already indicated, the strongly Raman-active vibration in calcite gives a frequency shift of 1086 cm.$^{-1}$ which corresponds to the case in which all the CO_3 groups vibrate in identical phases. Hence, the three other modes in which half of them vibrate in opposite phases may be expected to be of lower frequencies. Though, as already stated they would be Raman-inactive in the first approximation, various considerations indicate that they would be rendered feebly active by reason of the general similarity in the character of their vibrations and their close approximation in frequency to the strongly active mode.

We have seen in the preceding section that in the strongly exposed Raman spectra, the frequency shift of 1086 cm.$^{-1}$ is accompanied by weak satellites with lower frequency shifts which are respectively, 1075, 1072 and 1067 cm.$^{-1}$ Further, these satellites manifest themselves as octaves quite as strongly as the octave of the 1086 cm.$^{-1}$ frequency. These facts are in such excellent agreement with the theoretical considerations set forth above as to leave no doubt regarding the correctness of the explanation. It is also easy to understand why the 1086 cm.$^{-1}$ frequency exhibits the phenomenon of the satellites in such a clear and conspicuous manner. Being itself an extremely intense line, the satellites which derive from it have observable intensities and being themselves also sharp are seen resolved from it when a spectrograph of adequate power is brought to bear on them.

7. Satellites and Overtones of Other Frequency Shifts

Besides the three modes of internal vibration of the CO_3 groups appearing as frequency shifts in the Raman spectrum, there is still another in which the carbon and oxygen atoms in these groups oscillate in opposite phases along the trigonal axis of symmetry. Theory indicates that such an oscillation would be infra-red active but would not give a Raman shift of the same frequency, though it might give one with double that frequency. These indications of theory are in agreement with observation. A sharply defined maximum located at 877 cm.$^{-1}$ is observed in the infra-red absorption by thin layers of very finely powdered calcite. *Per contra*, no frequency shift in that vicinity is observable even in the most strongly exposed Raman spectra. Cabannes, Nisi and others noticed and recorded a sharp line with a frequency shift of 1749 cm.$^{-1}$ in the Raman spectrum of calcite. This is clearly identifiable as the octave of the mode of vibration referred to above. Fig. 5 (*c*) in Plate VIII recorded with the λ 4358 excitation exhibits this frequency shift with a notable intensity. In the excitation by λ 2536·5, the same frequency shift appears as a line falling between the second and third components of the triplet in the spectrum of the mercury arc; though it can be observed in that position, a detailed investigation is difficult. So far as is ascertainable, the frequency shift is a single line not accompanied by any satellites or companions.

As already reported in an earlier section, the frequency shift of 1436 cm.$^{-1}$ conspicuously exhibits an unsymmetrical broadening in strongly exposed spectra. In the microphotometer record reproduced in Fig. 2 of Plate V, three satellites can be recognized whose frequency shifts are respectively 1399, 1412 and 1418 cm.$^{-1}$ In the microphotometer record of the more heavily exposed spectrum reproduced in Fig. 4 of Plate VII, the unsymmetrical

broadening is clearly visible but the satellites are not resolved from the parent line. Their presence however is clearly indicated in the record obtained on a larger scale 1 : 50 and reproduced below as Fig. 3 in the text.

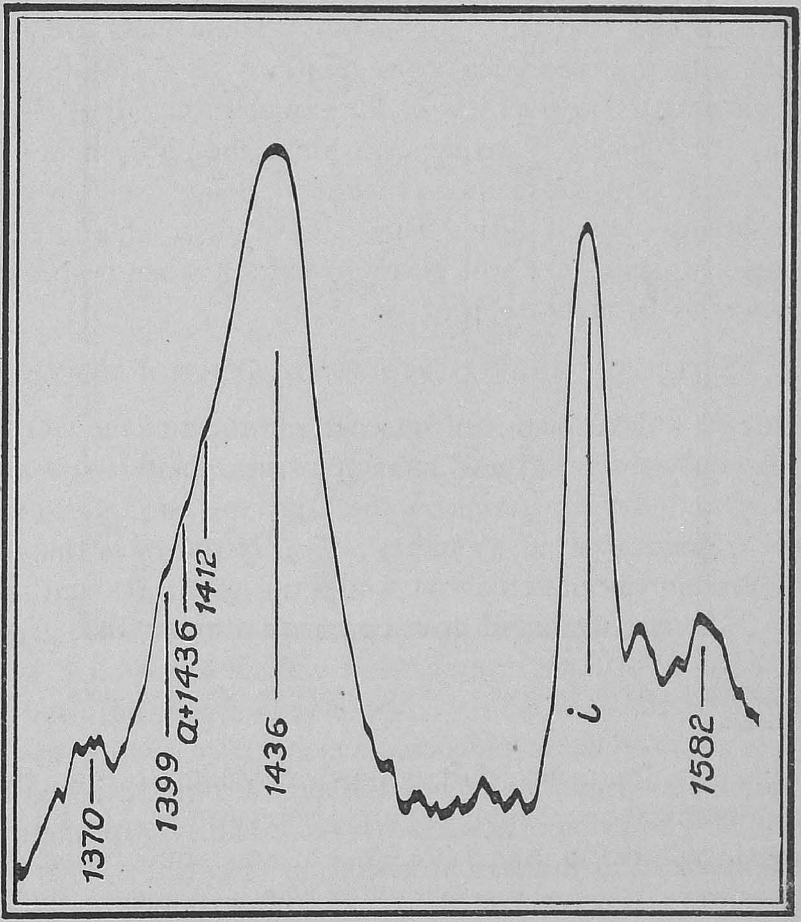

FIG. 3. Enlarged microphotometer record showing 1436 cm.$^{-1}$ line and other features.

In Fig. 4 (Plate VII), the positions where the octaves of the 1436 cm.$^{-1}$ shift and of its satellites appear are indicated in the microphotometer record. They fall on and near the triplet of Raman lines having a common frequency shift of 1086 cm.$^{-1}$ excited by the triplet of the mercury arc and this makes it difficult to describe them completely. It is evident, however, that the intensity of the overtones of 1436 cm.$^{-1}$ and its satellites is very small compared with the intensity of the octaves of the 1086 cm.$^{-1}$ and of its satellites. The enlarged microphotometer record reproduced in the text as Fig. 4 however makes it clear that the satellites of the 1436 cm.$^{-1}$ shift manifest themselves as octaves no less conspicuously than their parent line.

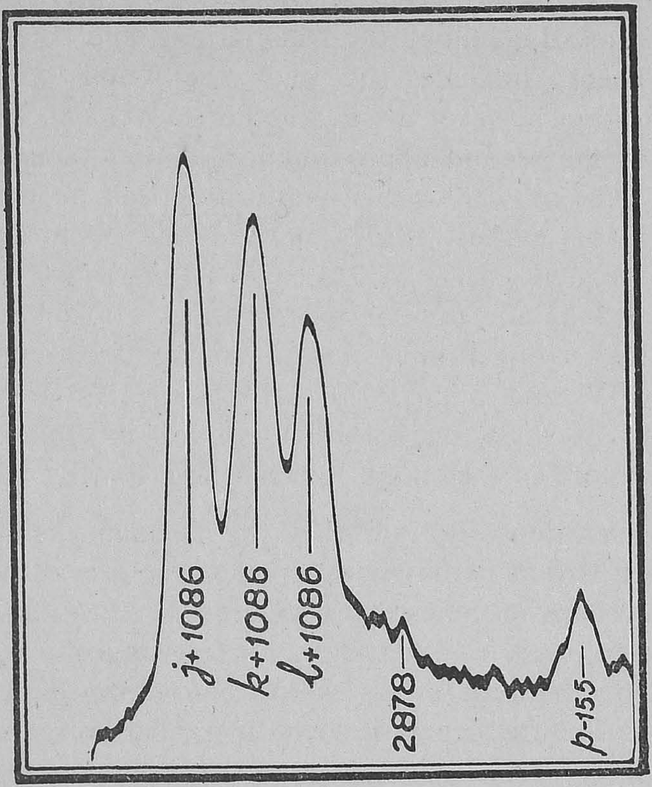

FIG. 4. Enlarged microphotometer record showing the overtones of 1436 cm.$^{-1}$ line and of its satellites.

The 712 cm.$^{-1}$ frequency shift is much less intense than the 1436 cm.$^{-1}$ and its unsymmetrical broadening is barely perceptible. The microphotometer record reproduced as Fig. 6 in Plate IX however shows a weak companion which may be interpreted as a satellite line with a frequency shift of 685 cm.$^{-1}$ It is however difficult to exclude the possibility that this may be only the 712 cm.$^{-1}$ shift excited by the weak λ 2534·8 line of the mercury arc.

The octave of the 712 cm.$^{-1}$ frequency may be expected to be extremely weak. Even otherwise, it could scarcely be expected to be observable, since it would overlap the 1436 cm.$^{-1}$ shift in the spectra recorded with the necessary exposures.

8. THE LOW-FREQUENCY SPECTRUM

We now proceed to consider the characters of the Raman spectrum in the region of the smaller frequency shifts ($<$ 600 cm.$^{-1}$). The most conspicuous features in this region are of course the frequency shifts of 155 cm.$^{-1}$ and 282 cm.$^{-1}$, the latter being much the stronger of the two. They have been identified as arising from the translatory oscillations of the CO_3 groups in their own plane combined with rotational oscillations about an axis also lying

in that plane. The two other types of oscillation of the CO_3 groups which are possible are translations along the trigonal axis and rotations also about the same axis. Theory indicates that such oscillations would be Raman-inactive. The question however arises whether movements of the latter two types might not in the second approximation exhibit themselves weakly as frequency shifts. The answer to this question appears to be in the affirmative. Cabannes in his earliest studies noticed and recorded a line in the spectrum with a frequency shift of 221 cm.$^{-1}$ The reality of this has been definitely established by the present investigation. It is visible as a sharp line between the two strong Raman lines in the spectrograms reproduced as Fig. 1 (*c*) in Plate IV and Fig. 5 (*a*) in Plate VIII. It also manifests itself conspicuously as peaks on both sides of the exciting radiation in the microphotometer record of the same spectrogram as Fig. 2 of Plate V.

Various considerations indicate that the frequency shift of 221 cm.$^{-1}$ the reality of which is thus definitely established represents the normal mode in which the CO_3 groups in the crystal oscillate in a direction normal to their planes, neighbouring layers of the CO_3 groups periodically approaching and receding from each other, the layers of Ca ions intermediate between them remaining at rest. The frequency of such an oscillation may be expected to be that actually observed. Confirmatory evidence of the correctness of this explanation of the 221 cm.$^{-1}$ shift of frequency comes to hand from a comparison of the low-frequency Raman spectra of calcite and aragonite. There are striking resemblances and also noteworthy differences between the two spectra, these being evidently consequences of the close similarities as well as the specific differences in the structures of the two crystals. Modes of oscillation of the CO_3 groups similar to those now under consideration are Raman-active in aragonite by reason of its lower symmetry of structure. Indeed, a close group of lines with an average frequency shift of 215 cm.$^{-1}$ and having a notable intensity is a very striking feature in the spectrum of aragonite.

Hibben in his book reports having observed frequency shifts of $\pm$ 86 cm.$^{-1}$ in the Raman spectrum of calcite. Some support for this claim is forthcoming in the present investigation, though the matter has not been placed completely beyond doubt. The rotational oscillation of the CO_3 groups about the trigonal axis of symmetry might be expected to have a frequency of that order of magnitude.

We may now briefly comment upon the explanation of the behaviour of the two principal Raman shifts in this region in strongly exposed spectra already described earlier in the present paper. Dynamical theory indicates that the unit cell in the calcite structure consisting of two CO_3 groups and two

Ca ions intervening between them has ten different normal modes of vibration. If the alternations in the phase of the vibration in adjacent unit cells along the three axes of the structure are also taken into account, this number would be increased to forty in all. The additional thirty modes would have frequencies different from those of the corresponding modes in the group of ten first referred to. Only two out of these forty modes would, strictly speaking, be Raman-active. But it appears inevitable that when one or the other of these two modes is excited, other modes approximating to them in frequency would also be excited, though only very feebly. The spectrum consisting of such a crowd of satellite radiations with different frequencies would naturally appear more or less continuous and this is what is actually observed.

The nature of the vibrations now under consideration is such that we could scarcely expect them to exhibit overtones with any notable intensities, and indeed no evidence is forthcoming of such overtones as *discrete* frequency shifts in the region under consideration. But we do observe a weak band of illumination in the spectrum covering the whole range of frequency shifts upto 600 $cm.^{-1}$ This may be regarded as a superposition of the effects arising from all the forty possible normal modes of vibration.

9. Combinational Frequency Shifts

We proceed to consider and report on the various features observed in the strongly exposed Raman spectra of calcite other than those already discussed above. It appears desirable to make some comments of a general nature regarding the principles on which the interpretations suggested are based. It is essential in the first place to make the most accurate measurements of the frequency shifts proposed to be interpreted as well as of the frequency shifts to which they might be related as overtones or combinations. It is not possible, however, to base interpretations solely on arithmetical agreements, as the latter might be purely fortuitous. Nor is it permissible to base the interpretations entirely on the selection rules which have been proposed on theoretical grounds. Frequency shifts might be permitted by those rules and yet be unobservable by reason of vanishingly small intensity or other circumstances. Further, the selection rules themselves rest on certain assumptions and are therefore not necessarily valid in all cases. In view of these remarks, it is important that other factors are also taken into consideration. The intensity and spectral character of the frequency shifts are factors of particular importance in this respect. These remarks are made, since the reservations which they imply have been overlooked in several

instances in the earlier literature and assignments have been proposed which are wholly unacceptable.

An examination of the strongly exposed spectra and of their microphotometer records reveals numerous features calling for explanation. After a careful review of the various possibilities, we find the most reasonable interpretation to be that they arise from combinations of the various normal modes of vibrations of the unit cells in the crystal structure with the two normal modes having frequencies respectively of 1086 and 875 cm.$^{-1}$ The former is the totally symmetric oscillation of the CO_3 groups which gives by far the most intense line in the Raman spectrum, while the other is an infra-red active mode which gives a Raman shift of double its frequency with notable intensity. We find it possible in the manner indicated to explain practically every one of the observed features in the spectrum. Table I gives a

TABLE I

Observed frequency shifts: Their characters and suggested origins

1186 cm.$^{-1}$	Diffuse and weak	1086+ 100 cm.$^{-1}$
1241 ,,	Sharp and weak	1086+ 155 ,,
1275 ,,	Diffuse and very weak	1086+ 189 ,,
1305 ,,	Sharp and very weak	1086+ 221 ,,
1370 ,,	Sharp and strong	1086+ 282 ,,
1795 ,,	Sharp but weak	1086+ 712 ,,
2522 ,,	Indication only	1086+1436 ,,

list of the combinations of the first kind and Table II a list of the combinations of the second kind. It is significant that while the octaves of the two frequencies 1086 and 875 cm.$^{-1}$ are conspicuous features in the Raman spectrum, no frequency shift in the vicinity of 1961 cm.$^{-1}$ which would represent a summation of them is observable even in the most strongly exposed spectra. This is readily understood, since the atomic vibrations in these two modes occur in mutually perpendicular directions and that while one of them is totally absent in the infra-red absorption spectrum, the other is conspicuously present.

The following comments may be offered on the entries in Table I. That the strongly Raman-active frequency 1086 cm.$^{-1}$ would combine with other

strongly Raman-active frequencies, *viz.*, 155, 282, 712 and 1436 cm.$^{-1}$ to give sharply defined summational shifts is only to be expected. That the strongest of them is also the combination with the strongly active 282 cm.$^{-1}$ is also intelligible. That no summations appear in Table I corresponding to the strongly infra-red active normal modes with frequencies 330 and 357 cm.$^{-1}$ might have been anticipated on theoretical grounds. The corresponding summations, *viz.*, 1416 and 1443 cm.$^{-1}$ would in any event, however, have been unobservable owing to their overlap with the strong 1436 cm.$^{-1}$ Raman shift. Table I also records summations with three other low frequencies, *viz.*, 100, 189 and 221 cm.$^{-1}$, the former two as weak and diffuse lines and the latter as a weak but sharp line. The first two frequencies are presumably to be identified with two normal modes which are infra-red active, while the 221 cm.$^{-1}$ represents a normal mode which itself appears weakly as a Raman shift and the nature of which has been discussed earlier in this paper.

In strong contrast with the entries in Table I, the frequency shifts listed in Table II appear in most cases as diffuse bands but with notable intensities. The two bands of lowest frequency are respectively a summational and a differential, the former being the more intense of the two, the frequency involved being in either case 84 cm.$^{-1}$ As remarked earlier in the paper, this frequency probably represents the rotational oscillations of the CO_3 groups in their own plane. The appearance in Table II of summations with the Raman-active frequencies of 155 and 282 cm.$^{-1}$ is very surprising, but there is no question as to their reality, since they are recorded with notable intensities and no alternative explanation of these features is forthcoming. Here, as in three other cases listed in Table I, there is a clear-cut violation of the selection rules of which the explanation must be left an open question. The other frequencies of which the summations are listed in Table II are those manifesting themselves strongly in infra-red absorption. Investigators in the latter field are agreed that the maximum which appears in nearly the same position as the Raman frequency shift of 712 cm.$^{-1}$ is a sharply defined one. It is therefore not surprising that the corresponding summation listed in Table II also appears as a strong sharp line. The position is however different with regard to the last two summations appearing in the table. Hunt and collaborators who have investigated the infra-red absorption by a very thin layer of powdered calcite record a peak at 1439 cm.$^{-1}$, but this is only the crest of a very broad maximum and it is therefore not surprising that the corresponding summation appears in Table II as a diffuse band. Perhaps the most remarkable entry in the table is that of the extremely diffuse band which corresponds to a summation with an infra-red absorption band having a maximum at 1340 cm.$^{-1}$ There is no place for such a frequency in the scheme of normal

TABLE II

Observed frequency shifts : Their characters and suggested origins

794 cm.$^{-1}$	Diffuse and weak	875 − 84 cm.$^{-1}$
957 ,,	Diffuse and strong	875 + 84 ,,
1025 ,,	Diffuse and strong	875 + 155 ,,
1159 ,,	Diffuse and strong	875 + 282 ,,
1207 ,,	Diffuse and weak	875 + 330 ,,
1232 ,,	Sharp and weak	875 + 357 ,,
1582 ,,	Strong and sharp	875 + 706 ,,
2215 ,,	Diffuse and strong	875 + 1340 ,,
2310 ,,	Diffuse and strong	875 + 1439 ,,

modes of vibration of the unit cell of the calcite structure. The suggestion may therefore be hazarded that this band is a satellite or an aggregate of satellites accompanying the infra-red absorption at 1439 cm.$^{-1}$ but distinctly separated from it and analogous to the satellites accompanying the 1436 cm.$^{-1}$ Raman frequency shift already discussed. This suggestion, it may be remarked, is strongly supported by the shape of the absorption curve reproduced in the paper by Hunt and collaborators. Their diagram shows that the absorption of which the crest appears at 1439 cm.$^{-1}$ is of a highly unsymmetrical shape; it rises steeply from nearly perfect transmission at 1650 cm.$^{-1}$ to almost complete opacity at 1439 cm.$^{-1}$ and then drops down quite gradually to nearly perfect transmission again only at 890 cm.$^{-1}$

In conclusion the author wishes to express his sincere thanks to Prof. Sir C. V. Raman, F.R.S., N.L., for the keen interest he took in this investigation and for the valuable suggestions that he gave for the preparation of this paper.

10. SUMMARY

The paper reports the results of a study of the Raman spectrum of calcite recorded with prolonged exposures.

(*a*) The principal Raman shift of 1086 cm.$^{-1}$ is accompanied by much weaker satellites whose frequency shifts are 1067, 1072 and 1075 cm.$^{-1}$ The octave of the principal mode is recorded as a sharp line with a frequency shift

of 2173 cm.$^{-1}$ with a diffuse companion of comparable intensity which is a superposition of the octaves of the three satellites. The 1436 cm.$^{-1}$ Raman shift likewise has satellites at 1399, 1412 and 1418 cm.$^{-1}$ and its octave is feebly recorded as a sharp line, while the octaves of the satellites are also observed in its vicinity. The origin of the satellite radiations is discussed and it is shown that they represent the superlattice vibration frequencies of the calcite structure which are feebly excited.

(*b*) The appearance of a sharp Raman line with a frequency shift of $\pm$ 221 cm.$^{-1}$ is confirmed and it is shown to arise from a normal mode usually considered as inactive.

(*c*) The two intense Raman shifts of 155 and 282 cm.$^{-1}$ exhibit a highly unsymmetrical broadening, as also wings of low intensity spread out over the whole range of frequency shifts between $-$ 300 cm.$^{-1}$ to $+$ 600 cm.$^{-1}$ This spectrum is explicable as arising from a very feeble excitation of the whole group of forty lattice and superlattice frequencies of the calcite structure and their overtones and combinations.

(*d*) Sixteen combinational frequency shifts have been recorded. Seven of them are explained as combinations with the 1086 cm.$^{-1}$ Raman line and the the nine others as combinations with 875 cm.$^{-1}$ Some of the observed combinations violate the selection rules.

REFERENCES

The literature on the Raman spectrum of calcite and its theoretical interpretation is very extensive. Only the papers which have been referred to in the text and which have a bearing on the results of the present investigation are quoted below.

1. Bhagavantam and Venkatarayudu .. *Proc. Ind. Acad. Sci.*, 1939, **9 A**, 224.
2. Cabannes, J. .. *Comptes Rendus*, 1929, **188**, 1041.
3. Couture, L. .. *Annales de Physique*, 1947, **2**, 5.
4. Hunt, Wishard and Bonham .. *Analyt. Chem.*, 1950, **22**, 1478.
5. Krishnan, R. S. .. *Proc. Ind. Acad. Sci.*, 1945, **22 A**, 182.
6. Nisi, H. .. *Proc. Imp. Acad. Tokyo*, 1929, **5**, 127.
7. Rasetti, F. .. *Nuovo Cimento*, 1932, **9**, 72.
8. Went, J. .. *Doctorate Thesis*, 1935, Utrecht.
9. Hibben, J. H. .. *Raman effect and its chemical applications*, 1939, pp. 428.

CONNEMARA PUBLIC ... 4 JAN 1965 MADRAS

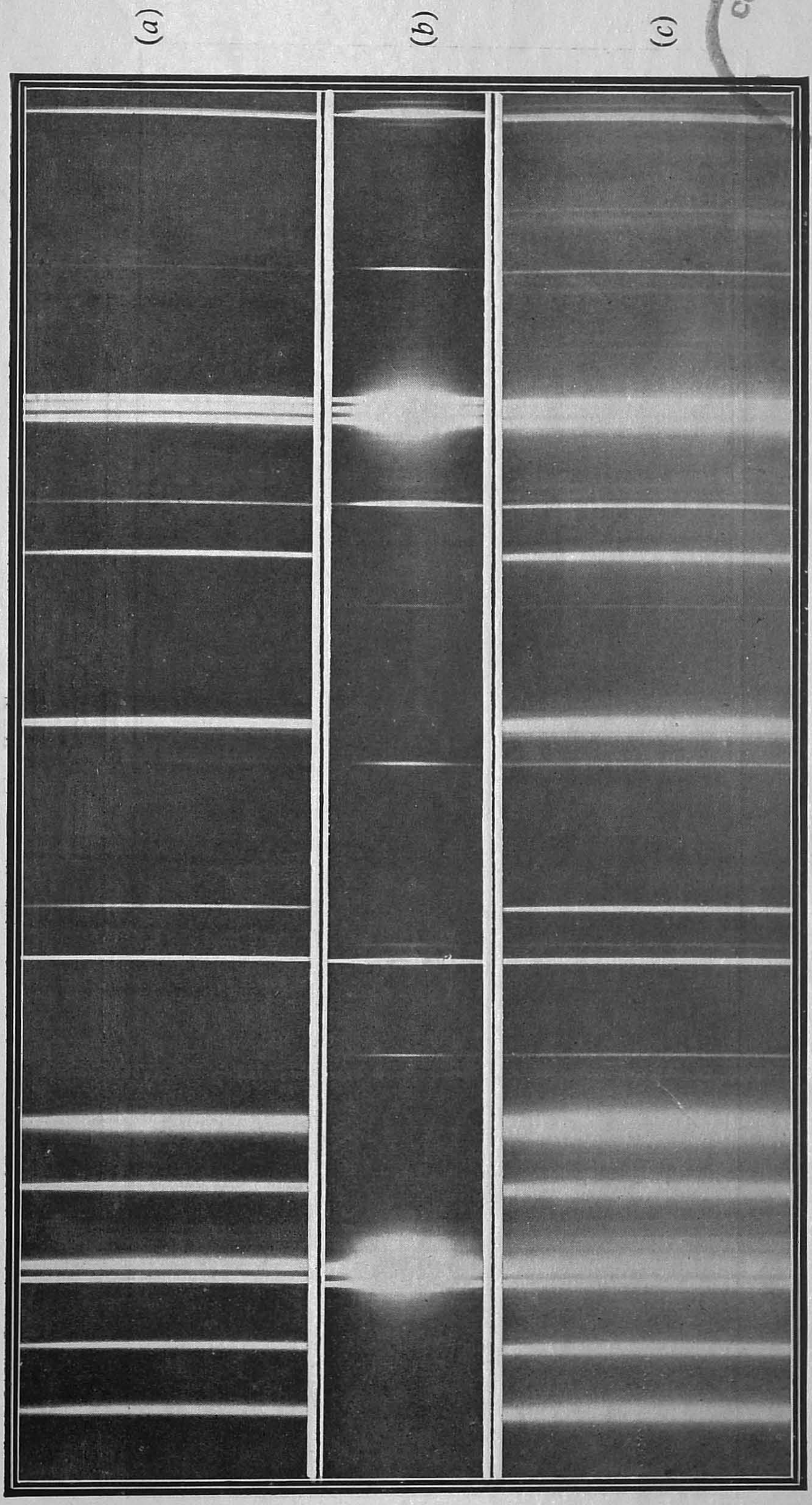

FIG. 1. The Raman spectrum of calcite recorded with Littrow spectrograph. (a) Deeply printed, (b) Spectrum of the mercury arc, (c) Lightly printed.

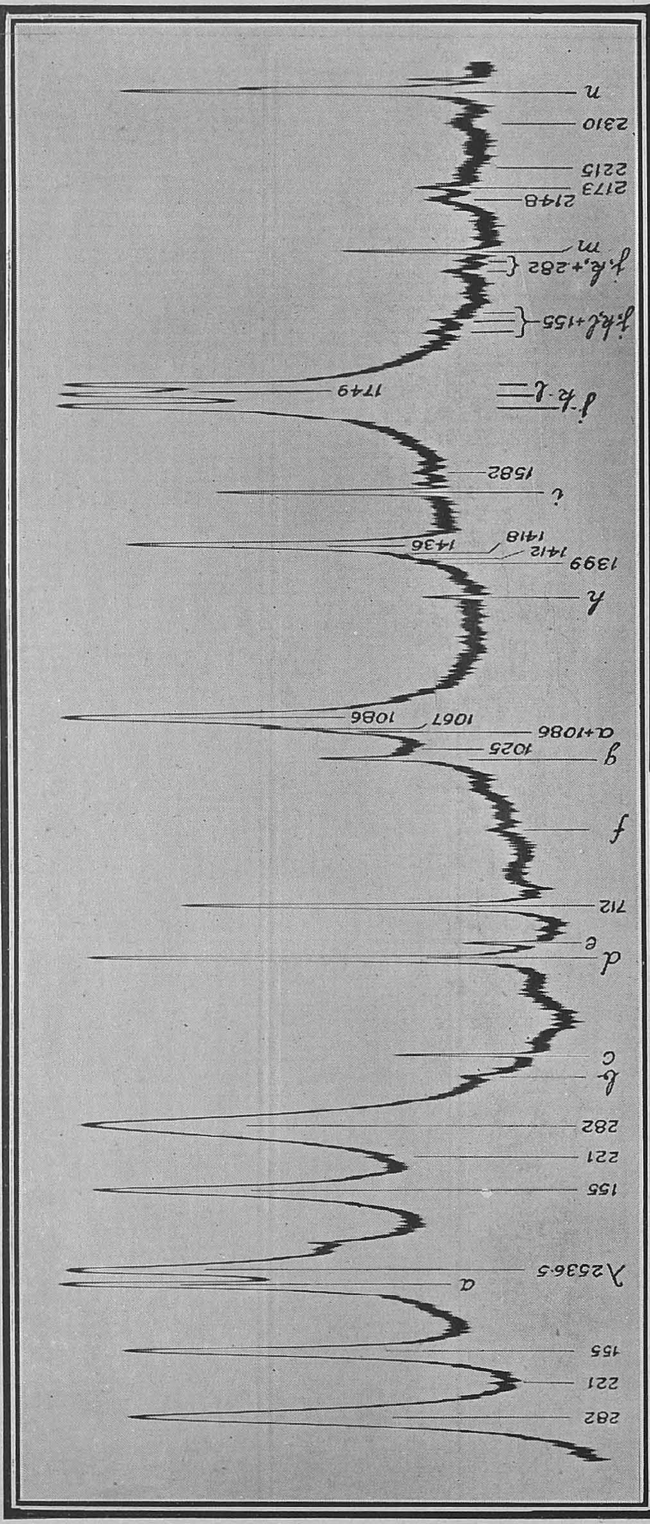

Fig. 2. Microphotometer record of the Raman spectrum of calcite recorded with the Littrow spectrograph.

Note.—The numbers denote the Raman shifts in $cm.^{-1}$ while *a*, *b*, *c*, etc., refer to the mercury arc lines.

CONNEMARA PUBLIC
4 JAN 1965
MADRAS

(a) (b) (c)

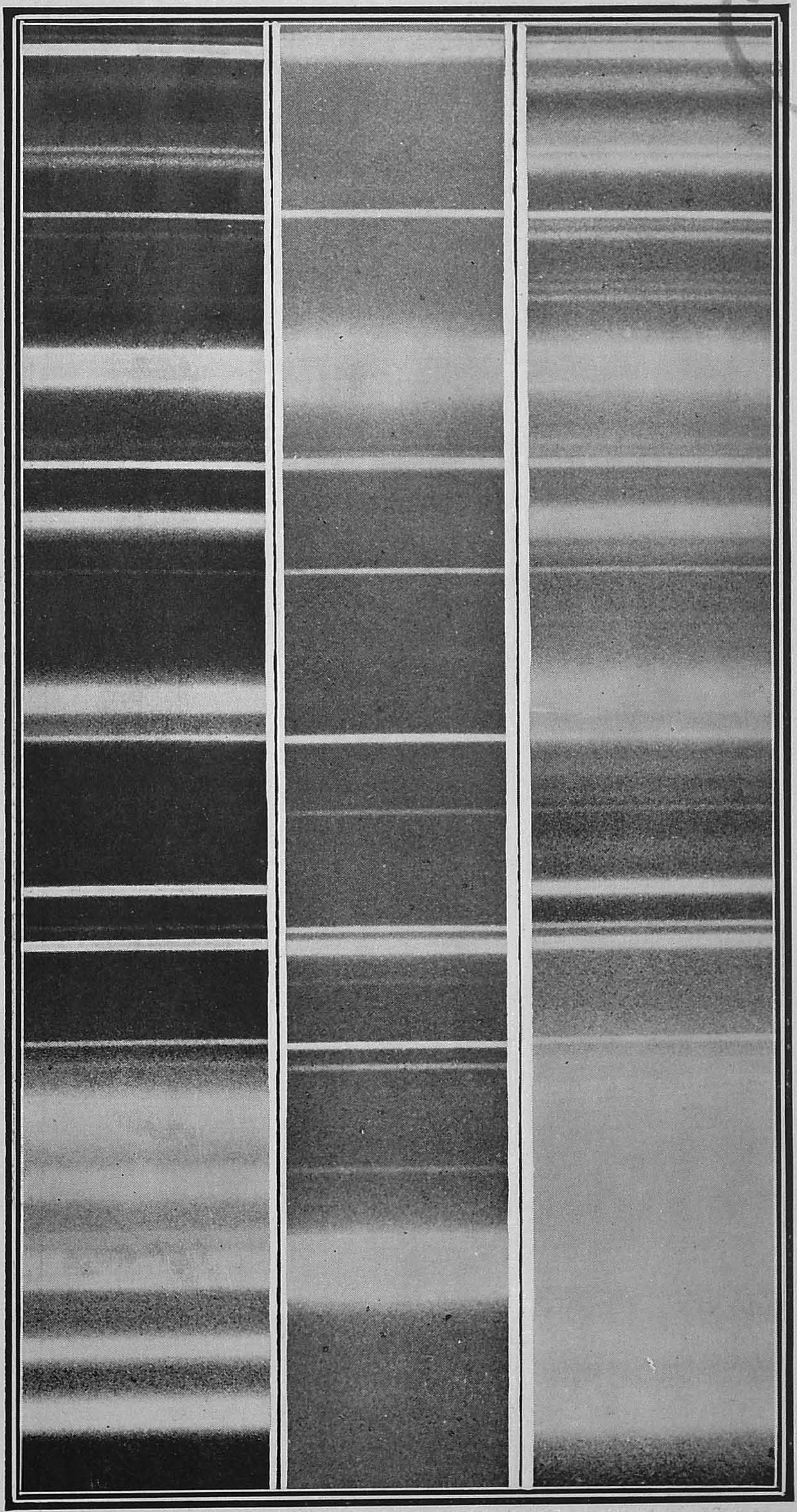

FIG. 3. The Raman spectrum of calcite recorded with the medium quartz spectrograph. (*a*) Deeply printed, (*b*) Spectrum of the mercury arc, (*c*) Lightly printed.

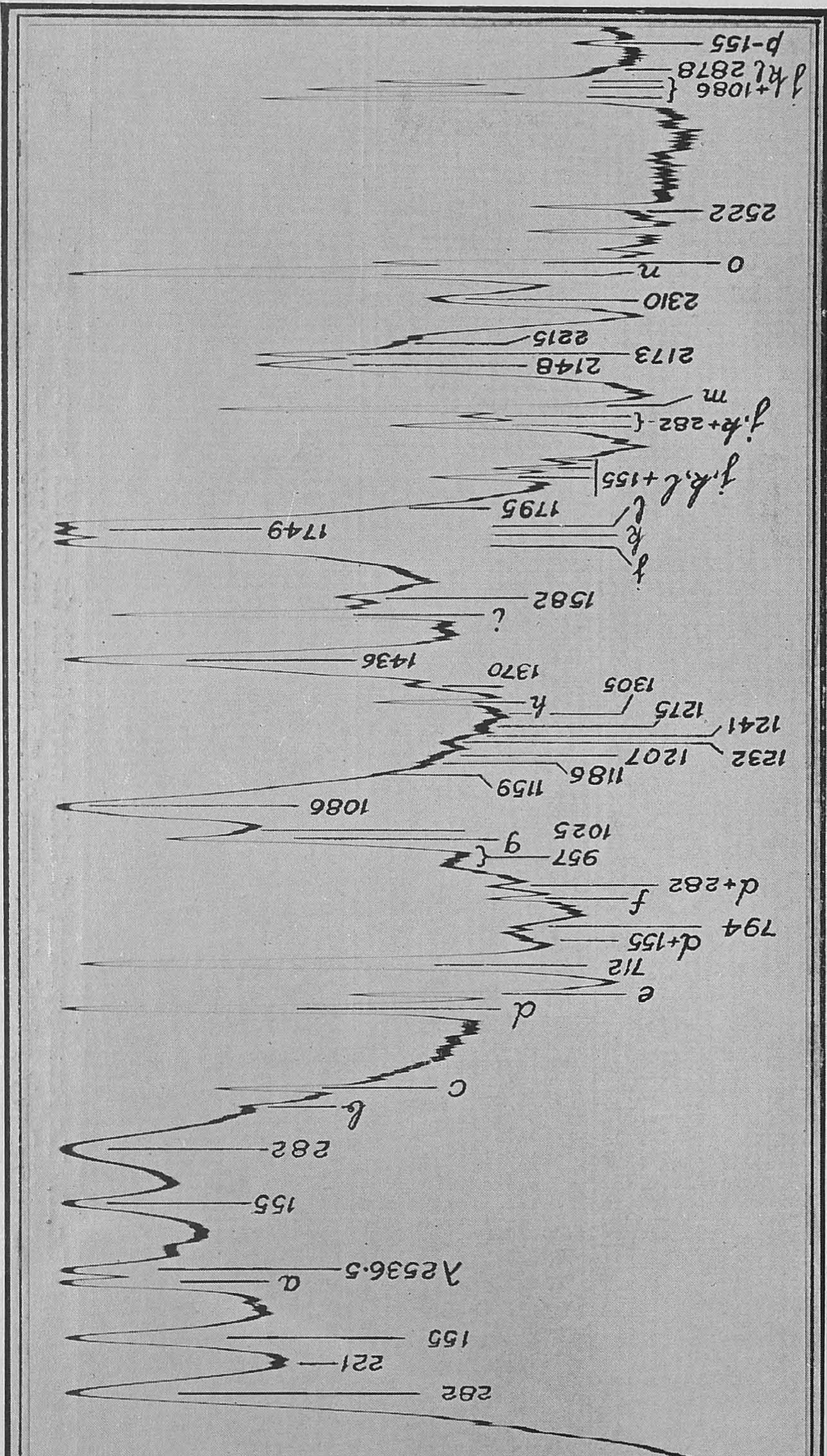

FIG. 4. Microphotometer record of the Raman spectrum of calcite recorded with the medium quartz spectrograph.

4 JAN 1965

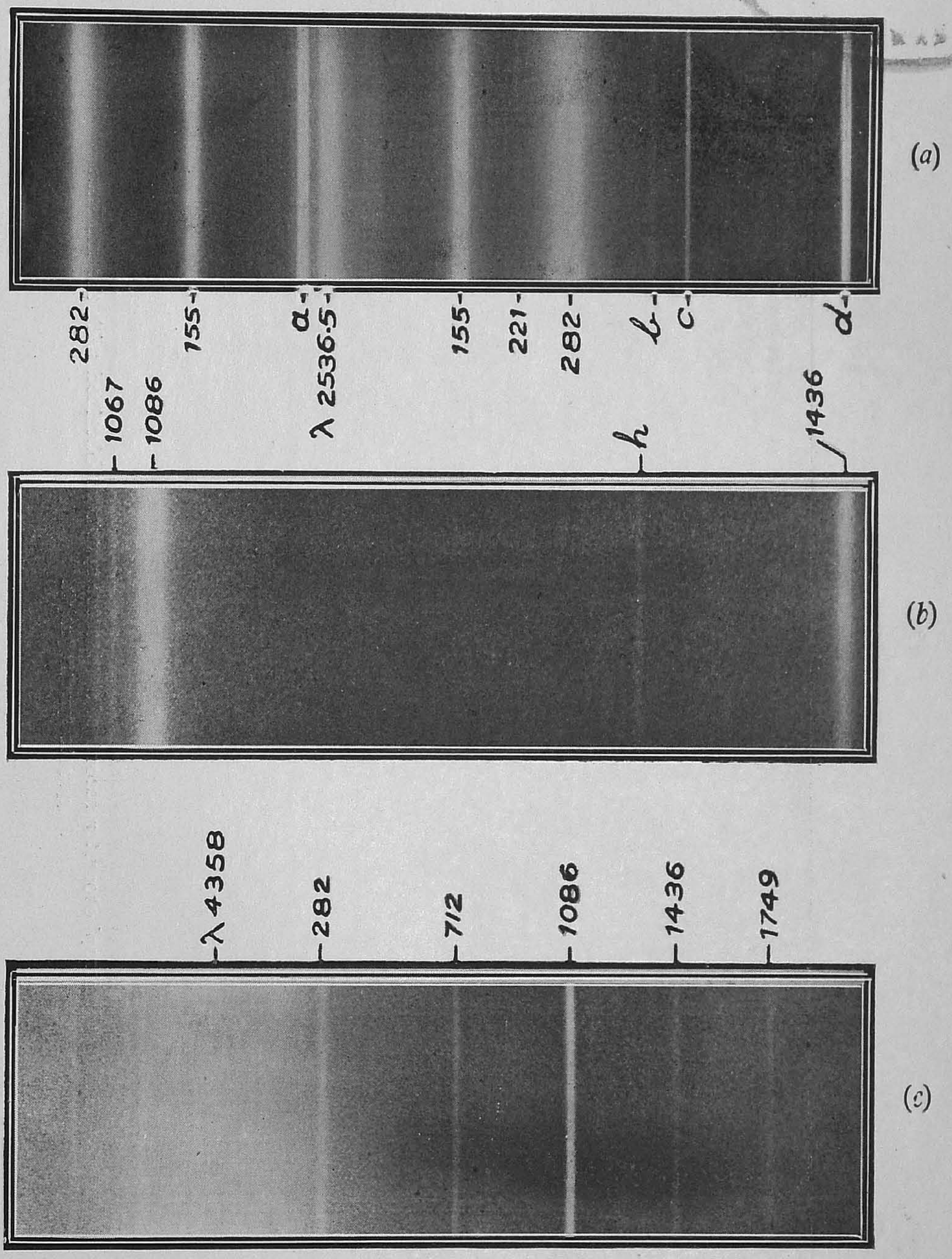

FIG. 5. The Raman spectrum of calcite; (*a*) and (*b*) Enlargements of some portions of Fig. 1 (*c*); (*c*) Spectrum recorded with λ 4358 excitation.

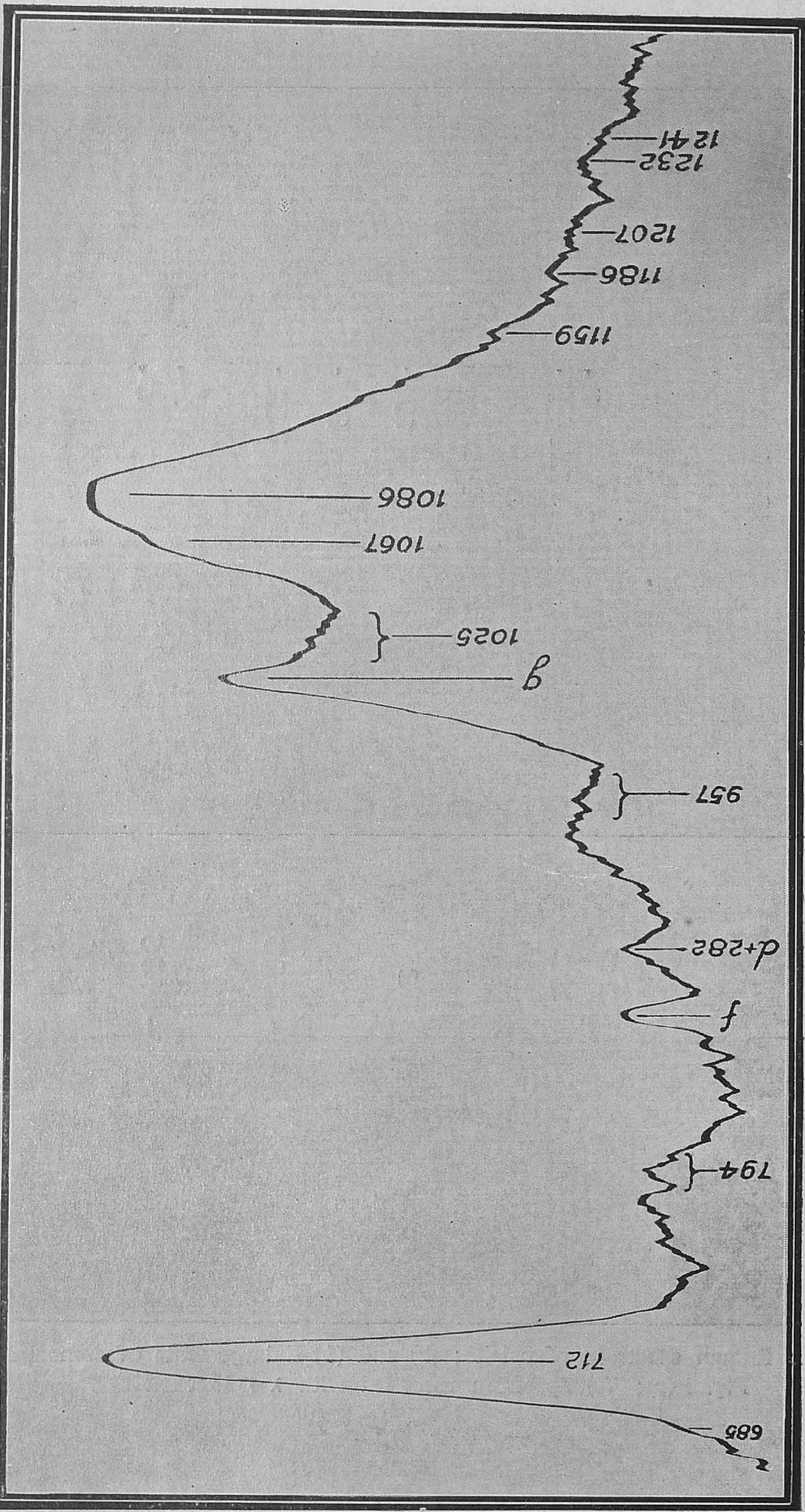

FIG. 6. Enlarged microphotometer record of an intense spectrum obtained with the medium quartz spectrograph.

THE SPECIFIC HEATS OF CRYSTALLINE SOLIDS: PART I*

By Sir C. V. Raman

(Memoir No. 101 *of the Raman Research Institute, Bangalore*-6)

A correct appreciation of the nature of the thermal agitation in a crystal is obviously of fundamental importance in the physics of the solid state. Closely related to it is the problem of evaluating the heat content of a crystalline solid as a function of the temperature. These topics have formed the subject of some recent studies by the present writer. From them has emerged a theory of the specific heats of crystalline solids which is both simple and comprehensive and which succeeds in establishing a quantitative relationship between the thermal properties and the spectroscopic behaviour of crystals and accounts for the facts of observation in both of these fields. It accordingly seems opportune to offer a connected review of the subject in which the basic principles are set forth as simply and clearly as possible.

2. Some General Considerations

A crystal is an assembly of great numbers of atoms (of the same or of several different species) in a three-dimensionally periodic array in space. Macroscopically regarded, a crystal of finite size is a single physical entity; and those problems concerning its physical behaviour in which the discrete atomic structure does not need to be specifically considered can be dealt with on that basis. But neither the evaluation of the thermal energy of the solid nor the determination of its spectroscopic behaviour is a problem of that nature. For, the discrete atomic structure of the solid is the very essence of both of these problems and it must therefore form the basis of any theoretical considerations regarding them. It is therefore a misconceived and irrational procedure to assume—as is done in the theories of Debye and Born—the macroscopic crystal to be itself the oscillating unit whose modes and frequencies of vibration determine the thermal properties and the spectroscopic behaviour of the solid. While we have necessarily to reject such an approach as inadmissible, we are also precluded from assuming that the individual atoms in the crystal are the oscillators with which we are concerned. This is obvious, for the atoms in a crystal are linked together by forces of a physico-chemical nature and hence they cannot oscillate independently of each other.

* Reprinted from *Current Science* for July 1957.

Thus, when both of these extreme suppositions are laid aside, we are left with the following questions requiring an answer. What are the oscillators which determine the thermal properties and the spectroscopic behaviour of a crystal? How are they to be enumerated, and in what manner are their modes and frequencies of vibration to be determined? The answers given to these questions stand at the very base of the problems now under consideration.

3. THE NORMAL MODES OF VIBRATION

The fundamental theorem in classical mechanics regarding the small vibrations of a system of connected particles, taken in conjunction with the three-dimensional periodicity of structure characteristic of the crystalline state, furnishes us with the key to the solution of our problem. The theorem referred to states that the possible vibrations of the system are superpositions of a set of normal modes, in each of which the particles of the system (in the present case, the atoms) vibrate with the same frequency and in the same or opposite phases. Hence, any mode of vibration which satisfies this description and which can be regarded as a characteristic property of the crystal must also satisfy the further criterion that it remains the same when the crystal is given a unit translation along any one of the three axes of its structure. This can obviously happen in two ways: following the unit translation, equivalent atoms in the adjacent cell retain their amplitudes and phases of vibration unaltered, or alternatively, while the amplitudes remain the same, the phases are all reversed. Thus, we have $2 \times 2 \times 2$ or 8 different possible situations. If there are p atoms in each unit cell of the crystal structure, each of the 8 possible situations give us $3p$ solutions of the equations of motion of the p atoms in the unit cell, in other words, indicates $3p$ normal modes of vibration with their respective frequencies which can be regarded as characteristic of the structure of the crystal. Thus, in all, we have $24p$ solutions of the equations of motion which may be divided into three groups: $(3p - 3)$ normal modes in which equivalent atoms in adjacent cells oscillate with identical amplitudes and phases; $21p$ other normal modes in which the amplitudes of equivalent atoms in adjacent cells are the same but their phases alternate along one, two or all three of the axes of the crystal structure; and finally, the 3 excluded translations.

4. THE OSCILLATORS AND THEIR ENUMERATION

We proceed to consider the physical significance of the results deduced and stated above. What they indicate is that we shall not be justified in identifying the groups of p atoms each which form the units of the crystal structure as the "oscillators" in specific heat theory, since their juxtaposition in the ordered structure of the crystal results in an eight-fold increase in

the number of distinct frequencies of internal vibration which these groups of p atoms each would possess if isolated from each other. We have also to recognize the existence of additional modes of vibration within the crystal made possible by the translatory movements of the atomic groups as distinct from their internal vibrations. It is to be remarked, however, that the $(24p - 3)$ normal modes of vibration with discrete frequencies indicated by the theory can be regarded as the *internal* modes of vibration of the groups of $8p$ atoms each to be found in volume elements whose dimensions are twice as large in each direction as those of the unit cells of the crystal structure. If the entire crystal encloses N unit cells, the number of groups of $8p$ atoms included in it would be N/8. Multiplying this by $(24p - 3)$ which is the number of their internal modes of vibration, and adding to the product the number of degrees of the translatory freedom of movement of the same groups, we recover $3Np$, which is the total of the number of degrees of freedom of atomic movement in the crystal.

5. The Vibration Spectra of Crystals

Thus, the atomistic approach to specific heat theory leads us directly to a result which is of fundamental importance in relation to the spectroscopic behaviour of crystals, namely, that by far the largest proportion of the atomic degrees of freedom of movement in crystals is manifested in their vibration spectra as a set of discrete monochromatic frequencies $(24p - 3)$ in number, p being the number of atoms in the unit cell, only the three omitted translations manifesting themselves in what may be designated as the " residual spectrum " comprising the lowest frequencies of vibration and having a different character which we shall consider presently. The nature of the vibration spectrum of a crystal as stated above which is indicated by the theory might have been anticipated *a priori* on general grounds. For, a crystal comprises within itself an immense number of similar and similarly situated groups of atoms which would necessarily be of identical dynamical behaviour. Hence, the modes and frequencies of internal vibration of these groups would all be the same and would be a characteristic property of the crystal. The reason why we have $(24p - 3)$ discrete frequencies and not $(3p - 3)$ is also readily understood. The additional $21p$ frequencies arise because of the coupling of the oscillators located along each of the axes of the structure, an effect analogous to that observed in the simple case of two similar oscillators which when coupled to each other exhibit two distinct frequencies of vibration instead of only one.

We must now consider the nature of the " residual spectrum " briefly alluded to above. This spectrum embodies the oscillatory movements arising

from the *translations* of volume elements of the crystal each containing $8p$ atoms; they may be described as *internal vibrations* in volume elements of still larger size and therefore having lower frequencies. The frequency ν of such a vibration can evidently range from a lower limit $\nu = 0$ to the upper limit $\nu = \nu_L$, ν_L being the lowest of the $(24p - 3)$ discrete frequencies of atomic vibration. The manner in which the disposable $3N/8$ degrees of freedom would be distributed over this range of frequencies can be deduced by a very simple argument. The total number of volume elements of any specified dimensions included in the crystal, and therefore also the number of degrees of freedom represented by their *translations* would diminish in inverse proportion to the cube of their linear dimensions, while the frequencies of their *internal vibrations* would vary inversely as the first power of the same. Hence the number of degrees of freedom appearing in the residual spectrum in the range of frequencies between 0 and ν would be proportional to ν^3. By differentiation, we obtain the result that the number of degrees of freedom appearing between frequencies ν and $\nu + d\nu$, in other words, the number of oscillators in the crystal having frequencies in that range, would be $3N/8 \times 3\, \nu^2 d\nu / \nu_L{}^3$.

6. QUANTISATION OF THE VIBRATIONAL ENERGY

In his classic paper of 1907 introducing the quantum theory of specific heats, Einstein showed that the acceptance of his theory of light quanta inevitably leads to the conclusion that the energy of the mechanical vibration of elementary oscillators—such as the molecules of a gas or the structural units in a crystal—would also be related to their respective frequencies by the quantum rules. He also indicated a procedure by which the thermal energy of a crystal could be evaluated as a function of the temperature on the basis of the quantum hypothesis. He identified the thermal energy of the crystal with the energy of mechanical vibration of an immense number of *individual* oscillators distributed over its volume. It was assumed that these oscillators could be grouped into sets, each set comprising a great number of individual oscillators characterised by a common frequency of vibration. The total number of the oscillators of all kinds was taken to be equal to thrice the number of the atoms comprised in the crystal. The oscillators themselves were assumed to be harmonic and to occupy the various energy levels allowed by the quantum hypothesis for the particular frequency. The thermodynamic principle of Boltzmann was then introduced, leading to the result that the numbers of the oscillators occupying the various permitted levels are in the relative proportions indicated by that principle, and determined by the respective energies and by the temperature. The average energy of the oscilla-

tors in each of the sets was then evaluated. Summing up over all the oscillators in each of the sets and then over all the sets, Einstein obtained an explicit formula for the thermal energy of a crystal as a function of the temperature.

Einstein's ideas necessarily form the basis of any rational approach to the solution of the specific heat problem for crystals. For, they are based on an atomistic approach to the problem and effect a synthesis of the results of classical dynamics with the notions of the quantum theory and the basic principles of thermodynamics, in other words, of all the three disciplines which find a place in the problem. Einstein's formulation, however, had the weakness that he left unanswered three important questions: What precisely are the individual oscillators contemplated in the theory? How are they to be enumerated? How should their frequencies of vibration be determined? Also, to enable his theory to be applied in the particular case of diamond, Einstein assumed that the individual atoms in that crystal were themselves the oscillators contemplated in his theory. This was an oversimplification which resulted in discrediting Einstein's theory. For, that assumption was theoretically unsustainable and it also led to values for the specific heats at low temperatures which were in disagreement with the experimental facts elicited by later investigations. It is not surprising in these circumstances that Einstein's approach to the specific heat problem was laid aside, and that other and totally different ways of approaching the same problem gained general acceptance.

The present approach to specific heat theory is in a sense a rehabilitation of Einstein's original ideas. It fills in the lacunæ left by him and we are thereby enabled to make use of Einstein's formulæ just as they stand for an evaluation of the thermal energy of the crystal. But, before we proceed to write down the expressions, it appears desirable to emphasize certain fundamental aspects of Einstein's theory which also find a place in the present approach to the subject. Einstein's application of Boltzmann's statistical-thermodynamical principle finds its logical justification in the fact that the crystal is regarded as an assembly of great numbers of similar oscillators capable of exchanging energy with each other and forming a system in thermodynamic equilibrium. The use of the principle implies that the energy of vibration of the individual oscillators of each sort exhibits fluctuations over the volume of the crystal both in space and in time, the magnitude of these fluctuations being naturally the greater, the higher the frequency of the oscillator considered. This picture of the thermal agitation in crystals is fundamentally in accord with the actual facts of crystal architecture as well as with

the principles of thermodynamics, but it is very remote indeed from any ideas of its nature based on the notions of macroscopic physics.

Another feature of Einstein's theory which he himself stressed is the intimate relationship which it indicates between the thermal properties and the spectroscopic behaviour of crystals. The same relationship is also a feature of the present theory. But, the latter goes further than Einstein's, since it specifies the number of sets of oscillators which are the carriers of the thermal energy and also indicates the procedure by which their frequencies may be evaluated. Properties descriptive of the macroscopic behaviour of solids, *viz.*, their elastic constants, do not as such find a place in the present theory of the specific heats of crystals.

7. EVALUATION OF THE SPECIFIC HEATS OF CRYSTALS

Making use of the reasoning employed by Einstein, we obtain the following expression for the heat content of a volume of a crystal containing N unit cells of the crystal structure as a function of the temperature, namely

$$\frac{N}{8}\left[\sum_{i=1}^{24p-3}\frac{h\nu_i}{e^{h\nu_i/KT}-1}+\frac{3}{\nu_L{}^3}\cdot\int_0^{\nu_L}\frac{3\,h\nu^3 d\nu}{e^{h\nu/KT}-1}\right]$$

The numerical factor 1/8 appears in the expression because each oscillator comprises 8 unit cells of the crystal structure. On differentiating the expression with respect to T, we obtain the formula for the specific heat.

The following remarks may be made regarding the numerical evaluation of the expression given above. All the $(24p-3)$ frequencies would be distinct from each other only in the case of a completely anisotropic crystal. If any symmetry elements are present, the number of distinct frequencies would be naturally diminished, but the formula remains the same. Such reduction in the number of distinct frequencies would appear both in respect of the $(3p-3)$ frequencies in which both the amplitudes and the phases are the same in adjacent unit cells and in the $21p$ others in which the phases may be opposite, as already explained. As an illustration of these remarks, we may consider a case in which $p=2$ and the crystal belongs to the cubic class and its structure consists of two interpenetrating face-centred cubic lattices. The $(3p-3)$ distinct frequencies then reduce to a single triply degenerate frequency: the $21p$ or 42 other vibrations reduce to only eight distinct frequencies, the modes relating to all of which may be readily described in geometric terms connected with the structure of the crystal.

Since the first term in the expression for the thermal energy is a summation extended over $(24p - 3)$ distinct modes of vibration, while the second represents the residual spectrum, it is evident that the latter would be of minor importance relatively to the first, especially in those cases where p is large, in other words when the crystal has a multi-atomic structure. The position is a little different when p is small, as for example, when p is equal to 1. The contribution from the second term would not then be altogether negligible in comparison with the first term. The second term also acquires some importance relatively to the first at very low temperatures. For, since the frequencies appearing in it are low, their contributions to the specific heat would survive when those due to the vibrations of the higher frequencies appearing in the first term have dropped out by reason of Boltzmann's principle.

THE SPECIFIC HEATS OF CRYSTALLINE SOLIDS: PART II*

By Sir C. V. Raman

(*Memoir No.* 101 *of the Raman Research Institute, Bangalore*-6)

The theory of the specific heats of crystals expounded in the first part of this review is similar in its approach to that originally proposed by Einstein in the year 1907, but it fills up the lacunæ left in that theory and succeeds in connecting the thermal energy of crystals with their spectroscopic behaviour, as also in explaining the facts of observation in both of these fields. It is hoped on some later occasion to set out the results following from the theory in greater detail and to illustrate them by specific examples. The present review will conclude with some comments on the theory of the specific heats of crystals put forward by Debye in the year 1912 and the closely analogous theory published by Born and Karman at about the same time. A whole generation of physicists and chemists has been persuaded to believe that these theories embody valid physico-mathematical thought and that they satisfactorily account for the facts of observation. These are circumstances which justify the inclusion in the present review of some critical remarks on those theories.

2. The Fundamentals of Specific Heat Theory

We may usefully commence our examination by recalling the ideas embodied in Einstein's paper of 1907 in the form of three distinct propositions.

I. A crystal is an assembly in thermodynamic equilibrium of an immense number of individual oscillators which are divisible into sets, each set consisting of a great number of oscillators characterised by a common frequency of vibration.

II. The total number of oscillators of all sorts is equal to thrice the number of atoms comprised in the crystal.

III. The vibrational energy of each individual oscillator is quantised and its average value taken over its different possible energy states may be determined by the aid of Boltzmann's principle.

The first of these propositions finds its justification in the known physical features of crystal architecture. The second proposition follows as a logical deduction from the first taken in conjunction with the results of classical

* Reprinted from *Current Science* for August 1957.

mechanics. The third proposition is a logical consequence of the principles of thermodynamics and the quantum theory when applied to the circumstances stated in the first proposition. In the earlier part of this review, it has already been shown how these propositions enable us to deduce both the thermal and the spectroscopic behaviour of crystals.

3. The Theories of Debye and Born

The basic idea underlying these other theories is that the thermal energy of a crystal may be evaluated in the same manner as the energy density of thermal radiation within a perfectly reflecting enclosure, in other words, by summing up the kinetic and potential energies of sets of wave-trains which are assumed to fill the volume of the solid and form stationary wave-patterns in its interior. J. H. Jeans who was the original proposer of this idea indicated in his paper of 1909 a way of escape from the more obvious difficulties which arise when it is sought to make use of it. Debye and Born who derived their inspiration from Jeans naturally also took over from his paper the special assumptions needed to put his ideas into quantitative form. These special assumptions figure prominently in both of the theories and are indeed their most characteristic feature.

The stationary wave-patterns considered by Debye were those contemplated in the classical theory of elasticity for a solid of finite volume. An enumeration on the basis of that theory shows the total number of modes of vibration to increase—without any upper limit—proportionately to the cube of the frequency up to which the enumeration is carried. To enable the enumeration thus made to form the basis of specific heat theory, Debye assumed that the enumeration is valid only up to a certain upper limit of frequency and that no modes of vibration with higher frequencies exist; the upper limiting frequency was so chosen that the number of wave-patterns is equal in number to thrice the number of atoms comprised in the crystal.

The waves considered by Born are of a more general type than those considered in the Debye theory. Whereas Debye limited himself to the consideration of crystals of comparatively simple type, *viz.*, those containing a single species of atom and belonging to the cubic system, the theory of Born accepts no such limitation and indeed claims to be applicable to all crystals. The special assumption which figures in the Born theory is the well-known " cyclic postulate " which selects the permitted wave-lengths of the stationary wave-patterns filling the solid in such manner that the total number of wave-patterns is equal to thrice the number of atoms comprised in the crystal.

The questions which arise and which need to be considered are the following: Are the approaches to specific heat theory briefly summarized above logically sustainable? Are the ideas on which they are based and the conclusions to which they lead compatible with the fundamental principles of classical mechanics, thermodynamics and the quantum theory? We shall consider these questions and presently find that the answer is in each case definitely in the negative.

4. THE LOGICAL FALLACY

A simple calculation shows that the frequencies of vibration which determine the variation of the specific heats of crystals with temperature lie in the infra-red region of the spectrum. It follows that the oscillators which are the carriers of the thermal energy are the ultimate structural elements in the crystal. This is further confirmed by the fact that when the atoms are firmly bound together in the structural elements of the crystal, as is the case for example with diamond, the specific heats are low and the vibrational frequencies estimated from them are high; the latter inference receives direct support from spectroscopic studies. It follows from these remarks that the approach to the specific heat problem made in the theories of Debye and Born is totally misconceived. These authors concern themselves with an entirely different and irrelevant subject, namely, the vibrations of a macroscopic solid and proceed to determine and enumerate them, treating it as a boundary-value problem in wave-propagation. It is easily shown that the results thus obtained are wholly unrelated to the specific heat problem. We have only to recall that wave-motion is a kinematic concept. Hence the stationary wave-patterns inside an enclosure can be described in purely geometric terms without any reference to the question whether the material traversed by the waves does or does not possess a discrete structure. In other words, there is no nexus or connection between the stationary wave-patterns assumed to exist in the medium and the discrete structure, if any, which it possesses. It is not surprising in these circumstances that Debye and Born are obliged to introduce postulates into their theories which assume the existence of such a relationship. We have only to remark that such postulates or assumptions savour of sophistry and that theories embodying them can lay no claim to logical validity.

5. FALSITY OF THE DYNAMICAL CONSEQUENCES

The theories of Debye and Born are attempts to carry over the ideas and methods of macroscopic physics into the fields of atomic dynamics, thermodynamics and quantum theory where they are inappropriate and indeed wholly out of place. The procedures they adopt naturally lead to consequences

which are irreconcilable with the basic principles of these disciplines and the results following from them.

Considering the matter first from the standpoint of atomic dynamics, it is clear that we are not concerned here either with wave-propagation or with any boundary value problem. Specific heat theory rests on the determination and enumeration of the normal modes of vibration of the ultimate particles of the material, in other words, of the atoms present in the structure of the crystal. Since the range of the interatomic forces is limited and small compared with the dimensions of any crystal of macroscopic size, these normal modes are determinable from the structure of the crystal without any reference to the size of the crystal or to the conditions at its external boundary. This also becomes evident when we compare the frequency of the atomic oscillations with the frequency of the elastic oscillations of a macroscopic crystal. The former is very great in comparison with the latter even for a crystal of colloidal dimensions. Hence the oscillations of the atoms in the interior of a crystal repeat themselves many thousands of times, thereby defining their frequency with all necessary precision, before any disturbance originating in the interior of the crystal could travel out to reach its surface and return after reflection to the place of its origin. Hence, whether the boundary is there or not makes no difference to the modes and frequencies of atomic vibration.

The fallacy of identifying the atomic vibrations with stationary wave-patterns is obvious even in such simple cases as those considered by Debye. The vast majority of the stationary wave-patterns assumed in his theory to be the carriers of the thermal energy of the crystal have wave-lengths of the same order of magnitude as its lattice spacings. These are precisely the circumstances in which it is not permissible to identify the dynamical behaviour of a discrete structure with that of a medium of uniform density. The consequence of such identification is to endow the crystal with an immense number of modes of vibration with frequencies all different from each other throughout the range under consideration and thus to present a false picture of the spectroscopic behaviour of the crystal.

Though Born's theory nominally takes account of the discrete lattice structure of crystals, his " postulate of the cyclic lattice " is equivalent to assuming that the normal modes of vibration of the atoms are similar to the oscillations of the volume elements in a continuous solid having the same shape as the unit cell of the crystal but of greatly enlarged size. The stationary vibrations permitted by the postulate accordingly appear in immense numbers with wave-lengths and frequencies all different from each other

and with their modes wholly unrelated to the structure of the crystal. It is important to remark in this connection that Born does not restrict himself to simple lattice structures but also claims his theory to be valid for all crystals. Any one who appreciates the nature of the results following from Born's lattice theory will realize that the ideology behind his dynamics is completely false. In effect, Born endows the atoms in a crystal with a vast number of modes and frequencies of vibration which are wholly unrelated to its internal architecture and which have a continuous spectrum of frequencies, a result which is in flagrant contradiction with the facts of observation revealed by spectroscopic investigations.

6. CONFLICT WITH THERMODYNAMICS

A stationary wave-pattern is a mode of vibration in which all the volume elements of the medium oscillate with the same frequency and in the same or opposite phases and with relative amplitudes which remain invariant with time. Vibrations of this type are characteristic of a macroscopic solid and can be considered as its normal modes of vibration and determined by the methods of the classical theory of elasticity. Such vibrations can also be set up and maintained in an elastic solid artificially, as for example, by the use of a piezo-electric oscillator attached to it.

The identification of the thermal agitation in crystals with stationary wave-patterns of the nature described above which is postulated in the theories of Debye and Born is however clearly irreconcilable with the statistical concept of the nature of thermal energy in material bodies. Thermal agitation is envisaged in Boltzmann's entropy-probability principle as a chaotic and fluctuating disturbance varying in its character and intensity from instant to instant and from place to place within the material. Atomic groups of similar nature which are located in parts of the crystal not contiguous to each other may indeed vibrate with the same frequency. But there can be nothing in the nature of definite relationships either in their amplitudes or in their phases of vibration persisting in time.

The issue can also be put a little differently. A crystal is an assembly of an immense number of individual atoms which are capable of moving from their positions of equilibrium. Hence the state of the system can only be described in terms of the values of a very large number of independent variables. The interactions between neighbouring atoms would naturally influence their relative movements and determine their modes and frequencies of vibration. But we cannot in any circumstances regard the entire assembly as a single unit in the thermodynamic sense or postulate constancy of ampli-

tude or coherence of phase in the atomic vibrations over its entire volume. A description of the thermal agitation in precisely defined terms is possible only for domains of space and periods of time which are small in comparison with macroscopic standards. In other words, the entire ideology behind the theories of Debye and Born is incompatible with the fundamental notions of the nature of thermal energy which lie at the base of the science of thermodynamics.

7. Misinterpretation of the Quantum Theory

As has been shown above, the theory of specific heats can be placed on a logically sustainable basis only if we recognize that the oscillators which are the carriers of the thermal energy are the structural elements in the crystal. We then obtain a picture of the thermal agitation in the solid which is consistent with the general principles of dynamics and of thermodynamics. Necessarily, therefore, it is these same oscillators whose vibrational energies must be assumed to be quantised. Since, further, these oscillators are present in large numbers distributed over the volume of the crystal, we have a logical justification for the use of Boltzmann's principle in conjunction with the quantum hypothesis for the evaluation of the average energy of the oscillators of any particular frequency and therefrom also the evaluation of the heat capacity of the entire crystal.

To the fallacies which vitiate the Debye and Born theories we have therefore to add one more, *viz.*, that they give a fantastic and altogether meaningless interpretation to the postulates of the quantum theory. They proceed to quantise the energy of the normal modes of vibration of a macroscopic crystal; in doing this, they ignore the fact that the theory of quanta possesses a meaning and significance only in relation to the behaviour of the physical entities which the language of determinism characteristic of macroscopic physics cannot successfully describe. For example, we can speak meaningfully of quantising the energies of rotation or vibration of a molecule of benzene; but it is patently absurd to quantise the vibrations of a tuning fork or the rotations of a flywheel.

Reprinted from "The Proceedings of the Indian Academy of Sciences",
Vol. XLVI, No. 4, Sec. A, 1957

LIGHT PROPAGATION IN ABSORBING CRYSTALS POSSESSING OPTICAL ACTIVITY

BY S. PANCHARATNAM

(*Memoir No.* 102 *from the Raman Research Institute, Bangalore-6*)

Received September 24, 1957

(Communicated by Sir C. V. Raman)

§ 1. INTRODUCTION

AN excellent though unsuspected example of a biaxial crystal possessing both optical activity and pronounced pleochroism was brought to light—in the shape of certain intensely coloured sectors of amethyst—during certain optical studies on this material. Interference figures of a remarkable nature—to be illustrated and discussed in a later paper—were exhibited by these areas. Indeed, it was the peculiarity of the optical phenomena displayed, which first invited the present investigation on the theory of light propagation in such media—a theory which provides, as we shall see, a simple basis for their explanation. Such a theory has also a more general interest: for instance, the measurement of the rotatory power of a biaxial crystal along an optic axial direction cannot be pursued into the absorbing regions of the spectrum without taking cognizance of its results (§§ 8 and 9*c*).

It has been established that the behaviour of both transparent active crystals (Pockels, 1906; Bruhat, 1930) and inactive absorbing crystals (Pancharatnam, 1955 *a*, *b*; Jones, 1942) may be physically pictured and quantitatively explained by a principle of the superposition of the 'elementary properties' associated with the medium. Thus linear birefringence has to be blended either with optical rotation (circular birefringence) or with linear dichroism—according as we are dealing with the former or latter class of crystals. Following the same geometrical method as was adopted for non-active absorbing crystals (Pancharatnam, 1955 *a*; hereafter referred to as P-*a*) we shall discuss the propagation in an active absorbing crystal as due to the superposed effects of linear birefringence, linear dichroism and optical rotation. For any particular direction of propagation, the last-mentioned properties are to be determined respectively, in the usual manner from the corresponding surfaces which characterise the optical properties of the medium; *viz.*, the index- and absorption-ellipsoids (*see* P-*a*, § 2 *a* and § 4 *d*), and the surface of optical rotation. Were this not the case, the method of superposition would have little practical value since the directional variation

of the properties of the medium—as revealed for example in convergent light phenomena—is naturally the most interesting part of the optics of anisotropic media.

It turns out that the two waves that can be propagated along any direction not only possess different velocities and coefficients of absorption, but are in different states of elliptical polarisation, the geometrical forms of which bear no simple relation to one another (§ 4)—except in certain special cases (§§ 7 and 8). The practical advantage of the method of superposition in such a complex case can be properly appreciated only in a later paper, where the principal results are experimentally confirmed. Sections 2–8 deal with media possessing no circular dichroism—the latter being a property which need not be exhibited in all the absorption bands (Lowry, 1935). The results may, however, be expected to apply fairly accurately for all crystals where linear dichroism is visible to the eye—since circular dichroism, even when present, is usually an extremely feeble effect. In § 9 we shall formally include the effects of circular dichroism, using again the principle of superposition.

For the case of absorbing crystals, the method of superposition was first introduced by Jones (1942, 1948) while developing a comprehensive matrix calculus treatment for general optical systems. Jones did not then pursue the method in sufficient detail as to give an overall picture of the optical properties of anisotropic absorbing media. He has, however, recently (Jones, 1956) attempted to correlate his method with the results of the electromagnetic theory; it will be pointed out in a later paper that this portion of his discussion contains an error as far as its applicability to optically active media is concerned.

Pending a more direct theoretical explanation (*see* § 6) as to why the method of superposition works even under the most diverse conditions (Ramachandran and Ramaseshan, 1952; Ramachandran and Chandrasekharan, 1951), its justification in the present instance has to be based on the equivalence of its results with those of the electromagnetic theory of light propagation in active absorbing crystals. The electromagnetic theory will be discussed in a later paper. We may mention that the theory has thus far been solved only for uniaxial crystals (Forsterling, 1912, quoted in Szivessy, 1928).

§ 2. Physical Description of the Method of Analysis

Consider a crystal plate cut perpendicular to an arbitrary direction of propagation Oz, which direction we may with advantage take as being normal to the plane of the paper (*see* Fig. 1 *a*). We first wish to find the states of polarisation of the two plane waves that can be propagated along this direction

(with specific velocities and coefficients of absorption). The principle of the method adopted may be described as follows. Suppose we are given the state of polarisation P, and the phase, of the elliptic vibration incident on the plane z in the medium. Then if the crystal possessed no linear dichroism, the state of polarisation P′ and the phase of the elliptic vibration emerging at the plane $(z + dz)$ could be completely determined from the theory of

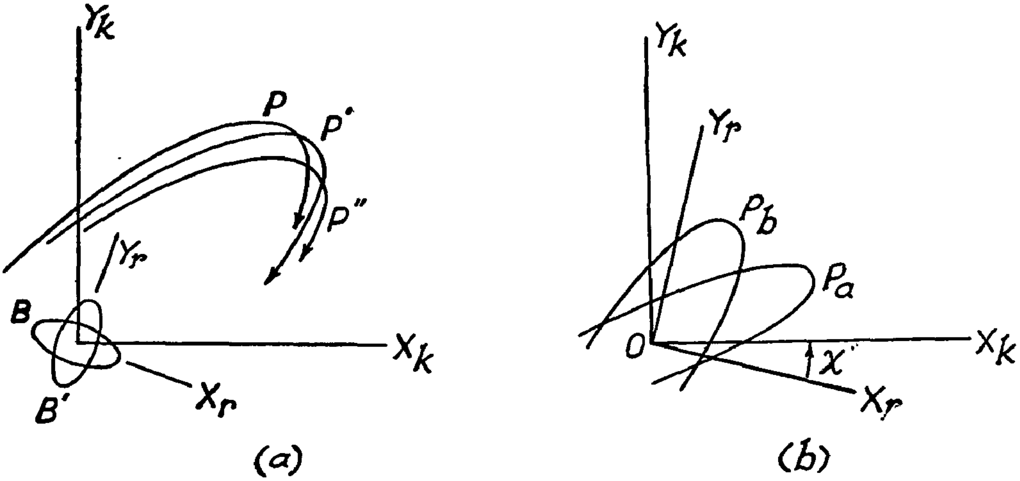

FIG. 1. P—State of polarisation at plane z. P′—State of polarisation at $(z + dz)$ if crystal were transparent. P″—State of polarisation at $(z + dz)$ with linear dichroism also present. P_a, P_b—States propagated unchanged in absorbing active crystal (*i.e.*, states for which P = P″). B, B′—States propagated unchanged in transparent active crystal (*i.e.*, for which P = P′). OX_k, OY_k—States propagated unchanged with linear dichroism *alone* present.

propagation in *transparent* active crystals. Since the crystal possesses linear dichroism, we regard the actual vibration emerging at the plane $(z + dz)$ as obtained by further subjecting the vibration P′ to the following operation of linear dichroism: the vibration P′ is first resolved into its components along the *principal planes of linear dichroism* OX_k and OY_k; the amplitudes of these components are then multiplied by the reducing factors $(1 - k_1 dz)$ and $(1 - k_2 dz)$ respectively, where k_1 and k_2 are the principal absorption coefficients if only dichroism were present. (OX_k and OY_k are parallel to the major and minor axes of the elliptic section of the absorption ellipsoid made by the xy plane.) The operation of dichroism not only causes a diminution in the intensity; because of the differential absorption of the two components the vibration at the plane $(z + dz)$ is now altered to the state of polarisation P″.

In general, however, we shall show that there will be two particular forms of the initial elliptic vibration P for which the vibration P″ at the plane $(z + dz)$ will be in the *same* state of polarisation as the vibration at the plane

z, being therefore altered only in intensity and phase.* These will therefore be the required states of polarisation P_a and P_b of the two waves that can be propagated along the z direction with specific velocities and coefficients of absorption (Fig. 1 *b*).

§ 3. Geometrical Formulation of the Problem

(*a*) *The Poincaré sphere.*—The problem of finding these states of polarisation P_a and P_b permits of an elegant solution if we take recourse to the Poincaré sphere (*see* Fig. 2)—as was done for inactive absorbing crystals (P-*a*). The state of polarisation of any particular elliptic vibration described in the *xy* plane is represented by a specific point on the surface of this sphere.

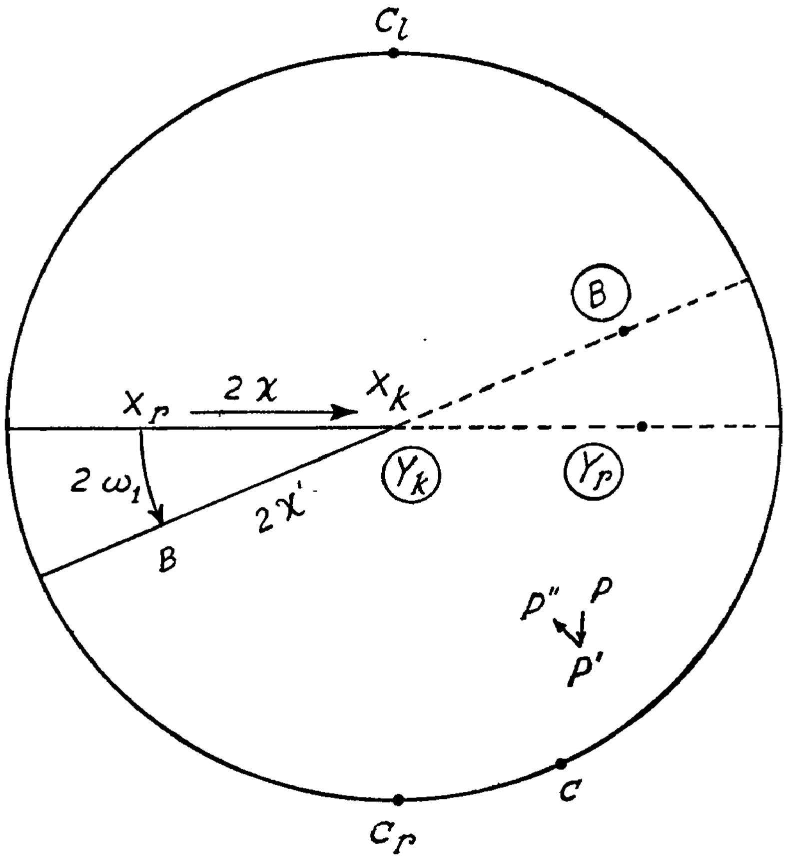

FIG. 2. Representation on the Poincaré sphere of the states described under Fig. 1 *a*. State P′ is obtained from P by a clockwise rotation Δdz of the sphere about BB. State P″ is obtained by displacing P′ towards the less absorbed component X_k through a distance $k\,dz \sin PX_k$.

* The sequence in which the two infinitesimal operations are applied is immaterial (if we neglect second order quantities). To prove this, consider the passage of light through a packet made up of infinitesimal lamellæ of two types, the odd members being transparent and the even members absorbing; the effect will not be modified (except to an infinitesimal extent) if the first transparent lamella is removed and placed last.

2

The definition of the mapping allows the form of the ellipse represented by any point to be directly visualised in terms of the longitude 2λ and the lattitude 2ω of the point; for λ is the azimuth of the major axis and ω the angle of ellipticity.

Thus two linear vibrations along OX_k and OY_k will be represented respectively by two diametrically opposite points X_k and Y_k on the *equator* of the sphere, Fig. 2 being drawn such that the diameter X_kY_k is normal to the plane of the paper. The states of elliptic polarisation of the slower and faster waves that can be propagated in the Oz direction in the absence of linear dichroism will be respectively represented by two diametrically opposite points B and B′. From the theory for transparent active crystals we may regard the oppositely polarised states B and B′ as known, as also the '*elliptic birefringence*' Δ in the absence of linear dichroism, *i.e.*, the phase retardation which the slower wave B suffers *relative* to the other per unit distance traversed.

The relevant results from the theory of propagation in *transparent active crystals* may be briefly recalled. The states B and B′ have respectively the same longitudes as the opposite points X_r and Y_r on the equator which represent the principal planes of linear birefringence OX_r and OY_r (drawn in Fig. 1). Denoting by $2\omega_1$ and $(-2\omega_1)$ the latitudes of B and B′ we have

$$\left.\begin{aligned} \tan 2\omega_1 &= -\frac{2\rho}{\delta} \\ \Delta^2 &= \delta^2 + (2\rho)^2 \end{aligned}\right\} \tag{1}$$

where ρ is the optical rotatory power for the direction of propagation considered, and δ the linear birefringence, as determined from the index-ellipsoid. The mean of the refractive indices of the waves is the same as in the absence of optical activity (Szivessy, 1928; *see* also § 9 *b* below); *i.e.*, if Δ_1 and Δ_2 be the absolute phase retardations suffered per unit distance by the slower and faster waves, δ_1 and δ_2 being the corresponding values in the absence of optical activity, then

$$\Delta_1 + \Delta_2 = \delta_1 + \delta_2 \tag{2}$$

(*b*) *Choice of co-ordinate axes in the Poincaré sphere.*—The state of polarisation of the arbitrary elliptic vibration at the plane z (referred to in the previous section) will be represented by a general point P on the Poincaré sphere. We wish to find the condition that the state P should be propagated unchanged. Hence the point P may be most conveniently specified by giving the cosines of the respective angular distances 2ψ, 2ϕ, 2ξ, which it makes with the reference points X_k, B, and a third point C

on the sphere: these points form a right-handed system, the point C being at an angular distance of $\frac{1}{2}\pi$ from X_k and B. (Since the squares of three direction cosines are not independent it is sufficient to specify $\cos 2\psi$ and $\cos 2\phi$ and give merely the sign of $\cos 2\xi$.) The specification of the state of polarisation P by 'direction cosines' is closely analogous to its specification by Stokes' parameters (Fano, 1949; Ramachandran, 1952; Pancharatnam, 1956 *b*). It must, however, be noted that our reference system does not form a rectangular co-ordinate system; the angular distance $2\chi'$ of X_k from B is in general different from $\frac{1}{2}\pi$, and we have

$$\cos 2\chi' = \cos 2\omega_1 \cos 2\chi = (\delta/\Delta)\cos 2\chi \tag{3}$$

where 2χ is the acute angle between OX_r and OX_k, and ω_1 the ellipticity of the slower vibration B in the absence of dichroism, as given by (1).

(*c*) *Operations of elliptic birefringence and linear dichroism.*—The state of polarisation P′—which would be described at the plane $(z + dz)$ if the crystal were a transparent active one—is obtained from P by an infinitesimal rotation of the sphere about the diameter BB′ through a clockwise angle Δdz (Pockels, *loc. cit.*). The infinitesimal movement $\overrightarrow{PP'}$ is therefore perpendicular to the arc BP and has a magnitude ds_R which is equal to $\Delta dz \sin 2\phi$ (*see* Fig. 2). To obtain the actual state of polarisation P″ at the plane $(z + dz)$, we subject the vibration in the state P′ to the infinitesimal operation of linear dichroism—whereupon we may expect it to move directly towards the state of polarisation X_k of the less absorbed component, and away from Y_k. It has been proved in a previous paper (Pancharatnam, 1955 *a*, § 4 *b*) that the infinitesimal movement $\overrightarrow{P'P''}$ *is* actually directed along the arc PX_k and has a magnitude ds_k equal to $kdz \sin 2\psi$, where k denotes the 'linear dichroism' $(k_2 - k_1)$.

§ 4. States of Polarisation of the Waves

We wish to find those states P $(2\psi, 2\phi, 2\xi)$ for which the state of polarisation P″ obtained after passage through a thickness dz is identical with P. The condition for this is obviously $\overrightarrow{PP'} = -\overrightarrow{P'P''}$, and this is equivalent to three conditions: (*a*) the magnitudes of the infinitesimal displacements due to elliptic birefringence and linear dichroism should be equal, *i.e.*, $ds_R = ds_k$; (*b*) the displacements $\overrightarrow{PP'}$ and $\overrightarrow{P'P''}$ should be collinear, *i.e.*, from what has been said above, $\angle X_kPB = \frac{1}{2}\pi$; (*c*) the diplacements should be opp ositely directed—which means that P is restricted to the hemisphere for which 2ξ lies between 0 and $\frac{1}{2}\pi$. Expressed mathematically the states P

which are propagated unchanged are those for which 2ψ and 2ϕ satisfy the relations:

$$\Delta \sin 2\phi = k \sin 2\psi \qquad (4)$$

$$\cos 2\phi \cos 2\psi = \cos 2\chi' \qquad (5)$$

together with the condition that $\cos 2\xi$ should be positive.

Let $P_a(2\psi_a, 2\phi_a)$ represent a state for which 2ϕ is less than $\frac{1}{2}\pi$, and which remains invariant under the operations of elliptic birefringence and linear dichroism (*see* Fig. 3). It is then geometrically evident that the state P_b which makes the same angular distances with the opposite points Y_k and B′, will also remain invariant under these operations; this may also be seen from the fact that equations (4) and (5) are unaltered *when* 2ϕ *and* 2ψ *are changed to their supplements.* These states are consequently propagated without change of form. It can be shown that in general there are only two such states, and no more [*see* equations (6) and (7) below]. From the figure it is seen that these states P_a and P_b are represented by two general points on the Poincaré sphere whose longitudes do not in general differ by π and whose latitudes are unequal. We thus arrive at the result that in a medium possessing optical activity, linear birefringence and linear dichroism, *the two polarised waves that can be propagated without change of form along any direction are in elliptical states of polarisation whose geometrical forms bear no simple relation to one another—i.e.*, the major axes of the elliptic vibrations are in general not crossed, their ellipticities are not numerically equal, and they may or may not be described in the same sense. Two polarised states such as P_a and P_b—not being represented by opposite points on the Poincaré sphere—are *non-orthogonally* polarised, and are capable of mutual interference (when coherent) to an extent determined by their ‘similarity factor’ $\cos^2 \frac{1}{2} P_aP_b$ (Pancharatnam, 1956 *a*). It is seen from the figure that the great circular arc P_aP_b is bisected by C, and hence the (common) third ‘direction cosine’ $\cos 2\xi$, of the two states acquires an importance as the factor expressing the degree of non-orthogonality of the two states of polarisation.

For the sake of completeness we shall give explicit expressions for the ‘direction cosines’ of the points P_a and P_b representing the states of polarisation of the two waves. By introducing in (5) the value of $\cos^2 2\psi$ obtained from (4) we obtain a quadratic in $k^2 \cos^2 2\psi$; the positive root of this quadratic (which alone will give a real solution for $\cos 2\psi$) is then found to be given by

$$k^2 \cos^2 2\psi = \tfrac{1}{2}\{(k^2 - \Delta^2) + \sqrt{(k^2 - \Delta^2)^2 + 4\Delta^2 k^2 \cos^2 2\chi'}\} \qquad (6)$$

Similarly, eliminating $\cos^2 2\phi$ between (4) and (5)

$$\Delta^2 \cos^2 2\phi = \tfrac{1}{2}\{(\Delta^2 - k^2) + \sqrt{(\Delta^2 - k^2)^2 + 4\Delta^2 k^2 \cos^2 2\chi'}\} \tag{7}$$

It may be recalled that in these equations $\cos 2\chi'$ is given by (3).

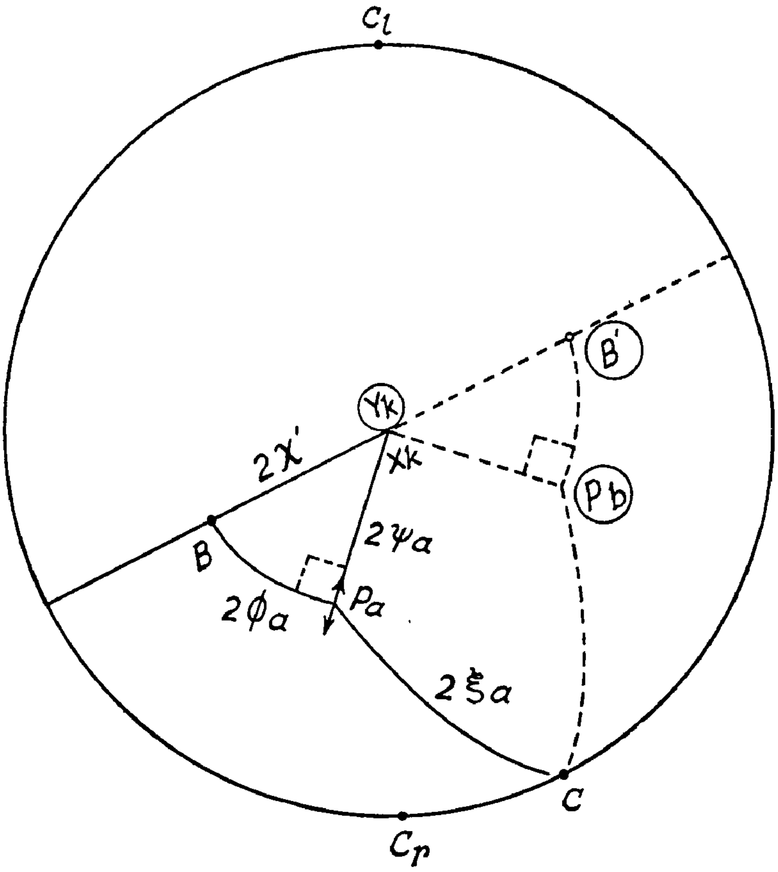

FIG. 3. P_a and P_b represent the states which remain invariant under the operations of elliptic birefringence and linear dichroism described under Fig. 2. The angular distances $2\psi_a$ and $2\phi_a$ of the slower state P_a from X_k and B, are also the angular distances of the faster state P_b from Y_k and B′.

Equation (6) gives two values of $\cos 2\psi$ which differ only in sign, while equation (7) gives two values of $\cos 2\phi$ which again differ only in sign. The corresponding pairs $(2\psi_a, 2\phi_a)$ and $(2\psi_b, 2\phi_b)$ are identified without ambiguity from the condition given by (5) that $\cos 2\phi$ and $\cos 2\psi$ have the same sign if $2\chi'$ lies between 0 and $\pi/2$, while they have opposite signs if $2\chi'$ lies between $\frac{1}{2}\pi$ and π.

The third 'direction cosine' $\cos 2\xi$ is always positive and is the same for both the states P_a and P_b; it is obtained from the first two by the following relation which we shall not prove here.

$$\cos 2\xi = \frac{\sin 2\phi \sin 2\psi}{\sin 2\chi'} \tag{8}$$

§ 5. Absorption Coefficients of the Waves

The absorption coefficients, k_a and k_b, of the waves in states P_a and P_b may be evaluated exactly as in the case of non-active crystals (Pancharatnam, 1955 *a*). The diminution of intensity $2k_a dz$ which a vibration of unit intensity in the state P_a suffers on travelling a distance dz arises entirely from the operation of dichroism; this operation diminishes the intensities of the X_k and Y_k components of the original vibration by $2\,k_1 dz \cos^2\psi_a$ and $2\,k_2 dz \sin^2\psi_a$. Hence we obtain, on addition,

$$\left.\begin{aligned} k_a &= \tfrac{1}{2}(k_1 + k_2) - \tfrac{1}{2}k\cos 2\,\psi_a \\ k_b &= \tfrac{1}{2}(k_1 + k_2) + \tfrac{1}{2}k\cos 2\psi_a \end{aligned}\right\} \tag{9}$$

so that

$$k_b - k_a = k\cos 2\psi_a \tag{10}$$

The absorption coefficients have thus been conveniently expressed as functions of the states of polarisation; they may also be otherwise expressed by using the explicit value of $k\cos 2\,\psi_a$ as obtained from (6). It may be recalled (P-*a*, equation 12) that for any one direction of propagation, k_1 and k_2 are proportional to b_1 and b_2—where $1/\sqrt{b_1}$ and $1/\sqrt{b_2}$ are the lengths of the corresponding principal radii of the absorption ellipsoid.

It is advantageous to anticipate here a small correction to the expression (9) and (10) given later by the electromagnetic theory; if the *extinction* coefficients of the waves be denoted by κ_a and κ_b, then the relations (9) derived by the method of superposition have to be replaced by

$$\left.\begin{aligned} 2\kappa_a v_a{}^3/c &= \tfrac{1}{2}(b_1 + b_2) - \tfrac{1}{2}(b_2 - b_1)\cos 2\psi_a \\ 2\kappa_b v_b{}^3/c &= \tfrac{1}{2}(b_1 + b_2) + \tfrac{1}{2}(b_2 - b_1)\cos 2\psi_a \end{aligned}\right\} \tag{11}$$

Because the velocities v_a and v_b of the waves have been dragged into these new expressions for the absorption coefficients, an exact application of (11) for directions near an optic axis is fraught with difficulty. Luckily for us, however, the error involved in using (9) will be negligible for such directions, since we may set $v_a \simeq v_b \simeq v_m$, where v_m is a mean velocity (*see* P-*a*, equation 14).

§ 6. Refractive Indices of the Waves

We shall next derive expressions for the refractive indices of the waves or, what is virtually the same thing, the respective phase retardations Δ_a and Δ_b which these waves suffer per unit distance of propagation. Our argument is somewhat involved but at the same time illuminating; for it very clearly indicates that the principle of superposition may be derived by regard-

ing the propagation in the medium as due to the forward scattering from induced doublets (*cf.* Jenkins and White, 1937; Kauzmann, 1957).

Let us consider the propagation through a distance dz of a vibration of unit intensity in the state of polarisation P_a. The effect of dichroism consists in diminishing the X_k and Y_k components (whose respective amplitudes are $\cos\psi_a$ and $\sin\psi_a$) by fractions k_1dz and k_2dz respectively. Alternatively the infinitesimal operation of dichroism is equivalent to the operation [which we denote by (a)] of *adding* to the original vibration the fractions $(-k_1dz)$ and $(-k_2dz)$ of its X_k and Y_k components. In the succeeding operation of elliptic birefringence the vibration thus obtained is resolved into its components in states B and B′, the phases of these components being then retarded by amounts $\Delta_1 dz$ and $\Delta_2 dz$ respectively (where Δ_1 and Δ_2 are the respective phase retardations per unit distance suffered by the two waves in the absence of dichroism). The operation of elliptic birefringence is therefore similarly equivalent to the operation [which we denote by (b)] of further adding on the fractions $(-i\Delta_1 dz)$ and $(-i\Delta_2 dz)$ of the B and B′ components of the original vibration itself (neglecting second order quantities). The occurrence of the imaginary $(-i)$ means that the added vibrations have a phase lag of $\frac{1}{2}\pi$ with respect to the corresponding B and B′ components of the original vibration; the 'amplitudes' of the latter components (that is, the square roots of their intensities) are $\cos\phi_a$ and $\sin\phi_a$ respectively.

But the original vibration in the state P_a is propagated without change of polarisation through the thickness dz under the combined effects of dichroism and elliptic birefringence. Hence—*insofar as its final contribution is concerned*—the effect of dichroism described in (a) becomes equivalent to the addition of two infinitesimal vibrations in the *same* state of polarisation P_a as the original vibration: these vibrations are really the resolved components in the state P_a of the corresponding vibrations described in (a); they will therefore have amplitudes $k_1dz\cos^2\psi_a$ and $k_2dz\sin^2\psi_a$; but they will be exactly opposed in phase to the original vibration, since only then will they diminish the intensity by $2k_adz$ as given by (9). It follows that the operation of elliptic birefringence (b)—*because of its complete formal similarity with* (a)—must be effectively equivalent to the addition of two infinitesimal vibrations (whose amplitudes are $\Delta_1 dz\cos^2\phi_a$ and $\Delta_2 dz\sin^2\phi_a$) which are in the same state of polarisation as the original vibration, but lag behind in phase by $\frac{1}{2}\pi$. The phase retardation per unit distance Δ_a, suffered by the wave is then equal to $(\Delta_1\cos^2\phi_a + \Delta_2\sin^2\phi_a)$. Or,

$$\left.\begin{aligned} \Delta_a &= \tfrac{1}{2}(\delta_1+\delta_2)+\tfrac{1}{2}\Delta\cos 2\phi_a \\ \Delta_b &= \tfrac{1}{2}(\delta_1+\delta_2)-\tfrac{1}{2}\Delta\cos 2\phi_a \end{aligned}\right\} \quad (12)$$

where we have used the fact that the mean refractive index in a transparent inactive crystal is the same as when optical activity is also present (Eq. 2). The birefringence is obtained from (12):

$$\Delta_a - \Delta_b = \Delta \cos 2\phi_a \tag{13}$$

When the refractive indices and the birefringence are not required as functions of the states of polarisation, we may introduce in (12) and (13) the explicit value of $\Delta \cos 2\phi_a$ as obtained from (7).

Since the arguments given above are somewhat involved it is worthwhile to indicate how the expression (13) for the birefringence (which alone is of much practical importance) may be *directly* derived. On travelling a distance dz, the alteration of the state of polarisation of any vibration (*e.g.*, from X_k to X_k'), may be evaluated by the method of superposition (as due to linear birefringence alone, in the example quoted). More properly, this alteration is connected with the relative phase retardation $(\Delta_a - \Delta_b)\, dz$ between the two waves (in states P_a and P_b) into which the original vibration will be decomposed; in fact the relative phase retardation must be equal to the area of the infinitesimal quadrilateral $P_a'X_kP_b'X_k'$ (Pancharatnam, 1956 *a*, equation 5 *b*), where P_a and P_b are points opposite to P_a and P_b. The area in question may be shown to be equal to $\Delta dz \cos 2\phi_a$, thus proving (13).

§ 7. Certain Special Cases

A noteworthy simplification in both uniaxial and biaxial crystals, is that along directions which are nowhere in the vicinity of an optic axis—and where, correspondingly, the linear birefringence δ becomes appreciable—the waves propagated may for most purposes be regarded as linearly polarised along the principal planes of linear birefringence: the reason is that for such directions the ratios (ρ/δ) and (k/Δ) occurring in (1) and (4) usually differ but little from zero. The refractive indices and absorption coefficients of the waves are then obtained from the index and absorption-ellipsoids by the usual constructions (*see* P-*a*, Eq. 12) since we may set $\Delta \simeq \delta$, $\cos 2\phi_a \simeq 1$ and $\cos 2\psi_a \simeq \cos 2\chi$, in (12) and (11).

(*a*) *Uniaxial crystals.*—In uniaxial crystals both the birefringence δ and the linear dichroism k are determined from *uniaxial* ellipsoids; consequently, the ratio (k/δ) is virtually constant for all directions of propagation, and—in accordance with what has been said in the previous paragraph—this ratio will differ negligibly from zero for *all* directions. The states of polarisation of the two waves are then the same as in a transparent active crystal (Eq. 1), since we may set $\sin \phi \simeq 0$ from (4). The refractive indices of the waves, being functions of the states of polarisation (Eq. 12), are also determined as in a

transparent crystal. The waves, however, possess absorption coefficients which are obtained by setting $\cos 2\psi_a \simeq \pm \cos 2\,\omega_1$ in (9), or more accurately, in (11)—the upper sign being chosen if both the index and absorption ellipsoids are of the same sign. The last substitution follows from the fact that in a uniaxial crystal the principal planes of linear birefringence and linear dichroism coincide, so that B will have the same longitude either as X_k or Y_k.

(*b*) *Biaxial crystals: directions not too near an optic axis.*—It is known that in both transparent active crystals as well as inactive absorbing crystals the *square* of the ellipticity of the waves may be neglected for directions not too near an optic axis. For such directions of propagation in an active absorbing crystal we shall show that the states of polarisation of the waves are related to each other in the following simple manner. *The major axes of the elliptic vibrations may be taken to coincide with the principal planes of linear birefringence; and the respective ellipticities ω_a and ω_b of the slower and faster waves will be given by*

$$\left.\begin{aligned} \omega_a &= \epsilon + \omega_1 \\ \omega_b &= \epsilon - \omega_1 \end{aligned}\right\} \qquad (14)$$

Here ω_1 and $(-\,\omega_1)$ represent as before the ellipticities of the slower and faster waves in the absence of dichroism alone as given by (1); and ϵ is the common ellipticity of the two waves in the absence of optical activity alone. Neglecting their squares in comparison with unity, ω_1 and ϵ will be given by

$$\omega_1 = -\,\rho/\delta; \qquad \epsilon = (k/2\,\delta)\sin 2X \qquad (15)$$

where X is the acute angle that OX_k makes with reference to OX_r (measured with the usual sign convention).

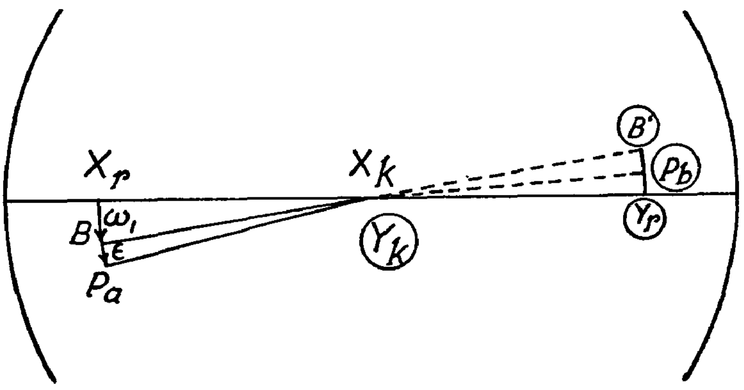

FIG. 4. For directions not in the vicinity of an optic axis each wave has an ellipticity which is the sum of the corresponding ellipticities which would obtain in the transparent active crystal and the inactive absorbing crystal.

For proving these relations we first remark that the directions under consideration are defined by the circumstance that the linear birefringence δ is sufficiently large (compared to both the rotatory power and the linear dichroism) to allow us to neglect the *squares* of (ρ/δ) and (k/δ) in comparison with unity. We may then also set Δ equal to δ according to (1). It follows that in Figs. 2 and 3, the arcs BX_r and $P_a B$ $(= 2\phi_a)$ may both be treated as infinitesimal, since their *squares* may be neglected, according to (1) and (4). The situation is illustrated in Fig. 4 which shows that P_a and P_b have respectively the same longitudes as X_r and Y_r (to our present order of approximation). Also the latitude $2\omega_a$ of P_a is equal to the sum of the *directed* arcs X_rB and BP_a (counted positive if they point to the upper hemisphere). The directed arc X_rB is however equal to $2\omega_1$. Hence for establishing the proposition of the previous paragraph it remains to show that the *directed* arc BP_a must be equal to 2ϵ. This is proved from the following consideration. If in accordance with our approximation we set $2\chi' \simeq 2|\chi|$ and $\Delta \simeq |\delta|$ in (4) and (5), those equations become formally identical with those holding for the case of a *non-active* absorbing crystal (for which case however B coincides with X_r); hence the infinitesimal arc $2\phi_a$ of the present case corresponds to twice the numerical ellipticity of the waves in the non-active absorbing crystal. Moreover, the sign of the directed arc BP_a being opposite to that of 2χ, will be the same as that of ϵ. This proves the first relation in (14) and a similar proof holds for the second relation.

[The approximate expression given in (15) for the ellipticity ϵ of the waves in a non-active absorbing crystal had not been derived in the author's previous paper on the subject (P-*a*). It is, however, immediately obtained either from Eq. (4) of the present paper or from the corresponding equation of the previous paper by setting $\sin 2\phi \simeq 2|\epsilon|$ and $\sin 2\psi \simeq \sin 2|\chi|$.]

The refractive indices and absorption coefficients of the waves may be determined by the usual index- and absorption-ellipsoid constructions, *as though* the waves were linearly polarised. This is because $\cos 2\phi_a \simeq 1$ and $2\psi_a \simeq |2\chi|$ in (12) and (11).

§ 8. PROPAGATION ALONG AN OPTIC AXIAL DIRECTION

In a biaxial crystal the linear dichroism does not in general vanish along an optic axial direction, since the circular sections of the index ellipsoid need not coincide with the circular sections of the absorption ellipsoid. In the absence of linear dichroism, however, the waves will be circularly polarised, so that $\Delta = 2|\rho|$, and the state B coincides with C_r if ρ is positive. The arc $2\chi'$ in Fig. 3 is then equal to a right angle, and from the condition that the angle it subtends at P_a should also be a right angle, it may be seen geometri-

cally [or from Eq. (5)] that P_a must lie either on the meridional arc C_rC ($2\psi = \pi/2$) or the equatorial arc CX_k ($2\phi = \frac{1}{2}\pi$)—as illustrated in Figs. 5 and 6 respectively. Two main cases may therefore be distinguished.

(*a*) *Circular birefringence* 2ρ *greater than linear dichroism* k.—The situation is illustrated in Fig. 5 for the case when ρ is positive (lævorotation).

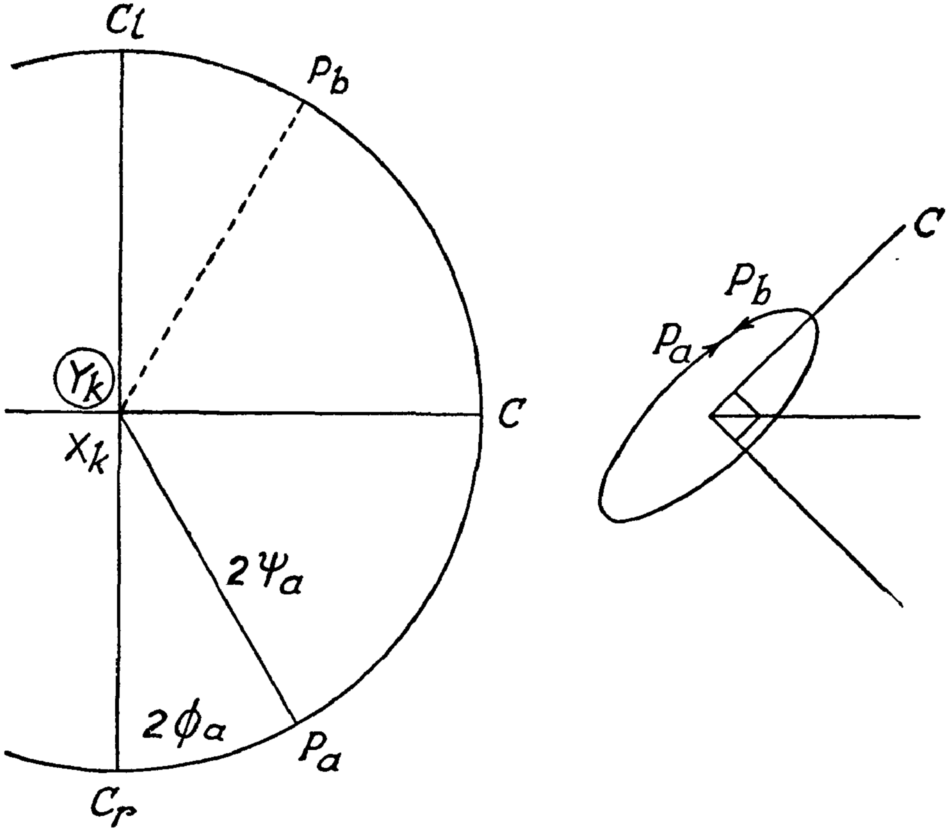

FIG. 5. Discussion of the elliptic states P_a and P_b propagated along an optic axial direction when $2\rho > k$.

Along the optic axis are propagated two elliptic vibrations exactly similar in form and orientation but described in oppsoite senses ($\omega_a = -\omega_b$). The sense of description of the slower elliptic vibration is the same as that of the slower circular vibration which would be propagated along the optic axis in the absence of linear dichroism; the major axes of the two elliptic vibrations are coincident and make an angle of 45° or —45° with reference to OX_k according as ρ is positive or negative. The numerical value of the ellipticity $|\omega_a|$ of the vibrations may be obtained from (4) since $2\phi_a = \frac{1}{2}\pi - |2\omega_a|$, and $2\psi = \frac{1}{2}\pi$.

$$\cos 2\omega_a = k/|2\rho| \tag{16}$$

The two waves have equal absorption coefficients, since $2\psi_a = \frac{1}{2}\pi$ in (10). But they possess different velocities of propagation, the phase retarda-

tion which one wave suffers *relative* to the other per unit distance of propagation being obtained from (13) and (16):

$$\Delta_a - \Delta_b = -2\rho \sin 2\omega_a = +\sqrt{(2\rho)^2 - k^2} \tag{17}$$

(*b*) *Circular birefringence* 2ρ *less than the linear dichroism* k.—Figure 6 illustrates this situation for the case when ρ is positive (the point P_a denotes the state of polarisation of the wave with the smaller absorption coefficient, *i.e.*, for which 2ψ is less than $\frac{1}{2}\pi$). *The waves propagated along the optic axis are linearly polarised, the angle between the linear vibrations being different from a right angle.* The azimuths of the two vibrations with reference to OX_k will be both positive (0 to $\frac{1}{2}\pi$) or both negative (0 to $-\frac{1}{2}\pi$) according as ρ is positive or negative. The numerical value of the azimuths of P_a and P_b (with reference to OX_k) will be ψ_a and $(\frac{1}{2}\pi - \psi_a)$; and if θ be the acute angle between the vibrations, then using (4)

$$\cos\theta = \sin 2\psi_a = |2\rho| / k \tag{18}$$

The two linearly polarised waves have the same velocity since $2\phi = \pi/2$ in (13). They are, however, propagated with different absorption coefficients as given by (10) and (18):

$$k_b - k_a = k\cos 2\psi_a = +\sqrt{k^2 - (2\rho)^2} \tag{19}$$

§ 9. MEDIA POSSESSING CIRCULAR DICHROISM

(*a*) *The operation of circular dichroism.*—Turning our attention now to the general example of an optically active absorbing crystal, we have naturally to suppose that even in the absence of optical rotation, linear birefringence and linear dichroism (*i.e.*, if we set $\rho = 0$, $\delta_1 = \delta_2 = \delta_m$ and $k_1 = k_2 = k_m$) the waves propagated in the *z*-direction will be circularly polarised with a difference σ between their coefficients of absorption (left *minus* right), the mean of their absorption coefficients being k_m. We therefore extend the discussion of § 2 in the following manner: the vibration at the plane $(z + dz)$ will now be given by further subjecting the vibration P″ (obtained after the operation of elliptic birefringence and linear dichroism) to the infinitesimal operation of circular dichroism; that is, the vibration P″ must be resolved into its right- and left-circular components, and the intensities of these components multiplied by $(1 - \sigma\, dz)$ and $(1 + \sigma\, dz)$ respectively (the phases being unaltered). It may be easily shown—using the results of a previous paper (Pancharatnam, 1956 *a*, § 6)—that, on the Poincaré sphere, the effect of the infinitesimal operation of circular dichroism will be exactly similar to that of the infinitesimal operation of linear dichroism (considered in P-*a*, § 4 *b*), since exactly the same argument is applicable to both cases; that is, *the state*

P'' will move directly towards the less absorbed circular state C_r, through an infinitesimal arc $\sigma dz \sin C_r P''$.

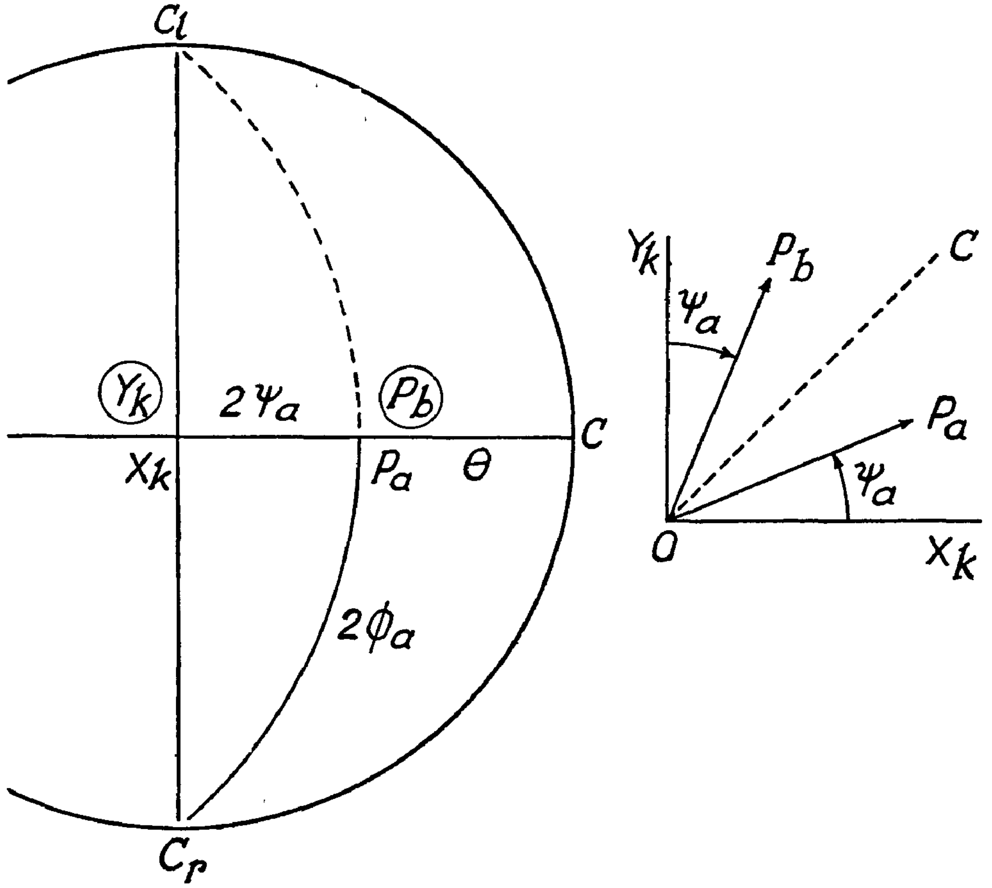

FIG. 6. Discussion of linearly polarised states P_a and P_b propagated along an axial direction when $2\rho < k$.

(*b*) *The superposition of linear and circular dichroism.*—A notable simplification of the analysis is effected by combining first the effects of the infinitesimal operations of linear and circular dichroism alone. [To fix our ideas we may for example consider the propagation along an optic axial direction for a wave-length where the rotatory power becomes zero, the circular dichroism being however near its maximum (Lowry, 1935)].

Just as the infinitesimal operations of linear birefringence and optical rotation (circular birefringence) may be compounded to yield the infinitesimal operation of elliptic birefringence as given by (1), we shall find that *the superposition of linear and circular dichroism results in elliptic dichroism.* More specifically, we shall show that vibrations in two oppositely polarised elliptic states D and D′ (with their major axes along OX_k and OY_k respectively) remain unaltered in form under the combined effects of the infinitesimal operations of linear and circular dichroism (applied in either order); and if

ω_2 be the angle of ellipticity of the less absorbed state D, and K the difference in the absorption coefficients of the vibrations in these two states D′ and D, then,

$$\left.\begin{aligned}\tan 2\omega_2 &= -\frac{\sigma}{k}\\ \mathrm{K} &= +\sqrt{\mathrm{K}^2+\sigma^2}\end{aligned}\right\} \qquad (20)$$

Consider a vibration initially in one of the states of polarisation D or D′ (*see* Fig. 7, where the diameter X_kY_k is drawn in the plane of the paper). Under the operation of linear dichroism its state will move towards X_k through a distance $kdz \sin |2\,\omega_2|$. Similarly, under the operation of circular dichroism the state of the vibration will be displaced towards C_r through an infinitesimal distance $\sigma dz \cos 2\,\omega_2$. These two movements are oppositely directed whatever be the sign of σ (since ω_2 has the opposite sign) and they will exactly cancel each other since $\tan 2\,\omega_2$ is given by (20). Thus vibrations in the respective states D and D′ suffer no alteration in their state of polarisation. The intensities of vibrations in these states will, however, be diminished by specific reduction factors, and correspondingly the absorption coefficients for these two states will have a specific difference K which we proceed to determine.

Consider a linear vibration initially in the state C which lies on the equator at a latitude of $-90°$ with respect to X_k (*see* Fig. 7). Under the operations of linear and circular dichroism its state suffers the successive displacements of kdz towards X_k and σdz towards C_r; in other words, *it suffers a displacement of* $\sqrt{k^2+\sigma^2}\,dz$ *directly towards the state D.* Since however the initial vibration could equally well be considered as the sum of two vibrations (of equal intensity) in states D′ and D, it follows that vibrations in these states suffer no relative phase retardation under the combined operations of linear and circular dichroism; and that the difference in the absorption coefficients of these states is given by the relation (20) which we wished to prove (*see* Pancharatnam, 1956, *a*, § 6).

Moreover, if the initial vibration in the state C be of unit intensity, the diminution of intensity under the operation of elliptic dichroism will be $(\mathrm{K}_1+\mathrm{K}_2)\,dz$, where K_1dz and K_2dz are the diminution in the intensities of the component vibrations (each with an initial intensity of one-half) in the states D and D′. This diminution of intensity may be equated to that occurring under the combined operation of linear and circular dichroism. Following the same argument as given above, it will be seen that the diminution of intensity arising from the operation of linear dichroism will be $(k_1+k_2)\,dz$; while the diminution of intensity arising from the operation

of circular dichroism—as described in § 9 *a*—will be zero. Hence, if K_1 and K_2 be the absorption coefficients of the waves which would be propagated in the absence of linear birefringence and optical rotation, then

$$K_1 + K_2 = k_1 + k_2 \tag{21}$$

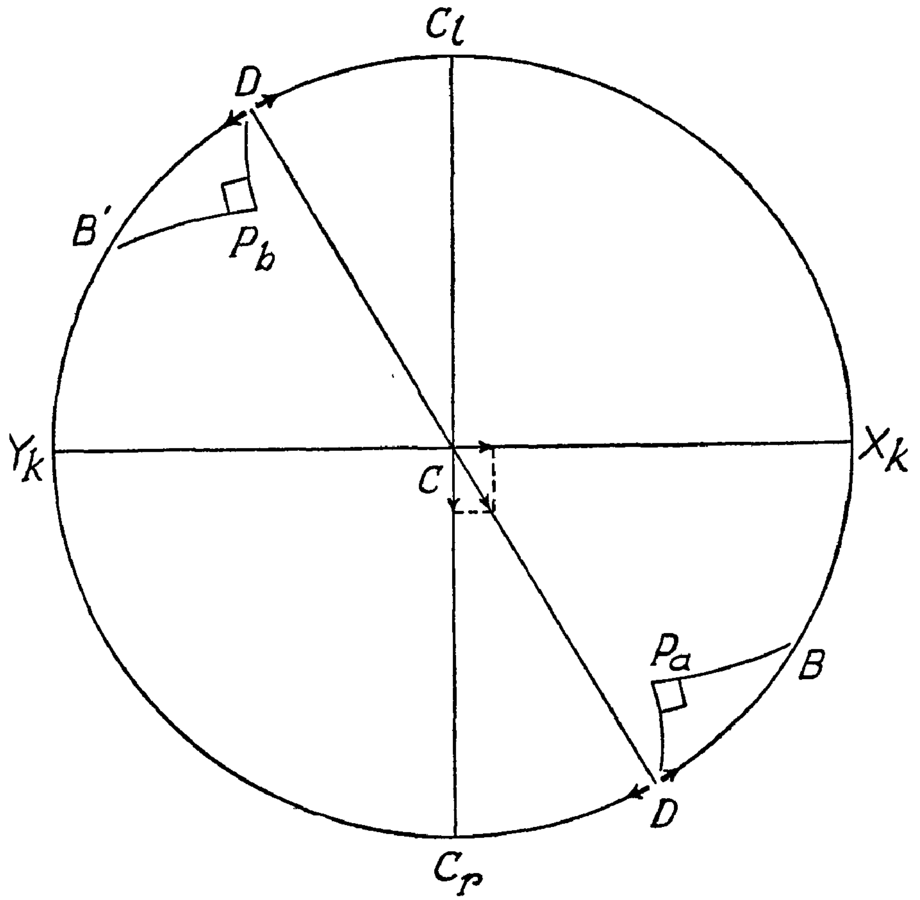

FIG. 7. Illustrating how linear dichroism and circular dichroism may be compounded by a vectorial law to yield elliptic dichroism. P_a and P_b represent the states of the waves propagated along a general direction in a uniaxial crystal possessing circular dichroism.

It has already been shown that the states which remain invariant under the infinitesimal operations of linear and circular dichroism are determined by the same vectorial law which holds for the composition of linear birefringence and optical rotation. Moreover, as in the discussion of § 6, it is easily seen that the infinitesimal operations of linear and circular dichroism are—from the formal mathematical standpoint—completely similar to the corresponding operations of linear birefringence and optical rotation (circular birefringence): the real constants K_1, K_2 and σ occurring in the former case being replaced by imaginary constants $i\delta_1$, $i\delta_2$ and $i\rho$ in the latter case. As a corollary it follows that since the states which remain invariant under the

successive infinitesimal operations of linear birefringence and optical rotation suffer no *absorption*, the states which remain invariant under the successive infinitesimal operations of linear and circular dichroism can suffer no alteration in *phase*. So also, by proving relation (21) above, we have also established the parallel relation given by Eq. (2).

(*c*) *The superposition of elliptic birefringence and elliptic dichroism.*—It will now be clear that along any direction in an optically active absorbing crystal, the effect of elliptic birefringence as given by (1) and (2), has to be combined with the effect of elliptic dichroism [which would be present in the absence of optical activity and linear birefringence, and is given by (20) and (21)]. Correspondingly, it becomes more convenient to specify any point on the Poincaré sphere by its 'direction cosines' with respect to the new reference points D, B and C, which form a right-handed set, and in which only the arc BD differs from $\frac{1}{2}\pi$ (*see* Fig. 8); if we denote arc BD by $2\chi'$, then we will have instead of (3), the following expression for $\cos 2\chi'$ obtained from triangle BDC_l:

$$\cos 2\chi' = \sin 2\omega_1 \sin 2\omega_2 + \cos 2\omega_1 \cos 2\omega_2 \cos 2\chi.$$

The problem has now been reduced to a form exactly similar to that considered in the previous sections. Hence the states of polarisation of the waves (*specified with reference to the new co-ordinate system*) and the refractive indices and absorption coefficients of the waves are given again by the relations (4), (5), (9) and (12)—except that *the symbol* k *representing the linear dichroism has to be replaced by* *K* (which represents the magnitude of elliptic dichroism). Because of (21), it becomes unnecessary to replace $(k_1 + k_2)$ in (9) by $(K_1 + K_2)$.

We have thus formally obtained the solution for the propagation in media possessing circular dichroism. For any particular direction of propagation the coefficient of circular dichroism σ is to be determined from the surface of circular dichroism. The media which possess circular dichroism to a striking extent and which at first sight would seem best suited for an easy qualitative test of the theory are certain of the so-called liquid crystals (Voigt, 1916); nevertheless in these liquid crystals, the large 'circular dichroism', the enormous rotation of the plane of polarisation and other phenomena indicate that the medium may not be homogeneous and that, on the contrary, it possesses a lamellar structure (Hl. de Vries, 1951). Since a suitable single crystal was not obtained for experimental study we shall not dwell at any length on the specific results of the theory, but content ourselves with mentioning a few of the results.

For directions which are nowhere in the vicinity of an optic axis the ratio k/Δ and ρ/δ will differ very slightly from zero, so that to a good degree of approximation the propagation will be as in non-active absorbing crystals (*see* § 7). Similarly, if the ratio of the circular to linear dichroism differ very

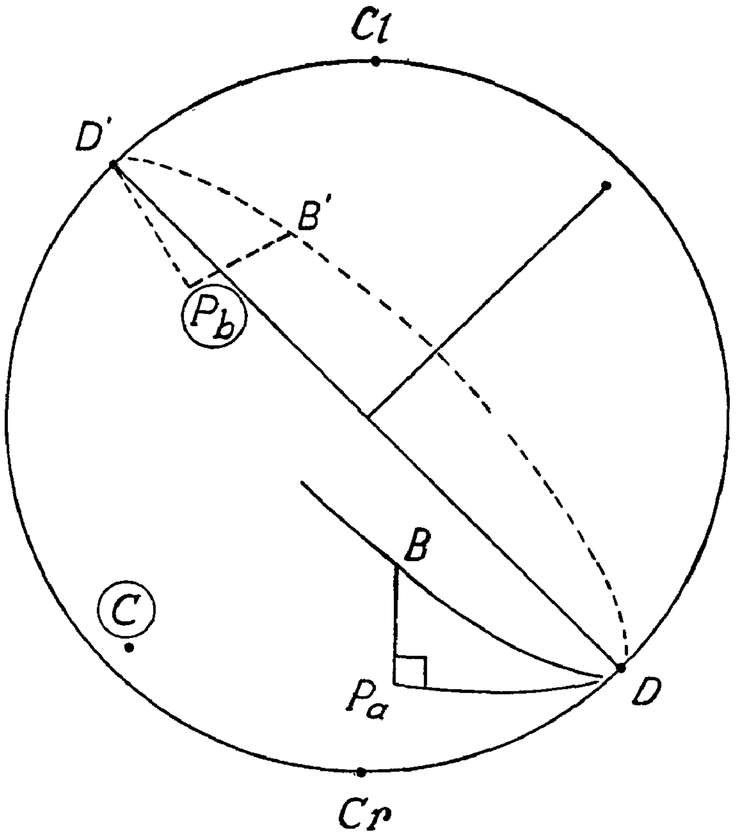

FIG. 8. Propagation in a crystal of the most general class (*i.e.*, possessing circular dichroism also). P_a and P_b represent the states propagated unchanged under the effects of elliptic birefringence Δ (axis BB′) and elliptic dichroism K (axis DD′).

slightly from zero, as may often be the case in biaxial crystals, we may according to (20) conveniently treat the crystal as though circular dichroism were absent.

For uniaxial crystals, since the principal planes of linear birefringence and dichroism coincide, the points B and D lie on the same great circle passing through the poles. It will then be seen from Fig. 7 that the elliptic states P_a and P_b propagated along any direction bear a simple geometrical relationship to one another; they have the same numerical ellipticity (though they are described in opposite senses); and the orientations of the major axes of the two ellipses are obtained from the principal planes OX_r and OY_r, by turning the latter directions through equal angles in *opposite* directions. This result has been obtained by Forsterling (quoted in Szivessy, 1928) from

the electromagnetic theory of propagation in uniaxial crystals. For directions not too close to the optic axis, the ellipticity of the waves will be the same as in a transparent crystal—since the square of (k/Δ) may be neglected in comparison with unity, so that the arc BP_a is an infinitesimal of the first order and lies along a parallel of latitude.

The states of polarisation of the waves propagated along a general direction in a biaxial crystal will bear no simple relation to one another (*see* Fig. 8); but along the optic axial direction the forms and orientations of the two elliptic vibrations will be simply related to one another—in the same fashion as those propagated along a general direction in a uniaxial crystal (*see* preceding paragraph).

§ 10. CONCLUDING REMARKS

It appears worthwhile to underline the essential difference between our procedure for applying the superposition principle and that customarily followed, *e.g.*, in the case of transparent active crystals by using the Poincaré sphere, or for any crystalline plate by using matrix calculus. The spirit of our method of analysis has *not* been so much to replace the effects produced by an absorbing crystalline plate (on light passing normally through it) by a geometrical or analytical *operation*; it has been to determine the states of polarisation of the two waves that can be propagated along each direction, as well as their velocities and absorption coefficients. This is because the characteristic interference phenomena exhibited by an absorbing crystalline plate, with the incident light partially or completely polarised, is naturally best understood as due to the *interference* and composition of the two non-orthogonally polarised waves emerging from the crystal plate—or their resolved components; in fact this method of analysis is useful for transparent and absorbing crystals alike (*see* Pancharatnam, 1956 *a, b*; 1957 *a, b*). Moreover, the two waves that can be propagated along any general direction have a physical reality that may otherwise be lost sight of. For example, each will in general have a different ray-direction. [The physical reason for this is that the wave-velocities as given by (12) vary with direction, and in any such medium the direction of propagation of an element of the wave-front will not always coincide with the wave-normal, but may be derived from it by a construction from the wave-surface.] One of the chief merits, then, of the use of the Poincaré sphere is that the states of polarisation of the waves, as well as their velocities and absorption coefficients are determined by extremely simple expressions [(4), (5), (9) and (12)] which remain essentially the same whether the crystal is optically active or not.

The peculiar interference figures exhibited by a sector of amethyst will be explained in detail in a later paper by the application of the method of superposition, so that an overall picture of the optics of such media in the vicinity of an optic axis will emerge. The possibility of the existence of *singular axes*, along which only *one* state of polarisation can be propagated without change of form, will also be investigated. That the properties of the singular axes as described by the method of superposition do not really flout the results of the electromagnetic theory (both in the case of active and non-active crystals) will be indicated in a later paper—which will present the electromagnetic theory of light propagation in active absorbing crystals.

The author is highly thankful to Prof. Sir C. V. Raman for his continued interest in the present investigation.

§ 11. SUMMARY

A light beam in an absorbing crystal may be looked upon as travelling under the superposed effects of the various 'elementary properties' associated with the medium, *viz.*, linear birefringence, linear dichroism, optical rotation and circular dichroism. For any general direction of propagation, this postulate yields completely (*a*) the states of polarisation of the two waves (specified conveniently by two corresponding points on the Poincaré sphere), and (*b*) their velocities and absorption coefficients (expressed conveniently as functions of their states of polarisation). The treatment is closely parallel to that for inactive absorbing crystals (Pancharatnam, 1955)—since for each direction, linear and circular birefringence combine to give elliptic birefringence, while linear and circular dichroism similarly combine to yield elliptic dichroism.

The case of biaxial media with negligible or no circular dichroism is dwelt upon at length. The waves along an optic axis are not circularly polarised: they may even be in two non-orthogonal linearly polarised states (if the dichroism exceed twice the rotatory power). For directions in the near vicinity of an optic axis the waves are in two *elliptic* states of unequal ellipticity with their major axes *not* crossed. For other directions, however, the orientations of the major axes—as also the velocities and absorption coefficients of the waves—become substantially the same as for an inactive absorbing crystal; but the ellipticity for each state now approximates to the sum of the corresponding ellipticities obtaining in the inactive absorbing crystal and the active transparent crystal—thus becoming negligible only when the inclination to both the optic axes becomes notable.

§ 12. REFERENCES

Bruhat .. *Traite de Polarimetrie*, 1930, 319.

de Vries .. *Acta Cryst.*, 1951, **4**, 219.

Fano .. *J. Opt. Soc. Am.*, 1949, **39**, 859.

Jenkins and White .. *Fundamentals of Physical Optics*, McGraw-Hill, 1937, 306.

Jones .. *J. Opt. Soc. Am.*, 1942, **32**, 486.

Ibid., 1948, **38**, 671.

Ibid., 1956, **46**, 126.

Kauzmann .. *Quantum Chemistry*, Academic Press, New York, 1957, 608, 618.

Lowry .. *Optical Rotatory Power*, Longmans, Green and Co., 1935, 393.

Pancharatnam .. *Proc. Indian Acad. Sci.*, 1955 *a*, *b*, **42 A**, 86, 235.

Ibid., 1956 *a*, *b*, **44 A**, 247, 398.

Ibid., 1957 *a*, **45 A**, 402.

Ibid., 1957 *b*, **46 A**, 1.

Pockels .. *Lehrbuch der Kristalloptik*, Teubner, 1906, 309.

Ramachandran .. *J. Madras Univ.*, 1952, **22 B**, 277.

——— and Chandrasekharan *Proc. Indian Acad. Sci.*, 1951, **33 A**, 199.

——— and Ramaseshan .. *J. Opt. Soc. Am.*, 1952, **42**, 49.

Szivessy .. *Handbuch der Physik, Band XX*, 1928, Springer, Kap 11, 901, 811.

Voigt .. *Physik. Z.*, 1916, **17**, 159.

Reprinted from "The Proceedings of the Indian Academy of Sciences", Vol. XLVI, No. 5, Sec. A, 1957

THE HEAT CAPACITY OF DIAMOND BETWEEN 0 AND 1000° K.

BY SIR C. V. RAMAN

(*Memoir No.* 103 *of the Raman Research Institute, Bangalore*-6)

Received November 14, 1957

1. INTRODUCTION

THE evaluation of the heat capacity of diamond on the basis of the theory of specific heats of crystals advanced by the author formed the subject of a recent publication[1] in these *Proceedings*. Since then, fresh experimental determinations have been reported which go down to temperatures at which the value of C_p for diamond is as low as 0·0001, in other words only a fifty-thousandth part of its value 5·0 at 1000° K. which is itself smaller than the theoretical maximum of 5·96 for a monatomic solid. We proceed here to consider the new experimental results. The theoretical evaluation already published succeeds in explaining the change of C_p with temperature over the whole of this enormous range of values in a highly satisfactory manner, but with certain reservations made necessary by the fact that the theoretical calculations are based on the spectroscopic behaviour of ideal diamonds, whereas the reported determinations have been made with material which is very far indeed from being ideal. To exhibit the closeness of the agreement which is observed over practically the entire temperature range as well as the minor differences which are noticeable in certain limited parts of it, the data have been plotted on adequate scales alongside of the theoretical values in a series of graphs which are reproduced in the present paper. The cause of the small differences which appear in the temperature range between 50 and 150° K. is discussed and it is shown that they are explicable in terms of the differences in the spectroscopic behaviour of ideal and non-ideal diamonds.

Diamond illustrates in a most striking manner the fundamental relationship between the specific heats of crystals and their spectroscopic behaviour. Being an elementary solid crystallising in the cubic system with an exceptionally simple structure, the characteristic modes of atomic vibration which determine both the thermal behaviour and the spectroscopic properties of diamond can be described in geometric terms without any reference to the magnitude of the interatomic force constants. Considerations of a general nature enable us to go further and arrange these modes in a scale of descending frequency, thereby greatly facilitating their identification.

Diamond being a transparent solid, the modes and frequencies of atomic vibration in it are also accessible to observation by a variety of spectroscopic methods. It is found possible to determine these frequencies with precision and compare them with the theoretically computed values. Thus theory and experiment agree to give us a complete and detailed picture of the atomic vibration spectrum of diamond. It thereby becomes possible to evaluate the heat capacity of the crystal in a completely independent fashion involving no assumptions of any sort. The agreement which emerges between the results of such evaluation and the experimental data is a convincing demonstration of the correctness of the theoretical approach.

2. THE VIBRATION SPECTRUM OF DIAMOND

The crystal structure of diamond consists of two distinct sets of atoms of carbon which appear separately in layers parallel to the faces of the octahedron and the cube respectively. The normal modes of atomic vibration of the structure can be readily described in terms of this arrangement. The principal mode of vibration is an oscillation of the two sets of atoms with respect to each other along any one of the three cubic axes and has therefore a degeneracy of 3. The atoms present in the layers parallel to the octahedral faces may oscillate with respect to each other either normally or transversely to themselves with degeneracies of four and eight respectively; but since the adjacent non-equivalent layers may oscillate either in the same or opposite phases, we have two such sets of modes. Likewise, we have two sets of modes in which the layers of atoms parallel to the cube faces oscillate normally or transversely to themselves with degeneracies of three and six respectively. Thus, we have 9 distinct normal modes with degeneracies of 3, 4, 4, 8, 8, 3, 3, 6 and 6 respectively, making a total of 45 modes in all. Considering the set of 16 atoms contained in a volume element which is twice as large in each direction as the unit cell of the crystal structure, the total number of atomic degrees of freedom of this group is 48. The 45 modes of vibration described above may be regarded as the *modes of internal vibration of this group*, while the three degrees of freedom left over represent *its three translations.*

In a lecture on the diamond delivered at Zurich, Freiburg and Bonn in July 1956, and subsequently published in these *Proceedings*[2] it was shown in detail how the frequencies of the nine normal modes described above may be evaluated and checked against the frequency shifts observed in the scattering of light by diamond when it is traversed by the $\lambda\, 2536 \cdot 5$ radiations of the mercury arc. We shall content ourselves here with reproducing below as Fig. 1 a chart showing the nine frequencies and their respective degeneracies.

The two modes of oscillation normal to the cubic planes have an identical frequency of 1088 cm.$^{-1}$ They have accordingly been shown as a single frequency with a degeneracy of 6.

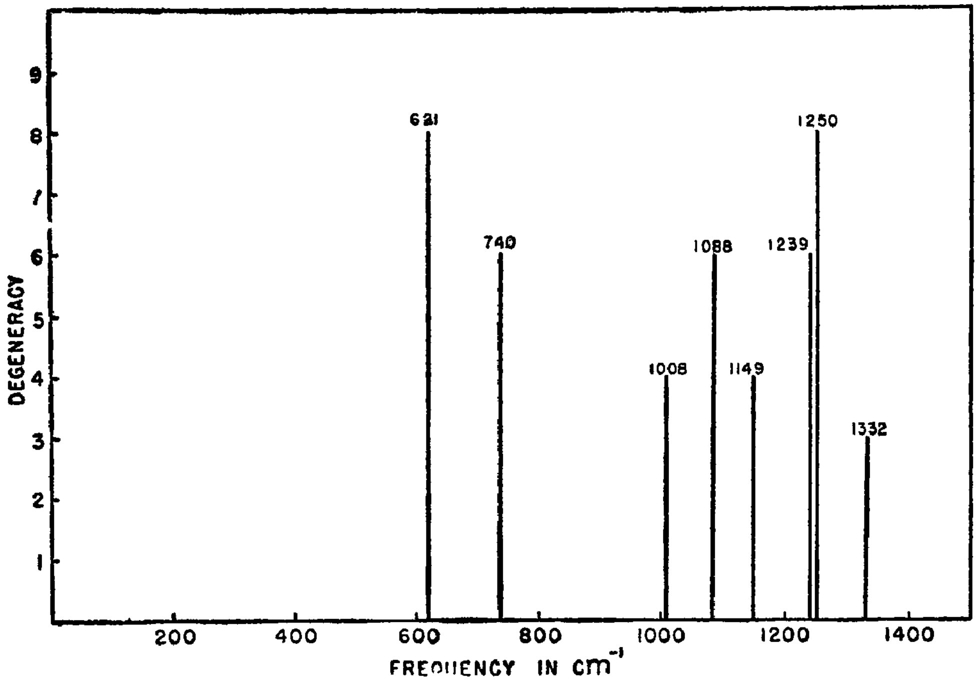

FIG. 1. Chart of the Vibration Spectrum of Diamond.

To complete the picture, we require to know how the three translatory movements of the 16-atom group manifest themselves in the vibration spectrum of the crystal. It is obvious that they would appear as internal vibrations in volume elements of larger size than the 16-atom group and therefore having lower frequencies. In dealing with vibrations of this nature, it is permissible to ignore the discrete atomic structure of the material. The larger the size of a volume element is, the lower would be the frequencies of its internal vibration. Considering volume elements of all possible sizes as the oscillators, their frequencies of internal vibration would evidently range from the lowest possible value $\nu = 0$ to an upper limit ν_L which may be taken equal to the lowest of the frequencies of vibration appearing in the chart (Fig. 1). The manner in which the disposable degrees of freedom of atomic movement are distributed over this range of frequencies is indicated by a simple argument. The number of volume elements of any specified dimension included in the crystal and hence also the number of degrees of freedom represented by their translations diminish in inverse proportion to the cube of the linear dimensions, while the frequencies of their internal vibration would vary inversely as the first power of the same. Hence the number of degrees of freedom appearing as internal vibrations of the volume

elements and having frequencies between 0 and ν would be proportional to ν^3. By differentiation, we obtain the result that the number of degrees of freedom appearing between frequencies ν and $\nu + d\nu$, in other words, the number of oscillators in the crystal having frequencies in that range would be proportional to $3\nu^2 d\nu$. The constant of proportionality may be deduced at once from the consideration that on integration between zero and the upper limit ν_L, we should obtain as the total number of oscillators three times the number of 16-atom groups comprised in the crystal.

3. THE HEAT CAPACITY OF DIAMOND

Having thus ascertained the nature of the complete vibration spectrum of diamond, we proceed to make use of the theory of Einstein and obtain an expression for the heat content of the crystal as a function of the temperature. This appears as a sum of two quantities; the first is a summation of the average energies of the individual oscillators having the discrete frequencies shown in the chart (Fig. 1) multiplied by their respective degeneracies and by the total number of 16-atom groups contained in the crystal. The second part is a summation of the average energies of vibration of the oscillators of larger sizes having various frequencies from 0 to ν_L, and this takes the form of an integral between these limits of frequency. The details of the calculations have already been given in the earlier paper and it is therefore sufficient to reproduce here the final results here in tabular form.

TABLE I

Theoretical Computation of the Atomic Heat of Diamond

(Calories per gram-atom per degree)

Absolute Temperature	Discrete Frequencies	Residual Spectrum	Total	Absolute Temperature	Discrete Frequencies	Residual Spectrum	Total
15°	..	0·00014	0·00014	200	0·4069	0·1631	0·5700
20	..	0·00033	0·00033	225	0·5894	0·1895	0·7789
25	..	0·00064	0·00064	250	0·7844	0·2124	0·9968
30	..	0·0011	0·0011	275	1·0137	0·2319	1·2456
40	..	0·0026	0·0026	300	1·2418	0·2486	1·4904
50	..	0·0051	0·0051	350	1·700	0·275	1·975
60	..	0·0088	0·0088	400	2·139	0·294	2·433
70	0·0005	0·0140	0·0145	450	2·538	0·308	2·846
80	0·002	0·0207	0·0227	500	2·892	0·319	3·211
90	0·0056	0·0290	0·0346	600	3·469	0·334	3·803
100	0·0128	0·0388	0·0516	700	3·899	0·344	4·243
120	0·0419	0·0619	0·1038	800	4·2[illegible]4	0·350	4·574
140	0·0957	0·0877	0·1834	900	4·465	0·355	4·820
160	0·1758	0·114	0·2898	1000	4·653	0·358	5·011
175	0·2517	0·1333	0·3850	1100	4·797	0·360	5·157

It will be seen that the contribution from the set of discrete frequencies becomes negligible at temperatures below 60° Abs. At and below that temperature, the residual spectrum of frequencies alone is responsible for the entire heat capacity of the crystal. At higher temperatures, however, the contribution of the spectrum of discrete frequencies rapidly increases and ultimately becomes responsible for all except 1/16th part of the specific heat.

In order to exhibit the over-all success of the theory in explaining the thermal behaviour of diamond, the figures for the atomic heat shown in Table I have been plotted as a curve (Fig. 2) on a scale which is adequate

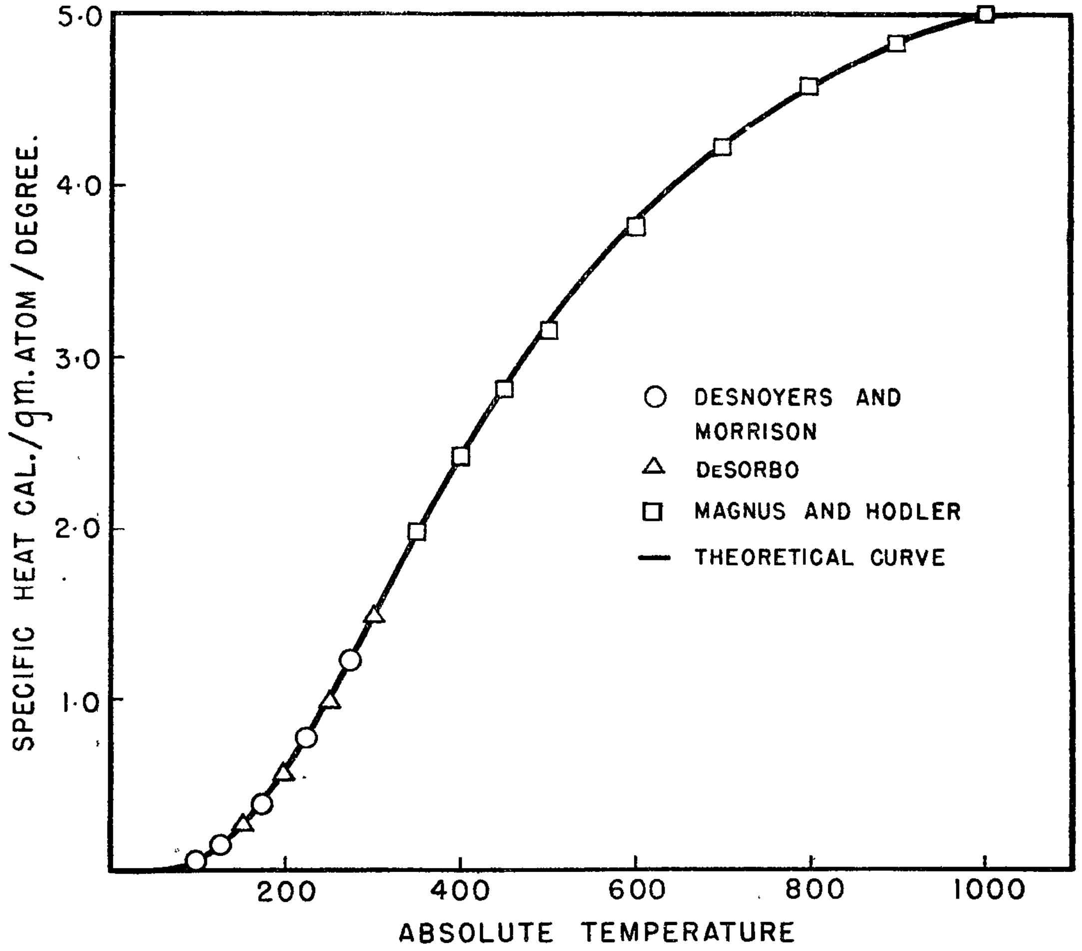

FIG. 2. Specific Heat of Diamond from 0 to 1000°.

to represent the data except in the region where it runs nearly parallel to the axis of temperature. In the temperature range between 300 and 1000° K., the values determined by Magnus and Hodler have been used, while in the

lower ranges, the data of DeSorbo as well as those reported by Desnoyers and Morrison have been put in. It will be seen that no deviations between theory and experiment which are at all significant are noticeable on the scale of the graph.

For temperatures below 300°, the determinations by Pitzer, DeSorbo and by Desnoyers and Morrison are available, but since the two latter sets of determinations are in good agreement, they have been plotted in a graph covering the temperature range between 160 and 300° K. (Fig. 3). The

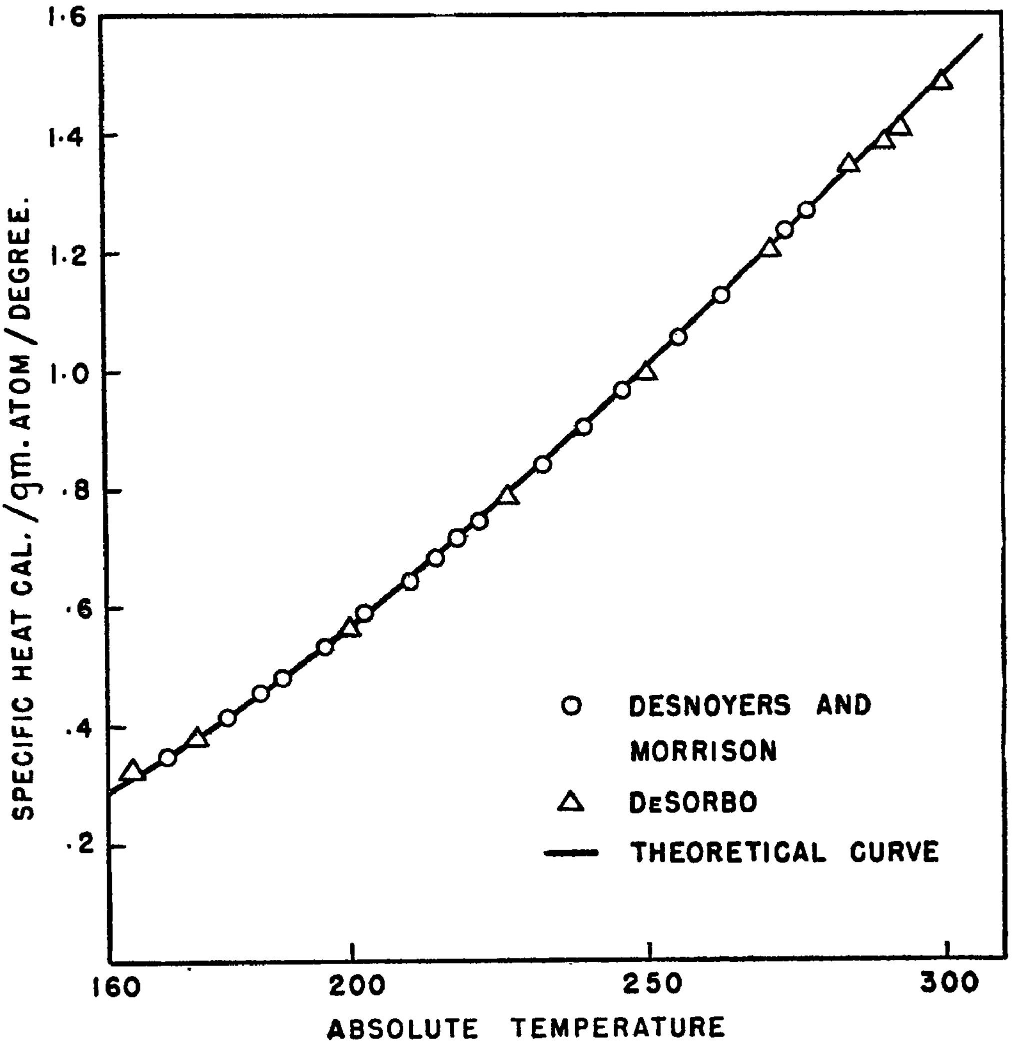

FIG. 3. Specific Heat of Diamond from 160 to 300°.

scale on which this figure has been drawn is adequate to disclose any systematic deviations between theory and experiment, had such existed. No such deviations are noticeable and hence it is evident that throughout the range of temperature in which the spectrum of discrete frequencies is principally

responsible for the heat capacity of diamond (160 to 1000° K.), the theory is in very satisfactory accord with the facts.

We shall next consider the very lowest temperatures where the value of C_p retreats into the third or fourth decimal place. The theoretical curve for this region has been drawn in Fig. 4, an adequately large scale being used for the ordinates, and the data reported by DeSorbo and by Desnoyers and Morrison have been plotted alongside of it. At the lowest temperatures the values of DeSorbo exhibit a distinct scatter, many of them lying above the theoretical curve. On the other hand, the more recent data of Desnoyers and Morrison lie smoothly on the curve up to 50°. The agreement between theory and experiment in this range made apparent by the graph must be considered highly satisfactory.

In the temperature range between 50° and 60° K., the experimental values plotted in Fig. 4 lie above the theoretical curve, the magnitude of the differences being a few units in the fourth place of decimals. From Fig. 5 which

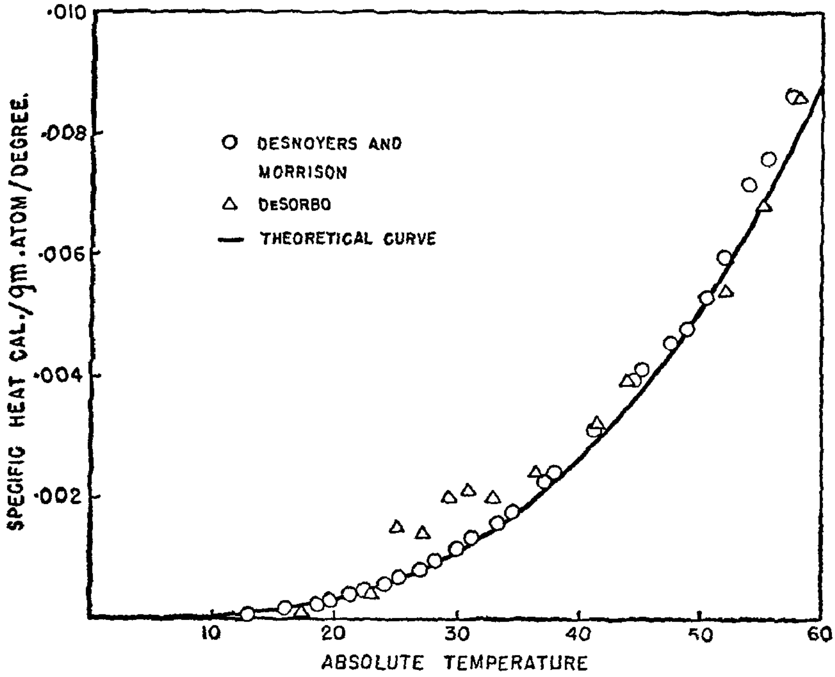

FIG. 4. Specific Heat of Diamond from 0 to 60°.

represents a comparison between theory and experiment in the range between 60 and 160° K. it will be seen that such differences become distinctly more pronounced at higher temperatures, reaching a maximum value of 0·007 at about 100°; they steadily diminish again at higher temperatures and finally cease to be noticeable on the graphs beyond 150° K. Since the value of the specific heat at 100° K. is itself very low, being only 0·059, the difference

between theory and experiment expressed as a percentage of the specific heat is 12%, but to express the difference in this way exaggerates its significance. Since, however, the discrepancy is real, we shall consider and comment upon its origin.

4. SPECTROSCOPIC BEHAVIOUR OF NON-IDEAL DIAMONDS

An explanation of the differences which are noticeable between theory and observation in the values of C_p in the range between 50 and 150° K. is not far to seek. The theoretical calculations refer to the case of an ideal crystal. They could therefore be expected to show a complete agreement with the experimentally determined specific heats if only the latter had also been made with ideal diamonds. Actually, however, determinations of specific heat require fairly large masses of material and it is therefore inevitable that they are made with diamonds of an inferior sort. It may be noted that DeSorbo used 80 grams of fragmented bort. He noticed that some of the crystals exhibited colour and also that about 20% of the material was fluorescent. Desnoyers and Morrison report that the sample used by them consisted approximately of 160 grams of industrial diamonds, their average dimensions being about 3 mm. They also remark that most of their diamonds were lightly coloured, either yellow, brown or green but that none contained occlusions. It is evident from these descriptions that we are concerned here with the class of diamond that exhibits its non-ideality of crystal structure in a visible manner, in other words, shows colour in daylight and luminescence under ultra-violet illumination.

The spectroscopic behaviour of diamonds of all sorts has been investigated by a variety of methods over a period of many years by the author and his collaborators. It will suffice here to refer to the results reported in a paper by Miss Anna Mani[3] recording a detailed study of the fluorescence and absorption spectra of twenty-two diamonds of various sorts. When the crystals are cooled down to liquid air temperature, these spectra sharpen notably, and it then becomes possible to analyse them *in detail*. Intercomparison of the fluorescence and absorption spectra enables the frequencies representing electronic transitions to be identified and distinguished from those due to the vibrational transitions appearing in combination with them. The result emerges clearly that the spectroscopic behaviour of diamonds which are colourless as seen by daylight and of those which exhibit various shades of brown, yellow or green is strikingly different. Diamonds of the former sort exhibit a blue fluorescence and the atomic vibration spectrum deduced from studies thereof is generally similar to that shown in the chart

reproduced above as Fig. 1 in the text. On the other hand, diamonds exhibiting visible tints by daylight fluoresce with a greenish yellow colour, the analysis of the spectrum of which discloses many features both in the electronic and atomic vibration spectra which are absent in the blue luminescence of

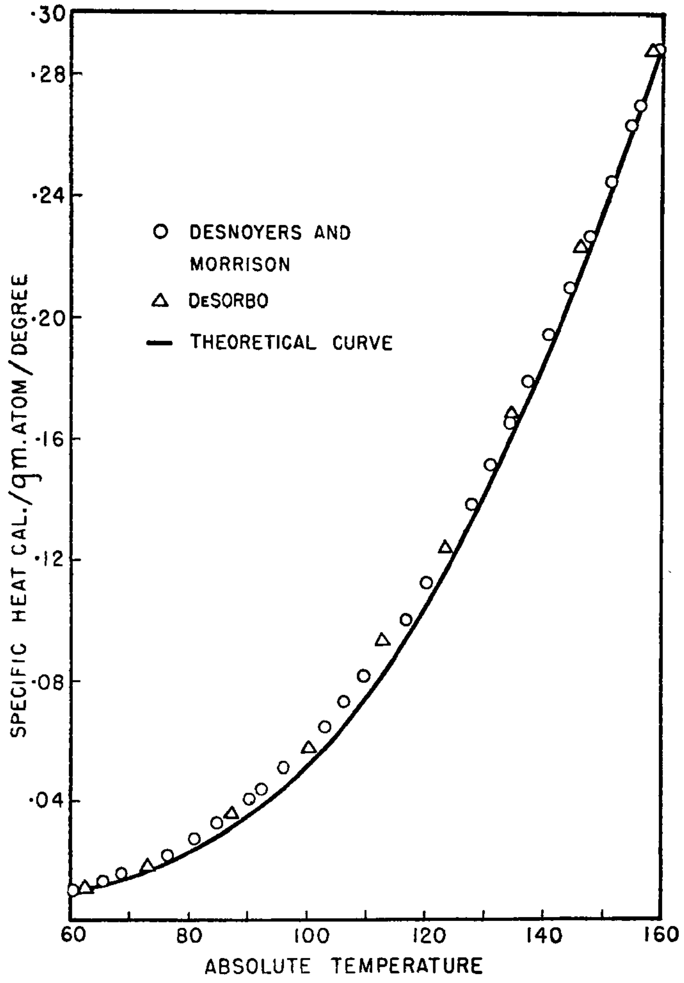

Fig. 5. Specific Heat of Diamond from 60 to 160°.

colourless diamonds. The most prominent of the additional features in the vibration spectrum is a band stretching from 257 to 443 cm.$^{-1}$ with its peak at 359 cm.$^{-1}$

It is clear from the facts recited above that the atomic vibration spectrum of non-ideal diamonds differs notably from that of the ideal material. The difference arises chiefly in the region of the residual spectrum of frequencies and may be described as an enhancement of its strength in the region of frequencies about 359 cm.$^{-1}$ Since the total number of atomic degrees of freedom is invariant, such enhancement would necessarily involve a diminu-

tion in the strength of the residual spectrum at higher frequencies between 359 cm.$^{-1}$ and the upper limit of 621 cm.$^{-1}$ A change in the character of the residual spectrum of the nature indicated would evidently result in altering the specific heat of the crystal. The Einstein function for a frequency of 359 cm.$^{-1}$ has a negligible value at temperatures below 50° K. It increases most rapidly in the temperature range in the vicinity of 100°, and at higher temperatures tends more slowly towards its limiting value. The change in the character of the residual spectrum would thus result in an increase of the specific heat of non-ideal diamonds which would be vanishingly small at very low and at very high temperatures and would be most prominent at about 100° K. This describes what is actually observed.

ACKNOWLEDGEMENT

The author much appreciates the courtesy of Messrs. Desnoyers and Morrison in having made the results of their valuable new determinations available to him in advance of publication.

SUMMARY

The evaluation of the heat capacity of diamond on the basis of the theory of specific heats advanced by the author is discussed and the results are compared graphically with the latest available experimental data. A striking over-all agreement emerges over the whole of the temperature range between 0 to 1000° K. The experimental values are however slightly in excess of the theoretical ones in the limited range between 50 and 150° K., the difference in the value of C_p being a maximum of 0·007 at about 100° K. and ceasing to be noticeable both below 50° K. and above 150° K. This small excess is explained as a consequence of the use in the experimental determinations of industrial diamonds whose spectroscopic behaviour is observably different from that of the ideal material.

REFERENCES

Raman, C. V. .. *Proc. Ind. Acad. Sci.*, 1956, **44**, 160.

———— .. *Ibid.*, 1956, **44**, 99.

Anna Mani .. *Ibid.*, 1944, **19**, 231.

Reprinted from "The Proceedings of the Indian Academy of Sciences",
Vol. XLVI, No. 6, Sec. A, 1957

THE TETRAHEDRAL CARBON ATOM AND THE STRUCTURE OF DIAMOND*

BY SIR C. V. RAMAN

(*Memoir No.* 104 *from the Raman Research Institute, Bangalore* 6)

1. INTRODUCTION

MY address to the Academy this year concerns itself with the element carbon and its chemical behaviour. The importance of this subject hardly needs to be stressed. Indeed, the amazing power which the atoms of carbon display of combining with themselves and with other atoms to form an immense variety of distinct compounds is one of the marvels of nature. It is perhaps part of the secret of life itself.

The science of chemistry made a great step forwards when it was realised that the structure of a chemical molecule can only be properly described in terms of the configuration in three-dimensional space of the atoms of which it is composed. This approach to chemical problems made its debut in the year 1874 when Van'T Hoff put forward his famous hypothesis of the tetrahedral carbon atom. What that description of the carbon atom really signifies, the physical and chemical evidence on which our belief in its validity is based and the explanation of the chemical behaviour of carbon in terms of the ultimate structure of its atoms are the topics which we shall proceed to consider. The ideas which emerge from the discussion will then be applied to an elucidation of the crystal structure of diamond and the explanation of the properties of that remarkable substance.

2. THE FOUR VALENCES OF CARBON

The simplest molecules exhibiting the disposition in space of the valences of the carbon atom are those in which an atom of carbon combines with four similar atoms or similar groups of atoms. This situation exists, for example, in the cases of methane (CH_4), deuteromethane (CD_4), carbon tetrafluoride (CF_4), carbon tetrachloride (CCl_4), carbon tetrabromide (CBr_4), tetramethyl methane [$C(CH_3)_4$] and so forth. In all these cases, the atoms or atomic groups which combine with the carbon atom are found to be disposed in space with perfect tetrahedral symmetry round it. This is most convincingly shown by the study of the vibration spectra of these molecules.

* Presidential Address to the Indian Academy of Sciences at the Tirupati Meeting on the 28th December, 1957.

A molecule composed of five atoms would in general exhibit nine modes of free vibration. On the other hand, the five-atom groups listed above exhibit only four fundamental frequencies of vibration. Such a reduction would follow as a necessary consequence of the molecule possessing perfect tetrahedral symmetry. It is therefore to be regarded as demonstrating that the atoms in these molecules are located at the vertices of a regular tetrahedron with the carbon atom itself at its centre.

The vibration spectra of molecules in which an atom of carbon combines with three atoms of one kind and a fourth of a different kind show that in every such case, they have six fundamental vibration frequencies and no more. As examples of this behaviour may be listed the molecules of DCH_3, HCD_3, HCF_3, FCH_3, $HCCl_3$, $DCCl_3$, $FCCl_3$, $ClCH_3$, $ClCD_3$, $BrCH_3$, $BrCD_3$ and ICH_3. Dynamical theory shows that a five-atom group possessing a triad axis of symmetry would exhibit only six distinct frequencies instead of nine. The observed facts are thus a clear proof that the molecules listed do possess such a symmetry. On the other hand, molecules containing carbon combining with two atoms of one kind and two atoms of another kind should exhibit all the nine modes of vibration, and this is in agreement with experience.

The symmetry of form of the molecules in each of the cases referred to above can also be inferred from the numbers respectively of polarised and depolarised lines observed as frequency shifts in the spectra of light-scattering. Here again, the experimental facts confirm the tetrahedral character of the atomic grouping around the central carbon atom.

Studies on the vibration spectra of various molecules of the kind quoted above also furnish us with a convincing proof of the non-existence of the several isomers which may be expected to be forthcoming if the four valences of carbon were not equivalent. For, the vibration frequencies of the molecules would be influenced by the atomic configurations and each isomer would therefore have its own set of vibration frequencies. As the characteristic frequencies reveal themselves as well-defined lines in the spectrum, multiplication of the number of observed frequencies would follow as a consequence of the existence of more than one form of the molecule. As no such effect is observed in the numerous cases which have been studied, we are justified in inferring that such isomers do not exist.

A question of great importance which arises in regard to molecules in which an atom of carbon is joined to four others which are not all the same is whether their joins with it make equal angles with each other as is

to be expected if the valences were directed along the axes of a regular tetrahedron. This question can only be answered if methods for precise determination of the atomic configurations were available. Two such methods have been employed for the determination of the atomic configurations in molecules, namely, X-ray diffraction and electron diffraction. Both of these methods involve recondite theoretical considerations besides complicated calculations. The results derived from them must therefore be considered as subject to some measure of uncertainty and this has to be borne in mind in assessing the significance of the reported results. Pauling, in his book '*On the Nature of the Chemical Bond*' (Second Edition, 1940, Table 14-I) gives a list of sixteen carbon compounds of varying degrees of complexity whose molecular structure has been investigated by electron diffraction methods. The table of results gives the bond angle subtended at the carbon atom for eight different species of bonds, namely, C–C–C, C–C–Cl, C–C–Br, F–C–F, Cl–C–Cl, Br–C–Br, F–C–Cl and N–C–N. In five of these cases, namely, C–C–Br, C–C–Cl, F–C–F, F–C–Cl and N–C–N the angles are indistinguishable from the tetrahedral angle of 109° 28′, while in the three other cases, namely, Cl–C–Cl, C–C–C and Br–C–Br the reported bond angles exceed the tetrahedral angles by a degree or two; but this difference cannot be regarded as significant since the reported experimental uncertainties are of the same order of magnitude.

We may sum up the conclusions which may be legitimately drawn from the facts of experiment cited above as follows: *When an atom of carbon combines with four others, the four valences are directed along the four axes of a regular tetrahedron but are otherwise indistinguishable from each other.*

3. The Atomic Structure of Carbon

The interpretation which has to be placed on the results stated above becomes clear when we take note of the position of carbon in a list of the chemical elements arranged in the order of atomic numbers, that is to say, according to the magnitude of charge on the nucleus of the atom or the number of the electrons outside the nucleus. In such a list, the chemically inert gas helium occupies the second position, and the chemically inert neon occupies the tenth, while carbon with its six electrons occupies a position midway between them. Likewise, silicon which in several respects exhibits a chemical behaviour similar to carbon and has fourteen electrons stands midway between the inert gases neon and argon which have respectively ten and eighteen electrons outside their atomic nuclei. This is an example of the periodicity in chemical behaviour which makes itself evident when the elements are listed in the order of their atomic numbers. Such periodicity

finds its explanation in certain general features manifested in the building up of the atoms, *viz.*, the arrangement of the extra-nuclear electrons in a series of shells denoted respectively as K, L, M, etc. When the K shell is complete with its two electrons, we have the inert gas helium; when the L shell is also complete with its eight additional electrons, we have the inert gas neon; when a further eight electrons have been put into the M shell, we have the inert gas argon. Thus it is clear that the quadrivalence of carbon arises from the fact that it has four electrons in the L shell, just half the full quota of eight electrons needed to complete that shell. Further, since the valences are directed along the four axes of a regular tetrahedron, we are evidently concerned here with a state of the atom in which the four electrons in the L shell by reason of their interactions with each other and with the force field of the charged core of the atom constitute a system which is electrically neutral but exhibits perfect tetrahedral symmetry. This system may therefore be rightly designated as the tetrahedral carbon atom. It can combine with four other atoms or groups of atoms to form molecules, but does not depart sensibly from its tetrahedral symmetry of structure as the result of such combination.

We have now to ask ourselves what precisely are the circumstances which favour the formation of the tetrahedral quartet of electrons referred to above. It is well known that helium, neon and argon besides being chemically inert are also diamagnetic in their behaviour. The explanation given for the latter circumstance is that in the building up of the electronic clouds, the magnetic moments arising from the inherent spins of the electrons as well as those, if any, arising from their orbital movements around the nucleus mutually cancel each other out. The same circumstance is also responsible for the chemical inertness of these gases. For this to happen in the L shell of an atom we require eight electrons, but since there are only four present in the L shell of carbon, the same situation cannot arise in its case. But the question does arise as to how the angular momenta associated with the orbital motion and the inherent spins of the four electrons are disposed. If the configuration resulting from the mutual interactions of the four electrons is to possess full tetrahedral symmetry, it is clearly necessary that the resultant angular momenta associated with each of the four electrons considered individually should be equal and that further, these momenta should set themselves respectively along the four axes of a regular tetrahedron. The total angular momentum of the quartet and hence also its magnetic moment would vanish in these circumstances, and hence *the quartet of electrons must be considered as diamagnetic. But it would not*

be chemically inert since the cancellation is a result of the tetrahedral setting of the individual angular momenta and not of their internal pairing off.

An interesting consequence of the foregoing ideas should be here referred to. The angular momentum of an electron and hence also the magnetic moment associated with it is a vector and hence must be regarded as having both a direction and a sign. As already remarked, the directions in the present case are along the four axes of a regular tetrahedron, and if the quartet is to possess tetrahedral symmetry, all the four vectors concerned should have the same sense. Hence, they should all be directed either outwards or inwards from the core of the atom. Thus we have two distinct possible states of the tetrahedral carbon atom which we might designate as the α and the β states respectively. These do not differ from each other except in the sense of the angular momenta of the individual electrons, these being directed respectively outwards or inwards from the charged core of the atom in the two cases.

4. The Crystal Structure of Diamond

Diamond furnishes a perfect illustration of Van'T Hoff's hypothesis of the tetrahedral carbon atom. For, X-ray analysis discloses its structure to consist of two sets of carbon atoms, each carbon atom in one set being chemically linked with perfect tetrahedral symmetry to four carbon atoms belonging to the other set and *vice versa*. The joins of the carbon atom in each set with the four others in the second set are all parallel to each other and to the four body-diagonals of a cube. Hence diamond exhibits the symmetry belonging to a crystal of the cubic class. Considering this situation in the light of the remarks made in the preceding section, it follows that diamond is a crystal whose properties would not be uniquely decided by the crystal structure alone as determined by the methods of X-ray analysis. Diamond consists of two interpenetrating lattices of carbon atoms. In an ideal crystal all the atoms belonging to one lattice should be the same, but as there are two possible types of tetrahedral carbon atom, it follows that an ideal diamond may belong to any one of four types, namely, $\alpha\alpha$, $\alpha\beta$, $\beta\alpha$, and $\beta\beta$. There is no reason to expect that these four types of diamond would exhibit any significant differences in such properties as lattice spacings, or the energy of formation, or the atomic vibration frequencies and so forth. But we should expect observable differences of a less obvious kind arising from the fact that the $\alpha\alpha$ and $\beta\beta$ types of diamond would possess a perfect octahedral symmetry in their crystal structure, whereas the two other types $\alpha\beta$ and $\beta\alpha$ would exhibit only the lower or tetrahedral symmetry.

Thus our present approach to the basic problems of organic chemistry leads to a natural and intelligible explanation of the fact that some diamonds exhibit infra-red absorption in the region of wave-lengths about 8 μ including the characteristic lattice frequencies of vibration, while other diamonds do not exhibit this absorption. The diamonds which exhibit such absorption are those whose structure is of the $\alpha\beta$ or $\beta\alpha$ type, while those that do not are those whose structure is of the $\alpha\alpha$ or $\beta\beta$ type. Considerations of the same nature would also account for the differences exhibited by diamond in respect of other properties including expecially the presence or absence of absorption of light in the near ultra-violet, which as is well known accompany the presence or absence of infra-red absorption in the 8 μ region. We shall not enter into these questions here in detail but shall content ourselves with making two further remarks. The difference between the diamonds exhibiting octahedral and tetrahedral symmetry respectively cannot be expected to manifest itself in any difference in piezo-electric behaviour. The other remark is to recall the fact long known to mineralogists that the external forms of the diamond crystals found in nature more often than not indicate the lower or tetrahedral symmetry instead of the higher or octahedral one. This fact ceases to be surprising in the light of the considerations set forth above.

5. THE THEORY OF HYBRID BOND ORBITALS

We cannot avoid making some reference here to the attempts that have been made to explain the directed valences of the carbon atom in terms of ideas based on the Schrodinger solution of the wave-equation for the hydrogen atom. The theory of hybrid bond orbitals, as it is called, can be summarised as follows: The solution of the hydrogen problem by the Schrodinger method yields a series of solutions (*s*, *p*, *d*, etc.) which indicate the possible distributions of electron density around the nucleus. The wave-function *s* indicates a distribution of electron density spherically symmetrical round the nucleus, where there are three wave-functions denoted by p_x, p_y and p_z respectively which represent density distributions whose maximum extensions are respectively along the x, y and z axes in both directions. All these wave-functions represent the same energy and hence it is possible to construct linear combinations of them so as to produce new wave-functions which are orthogonal to each other. By giving equal weights to the wave-functions p_x, p_y and p_z but different signs in different cases and adding the *s* wave-function, it is possible to obtain four wave-functions which are tetrahedrally symmetric with respect to the nucleus.

The four orbitals thus derived are put forward as a representation of the directed valences of a carbon atom.

Several criticisms of a fundamental nature regarding the theory thus briefly summarised may be put forward. The first objection is that we are not concerned here with a hydrogen atom having a single electron but with a carbon atom having two inner and four outer electrons; the interactions of these with each other and with the atomic nucleus are of the very essence of the problem but they are left out of consideration in the theory. A second objection is that the theory does not explicitly consider the spin of the electrons, though they play a fundamental role in the theory of atomic structure. Apart from these difficulties, one is also confronted with the fact that we have an infinite number of possible sp^3 hybrids and the question may well be asked why the particular set which gives four orbitals indicative of a tetrahedral orientation of the valences should be chosen out of them all. The fundamental feature of the quadrivalence of carbon is that the tetrahedral disposition of the valences is maintained even when the four atoms with which the combination occurs differ from each other enormously, as for example, hydrogen, carbon, nitrogen, fluorine, bromine, chlorine and iodine—to mention no others. *It is this circumstance which indicates that the determining factor which gives rise to the tetrahedral configuration of the valences is not the energy of formation of the bond or bonds, but is an inherent property of the carbon atom itself.* In other words, it is to be found in the mutual interactions between the quartet of electrons which compel them to set themselves in a uniquely determined tetrahedral configuration.

6. Summary

The experimental evidence derived from the study of the vibration spectra of molecules and of their electron diffraction patterns shows unequivocally that the four valences directed outwards from a carbon atom are parallel to the four axes of a regular tetrahedron. That this disposition is maintained even when the four atoms combining with the carbon atom differ enormously from each other indicates that we are concerned here with an intrinsic property of the carbon atom, namely, that the quartet of electrons in the L shell as a result of their mutual interactions can set themselves so as to constitute a structure possessing perfect tetrahedral symmetry. Such a structure would be diamagnetic but not chemically inert, since the individual angular momenta cancel out as a result of the tetrahedral setting and not as a consequence of the internal pairing off as in the inert as molecules,

It follows from these considerations that there are two possible states of the carbon atom and hence also four possible forms of diamond, which may be designated as $\alpha\alpha$, $\alpha\beta$, $\beta\alpha$ and $\beta\beta$ respectively. The first and the last would have true octahedral symmetry, while the second and the third would have the lower or tetrahedral symmetry. The differences in physical behaviour exhibited by even ideal diamonds in various respects, including especially their infra-red absorption spectra, thus receive a natural and intelligible explanation.

Reprinted from "The Proceedings of the Indian Academy of Sciences", Vol. XLVII, No. 2, Sec. A, 1958

ANHARMONICITY OF VIBRATION IN MOLECULES

By K. S. Viswanathan

(*Memoir No.* 105 *of the Raman Research Institute, Bangalore–6*)

Received December 19, 1957

1. Introduction

Anharmonicity of vibration is responsible for several of the finer features observed in the vibration spectra of molecules, *viz.*, the uneven spacing of the overtone levels of the different normal modes and the splitting of levels that are degenerate in the harmonic oscillator approximation. The spectrum of the vibrational energy levels, when the effect of anharmonic terms in the potential energy of the molecule is taken into account, has been the subject of several investigations, references to which can be had from the well-known books on the subject by Herzberg[1] and by Wilson, Decius and Cross.[2] In a detailed and elaborate piece of work, Nielson[3] has considered the problem for a general molecule taking account of one more complication, *viz.*, the vibration-rotation interaction in the molecule.

In the harmonic oscillator approximation, the normal modes of vibration of the molecule are independent of each other and the energy of the system is the sum of the energies of the $(3n - 6)$ normal modes of the molecule. When anharmonicity is taken into account, product terms of the third and higher powers in the normal co-ordinates are introduced in the potential energy of the system, and as a consequence the normal modes are no longer independent but interact with each other. The standard procedure for obtaining the corrections to the energy levels due to the anharmonic terms is by the perturbation method applied to $N = (3n - 6)$ variables and the results of the theory indicate that the energy levels get altered by the introduction of additional quadratic terms in the vibrational quantum numbers of the normal modes of the molecule. In the present paper, we adopt a different method and follow a procedure well known in the treatment of electronic motion in atoms and molecules, namely the method of the self-consistent field proposed by Hartree. Each normal mode of the molecule is assumed to be moving in the average potential field of vibration of the remaining ones, and the eigenfunctions and energy levels of each of the normal modes are calculated accordingly. Apart from the academic interest of the fact that the Hartree method can be applied to the problems of vibrational motion of the molecule, the procedure deserves attention

since it enables one to regard a molecule as an assembly of anharmonic oscillators and calculate the anharmonicity constants in terms of the force constants of the molecule, and also because it enables one to evaluate a measure of the interaction exerted on each mode by the remaining ones. Thus it is shown in Section 2 that a normal mode of the anti-symmetric species does not interact with the rest even in the first order of approximation. In Section 3, the question of degeneracy has been considered and eigen-functions and energy values for the case in which one of the modes is doubly degenerate have been evaluated.

2. THE ENERGY LEVELS

We start from the equilibrium configuration of the molecule, that is the configuration in which the forces acting on each atom of the molecule is zero. Referred to this state, the potential energy of the system will not contain any terms linear in the displacements of the atoms. If further we use normal co-ordinates, the potential and kinetic energies will not contain any quadratic cross terms and we can write therefore

$$T = \frac{1}{2}\sum_{i=1}^{N} \dot{\eta}_i^2 \tag{1}$$

$$V = \frac{1}{2}\sum_{i=1}^{N} \lambda_i \eta_i^2 + \frac{1}{3!}\sum_i\sum_j\sum_k a_{ijk}\,\eta_i\,\eta_j\,\eta_k + \frac{1}{4!}\sum_i\sum_j\sum_k\sum_l \beta_{ijkl}\,\eta_i\,\eta_j\,\eta_k\,\eta_l \tag{2}$$

where $\eta_1, \eta_2, \ldots\ldots\ldots \eta_N$ ($N = 3n - 6$ or $3n - 5$ as the case may be) are the normal co-ordinates of the system. We first consider the case in which the system is non-degenerate. The constants $\lambda_1, \lambda_2, \ldots\ldots\ldots \lambda_N$ in (2) are then all different.

The wave function $\psi(\eta_1 \ldots\ldots \eta_N)$ describing the state of the molecule is given by the solution of the variational principle

$$\delta\,[J] = \delta \int \psi^* H\psi dV = 0 \tag{3}$$

subject to the condition

$$\int \psi^* \psi dV = 1 \tag{4}$$

where

$$H = (T + V) \qquad \text{and} \qquad dV = \prod_{i=1}^{N} d\eta_i.$$

We now try to approximate ψ in terms of the 'one normal co-ordinate' wave functions $\psi_i(\eta_i)$, each of which depending on one normal co-ordinate only. We set

$$\psi = \psi_{v_1}(\eta_1)\,\psi_{v_2}(\eta_2)\ldots\ldots\ldots\psi_{v_N}(\eta_N) \tag{5}$$

where $v_1, v_2\ldots\ldots\ldots v_N$ are integral numbers denoting the degree of excitation of the different normal modes, each moving in the field of the rest. The functions $\psi_{v_i}(\eta_i)$ are all assumed to be normalised, and the best possible choice of these which approximate the physical system as closely as possible are obtained as the solution of the variational principle (3). This leads to the following set of differential equations which the ψ's must satisfy.[4]

$$(H_i - \epsilon_i)\,\psi_{v_i} = 0 \tag{6}$$

where

$$H_i = \int \Big(\prod_{k\neq i} \psi_{v_k}{}^*\Big)\, H \Big(\prod_{k\neq i} \psi_{v_k}\Big) \prod_{k\neq i} d\eta_k \tag{7}$$

ϵ_i is independent of the suffix i and denotes the energy of the whole molecule.

To evaluate the Hamiltonian of the i-th normal mode as well as to determine its eigenfunction, we adopt the procedure of variation-iteration. To a first approximation, we ignore the quartic terms in (2) and substitute for all the wave functions $\psi_{v_k}(\eta_k)\,(k \neq i)$ in (7) the harmonic oscillator eigenfunctions of these normal co-ordinates. The integrals that arise in this process, like $\int \psi^*_{v_k}\,\eta_k{}^2\psi_{v_k} d\eta_k$ have been tabulated in Wilson's[2] book and making use of these, we find that equation (6) reduces to

$$\Big\{-\frac{h^2}{8\pi^2}\frac{\partial^2}{\partial\eta_i{}^2} + (A_{i0}{}^{(1)} - \epsilon_i{}^{(1)}) + A_{i1}{}^{(1)}\eta_i + A_{i2}{}^{(1)}\eta_i{}^2$$

$$+ A_{i3}{}^{(1)}\eta_i{}^3\Big\}\,\psi_{v_k}(\eta_i) = 0 \tag{8}$$

where

$$A_{i0}{}^{(1)} = \sum_{l\neq i}(v_l + \tfrac{1}{2})\,h\nu_l;$$

$$A_{i1}{}^{(1)} = \tfrac{1}{2}\sum_{\substack{m \\ m\neq i}} \frac{a_{mmi}(v_m + \tfrac{1}{2})}{\gamma_m};$$

$$A_{i2}{}^{(1)} = \frac{\lambda_i}{2};$$

$$A_{i3}^{(1)} = \tfrac{1}{6}\, a_{iii}; \text{ and}$$

$$\gamma_m = \frac{4\pi^2 \nu_m}{h}. \tag{9}$$

The upper suffix in the above indicates the order of approximation.

Further $\epsilon_i^{(1)} = \int (\Pi\, \psi^*_{v_i})\, H\, (\Pi\, \psi_{v_i}) \Pi\, d\eta_i$ and by substitution of the harmonic oscillator wave-functions in this we get

$$\epsilon_i^{(1)} = \sum_{l=1}^{N} (v_l + \tfrac{1}{2})\, h\nu_l.$$

Hence the eigenvalue of the i-th mode (*i.e.*) $(\epsilon_i^{(1)} - A_0^{(1)})$, is equal to $(v_i + \frac{1}{2})\, h\nu_i$. The first order approximation therfore does not introduce any corrections to the eigenvalues of the different normal modes from their harmonic oscillator values.

From (8) it follows that the Hamiltonian of the oscillator contains an anharmonic cubic term whose coefficient is the same as the coefficient of η_i^3 in the potential energy of the molecule and also a term linear in η_i. The linear term arises out of the process of averaging terms of the type $\eta_i\, \eta_l^2$ and it gives a measure of the action exerted by the other normal modes on the i-th one. It further suggests that the vibrations of the remaining modes tend to displace the equilibrium position of the i-th one from the place it occupies in the equilibrium configuration of the molecule as a whole.

The coefficient of the linear term is much smaller than the coefficient of the cubic one and their ratio is of the order of $1/\gamma \sim 10^{-16}$. But since the region wherein the displacement of the oscillator has a finite probability is of the order of $\gamma^{-\frac{1}{2}}$, both these terms are of the same order of smallness.

If the i-th mode belongs to an antisymmetric species of vibration of the molecule, all the coefficients of the type a_{mmi} and a_{iii} should be equal to zero. This is because the potential energy, including third and higher order terms, should be invariant under all the symmetry operations of the molecule and there will be at least one operation which will change the sign of a normal co-ordinate falling under an antisymmetric species of the molecule. Thus from (9) it follows that *to a first approximation a normal mode belonging to the antisymmetric species of vibration of the molecule does not interact with the rest and also it suffers no anharmonicity.*

The first order eigenfunctions of (8) may be obtained by the perturbation method. The normalised eigenfunctions are given by

$$\psi_{v_i}^{(1)} = a_i \psi_{v_i}^{(0)} + a_{i-3}^{(0)} \psi_{v_i-3}^{(0)} + a_{i-1}^{(0)} \psi_{v_i-1}^{(0)} + a_{i+1}^{(0)} \psi_{v_i+1}^{(0)} + a_{i+3}^{(0)} \psi_{v_i+3}^{(0)} \tag{10}$$

where

$$a_i = 1 - \frac{f_i}{2h^2\nu_i^2(8\gamma_i^3)} + \tfrac{3}{8}\frac{f_i^2}{(8h^2\nu_i^2\gamma_i^3)^2}$$

with

$$f_i = \frac{1}{9}\, v_i(v_i - 1)(v_i - 2)\,\alpha_i^2 + v_i(3v_i\alpha_i + \beta_i)^2$$
$$+ (v_i + 1)\,[3(v_i + 1)\,\alpha_i + \beta_i]^2$$
$$+ \frac{1}{9}(v_i + 1)(v_i + 2)(v_i + 3)\,\alpha_i^2;$$

$$a_{i-3} = \frac{-a_i}{3h\nu_i(8\gamma_i^3)^{\frac{1}{2}}}\,[v_i(v_i - 1)(v_i - 2)]^{\frac{1}{2}}\,\alpha_i;$$

$$a_{i-1} = \frac{-a_i}{h\nu_i(8\gamma_i^3)^{\frac{1}{2}}}\,v_i^{\frac{1}{2}}\,(3v_i\alpha_i + \beta_i); \qquad (11)$$

$$a_{i+1} = \frac{a_i}{h\nu_i(8\gamma_i^3)^{\frac{1}{2}}}\,(v_i + 1)^{\frac{1}{2}}\,[3(v_i + 1)\,\alpha_i + \beta_i]$$

$$a_{i+3} = \frac{a_i}{3h\nu_i(8\gamma_i^3)^{\frac{1}{2}}}\,[(v_i + 1)(v_i + 2)(v_i + 3)]^{\frac{1}{2}}\,\alpha_i$$

and

$$\alpha_i = \frac{-\alpha_{iii}}{6} \quad \text{and} \quad \beta_i = -\gamma_i \sum_{m \neq i} \frac{\alpha_{mmi}(v_m + \frac{1}{2})}{\gamma_m}$$

The upper suffix in (10) denotes the order of approximation. The zeroth order functions are chosen as the harmonic oscillator eigenfunctions.

To obtain the eigenvalues and eigenfunctions correct to the second order, we substitute the first order eigenfunctions (10) in (7). We now take into account of the quartic terms in the Hamiltonian also. After considerable simplification, the wave function of the *i*th mode can be written as

$$\left\{-\frac{h^2}{8\pi^2}\frac{\partial^2}{\partial\eta_i^2} + A_{i1}^{(2)}\eta_i + A_{i2}^{(2)}\eta_i^2 + A_{i3}^{(2)}\eta_i^3 + A_{i4}^{(2)}\eta_i^4\right\}\psi_{v_i}$$
$$= W_i^{(2)}\psi_{v_i} \qquad (12)$$

where

$$A_{i_1}^{(2)} = \sum_l{}' \frac{\alpha_{lli}(v_l + \frac{1}{2})}{2\gamma_l} + \sum_l{}' \frac{\alpha_{lli}}{16h^2\nu_l^2\gamma_l^4} Q_l$$

$$+ \sum_l{}' \frac{\beta_{llli}}{24\gamma_l^3 h\nu_l} T_l + \sum_{\substack{lm \\ l<m}}{}' \frac{\alpha_{lmi}}{4\gamma_l^2\gamma_m^2 h^2\nu_l\nu_m} R_l R_m$$

$$+ \sum_{lm}{}' \frac{\beta_{llmi}(v_l + \frac{1}{2}) R_m}{4\gamma_m^2\gamma_l h\nu_m};$$

$$A_{i_2}^{(2)} = \frac{\lambda_i}{2} + \sum_l{}' \frac{\alpha_{lii}R_l}{4\gamma_l^2 h\nu_l} + \sum_l{}' \frac{\beta_{llii}}{4\gamma_l}(v_l + \tfrac{1}{2});$$

$$A_{i_3}^{(2)} = \frac{\alpha_{iii}}{6} + \frac{1}{12}\sum_l{}' \frac{\beta_{liii}}{h\nu_l\gamma_l^2} R_l; \tag{13}$$

$$A_{i_4}^{(2)} = \frac{1}{24}\beta_{iiii}$$

and

$$W_i^{(2)} = (v_i + \tfrac{1}{2}) h\nu_i + \frac{K_i}{(8\gamma_i^3) h\nu_i} + \frac{\alpha_{iii}}{24\gamma_i^3 h\nu_i} T_i$$

$$+ \frac{\beta_{iiii}}{32\gamma_i^2}\{2(v_i + \tfrac{1}{2})^2 + \tfrac{1}{2}\}$$

$$+ \sum_l{}' \frac{\beta_{llii}}{4\gamma_l\gamma_i}(v_l + \tfrac{1}{2})(v_i + \tfrac{1}{2})$$

$$+ \left\{\sum_m{}' \frac{\alpha_{iim}}{4\gamma_m^2\gamma_i h\nu_m}(v_i + \tfrac{1}{2}) R_m\right.$$

$$\left. + \sum_m{}' \frac{\alpha_{mmi}}{4\gamma_i^2\gamma_m h\nu_i}(v_m + \tfrac{1}{2}) R_i\right\}$$

In the above the accent indicates that the sum excludes the term l or $m = i$.

The quantities R_l, K_l, T_l and Q_l are given by

$$R_l = 3(2v_l + 1)\alpha_l + \beta_l;$$

$$K_l = 30\alpha_l^2\left\{(v_l + \tfrac{1}{2})^2 + \frac{7}{60}\right\} + 12\alpha_l\beta_l(v_l + \tfrac{1}{2}) + \beta_l^2;$$

$$T_l = 30\alpha_l\left\{(v_l + \tfrac{1}{2})^2 + \frac{7}{60}\right\} + 6\beta_l(v_l + \tfrac{1}{2}); \tag{15}$$

$$\begin{aligned} Q_l = K_l &+ \tfrac{1}{3}v_l(v_l - 1)(v_l - 2)(3v_l\alpha_l + \beta_l)\alpha_l \\ &- v_l(v_l + 1)(3v_l\alpha_l + \beta_l)(3v_l + 1\alpha_l + \beta_l) \\ &+ \tfrac{1}{3}(v_l + 1)(v_l + 2)(v_l + 3)[3(v_l + 1)\alpha_l + \beta_l]\alpha_l \end{aligned}$$

$W_i^{(2)}$ gives the expression for the energy of the ith normal mode.

The energy of the whole molecule is

$$\begin{aligned} \epsilon_i^{(2)} = &\sum_l (v_l + \tfrac{1}{2})h\nu_l + \sum_l \frac{K_l}{(8\gamma_l^3)h\nu_l} + \sum_l \frac{\alpha_{lll}}{24\gamma_l^3 h\nu_l}T_l \\ &+ \sum_l \frac{\beta_{llll}}{32\gamma_l^2}\{2(v_l + \tfrac{1}{2})^2 + \tfrac{1}{2}\} + \sum_{\substack{lm \\ l\neq m}} \frac{\alpha_{llm}R_m}{4\gamma_m^2\gamma_l h\nu_m}(v_l + \tfrac{1}{2}) \\ &+ \sum_{\substack{lm \\ l<m}} \frac{\beta_{llmm}}{4\gamma_l\gamma_m}(v_l + \tfrac{1}{2})(v_m + \tfrac{1}{2}) \end{aligned} \tag{16}$$

Remark

We shall define W^{im} by

$$\begin{aligned} W^{im} = &\left\{\frac{\alpha_{iim}}{4\gamma_m^2\gamma_i h\nu_m}(v_i + \tfrac{1}{2})R_m + \frac{\alpha_{mmi}(v_m + \tfrac{1}{2})R_i}{4\gamma_i^2\gamma_m h\nu_i}\right. \\ &\left. + \frac{\beta_{mmii}}{4\gamma_m\gamma_i}(v_m + \tfrac{1}{2})(v_i + \tfrac{1}{2})\right\} \end{aligned} \tag{17}$$

W^{im} denotes the average interaction energy of the ith and mth modes correct to the second order of approximation. The energy of the whole molecule is related to the energy of the individual modes by means of the relation

$$\epsilon_i^{(2)} = \sum_i W_i^{(2)} - \tfrac{1}{2}\sum_i \sum_m W^{im} \tag{18}$$

3. DEGENERACY

We now consider the case of degeneracy of vibrations. For the sake of preciseness, we consider the case in which one of the modes of vibrations of the molecule is doubly degenerate and the remaining modes are all non-degenerate. The more general cases can be discussed on exactly the same lines. Let us denote the modes that are degenerate with one another by the suffixes (N − 1) and N so that $\nu_{N-1} = \nu_N$. Our problem then is to evaluate the energy values and eigenfunctions of the degenerate mode and to find a measure of its splitting due to anharmonicity.

Let us fix our attention on a state in which the different normal modes of the molecule are excited by $v_1, v_2, \ldots\ldots v_{N-2}$ and v_N quantas respectively. The degeneracy of the overtone level of the doubly degenerate mode is then (v_{N+1}). It is well known that the eigenfunctions for the degenerate mode may be written as

$$\psi_m = N_m e^{(-\gamma_N/2)\rho_N^2} F_{v_N}^{l_N} (\sqrt{\gamma_N}\rho_N)\, e^{\pm i l_N \phi_N} \tag{19}$$

where $F_{v_N}^{l_N}(\sqrt{\gamma_N}\rho_N)$ is a polynomial of degree v_N in ρ_N $[= (\eta_{N-1}^2 + \eta_N^2)^{\frac{1}{2}}]$, and l_N is an integer which can assume the values v_N, v_{N-2}, $v_{N-4} \ldots .1$ or 0 depending on whether v_N is odd or even.

Now the symmetry of an overtone level of degree v_N of a mode which falls under a species Γ of the molecule is given by $(\Gamma)^{v_N}$ and this is in general, a linear sum of the irreducible representations of the point group of the molecule. Thus the wave-functions (19) will transform, under a symmetry operation, like a linear sum of the different irreducible representations of the molecule. Or, alternatively, one can form linear combinations of the above $(v_N + 1)$ wave-functions in such a way that the resulting functions fall exclusively each under any one of the irreducible representations of the symmetry group of the molecule.

Let us suppose that the structure of the level under consideration is given by $\sum_{\gamma} n^{(\gamma)}\Gamma^{(\gamma)}$ where $\Gamma^{(\gamma)}$ stands for the γth species and $n^{(\gamma)}$ is the number of times this species occurs in the reduced representation of the level. It has been shown by Tisza[5] that only wave-functions which either belong to different irreducible representations or to different matrix representations of the same species can have different energy levels and thus the *maximum* number of components into which the level can be split up by the anharmonic terms is $\Sigma n^{(\gamma)}$.

Let us now subject the set of wave-functions (19) to an orthogonal transformation and obtain a new set of functions $\psi_s^{\gamma a}$ $(s = 1, 2, \ldots . v_{N+1})$ such

that each one of these fall exclusively under one of the irreducible representations of the symmetry group of the molecule. In symbols,

$$\psi_S{}^{\gamma a} = \sum_{m=1}^{v_{N+1}} C_{sm}{}^{\gamma a} \psi_m \qquad (s = 1, 2, \ldots . v_{N+1}) \tag{20}$$

where

$$\sum_{m=1}^{(v_{N+1})} (C_{sm}{}^{\gamma a})^2 = 1 \tag{21}$$

and

$$\sum_{m=1}^{v_{N+1}} C_{sm}{}^{\gamma a} C_{s'm}{}^{\gamma' a'} = 0 \qquad (s \neq s')$$

In the above the upper suffix γ denotes the irreducible representation $\Gamma^{(\gamma)}$ under which $\psi_S{}^{\gamma a}$ falls, and a denotes the matrix representation of the irreducible representation. All functions with different γ and a may therefore be expected to have different energies.

The wave function for the ith mode is now given by

$$(H_i - \epsilon_i)\, \psi_{v_i} = 0 \tag{22}$$

where

$$H_i = \int (\Pi_{k \neq i} \psi^*_{v_k})\, H\, (\Pi_{k \neq i} \psi_{v_k}) \Pi_{k \neq i}\, d\eta_k \tag{22 a}$$

In evaluating the above expression, we may notice that the potential energy of the system does not contain the factors η_{N-1} or η_N individually, but involves these only through the sum of their squares (*i.e.*) through

$$(\eta_{N-1}{}^2 + \eta_N{}^2) = \rho_N{}^2.$$

Thus, we have

$$a_{ijN-1} = a_{ijN} = 0$$

$$(i, j = 1, 2, \ldots . N - 2); \quad a_{N-1\ N-1\ N-1} = a_{NNN} = 0;$$

$$\beta_{ijkN-1} = \beta_{ijkN} = \ldots . = \beta_{iNNN} = 0 \ldots .$$

$$(i, j, k = 1, 2, \ldots . N - 2)$$

and

$$a_{iN-1\ N-1} = a_{iNN}; \quad \beta_{ijN-1\ N-1} = \beta_{ijNN}, \text{ etc.}$$

The first-order energy values and eigenfunctions may be obtained by substituting the harmonic oscillator wave functions for the non-degenerate modes and the function $\psi_S^{\gamma a}$ for the degenerate one. We get $\epsilon_i^{(1)} = \Sigma (v_i + d_i/2)\, h\nu_i$ where the sum is over all modes with distinct frequencies and d_i denotes the degeneracy of the ith mode. The wave equation is given by the same formulæ (8) and (9) with this difference that the constants $A_{i0}^{(1)}$ and $A_{i1}^{(1)}$ get modified in this by

$$A_{i0}^{(1)} = \sum_j{}' \left(v_j + \frac{d_j}{2}\right) h\nu_j$$

and

$$A_{i1}^{(1)} = \tfrac{1}{2} \sum_m{}' \frac{a_{mmi}\left(v_m + \frac{d_m}{2}\right)}{\gamma_m} \tag{23}$$

The first order wave equation is therefore still given by (10) with this change that β_i should be defined here by

$$\beta_i = -\gamma_i \Sigma' \frac{a_{mmi}\left(v_m + \frac{d_m}{2}\right)}{\gamma_m} \tag{24}$$

For the degenerate mode, the wave equation is given by

$$\left\{-\frac{h^2}{8\pi^2}\left(\frac{\partial^2}{\partial \eta^2_{N-1}} + \frac{\partial^2}{\partial \eta_N{}^2}\right) - W_N^{(1)} + \frac{\lambda_N}{2}\rho_N{}^2\right\}\psi_{v_N} = 0 \tag{25}$$

where

$$W_N^{(1)} = (v_N + 1)\, h\nu_N.$$

We see that in the first order approximation, anharmonicity does not affect the degenerate mode at all.

The Hamiltonian as well as the eigenvalue for the degenerate mode correct to the second order may be obtained by substituting the wave functions given by (10) and (24) in the variational principle (6). One gets

$$\left\{-\frac{h^2}{8\pi^2}\left(\frac{\partial^2}{\partial \eta^2_{N-1}} + \frac{\partial^2}{\partial \eta_N{}^2}\right) - W_N^{(2)} + A_N^{(2)}\rho_N{}^2 + A_N^{(4)}\rho_N{}^4\right\}\psi_{v_N} = 0 \tag{26}$$

where

$$A_N^{(4)} = \frac{1}{24}\beta_{NNNN};$$

$$A_N^{(2)} = \frac{\lambda_N}{2} + \sum_{l=1}^{N-2} \frac{\alpha_{NNl}}{4\gamma_l^2 h\nu_l} R_l + \sum_{l=1}^{N-2} \frac{\beta_{NNll}(v_l + \frac{1}{2})}{4\gamma_l};$$

$$W_N^{(2)} = (v_N + 1) h\nu_N + \sum_{m=1}^{N-2} \frac{\alpha_{NNm}(v_N + 1)}{4\gamma_m^2 \gamma_N h\nu_m} R_m$$

$$+ \sum_m \frac{\beta_{NNmm}}{4\gamma_m \gamma_N}(v_N + 1)(v_m + \tfrac{1}{2})$$

$$+ \frac{\beta_{NNNN}}{16\gamma_N^2}\{(v_N + 1)^2 + \tfrac{1}{3}\} - \frac{\beta_{NNNN}}{48\gamma_N^2}$$

$$\times \{\sum_{m=1}^{v_N+1} (C_{sm}^{\gamma a})^2 l_m^2\} \quad (27)$$

Since the last term in the above may be expected to be different for functions with different γ and a (*i.e.*) for wave functions falling under different irreducible representations or different matrix representations of the same irreducible representation, each level of the degenerate mode will get split into not more than (Σn^γ) sublevels.

The energy of the whole molecule is

$$\epsilon_i^{(2)} = \sum_l \left(v_l + \frac{d_l}{2}\right) h\nu_l + \sum_{l=1}^{N-2} \frac{K_l}{(8\gamma_l^3) h\nu_l}$$

$$+ \sum_{l=1}^{N-2} \frac{\alpha_{lll}}{24\gamma_l^3 h\nu_l} T_l + \sum_{\substack{lm \\ m \neq N}} \frac{\alpha_{llm}\left(v_l + \frac{d_l}{2}\right)}{4\gamma_m^2 \gamma_l h\nu_m} R_m$$

$$+ \sum_{l=1}^{N-2} \frac{\beta_{llll}}{16\gamma_l^2}\{(v_l + \tfrac{1}{2})^2 + \tfrac{1}{4}\}$$

$$+ \sum_{\substack{lm \\ l<m}} \frac{\beta_{llmm}}{4\gamma_l \gamma_m}\left(v_l + \frac{d_l}{2}\right)\left(v_m + \frac{d_m}{2}\right)$$

$$+ \frac{\beta_{NNNN}}{16\gamma_N^2}\{(v_N+1)^2+\tfrac{1}{3}\} - \frac{\beta_{NNNN}}{48\gamma_N^2}$$

$$\times \{\sum_{m=1}^{v_{N+1}} (C_{sm}^{\gamma a})^2 l_m^2\} \qquad (28)$$

Nielson has given explicit expressions for the vibrational energy levels of the molecule. His formula for the energy of the molecule may be written as

$$G(v_1, v_2, \ldots .)$$

$$= \sum_i \left(v_i + \frac{d_i}{2}\right) h\nu_i + \sum_{i} \sum_{\substack{k \\ k > i}} x_{ik}$$

$$\times \left(v_i + \frac{d_i}{2}\right)\left(v_k + \frac{d_k}{2}\right) + \sum_i \sum_{k \geqslant i} g_{ik}\, l_i\, l_k \qquad (29)$$

In the above, the cross coefficient g_{ik} of the azimuthal quantum numbers l_i and l_k depends on the vibration-rotation interaction of the molecule which is a feature considered in Nielson's work. This explains the absence of the cross terms in the quantum number 'l' in the equation (28). Further, as has been pointed out by Herzberg, the formula (29) gives in general a splitting into fewer levels than what a group theoretical theory would indicate. This is because the wavefunctions used in the evaluation of energy in (29) are the functions (19) and not linear combinations of these falling under different representations of the point group of the molecule. A comparison of (28) with (29) however indicates that the difference is only slight and consists in the replacement of g_{ll} by a coefficient $g_{ll}^{\gamma a}$ depending on the symmetry of the state of the sublevel.

For a molecule with several degenerate modes of vibration, the symmetry of a general vibrational level is given by the formula

$$\Gamma = (\Gamma_1)^{v_1} \text{X} (\Gamma_2)^{v_2} \qquad \text{X} (\Gamma^f)^{v_f} \qquad (30)$$

where the 'X' denotes the direct product multiplication of groups and $v_1, v_2 \ldots . v_f$ are the degrees of excitation of the modes 1, 2,. . . . f respectively. Γ is a linear sum of the different irreducible representations of the molecule, and thus by forming linear sums of products of the wavefunctions of the type (19) which fall exclusively under one of the matrix representation of an irreducible representation of the symmetry group of the molecule, one can evaluate the energy levels of the molecule. If one adopts the standard

perturbation method involving N variables, the expected energy levels may be written in the form

$$G^{\gamma a}(v_1 v_2 \ldots v_N)$$
$$= \sum \left(v_i + \frac{d_i}{2}\right) h\nu_i + \sum_i \sum_{k>i} x_{ik}^{\gamma a}$$
$$\times \left(v_i + \frac{d_i}{2}\right)\left(v_k + \frac{d_k}{2}\right) + \sum_i \sum_{k>i} g_{ik}^{\gamma a} l_i l_k \qquad (31)$$

In the above, all coefficients $x_{ik}^{\gamma a}$ pertaining to non-degenerate modes will be independent of γ and a, but the coefficients $x_{ik}^{\gamma a}$ pertaining to degenerate modes and the coefficients $g_{ik}^{\gamma a}$ will, in general, be different for levels of different symmetries.

The author's thanks are due to Professor Sir C. V. Raman for his kind interest in this work.

SUMMARY

The presence of anharmonicity entails the interactions of the normal modes of vibrations, which are independent in the harmonic oscillator approximation. The method of Hartree has been applied to study the mutual interaction of the normal modes, each assumed to be moving in the average potential field of the rest, and to evaluate their wave functions and eigenvalues. It is shown that, to a first order of approximation, normal vibrations belonging to the antisymmetric species do not interact with the rest and suffer no anharmonicity at all. The wave functions and eigenvalues of the different normal modes have been evaluated correct to the second order. The question of degeneracy has been considered and expressions have been given for the energy values of the different sublevels into which an overtone level of a degenerate system may be expected to split up according to group-theoretical considerations.

REFERENCES

1. G. Herzberg .. *Infra-Red and Raman Spectra*, Van Nostrand, New York, 1945, pp. 201–226.
2. Wilson, E. B., Decius, J. C. and P. C. Cross .. *Molecular Vibrations*, McGraw Hill Book Co., 1955.
3. Nielson, H. H. .. *Physical Review*, 1941, **60**, 794.
4. Frenkel, J. .. *Wave Mechanics, Advanced General Theory* (Oxford), 1934, 423–28.
5. Tisza, L. .. *Z. Physik.*, 1933, **82**, 48.

Reprinted from "The Proceedings of the Indian Academy of Sciences"
Vol. XLVII, No. 3, Sec. A, 1958

RECIPROCAL LATTICE PHOTOGRAPHY

By A. Jayaraman

(*Memoir No.* 106 *from the Raman Research Institute, Bangalore*-6)

Received February 24, 1958

1. Introduction

Of the single-crystal X-ray photographic methods, the method of reciprocal lattice photography yields undistorted records of the reciprocal lattice. The photographs obtained are not only symmetry-true but also enable one to index the spots by visual inspection.

The well-known De-Jong Bouman camera was the first of its kind. Improved types of cameras were later designed and constructed by M. J. Buerger. A publication bearing the title "The Photography of the Reciprocal Lattice" by M. J. Buerger published as a A.S.X.R.E.D. Monograph, No. 1, 1944 gives in detail the principles involved in reciprocal lattice photography and describes a reciprocal camera, its uses, and advantages over other methods. The principle involved can be stated very briefly as follows: The Ewald construction for the reflection of X-rays by a set of planes indicates that an X-ray reflection occurs whenever a reciprocal lattice point intersects the sphere of reflection. The direction of the reflected beam is got by joining the centre of the reflecting circle and the reciprocal lattice point. If one can always keep the film plane parallel to the reciprocal lattice plane that is being investigated, the record obtained under such conditions represents a scaled replica of the reciprocal lattice plane. This can be shown to be the case with a simple geometric construction shown in Fig. 1. In order to cover as many points of the reciprocal plane as is convenient, a very ingenious kind of rotation has been introduced, in which the normals to the reciprocal lattice plane and the film plane follow a motion, similar to that of a precessing top about an axis which is the direction of the incident X-ray beam. Hence the instrument was given the name "X-ray precession camera". An arrangement is provided in the camera for this type of precessional motion wherein it is possible to set different angles of precession. In order that the film and the reciprocal lattice should remain parallel to each other during the motion, a link system is incorporated in the design of the camera. Further, a layer-line screen whose distance can be altered with

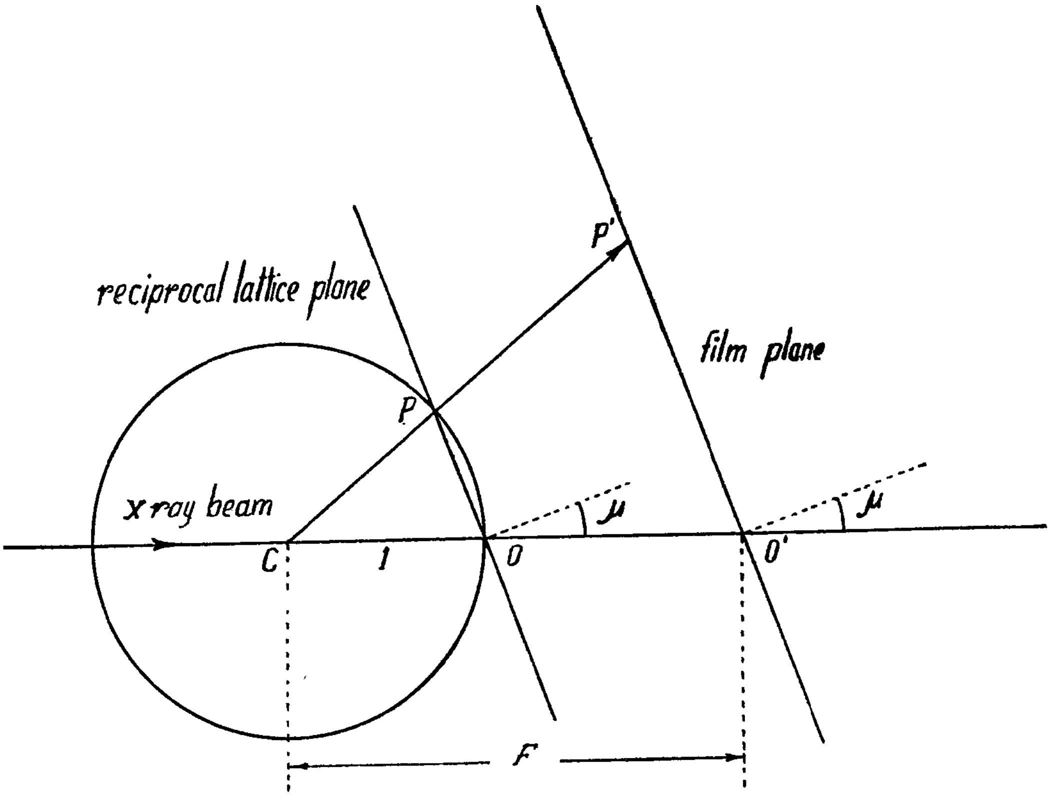

FIG. 1

$$\frac{O'P'}{OP} = \frac{CO'}{CO} = \frac{F}{1} \therefore O'P' = F.OP$$

respect to the crystal is provided, with a view to isolate reflections of a particular layer. A movement for translating the film towards the crystal is also provided so that different reciprocal planes can be recorded without distortion. The geometric conditions necessary for obtaining these results are described and discussed in detail in the book referred to above.

The construction of such a camera was undertaken at this Institute and the present communication describes the same. It is not claimed that the instrument incorporates any new features. It appeared worthwhile however to describe our experience in making and using such a camera for the benefit of those interested in such work.

2. THE CONSTRUCTIONAL FEATURES

A photograph of the reciprocal camera is reproduced in Fig. 2. The different parts of the camera described in this section can be clearly seen on an inspection of the same. The arc-shaped arm which is the principal part of the driving mechanism of the camera can be seen. The arc was cut out

of ¼″ brass plate and represents a part of a circle of radius 16·5 cm., the segment subtending an angle of about 40° at the centre. It is mounted on a bush bearing which is supported on a pillar fixed to the base. The arm can be rotated by a motor about the X-ray beam as its axis. A sliding block on the arm carries the driving axis which goes and fits into a cylindrical brass bush attached to the back of the film holder carrier. The sliding piece at its lowest setting represents a precession angle of 0°, while at the maximum it represents a precession angle of 30°. A square frame which carries the film holder is mounted on a two-axis universal joint. The unmoved point of the universal joint is precisely set in the centre of the circle mentioned above. A sliding arrangement is provided for translating the film holder towards the crystal. The crystal holder assembly is mounted on another two-axis universal joint. The distance between the film and the crystal universal joint centres represents the specimen to film distance, which has been set at 6 cm. in the instrument. The crystal holder assembly supports an L-shaped arm, and this carries a movable layer-line screen. The layer-line screen is made out of brass sheet, 10 cm. square, with an annular opening of 15 mm. in radius. A layer-line screen with an annular opening of 30 mm. in radius will also be found useful. Provision has therefore been made to be able to use the desired layer-line screen. A parellelogram link motion with ball and socket joints at the upper two corners serves as the link between the reciprocal lattice plane and the film plane. The precessional motion executed by the latter is transmitted by this link to the former, maintaining at the same time both the planes strictly parallel. The link is attached at its two lower ends to the projecting horizontal, film and crystal axes. For facilitating initial setting of the crystal, the link at the crystal axis end can be decoupled, leaving the crystal axis free. Further, the platforms which support the film holder carrier and the crystal holder are coupled by two brass links. This serves as a parallelogram link in the horizontal plane. The former link has to be of the ball and socket type, since it has to take care of parallelogram motions in two mutually perpendicular planes. The latter link is absolutely necessary, but is of a very simple type as it has to take care of a parallelogram motion in one plane only, namely, the horizontal plane. The X-ray collimator is carried by the pillar which is seen at the extreme left of the photograph. There is a lead stop which serves to screen off the incident beam after it has emerged from the crystal.

The universal joint carrying the film holder is capable of being moved along the axis of the instrument, while the universal joint carrying the crystal is capable of being moved at right angles to this axis. The X-ray collimator can similarly be moved at right angles to the axis of the instrument. After

proper alignment, these can be firmly clamped. The geometry of the instrument strictly demands that the incident X-ray beam should pass through the two universal joint centres which remain unmoved during the motion. The beam should be set parallel to the axis of the instrument.

In making these universal joints, a tapered cone assembly was used for the vertical axis. Very smooth and satisfactory running is ensured by putting a steel ball on top of the male cone, such that the hollow cone part rests on the steel ball, at the same time remaining just in contact with the male cone. This arrangement helps in reducing the grip between the two members which would otherwise result, and has been found to be very satisfactory. For the horizontal axis two ball bearings were used. A major portion of the instrument was made by machining $\frac{1}{2}''$ thick perspex sheet. It is very easy to shape this material and stick pieces of these together with trichloroethylene. Wherever necessary, pieces were stuck and strengthened by screws and nuts. Since the instrument was at the outset started as a model, the above materials were used, but to our surprise, the materials have been found to be very satisfactory.

Smooth running of the instrument depends on accurate alignment and accurate balancing of the different parts. It may not be out of place to mention here that the camera can be made at a cost much less than one has to pay for the commercially available ones.

3. Photography by the Precession Method

A preliminary step in recording reciprocal lattice photographs is to set the chosen axis of the crystal, parallel to the X-ray beam. If the axis of the crystal is roughly set by trial photographs, or from its known optical properties, accurate setting can be made by taking a series of precession photographs at small precession angles. Such photographs can be taken with short exposure times. The procedure for setting is explained in the book referred to. Once the axis is set parallel to the X-ray beam, the instrument is ready for recording the reciprocal lattice. For recording the zero layer, the film is kept such that its centre coincides with the unmoved point of the universal joint through which the X-ray beam also passes and intersects the film normally. The desired precession angle is then set. The appropriate layer-line screen is chosen and its distance from the crystal is set according to the equation

$$r_s/S = \tan \cos^{-1}(\cos \mu - d^*)$$

where r_s is the radius of the annular opening, S is the screen to crystal distance, μ is the precession angle and d^* is the reciprocal lattice spacing. For

zero layer, d^* is zero and the equation reduces to $r_s/S = \tan \mu$. For recording of higher planes, the appropriate value of d^* should be substituted in the equation.

For recording n levels without distortion, it is necessary to displace the film away from the universal joint centre towards the crystal, by a distance:

$$d' = Fd^*$$

where F is the crystal to film distance, and d^* the reciprocal lattice plane spacing.

Three X-ray precession photographs are reproduced in the plate accompanying this paper. Fig. 3 is a zero layer reciprocal lattice photograph of quartz recorded with the trigonal axis as the precession axis. Mo white radiation was employed. Fig. 4 is again a zero layer photograph of quartz taken with MoKα radiation. Fig. 5 represents the zero layer reciprocal lattice photograph recorded with the b-axis, of the monoclinic crystal cobalt nitrate hexahydrate, as the precession axis. In this case MoKα radiation was used.

The chief advantages of the method are, that it gives a scaled replica of the reciprocal lattice and indexing can be carried out by visual inspection. With crystals of large spacing, the determination of the space-group is comparatively quicker. Another advantage is that if a crystal is set with one crystallographic axis parallel to the goniometer axis, information regarding two reciprocal cell-axes can be obtained without having to remount the crystal, as in the case of other methods. After obtaining photographs about one axis, one has to rotate the crystal through the appropriate angle to bring the second reciprocal cell-axis along the X-ray beam to obtain the records. This is decidedly a great advantage over other methods and especially so when one is dealing with crystals of small dimensions and in low temperature X-ray crystallography.

The author wishes to express his grateful thanks to Professor Sir C. V. Raman, F.R.S., N.L., for his interest in the work. It is a pleasure to thank Dr. S. Ramaseshan for the many illuminating discussions the author had with him.

SUMMARY

A precession X-ray camera constructed at this Institute is described. Reciprocal lattice photographs of quartz and $CO(NO_3)_2\,6H_2O$ recorded with the camera are reproduced and the general principles involved in X-ray reciprocal lattice photography are discussed.

CONNEMARA PUBLIC LIBRARY
4 JAN 1965
MADRAS

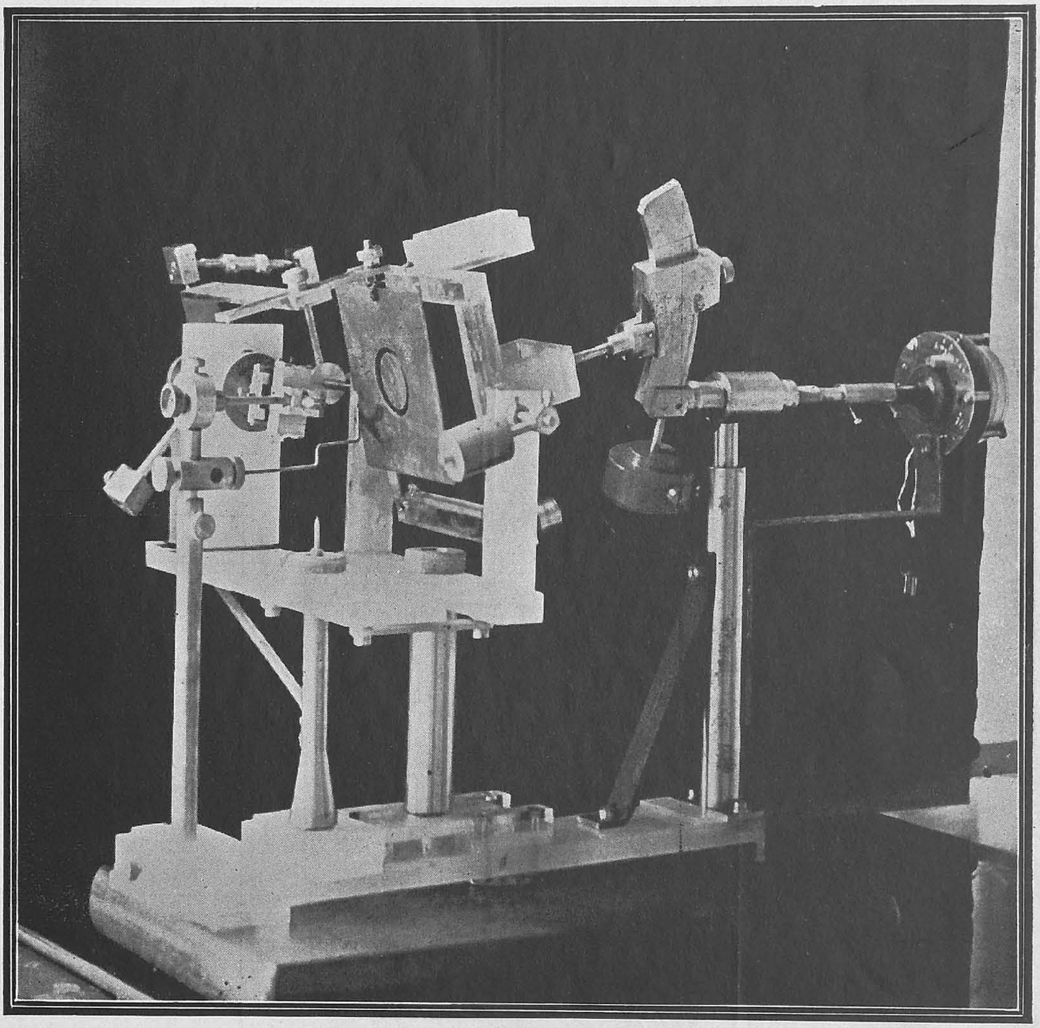

FIG 2

FIG 3

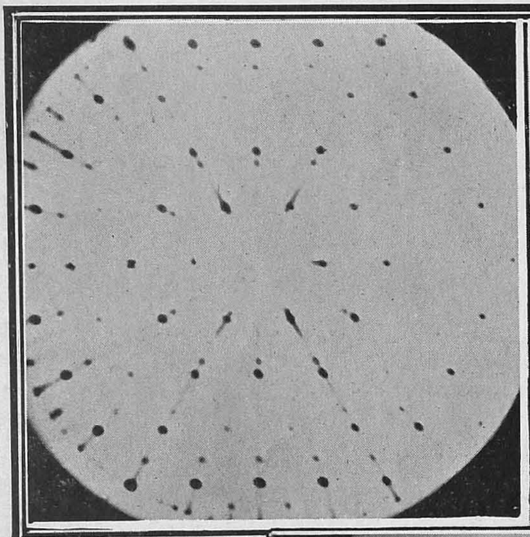

FIG. 4

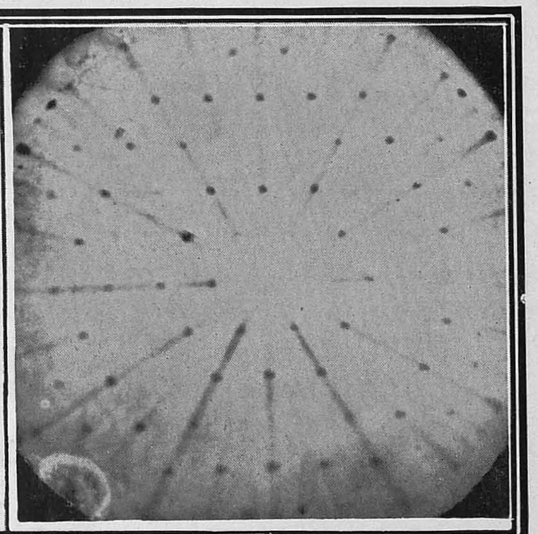

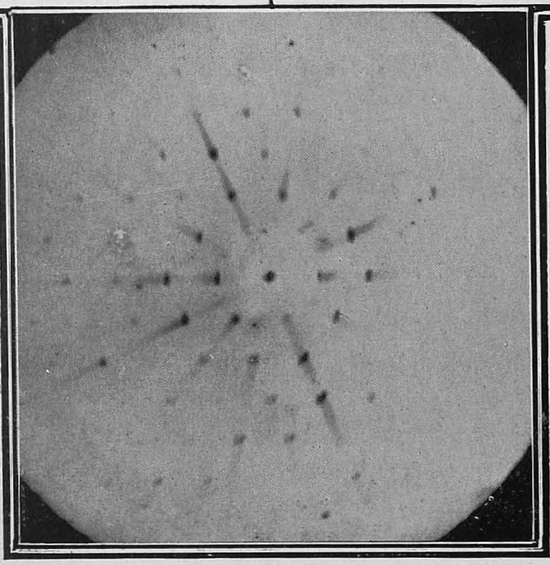

FIG. 5

Reprinted from "The Proceedings of the Indian Academy of Sciences",
Vol. XLVII, No. 3, Sec. A, 1958

UNIT CELL PARAMETERS, SPACE-GROUP AND OPTICAL PROPERTIES OF COBALT NITRATE HEXAHYDRATE

BY A. JAYARAMAN

(Memoir No. 106 *from the Raman Research Institute, Bangalore-6)*

Received February 24, 1958

Cobalt nitrate hexahydrate crystallises from aqueous solution as large platy crystals which are highly deliquescent. According to Groth the crystal belongs to the monoclinic system with axial ratios $a:b:c::1\cdot172:1:1\cdot925$ and $\beta = 101°$. The density is given as 1·88 gm./c.c. In a previous paper in these *Proceedings* (1957, **45,** 263), the unit cell parameters and optical properties of nickel nitrate hexahydrate were reported. In the same connection it was thought worthwhile to investigate the structure and optical properties of cobalt nitrate hexahydrate. In the present communication the unit cell parameters, space-group and optical properties of the crystal are reported.

Cobalt nitrate hyxahydrate was crystallised by making a saturated solution and allowing the same to crystallise in an air-tight enclosure containing anhydrous calcium chloride in a dish. Large platy crystals reddish orange in colour were obtained in this manner, which were dried between filter-papers and kept immersed in kerosene. Examination of one of the plates under the polarising microscope exhibited straight extinction. The crystal was mounted on the Federov stage, with kerosene as the immersion medium and rotated about the straight extinction edge as the axis. The crystal continued to remain extinguished and exhibited a biaxial figure when examined in convergent polarised light.

For X-ray work, a thin rod-shaped piece ground parallel to the straight extinction edge was employed, and this was enclosed in a thin-walled glass capillary tube sealed at one end and blocked at the other with wax. Since the crystal is highly deliquescent, it had to be protected from attack by moisture during X-ray exposure in the above manner.

One rotation, and three Weissenberg photographs were taken with the crystal rotated about the axis chosen, employing NiKα radiation. The three

Weissenberg photographs were respectively, the zero, first and second layer photographs. A perusal of the rotation and zero layer Weissenberg photographs revealed that the axis of rotation was the *b*-axis of a crystal belonging to the monoclinic system. One more rotation and zero layer Weissenberg photograph was recorded rotating the crystal about another crystallographic axis, perpendicular to the *b*-axis. Axial dimensions were calculated from rotation and Weissenberg photographs and are as follows:

$$a = 15 \cdot 09 \text{ AU}$$

$$b = 6 \cdot 12 \text{ AU} \qquad \beta = 119°$$

$$c = 12 \cdot 69 \text{ AU}$$

From the measured density of 1·9 and the calculated volume on the basis of the above dimensions, the number of molecules per unit cell turns out to be 4.

The Weissenberg photographs were indexed and the following conditions for the presence of reflections were noted.

$$hkl : h + k = 2n$$

$$hol : l = 2n \; ; (h = 2n)$$

$$oko : k = 2n$$

On looking up the *International Tables*, the monoclinic space-groups C/*c* and C2/*c* satisfy these conditions. Of these two, C/*c* has no centre of symmetry. Optical examination did not reveal the presence of optical activity, the brush crossing the eye being quite definitely dark. It is highly probable that the crystal belongs to the monoclinic space-group C2/*c*. Complete structure determination is under progress.

OPTICAL PROPERTIES

The convergent light figure is observed on the habit plane which corresponds to the ($\bar{1}01$) face of the crystal, when referred to the axes chosen on the basis of the X-ray results. The principal vibration direction parallel to the *b*-crystallographic axis is found to be the intermediate or β index of refraction. The orientation of the optical elements are shown in Fig. 1.

The refractive indices for sodium light were measured by employing the immersion method with a polarising microscope and an universal stage. The values determined are as follows;

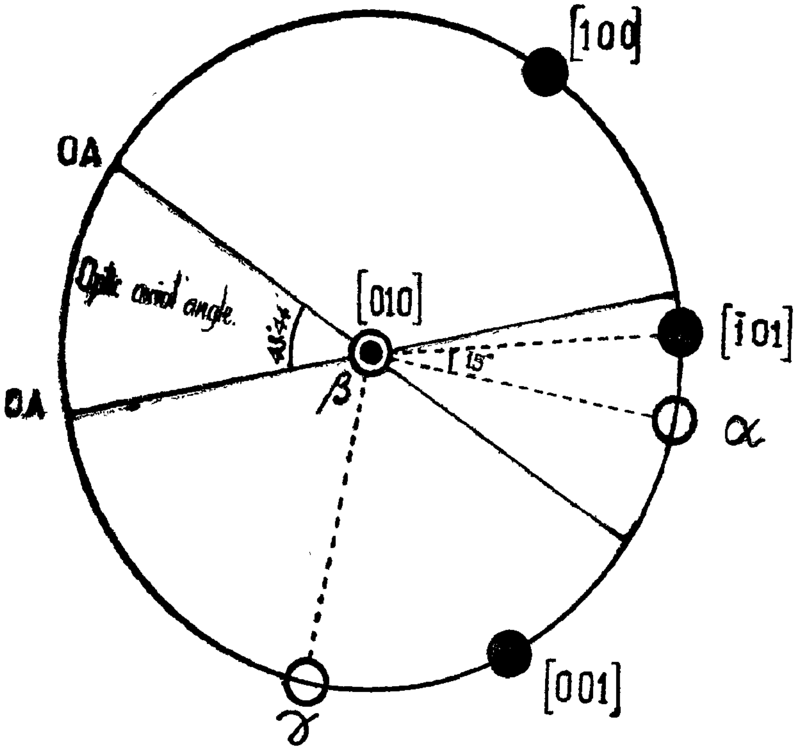

Fig. 1

$\alpha = 1 \cdot 38$

$\beta = 1 \cdot 52$ $2V = 43° 44'$

$\gamma = 1 \cdot 547$

The crystal is biaxial negative.

Pleochroism is not marked for the vibration direction parallel to β and γ. But for a vibration parallel to α and γ the effect is very vivid. For the former the colour is purple and for the latter it is orange yellow.

The author in conclusion wishes to express his thanks to Professor Sir C. V. Raman for his interest in the investigation.

Reprinted from "The Proceedings of the Indian Academy of Sciences",
Vol. XLVII, No. 4, Sec. A, 1958

THE OPTIC INTERFERENCE FIGURES OF AMETHYSTINE QUARTZ—PART I

BY S. PANCHARATNAM
(*Memoir No.* 107 *of the Raman Research Institute, Bangalore*-6)

Received April 11, 1958
(Communicated by Sir C. V. Raman)

§1. INTRODUCTION

AMETHYST is the familiar purple modification of quartz having an absorption band in the yellow-green region of the spectrum, a study of whose optical properties had been reported in an earlier paper.[1] Observations on untwinned amethystine sectors through a polaroid, showed that they exhibited pronounced pleochroism even when observed along the *c*-axis—showing that the *c*-axis was *not* an axis of uniaxial symmetry for the absorption ellipsoid. It followed that the material could not be strictly uniaxial. This was indeed confirmed, though only in the cases of very intensely coloured sectors, was the biaxial nature quite pronounced—the *c*-axis being the acute bisectrix. A sector of this type which was pre-eminently suited for the present study (*i.e.*, which did not possess certain extraneous complicating features characteristic of most quartz-amethyst plates) had been obtained by careful selection during our previous investigation. Of the various conclusions which emerged from that investigation it is sufficient for our present purpose to accept the following particular results, which may be independently deduced from certain observations described in the present paper itself (§§3 and 4):

(*a*) The amethystine sector used is an optically untwinned and genuinely biaxial medium possessing optical activity.

(*b*) The sector is pleochroic, the elliptic section of the absorption ellipsoid normal to the acute bisectrix having its major and minor axes lying respectively parallel and perpendicular to the axial plane.

The optic interference figures displayed in convergent light by this class of media (*viz.*, the class of biaxial media possessing both pronounced pleochroism and optical rotatory power) have not been investigated and are therefore of interest. In the present paper we reproduce and discuss the remarkable types of interference figures exhibited under various conditions by the selected amethystine sector. These interference figures are found to

differ considerably from those displayed both by inactive absorbing crystals and active transparent crystals. It will be shown however that the observations described become explicable in detail in the light of the theory of light propagation in absorbing crystals possessing optical activity; this theory was presented in an earlier paper[2] hereafter referred to as P–*a*. We shall also have frequent occasion to refer to a paper[3] (hereafter referred to as P–IV) where the interference figures of absorbing biaxial crystals had been discussed.

Though it should certainly be possible to repeat our experiments with other deeply coloured sectors of comparable intensity, the impression should not be created that this can be done with any densely coloured area in a basal section of amethyst randomly selected. According to our previous investigation, this is because of certain very interesting—though, from our present point of view, extraneous—complicating factors which feature prominently in most quartz-amethyst plates. In the appendix at the end of Part II, attention is briefly drawn to these complicating factors, and also to the fact that it becomes difficult to compare our results directly with those of other workers.

§2. Preliminary Remarks

In the present study we have used an intensely coloured amethystine sector occurring in a roughly basal section-plate of the quartz-amethyst about 3 mm. thick. In our previous investigation, an examination of the etch patterns shown by the two surfaces of the plate had revealed that the portion to be used was untwinned and was *right-rotating*, the sector being associated with a secondary rhombohedral face. The tremendous depth of absorption may be estimated from the wedge-spectrograms published in that paper—taken with this coloured area. Because of the large absorption the optic interference figures reproduced in the present paper had to be photographed by focussing a reduced image of a sodium (or mercury) arc directly on the sector using a battery of lenses which also served as the converger. Only an area about 3 mm. square in the body of the sector was used: the remainder of the plate was blackened on both sides with paint to exclude light from adjoining uncoloured and twinned areas. In what follows (particularly in Part II) an acquaintance with the behaviour in convergent light of transparent biaxial crystals—both inactive and active—will be presumed.

§3. Observations in Blue Light

Figures 1, 2 and 3 (Plate IX) exhibit the interference figures observed in blue light (λ 4358) at three different settings of *crossed* polaroids. They

prove clearly the biaxial nature of the material, the axial angle for this wavelength being about 8°; the axial plane has been kept horizontal in these photographs—as well as in all the others reproduced in this paper. In Fig. 1 the vibration-directions of the polariser and the analyser lie along and perpendicular to the axial plane while in Fig. 2 they are at 45° to the axial plane. Fig. 3 has been obtained by interchanging the positions which the polariser and analyser occupy in Fig. 2. In these as well as in all other settings of the crossed polaroids it was observed that—unlike the behaviour obtaining in transparent inactive crystals—the optic axial directions were never extinguished; though at the border of the figure the isogyres were fairly dark and appeared at the same position as in non-active crystals, they became diffuse and vanished as the optic axial directions were approached. *This behaviour is characteristic of an ordinary optically active crystal*; and the fact that there is no sensible difference between Figs. 2 and 3 is only what is to be expected for a *transparent* crystal of this class. (This may be shown from reference 4, Eqns. 1 and 2.) In a transparent optically active crystal the optic axial directions may be extinguished by keeping the polariser setting fixed, and rotating the analyser away from the crossed position by an amount equal to the rotation of the plane of polarisation along the optic axial directions. This has been done in Fig. 4, where in addition—purely for achieving a symmetrical interference figure—the polariser and analyser have been adjusted so as to be symmetrically situated with respect to the axial plane. The mean value of the rotation measured in this approximate manner for six azimuths of the polariser was found to be about − 115°. This being also the rotation for a plate of quartz of the same thickness (*viz.*, 0·28 cm.) the untwinned nature of the medium is again confirmed. (That the material was right-rotating was established—independent of the etch study—by the fact that the rings expanded when the analyser was rotated clockwise).

A curious property not displayed by transparent crystals was however detected. The measured rotation varied systematically with the azimuth of the incident vibration, deviating by as much as ten per cent. from the mean value. This phenomenon will be theoretically explained later (§5); it arises from the fact that the plate is so intensely coloured that even for the blue region of the spectrum the dichroism is not altogether absent, though it is small especially when compared to the optical rotation. Since the latter diminishes with increasing wavelength such effects of dichroism may be expected to be even more prominent for corresponding wavelengths on the long wavelength side of the absorption band. Before proceeding to describe such observations with red light, it is well to confirm also the property

(*b*) mentioned in the introduction: this can be best done by using a wavelength (λ 5890) lying in the heart of the absorption band.

§4. Brewster's Brushes

Figure 5 shows the so-called Brewster's brushes as revealed without the use of either polariser or analyser in the unpolarised yellow light of a sodium lamp. It will be seen that they consist of two pairs of brushes, one pair of brushes being associated with each optic axis. For the present we may consider the phenomenon from the elementary standpoint that the behaviour should approximate to that of inactive absorbing crystals as we approach directions represented by points near the border of the field of view. The position of the brushes is in fact the same as exhibited in a crystal such as yttrium platinocyanide[5] which has a small axial angle and is inactive.

In non-active crystals Brewster's brushes will be seen only when there is pronounced dichroism along the optic axial directions; and they will then lie along zones for which the principal planes of linear birefringence are inclined at 45° to the principal planes of linear dichroism. In the present case the brushes are seen to lie along the same zone as the isogyres of the biaxial interference figure when the polariser and analyser are at 45° to the axial plane (refer *e.g.* Fig. 2). This means that the principal radii of the elliptic section of the absorption ellipsoid (taken normal to the acute bisectrix) lie along and perpendicular to the axial plane, *i.e.*, along $O'X_k$ and $O'Y_k$ in Fig. 1, text, of Part II: this diagram represents the field of view of the convergent light figure, O' representing the acute bisectrix, while O_1 and O_2 represent the two optic axes.

Which of the directions $O'X_k$, $O'Y_k$ correspond to the less absorbed vibration in the absence of optical activity could be determined in the following manner. The plate was tilted first about a horizontal axis (so as to effectively eliminate the effects of optical activity) and the depth of absorption for the horizontal vibration direction was noted in *parallel* light. An analogous procedure was adopted for observing the depth of absorption for a vibration parallel to $O'Y_k$; this was seen to be enormously greater than that for the vibration $O'X_k$, thus independently confirming the statement (*b*) made in the introduction.

Though the explanation of Brewster's brushes given in this section appears to have completely neglected the presence of optical activity, it actually holds to a higher degree of approximation than is to be suspected from such a statement. According to P–*a*, §7 *b*, we may—for directions not too close to an optic axis—neglect the *squares* of the ellipticity of the waves

(and hence the square of the non-orthogonality factor cos $\frac{1}{2}c$) even though the first power of these quantities may not be negligible. For such directions it has also been shown that the absorption coefficients of the waves propagated along any direction will be virtually the same as in the absence of optical activity. Referring now to Eqn. (11) of P–IV it follows that the intensity at any point in the field seen directly in unpolarised light will be the same as in an inactive crystal (neglecting the squares of the ellipticity of the waves, in both cases). Hence the explanation of Brewster's brushes as customarily presented for an inactive absorbing crystal (Pockels,[6] p. 424) may be also applied in the present case—(*see* also Part II, §7).

In the present paper *we shall be making the following approximation* which is quite customary, *viz.*, that the elliptic section of the absorption ellipsoid made by the plane of the paper in Fig. 1, text, Part II, is practically the same (in orientation and dimension) as the section normal to any direction of propagation in the angular range considered. [That this approximation is not strictly true is shown by the asymmetry of the intensity of Brewster's brushes with respect to the axial plane (*see* Appendix)]. For the purpose of our qualitative discussion we shall also take the rotatory power to be constant over the range of directions under consideration.

§5. Observations in Red Light

Figures 6, 7 and 8 (Plate X) show the biaxial interference figures exhibited in red light (6450–6900 Å) at three different settings of *crossed* polaroids which correspond respectively to the three settings already used in Figs. 1, 2 and 3 with blue light. Apart from the very appreciable increase of the axial angle (relative to blue light), the most striking feature is that Figs. 7 and 8 are *not* identical since the brush apparently goes through the eyes in the latter. Any such alteration in the interference figure caused by a mere interchanging of crossed polaroids implies that the waves propagated along a general direction are in two general non-orthogonally polarised states, and that *the relation between these states of polarisation is necessarily different from that obtaining in inactive absorbing crystals* (*see* P–IV, §8 *a*).

It was observed that in the setting of Fig. 8—for which the vibration-direction of the polariser is inclined at − 45° with respect to the axial plane—the portion of the brush which apparently passes through the eyes was really not perfectly dark; and that the optic axial directions could be more perfectly extinguished by turning the analyser clockwise, away from the crossed position, through a small angle—the mean value of this angle for obtaining best extinction being estimated to be 31°. On the other hand when the vibration-direction

of the polariser made an angle of $+45°$ with respect to the axial plane (as in Fig. 7), the analyser had to be turned (from the crossed position) through the much larger angle of 50° to reach a position where the optic axis appeared best extinguished. For any general setting of the polariser the axial directions can be extinguished by a similar procedure, as illustrated in Fig. 9 (where, in addition, the polariser and analyser have been oriented symmetrically with respect to the axial plane).

Along an axial direction in a *transparent* active crystal two oppositely polarised circular vibrations are propagated with 'circular birefringence' $|2\rho|$. In the present case such a supposition cannot account for the phenomenon noted in the previous paragraph—which had also been exhibited less conspicuously in blue light, *viz.*, the variation of the apparent rotation with the azimuth of the incident vibration. But in P–*a*, §8 *a*, it had been theoretically deduced that in an optically active crystal with weak linear dichroism ($k < |2\rho|$) the waves propagated along an axial direction will be *elliptically* polarised: the two elliptic vibrations will be exactly similar in form and orientation but will be described in opposite senses. The major axes of the ellipses will be coincident and—since the rotatory power is negative in the present case—will make an angle of $-45°$ with respect to the line $O'X_k$ (Fig. 1, text, Part II) which is the trace of the axial plane as well as the trace of a principal plane of linear dichroism.

Before proceeding further we shall describe an experiment confirming the theoretical results stated in the last paragraph. The crystal was as usual kept in the conoscopic arrangement between crossed polaroids which could be turned around *together*; but a mica retardation plate was set immediately behind the first polaroid and an *identical* retardation plate was set immediately in front of the second polaroid with its principal planes turned round by 90° with respect to the first. The two retardation plates were coupled so that they could be turned around *together*. The arrangement in front of the crystal constitutes an '*elliptic polariser*'. The arrangement behind the crystal constitutes a '*crossed elliptic analyser*' which, if the crystal plate were absent, would *automatically* cut out the elliptically polarised light produced by the arrangement in front—independent of the setting of the coupled polaroids and the coupled retardation plates. In the present case, $\lambda/4$ retardation plates were used, the principal planes being oriented at an angle of 45° to the axial plane. Thus the principal axes of the incident elliptic vibration were equally inclined to the axial plane, though the ellipticity could be altered by turning the coupled polaroids. It was observed that there were two settings of the coupled polaroids at which the optic axial

directions were extinguished—the figure for one of these settings being reproduced in Fig. 10. These were the two settings at which the vibration-direction of the first polaroid made angles of + 34° and − 34° with respect to O′M (Fig. 3 *b*, text, Part II) as roughly determined by the fact that the spots had moved exactly into the axial plane at these settings. *This confirms that the two waves propagated along each optic axis are elliptically polarised* as described above—the numerical value of the ellipticity $|\omega|$ of both vibrations being about 34°. On the Poincaré sphere (Fig. 1, text), the states of polarisation of these two waves are denoted by the points A and B lying on the same meridian of longitude but at latitudes -2ω and $+2\omega$ respectively.

The variation of the measured rotation with the azimuth of the incident vibration may now be understood by applying the results of ref. 7, §§4 and 5, for discussing the dissolution of the incident vibration into two elliptic vibrations, and the compounding of the latter after their propagation through the plate with different velocities but equal absorption coefficients. The actual rotatory power along an axial direction can in fact be calculated from the apparent rotations α_1 and α_2 observed with the incident vibration lying respectively parallel and perpendicular to the major axes of the elliptic vibrations propagated. Considering first the former case the incident vibration will be represented on the Poincaré sphere by the point M on the equator (Fig. 1, text, Part I). It will be decomposed into two vibrations in states A and B whose intensities will be equal and whose initial ‘phase difference’ will be zero since M lies on the arc AB (reference 7, §4). Hence if the slower wave B suffers a phase retardation of ϕ relative to the other on propagation through the plate along an axial direction, then ϕ also represents the absolute phase advance of vibration A over B when they emerge from the plate. These vibrations will still be of equal intensity—their absorption on passage through the plate being equal according to P–*a*, §8 *a*—so that they will compound to give a *linear* vibration represented by a point C_1 on the equator (reference 7, §5); if E_1' be the area of the triangle $C_1'BA$, where C_1' is the point opposite to C_1, then $\frac{1}{2}E_1'$ should be equal to the supplement of the absolute phase advance of vibration A over B (*see* reference 7, Eq. 5 *b*). The spherical excess $\frac{1}{2}E_1'$ of the right-angled triangle $C_1'BM$ may be obtained from spherical trigonometry:

$$\tan \tfrac{1}{4}E_1' = \tan \omega \tan \tfrac{1}{2}(\pi - 2\alpha_1).$$

Hence

$$\cot \tfrac{1}{2}\phi = \tan \omega \cot \alpha_1 \qquad (1)$$

On the other hand, if the incident vibration is turned to the orthogonal state M′, the two vibrations into which it is split along an optic axial direction will have an initial phase difference of $-\pi$ and a final phase difference

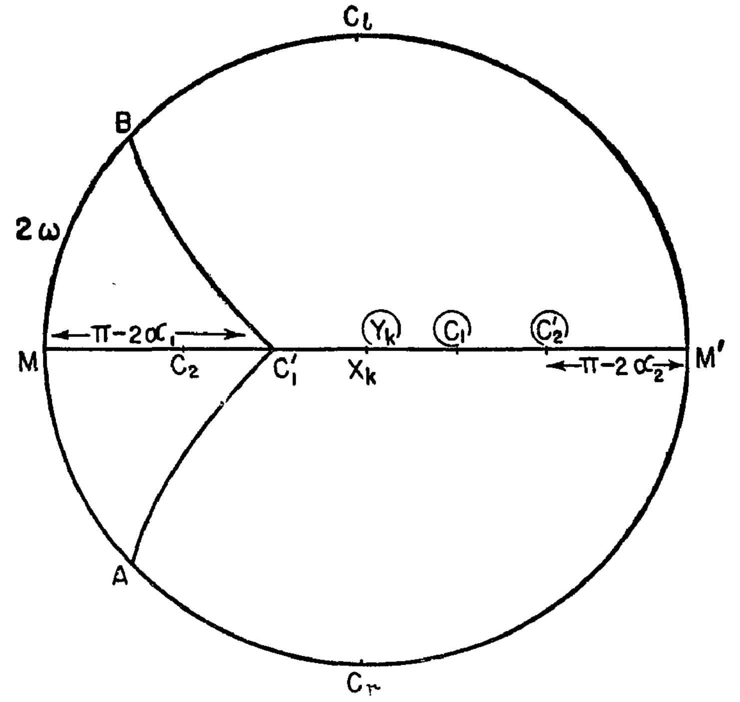

TEXT-FIG. 1. The Poincaré sphere as used for explaining the apparent variation of optical rotation with the azimuth of the incident vibration. Symbols enclosed in circles represent points on the hemisphere below the plane of the paper.

of $(\phi - \pi)$, compounding finally to give the linear vibration in state C_2. Hence if C_2' represent the state orthogonal to C_2, then ϕ should be equal to half the spherical excess of the triangle $C_2'AB$. Proceeding as before we get from spherical trigonometry,

$$\tan \tfrac{1}{2}\phi = \tan \omega \tan \alpha_2 \tag{2}$$

From (1) and (2) we obtain

$$\tan^2 \omega = \frac{\tan \alpha_1}{\tan \alpha_2} \tag{3}$$

$$\tan^2 \tfrac{1}{2}\phi = \tan \alpha_1 \tan \alpha_2 \tag{4}$$

The apparent rotations α_1 and α_2 observed in the respective cases when the incident vibration lies parallel to O′M and O′M′ (Fig. 3 *b*, text, Part II) have been roughly measured to be 31° and 50° respectively (refer above). Inserting these values in (3) and (4) we find firstly that the numerical ellipticity $|\omega|$ of the vibrations propagated along an optic axis should be 35·5°—in

4 JAN 1965

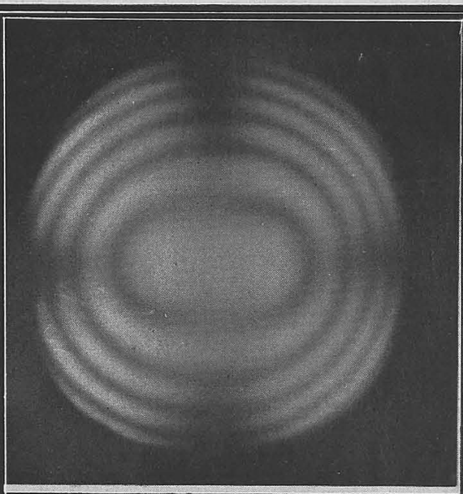

FIG. 1

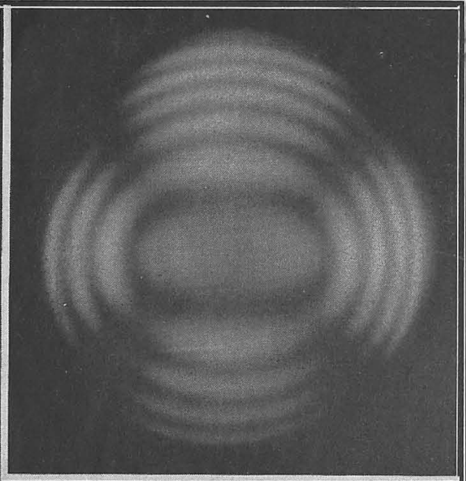

FIG. 2

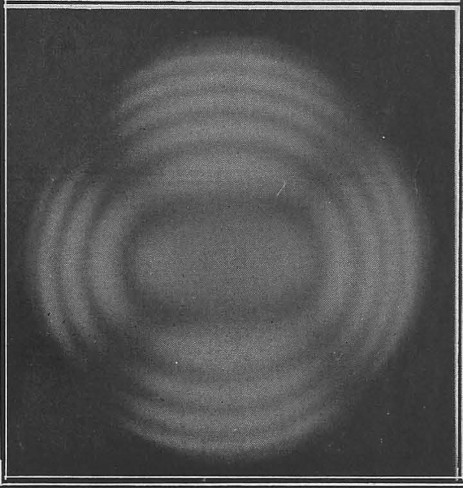

FIG. 3

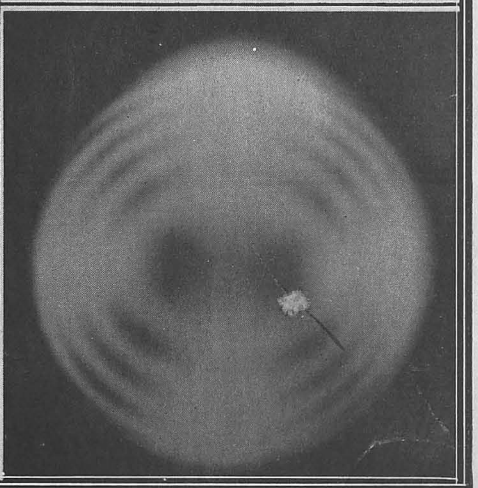

FIG. 4

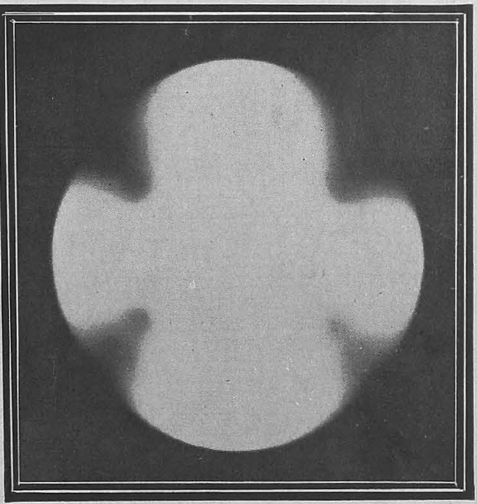

FIG. 5

FIGS. 1-5

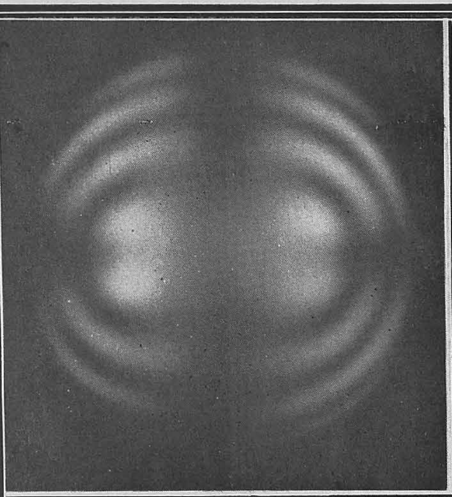

FIG. 6

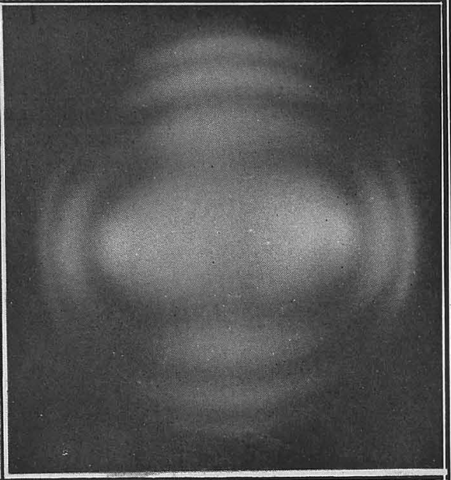

FIG. 7

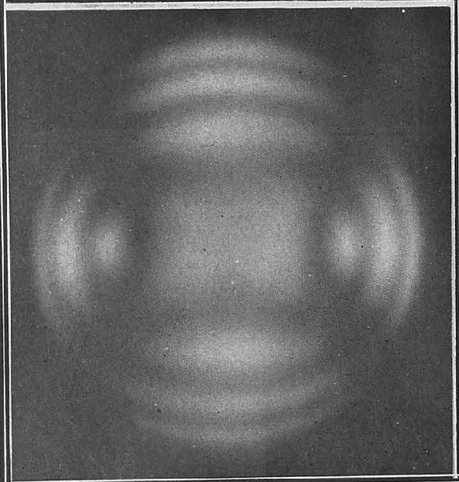

FIG. 8

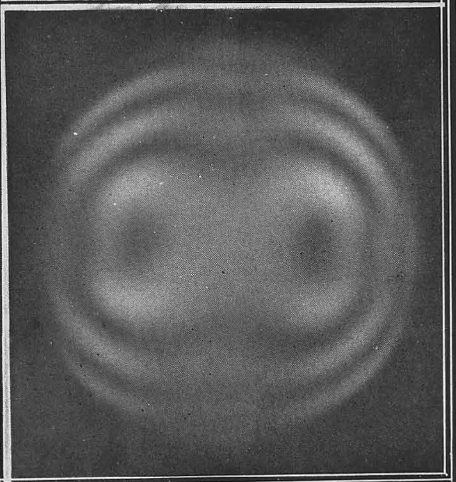

FIG. 9

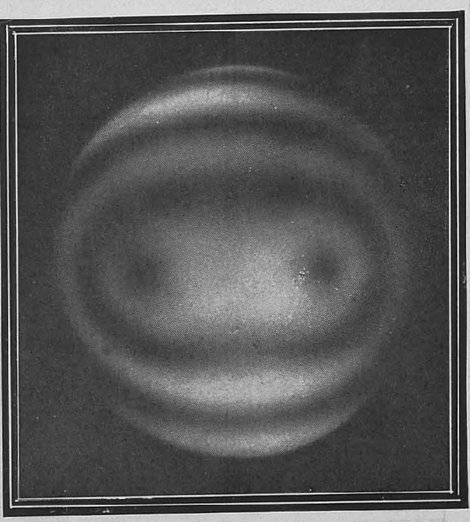

FIG. 10

FIGS. 6–10

agreement with the experimentally estimated value of 34°, previously quoted; secondly, the relative phase advance ϕ gained by the faster wave over the slower wave on passage through the plate is found to be 80·5°. Since the waves are not circularly polarised, the relative phase difference per unit path (ϕ/d) is *not* directly equal to $|2\rho|$ but is related to it by Eq. (17) of P-*a*:

$$|\rho|\, d = \frac{\frac{1}{2}\phi}{\sin|2\omega|} \tag{5}$$

The true optical rotation $|\rho|\, d$ which would be exhibited by the plate in the absence of dichroism may be calculated from (5) by substituting the values of ω and ϕ obtained from (3) and (4). In the present case it is found to be 42·5°. (Though this is somewhat lower than the optical rotation for a plate of transparent quartz, the difference may be entirely due to the large experimental errors involved).

§6. Summary

The interference figures exhibited by an intensely coloured amethystine sector at two wavelengths which lie practically outside the absorption band are reproduced. In blue light the interference figures are characteristic of a transparent biaxial crystal possessing the rotatory power of quartz. In red light the axial angle is larger, and effects due to weak linear dichroism are also exhibited. Thus the rotation of the plane of polarisation along the optic axes varies with the azimuth of the incident vibration; and the method of determining the rotatory power from the apparent rotation is illustrated.

§7. References

1. Pancharatnam .. *Proc. Ind. Acad. Sci.*, 1954, **40 A**, 196.
2. ———— (P-*a*) .. *Ibid.*, 1957, **46 A**, 280.
3. ———— (P-IV) .. *Ibid.*, 1957, **45 A**, 2.
4. ———— .. *Ibid.*, 1957, **45 A**, 402.
5. Boguslowski .. *Ann. der Physik*, 1914, **44**, 1084.
6. Pockels .. *Lehrbuch der Kristalloptick*, *Teubner*, 1906.
7. Pancharatnam .. *Proc. Ind. Acad. Sci.*, 1956, **44 A**, 247.

THE OPTIC INTERFERENCE FIGURES OF AMETHYSTINE QUARTZ—PART II

BY S. PANCHARATNAM

(*Memoir No.* 107 *of the Raman Research Institute, Bangalore*-6)

Received on April 9, 1958
(Communicated by Sir C. V. Raman)

§1. INTRODUCTION

IN the remaining part of the paper, observations on the interference figures of the amethystine sector are continued, using a wavelength lying in the heart of the absorption band (λ 5890). Here the effects of dichroism gain such ascendancy ($k > 2\,|\,\rho\,|$) that the existence of optical rotatory power is itself only indirectly manifested—through the exceptional nature of the observed phenomena.

§2. OBSERVATIONS BETWEEN CROSSED POLAROIDS

Figures 1–6 (Plate XI) demonstrate the singular behaviour of the isogyres observed between *crossed* polaroids as the latter are turned around *together* in a clockwise sense—starting with the setting in which the vibration-direction of the polariser is parallel to the axial plane. (The settings of polariser and analyser have been respectively marked in the upper and lower circles drawn by the side of each figure, the axial directions themselves being marked by white dots in some of the photographs.) *There are only two settings of the incident vibration, viz.*, when it is parallel to either $O'A_1$ or $O'A_2$ in Fig. 1, text, *for which genuine isogyres are observed* passing unmodified through the two optic axes, as seen in Figs. 2 and 3 (Plate XI). For all other settings of the crossed polaroids it was observed that the 'isogyres' appeared really dark only towards the border of the figure. This is true even in Figs. 5 and 6 though the crossed polaroids are in orientations obtained merely by interchanging the polariser and analyser in the settings of Figs. 2 and 3 respectively.

§ 3. PROPERTIES OF THE OPTIC AXES

The observations of the previous paragraph clearly mean that when the incident vibration is parallel to either $O'A_1$ or $O'A_2$ (Fig. 1, text) it is propagated without resolution along each axial direction. We thus arrive experimentally at the conclusion that *the waves propagated along an optic axis, e.g.*, along O_1, *are linearly polarised along two non-orthogonal directions*

parallel to $O'A_1$ and $O'A_2$, as marked at O_1 in Fig. 1, text. These directions are found to be equally inclined to the lines bisecting the angle between $O'X_k$ and $O'Y_k$, and lie in the negative quadrant. These results are exactly what have been already derived* theoretically in P–a^1, §8 *b*, for the propagation along an axial direction when the dichroism is sufficiently large ($k > |2\rho|$). For the purpose of discussion it is convenient to refer to Fig. 2 *a* text, which represents a plate cut exactly normal to an optic axis on which have been marked the principal planes of linear dichroism OX_k and OY_k. The linearly polarised states P_a and P_b of the waves that can be propagated normal to the plate should both lie in the negative quadrant (since ρ is negative) at azimuths whose numerical values ψ_1 and $(\frac{1}{2}\pi - \psi_1)$ are the roots of

$$\tfrac{1}{2}k \sin 2\psi = |\rho| \tag{1}$$

Furthermore, these waves should differ not in their velocities, but only in their coefficients of absorption k_a and k_b:

$$(k_b - k_a) = k \cos 2\psi_1 \tag{2}$$

When the vibration incident along an axial direction is in a general setting (*i.e.*, other than $O'A_1$ or $O'A_2$), it will be decomposed into two non-orthogonal vibrations in states P_a and P_b according to the parallelogram law (*see e.g.*, reference 2, Fig. 3); while according to the same law the attenuated vibrations emerging from the plate should compound to yield a linear vibration whose azimuth would have turned towards the plane of the less attenuated state P_a. In accordance with this it was always found possible to extinguish the optic axial directions by turning the analyser away from the crossed position. This is illustrated in Figs. 7 and 8 (Plate XII); in Fig. 7 the angles that the vibration-directions of the polariser and analyser made with respect to $O'X_k$ were $-59°$ and $+59°$ respectively; while for Fig. 8 the corresponding angles were $-84\frac{1}{2}°$ and $+84\frac{1}{2}°$. A straightforward calculation—based on the explanation given above of the extinction of the optic axes—enables the difference in the absorption coefficients of the waves propagated along an axial direction to be estimated. If *d* be the thickness of the plate, it is easily shown that for an axial direction $(k_b - k_a)\, d$ is equal to 2·5, this being the mean of the two values calculated from the settings of Figs. 7 and 8 respectively. The angle between $O'A_1$

---

* These results may also be derived analytically by directly applying the principle of superposition. Thus, if both sides of (1) be multiplied by dz, the left-hand side and right hand side denote respectively the angles through which a plane vibration at azimuth ψ turns during the infinitesimal operations of dichroism and rotation respectively; for these to be equal and opposite, eq. (1) should be satisfied, and the plane of vibration should lie in the negative quadrant, if ρ is negative.

and $O'A_2$ (*i.e.*, between the settings of the polariser in Figs. 2 and 3) was required in the calculation; it was estimated to be 50°, this being done more accurately from observations using a polariser alone and an analyser alone (§8). (It may be noted that this angle may also be *calculated* by measuring the turning of the plane of polarisation along the axial directions for *two* azimuths of the incident vibration, as in Figs. 7 and 8.) We then obtain $kd = 3 \cdot 25$ from (2), giving an estimate of the 'pure' linear dichroism.

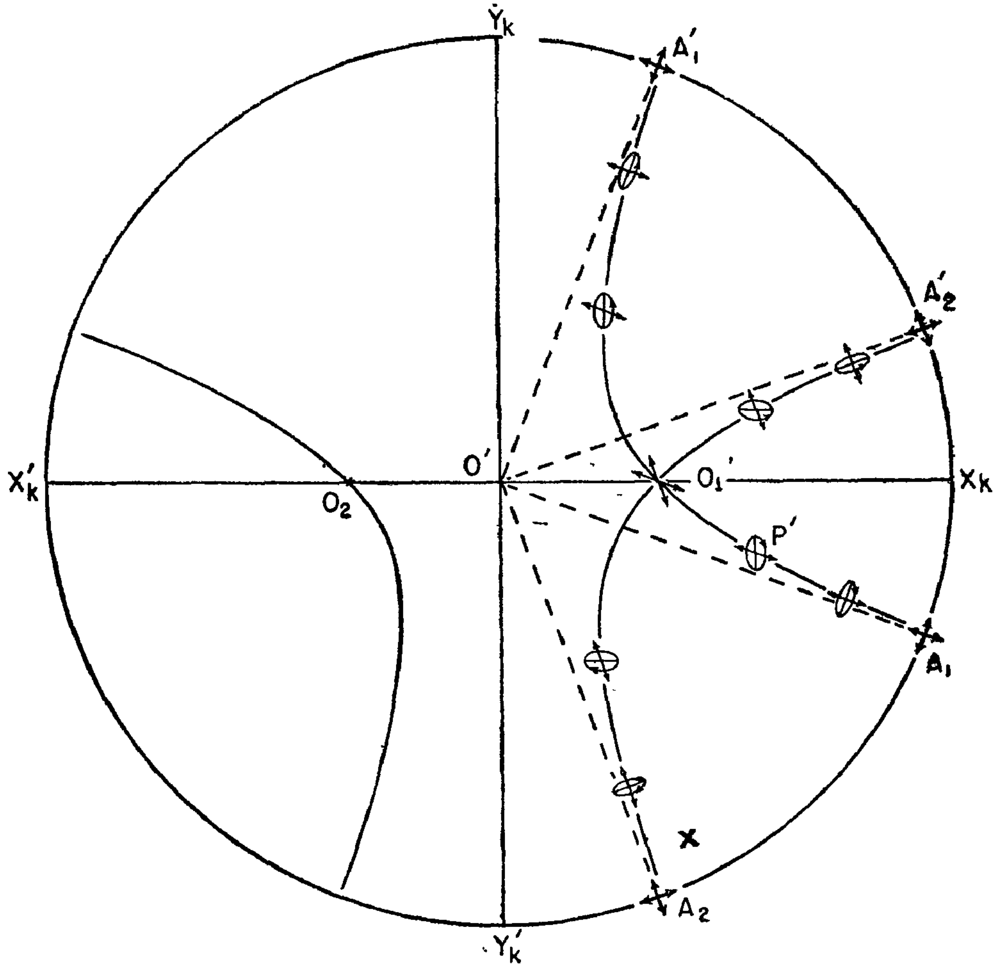

TEXT-FIG. 1. Convergent light figure depicting the variation of the states of polarisation of the waves with the direction of propagation for particular zones in the field of view. O_1 and O_2 are the optic axes.

The optical rotatory power along the axial directions—though masked by the effects of dichroism—may now be indirectly estimated by substituting the values $\psi_1 = 20°$, and $kd = 3 \cdot 25$ in (1). The total optical rotation $|\rho| d$ (which would be exhibited along the axial directions in the absence of dichroism) turns out to be about $59 \cdot 5°$—after conversion from radians to degrees. Since this is practically the same as the rotation for a plate of transparent

quartz of the same thickness (*viz.*, 2·8 mm.), we have here a semi-quantitative check on the results of our theory.

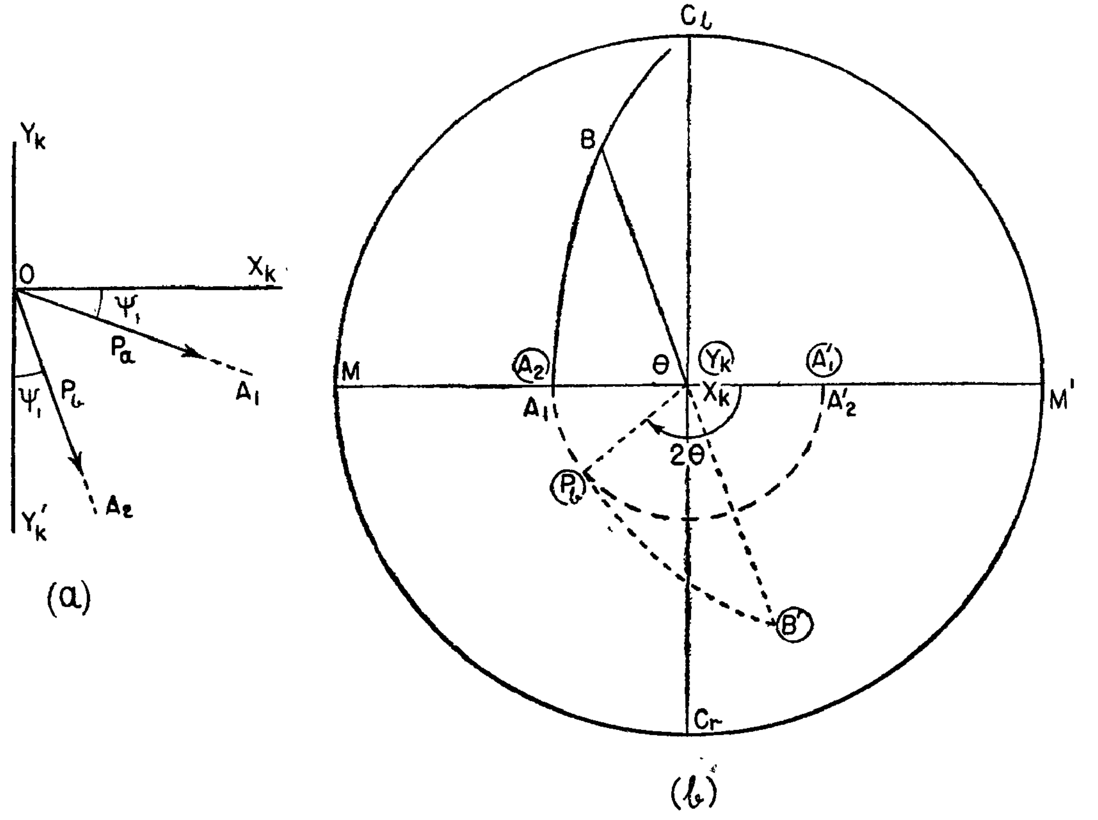

TEXT-FIG. 2. (*a*) Plate cut normal to an optic axis along which the waves propagated are linearly polarised in non-orthogonal states P_a and P_b.

(*b*) Construction on the Poincaré sphere determining the points A_1 and P_b which represent the states propagated unchanged along the direction P′ of Fig. 1, Text.

§4. EXPLANATION OF THE FORMATION OF ISOGYRES

We now turn to the fact that in Fig. 2 for example—where the vibration-direction of the polariser is parallel to $O'A_1$ (Fig. 1, text)—it is not the two optic axial directions *alone* that are extinguished; all the directions represented by points on the dark isogyres are extinguished (in sharp contrast to the behaviour of transparent active crystals). These isogyres form a rectangular hyperbola (with $O'A_1$ and $O'A_1'$ as asymptotes) one branch of which has been marked $A_1O_1A'_1$ in Fig. 1, text. We may conclude from our observation that along any direction represented by a point on this hyperbola (*e.g.*, the point P′), a vibration parallel to $O'A_1$ can be propagated unchanged—so as to be completely extinguished by the crossed analyser; while for the same direction P′ a vibration parallel to $O'A_1'$ is *not* propagated

unchanged—as is shown by the absence of isogyres in Fig. 5, obtained by interchanging the polariser and analyser settings of Fig. 2.

This conclusion may be theoretically explained by the method of superposition presented in P–*a*: for a general direction of propagation we will observe the superposed effects not only of linear dichroism and optical rotation (as along the axial directions) but also of the linear birefringence which would be present even in a transparent inactive crystal. The clue to the explanation of the isogyres which form when the vibration-direction of the polariser is parallel to $O'A_1$ (Fig. 1, text) is given by the fact that the isogyres (one branch of which is marked $A_1O_1A_1'$) would have occurred in the same position even in the absence of optical activity and linear dichroism (*see e.g.*, Johannsen[3]). That is to say, any point such as P′ lying on these isogyres represents a direction for which one of the principal planes of linear birefringence lies parallel to $O'A_1$. Hence, for such a direction a vibration parallel to $O'A_1$ will remain unchanged under the effect of the infinitesimal operation of linear birefringence. The same vibration will also remain unaltered under the *combined* effects of the two succeeding infinitesimal operations of linear dichroism and optical rotation—as is evidenced by the fact that it is propagated unchanged along the axial directions where these two factors alone subsist (§3). It follows that a vibration parallel to $O'A_1$ can be propagated unaltered (along the zone of directions represented by the isogyres) under the combined effect of all three factors, *viz*., linear birefringence, linear dichroism and optical rotation. It may be similarly proved that a vibration parallel to $O'A_1'$ cannot be propagated unchanged along these directions; for it is *not* propagated unchanged under the combined effects of the second two factors alone—as is evidenced by the fact that it is not propagated unchanged along an axial direction. This explains the presence of genuine isogyres in Fig. 2 and their absence in Fig. 5.

The isogyres in Fig. 3 form a rectangular hyperbola—with asymptotes $O'A_2$ and $O'A_2'$—one branch of which has been marked $A_2O_1A_2'$. It may be shown by an exactly similar argument that along the zone of directions represented by this hyperbola a vibration parallel to $O'A_2$ can be propagated unchanged, but not a vibration parallel to $O'A_2'$; this explains the presence of genuine isogyres in Fig. 3 and their absence in Fig. 6.

The main result of this section may be summarised in a form applicable to crystals of arbitrary axial angle and of any symmetry (in a region where $k > |2\rho|$). *Isogyres are formed between crossed polaroids only when the polariser setting is parallel to one of the vibration-directions of the waves propagated along an optic axis*; the isogyres then occupy the same position

as they would in a transparent inactive crystal with the same axial directions. It is, of course, assumed that the optical rotatory power and linear dichroism do not vary rapidly in the neighbourhood of the optic axis considered.

§5. States of Polarisation of the Waves

(*a*) *Co-ordinates for points in convergent light figure.*—We shall now see what will be the states of polarisation of the waves propagated along the direction represented by the arbitrary point P in the convergent light figure (Fig. 3 *a*, text). In the present case, it is best to specify the point P in curvilinear co-ordinates δ, χ. In the region of view in Fig. 3 *a*, text, we can draw two families of intersecting curves. The point P has been depicted as the point of intersection of two of these curves. The first is a curve of constant linear birefringence characterised by the parameter δ which is equal to the linear birefringence, *i.e.*, the birefringence in the absence of optical activity and linear dichroism; this curve takes the form of an 'oval of Cassini' (*see e.g.*, Wooster[4]). The second curve is a branch of a rectangular hyperbola which is drawn passing through the two optic axes, having as its asymptotes two perpendicular lines O′L and O′L′ drawn through the centre of the figure. This hyperbola really represents a curve of like polarisation in the absence of optical activity and linear dichroism, since it would then represent the position of the isogyres formed when the crossed polaroids are set parallel to O′L and O′L′ (*see* Johannsen[3]). The hyperbolic segment O_1PL may be characterised by the parameter χ, where $(-\chi)$ is the angle that its asymptote O′L makes with respect to $O'X_k$. For any point on this hyperbolic segment χ the principal plane of linear birefringence OX_r (corresponding to the slower wave in the absence of optical activity and dichroism) makes an angle $-\chi$ with $O'X_k$.

For a point in the convergent light figure which is related to P by inversion about the central point O′, the orientation of the principal planes of linear birefringence, as well as the magnitude of the linear birefringence will be the same as for the point P itself. All other factors being taken to be constant over the field of view, *the interference figures in convergent light must always be centrosymmetric about O′*. That this is not strictly what is observed (*see e.g.*, Brewster's brushes, Part I, Fig. 5, Plate IX) is mainly because the coefficients of linear dichroism exhibit some variation over the field of view. For the sake of our qualitative discussion we may neglect this variation. Accordingly *it is sufficient to consider only the field of view on the right of the vertical line* Y_kY_k'.

(*b*) *Approximate discussion.—For directions of propagation lying towards the border of the figure*, the variation of the states of polarisation of the two

waves as we proceed round a curve of constant linear birefringence δ may be easily studied in a fairly comprehensive manner. The two waves propagated along the direction P will be elliptically polarised; and according to the approximate results of P–a^1, §7 *b*, we may take the major axes of the

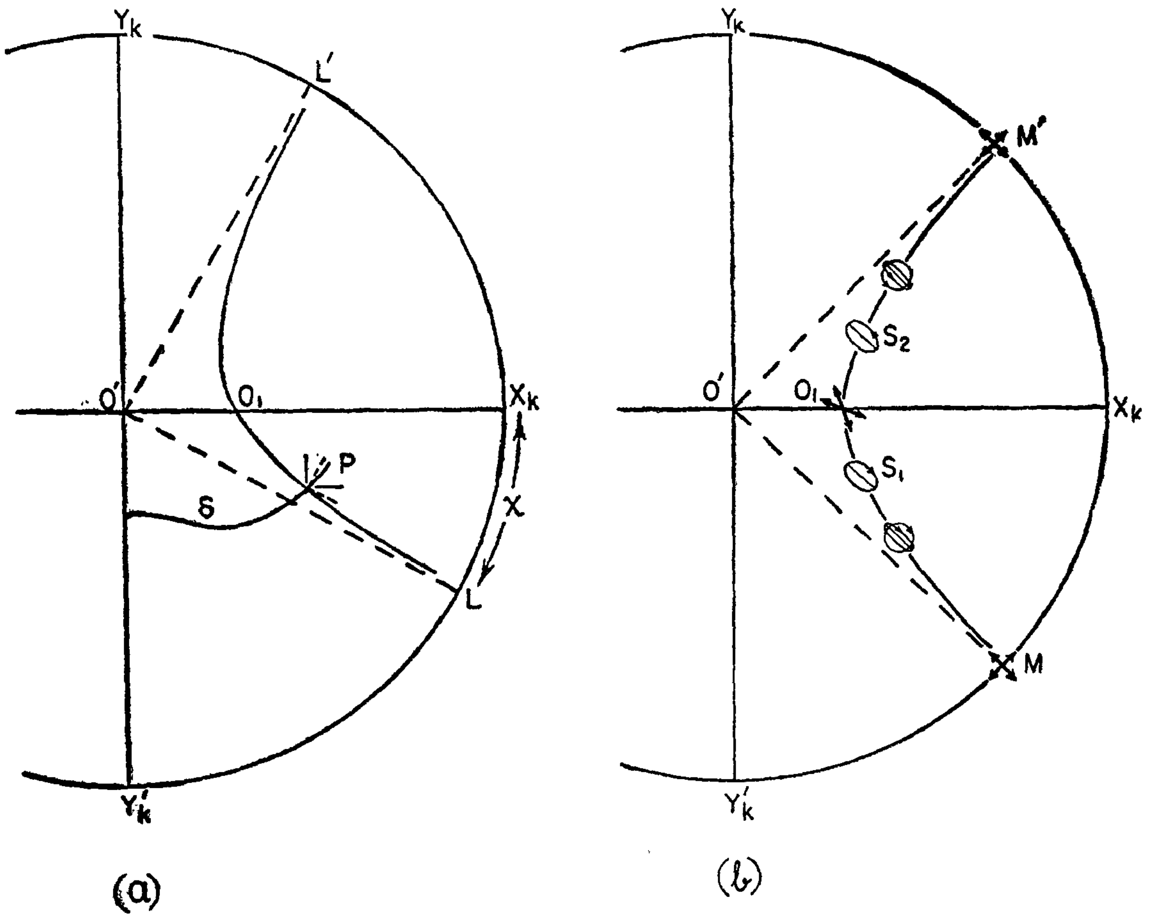

TEXT-FIG. 3. (*a*) Curvilinear co-ordinates (δ, χ) for the point P in the convergent light figure. (*b*) States of polarisation of the waves propagated along directions represented by points on MO_1M'; S_1 and S_2 are the singular axes.

slower and faster ellipses to lie along the corresponding principal planes of linear birefringence (OX_T and OY_T); and if ω represent the ellipticity of one of these elliptically polarised waves propagated along P (δ, χ), then since ρ is negative in the present case,

$$\omega = \pm \mid \rho \mid / \delta - \tfrac{1}{2} k \sin 2\chi / \delta \qquad (3)\dagger$$

the first term being taken with a positive or negative sign according as the ellipticity of the slower or faster wave is required.

† We had inadvertantly omitted, in P–*a*, eq. 15, to include a negative sign before the expression for ϵ, the common ellipticity of the waves in the absence of optical activity.

The variation of the ellipticity of the waves with direction (for points near the border of the figure) may be obtained from (3). We shall not proceed to describe this variation, since for such directions, the ellipticity is so small, that any experimental test using elliptically polarised light becomes difficult. It is to be noted that (3) may also be used for discussing the propagation for wavelengths in the red (where $k < |2\rho|$). But a characteristic difference which arises only in the present case (where yellow light is used) may be mentioned: there exists a zone of directions, *viz.*, those included between the segments O_1A_2 and O_1A_1 as also those between O_1A_2' and O_1A_1', for which both ellipses have the same sense of description—this common sense of description being the same as that in an inactive absorbing crystal.

(*c*) *General direction of propagation.*—The principal planes of linear birefringence and linear dichroism corresponding to the direction P have been marked at P itself in Fig. 3 *a*, text, while they have also been marked in P–*a*, Fig. 1 *a*, for a plate cut normal to the direction represented by P. The states of elliptic polarisation of the waves propagated along the general direction P (δ, χ) may now be accurately determined using the results proved in P–*a* which we may briefly recapitulate.

The horizontal and vertical directions will be represented on the Poincaré sphere by two opposite points X_k and Y_k on the equator—the diameter $X_k Y_k$ being kept perpendicular to the paper in our diagrams. From the theory for transparent active crystals we may regard as given (*a*) the elliptic birefringence Δ in the absence of dichroism, (*b*) the diametrically opposite points B and B′ which represent the states of elliptic polarisation of the slower and faster waves propagated along the direction P in the absence of dichroism (*vide* P–*a*, Fig. 2 and §3 *a*). The states of polarisation of the waves actually propagated in the direction P (*i.e.*, with linear dichroism present) will be represented on the Poincaré sphere by two points P_a and P_b which we wish to determine. Now the angular distances $2\psi_a$ and $2\phi_a$ of the slower state P_a from X_k and B are also the angular distances of P_b from the opposite points Y_k and B′; and further, P_a and P_b lie on the same side of the great circle passing through X_k and B—the hemisphere on which they lie being fixed by the fact that the vertices B, P_a and X_k describe the triangle BP_aX_k in a positive sense. Because of this relation it becomes sufficient to locate geometrically the position of P_a; this may be done from the following additional features regarding the triangle BP_aX_k; (*i*) the angle at P_a is a right angle; (*ii*) the ratio of the sines of the angular distances $2\phi_a$ and $2\psi_a$ of P_a from B and X_k is equal to k/Δ. The absorption

coefficients and refractive indices of the states P_a and P_b are given by P–*a*, Eqns. 9 and 12.

The region of the convergent light figure which need be theoretically studied is considerably reduced by the following relation which may be proved from the results of P–*a*. The points on the Poincaré sphere, representing the states of polarisation of the waves propagated along the direction P $(\delta, \chi - \frac{1}{2}\pi)$ are obtained from those representing the states propagated along P (δ, χ), by reflection about the equatorial plane of the sphere: the refractive indices of the states are interchanged after reflection but not the absorption coefficients. So also the points on the Poincaré sphere representing the states propagated along P $(\delta, \frac{1}{2}\pi - \chi)$ may be obtained from those representing the states propagated along P (δ, χ) by reflection about the plane $C_l M C_r$: the absorption coefficients of the states are interchanged after reflection but not the refractive indices. We shall proceed to apply the results quoted in this sub-section to discuss in detail the propagation along particular zones of directions.

§6. Observations with Elliptically Polarised Light

Let us now consider a direction of propagation such as P′ lying on the hyperbolic segment O_1A_1 (Fig. 1, text). For such a direction the principal plane of linear birefringence OX_r lies parallel to $O'A_1$ and is represented on the Poincaré sphere by the point A_1 on the equator (*see* Fig. 2 *b*, text). The point B representing the state of polarisation of the slower wave in the absence of absorption, will lie on the meridian A_1C_l—since this state will be left-elliptically polarised with its major axis parallel to $O'A_1$. In §4 we have seen that a vibration parallel to $O'A_1$ is propagated unchanged along the direction P′ in the convergent light figure. Hence the point P_a—representing the state of polarisation of one of the waves propagated in this direction—coincides with A_1. The state P_a being given, the state P_b may be immediately located as described in §5 *c*. Thus since the arc P_bY_k should be equal to arc A_1X_k *the state P_b must lie on the dotted small circle* of angular radius Y_kA_2 drawn about Y_k as centre. Further P_b and A_1 should lie on the same side of the great circle drawn through B, X_k and B′, and arc P_bB' should be equal to arc A_1B. From the symmetry of the figure, P_b is clearly determined by the point of intersection of the dotted small circle (mentioned above) with the arc Y_kP_b which is drawn at an angle 2θ to the equator as indicated, θ being the angle A_1X_kB. Turning to the convergent light figure (Fig. 1, text) suppose the point P′ on which we have fixed our attention moves outwards from the optic axis O_1 along the hyperbolic segment O_1A_1; the state of elliptic polarisation B (which would have been propagated along

the direction P′ as the slower wave *in the absence of absorption*) changes progressively from a left-circular vibration (for P′ coinciding with the optic axis O_1) towards the state of a linear vibration parallel to $O'A_1$: that is, on the Poincaré sphere (Fig. 2 *b*, text) the point B moves down from C_l towards A_1 along the arc C_lA_1, θ decreasing from $\frac{1}{2}\pi$ to zero. At the same time the state P_b of the faster wave being determined by the angle 2θ moves from A_2 towards A_1' along the dotted small circle whose diameter is A_2A_1' (the locus of P_b being in the lower hemisphere).

We shall now express the above results in physical terms. For all points on the hyperbolic segment O_1A_1 the state of polarisation P_a of the slower wave remains linearly polarised parallel to $O'A_1$ (§4). But as we proceed outwards from the optic axis O_1 along this hyperbolic segment, the state of polarisation P_b of the faster wave progressively alters in a manner which may be described thus: the state P_b—which is initially linearly polarised parallel to $O'A_2$—opens out into a right-elliptic vibration the ellipticity of which initially increases, the major axis at the same time turning rapidly towards the direction $O'A_1'$ orthogonal to $O'A_1$; further out the ellipticity again decreases though the turning of the major axis towards $O'A_1'$ continues, so that towards the border of the figure the states of the two waves approximate to those given in §5 *b*—and thence towards vibrations linearly polarised along the principal planes of linear birefringence (*see* Fig. 1, text).

As we proceed outwards from the optic axial direction O_1 along the hyperbolic segment O_1A_1', the state P_b of the faster vibration will, on the Poincaré sphere, remain fixed at A_1: but the state P_a of the slower vibration may be shown (by a similar analysis) to move from A_2 towards A_1' along the arc of a small circle which again has A_1A_2' as diameter, but which now lies in the *upper* hemisphere. So also, as we proceed along the hyperbolic branch $A_2O_1A_2'$ from A_2 to A_2', the state of polarisation of *one* of the waves will, according to §4, remain fixed at A_2 on the Poincaré sphere. (This state represents the slower state for points on the segment O_1A_2 but becomes the faster state for points on segment O_1A_2'). At the same time the state of the other wave moves on the Poincaré sphere from A_2' to A_1 and back to A_2' tracing (in a clockwise sense) the small circle of diameter $A_2'A_1$. (The results of this paragraph follow from those quoted at the end of §5*c*.) The variation of the states of polarisation of the waves for points on the hyperbolic branches $A_1O_1A_1'$ and $A_2O_1A_2'$ has been illustrated in Fig. 1, text.

According to a well-known property of the Poincaré sphere, the elliptic state P_b in Fig. 2 *b*, text, may be produced by passing a linear vibration in the state A_1' through a mica plate of retardation 2θ whose slow

vibration-direction is represented by X_k; *i.e.*, by passing light first through a polaroid whose vibration-direction is parallel to $O'A_1'$ and then through a retardation plate whose slow vibration is parallel to the axial plane. In Fig. 9 this arrangement was kept in front of the crystal plate, while behind the crystal plate was placed an 'elliptic analyser' which was kept automatically crossed with respect to the elliptic polariser (the arrangement used being that described in Part I, §5); it will be seen that, in conformity with theory, a particular point (such as P′) on the hyperbolic segment O_1A_1 is extinguished—this point representing the direction where the incident elliptic vibration is propagated unchanged. When the coupled retardation plates are rotated around together by 90° (so that X_k becomes the *fast* vibration-direction of the first retardation plate), a corresponding point on the hyperbolic segment O_1A_1' is extinguished—as seen in Fig. 10. In Figs. 11 and 12 (Plate XII) the coupled polaroids have been turned so that in both cases the vibration-direction of the first polaroid is parallel to $O'A_2'$ (represented by A_2' on the Poincaré sphere); the slow vibration-direction of the first retardation plate lies along the axial plane in Fig. 12 but perpendicular to it in Fig. 11. In the former case the point near O_1 which is extinguished lies on the hyperbolic segment O_1A_2, while in the latter (Fig. 11) it lies on O_1A_2'. In all the four photographs (Figs. 9–12, Plate XII) the extinguished points should lie on a curve of constant linear birefringence —a point which is difficult to confirm exactly. It was however verified that when the experiments were repeated with mica plates of lower retardation, the extinguished spots had in all cases moved outwards along the respective hyperbolic arcs. All these observations confirm the theoretical results stated in this section.

§7. SINGULAR AXES

We shall now consider directions of propagation for which the principal planes of linear birefringence are equally inclined to the axial plane. Considering first a point on the hyperbolic segment O_1M (Fig. 3 *b*, text), the orientation of the principal plane of linear birefringence OX_r will be parallel to $O'M$, and will be represented by the point M on the Poincaré sphere (Fig. 4 *a*, text). Hence for this direction of propagation the state B (representing the slower wave in the absence of dichroism) will be a point on the meridian C_lM, at latitude $2\omega_1$; and the elliptic birefringence Δ in the absence of dichroism will [according to P–*a* Eq. (1)] be equal to $|2\rho|$ cosec $2\omega_1$. The great circle CX_kC' is drawn having B and B′ as its poles. The arc X_kB is a quadrant, and from the condition that the angle it subtends at P_a should be a right angle, it may be seen geometrically [or from P–*a*, Eq. (5)] that P_a

must lie either on the arc CX_k ($2\phi_a = \frac{1}{2}\pi$) or on the meridional arc BC ($2\psi_a = \frac{1}{2}\pi$). The former situation is illustrated in Fig. 4 *a*, text, and holds when the direction under consideration is still sufficiently close to the axial direction O_1 for k to be greater than Δ. It may be shown [using Eq. (1) above, and P-*a*, Eq. (4)] that the states P_a and P_b are the points of intersection of the great circular arc X_kCY_k with the small circle $E_2A_1E_1$ of spherical radius MA_1 drawn about M as centre. As we proceed outwards from the optic axis O_1 along the segment O_1M, Δ increases while at the same time the latitude $2\omega_1$ of the point B decreases: thus the states P_a and P_b which originally coincide with A_1 and A_2 move along the small circle towards the state E_1.

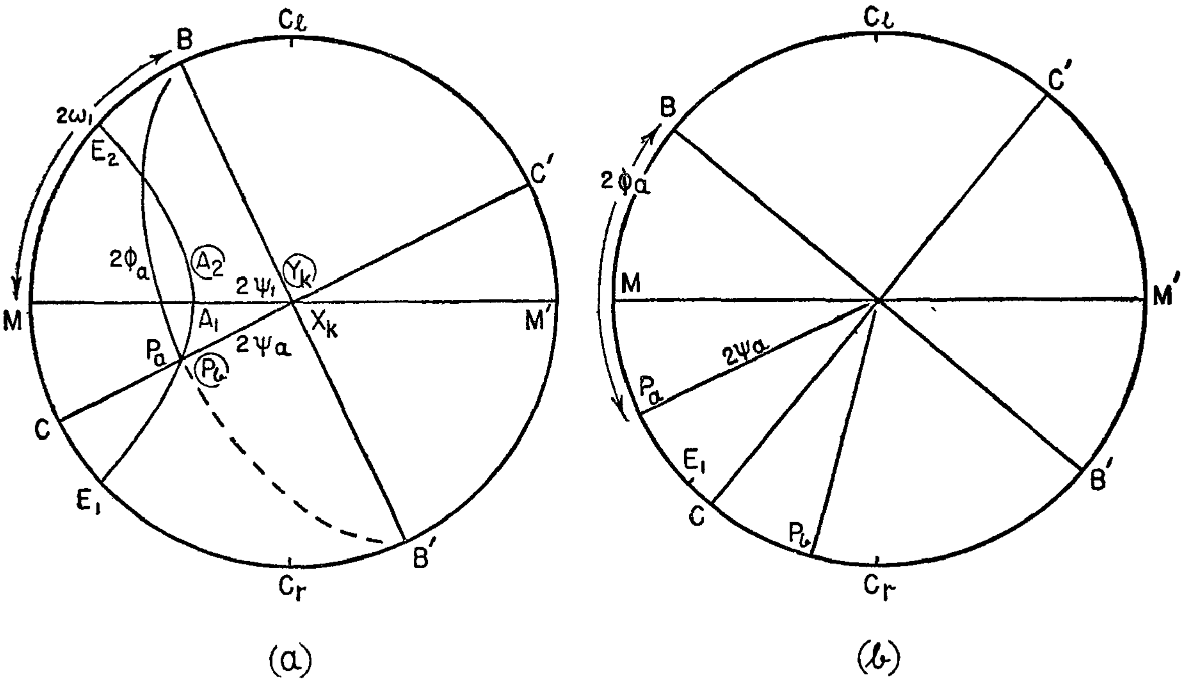

Text-Fig. 4. Construction for determining the states of polarisation of the propagated waves (*a*) for points on O_1S_1 in Fig. 3 *b*, text, (*b*) for points on S_1M in Fig. 3 *b*, text. The states E_1 and E_2 are respectively propagated unchanged along the singular axes S_1 and S_2.

In Fig. 3 *b*, text, S_1 denotes the direction of propagation on the segment O_1M for which Δ has become equal to k: since $\Delta = |2\rho| \operatorname{cosec} 2\omega_1$, it may be seen from Eq. (1) that for this direction $\omega_1 = \psi_1$ so that the point C of Fig. 4 *a*, text, now coincides with E_1. *For the direction of propagation S_1 there are no longer two distinct states of polarisation which can be propagated unchanged* since both states P_a and P_b have coalesced with the state represented by E_1 on the Poincaré sphere. Thus there is only *one* state of vibration which can be propagated without change of form along the '*singular*

axis' S_1—as may be directly shown from P–*a*, Eqns. (4) and (5) by setting $k = \Delta$, and $2\chi' = \frac{1}{2}\pi$. As we proceed further outwards along the segment O_1M, we will have $\Delta > k$; the states of polarisation P_a and P_b of the waves become again separate, moving from E_1 towards M and M′ respectively, along the arcs joining E_1 to these points. Thus Fig. 4 *b*, text, illustrates the position of the states P_a and P_b for a direction of propagation on the segment S_1M. The variation of the states of polarisation of the waves as we proceed outwards along O_1M' may be similarly traced on the Poincaré sphere using the relations stated in the concluding paragraph of §5 *c*. The direction S_2 for which $k = \Delta$, is again a singular axis where *only* the state of polarisation E_2 can be propagated unchanged—the points E_2 and E_1 being related to one another by reflection about the equatorial plane of the sphere.

The results proved above have been expressed in terms of the Poincaré sphere. They may be easily translated into physical terms, and the actual variation of the states of polarisation of the waves along the segments O_1M and O_1M' has been depicted (in an exaggerated form) in Fig. 3 *b*, text. The single wave which can be propagated along the singular axis S_1 differs from that which can be propagated along S_2, only in the sense of description; but both states are elliptically polarised and are not orthogonal to one another—unlike the case in inactive absorbing crystals.

Fig. 13 (Plate XIII) shows the photograph obtained with an elliptic polariser and a crossed elliptic analyser (*see* Part I, §5), the elliptic polariser being adjusted to produce the state of polarisation E_2 which can be propagated unchanged along the singular axis S_2; the vibration-direction of the first polaroid was kept along the direction $O'A_2$ (which is represented by the state A_2 in Fig. 4 *a*, text), this being followed by a quarter-wave plate with its slow axis along O′M (represented by M in Fig. 7). The singular axis S_2 and a corresponding singular axis associated with the other optic axis, appear extinguished in Fig. 13, Plate XIII. By turning the coupled polaroids so that the vibration-direction of the first polaroid is parallel to $O'A_1$ we observe the figure presented with an elliptic polariser E_1 and a crossed elliptic analyser. Fig. 14 shows this photograph, the singular axis S_1 and a corresponding singular axis associated with the optic axis O_2, being extinguished. (The singular axes have been indicated by spots in Figs. 13 and 14.) Fig. 15 shows the photograph obtained with the elliptic analyser removed in the arrangement of Fig. 14. This has to be compared with Fig. 16 which has been obtained by turning the polaroid by 90° relative to its orientation in Fig. 15. In Fig. 16, therefore, the elliptic vibration incident on the crystal is *orthogonal* to that which alone can be propagated unchanged along the singular axis S_1. Nevertheless, *the light incident along*

this singular direction is not reflected away; in fact the intensity of the light emerging along S_1 in Fig. 16, Plate XIII is *greater* than in Fig. 15, though in the latter case the incident vibration is in a state which is propagated unchanged along S_1. We need not enter into the explanation of this phenomenon, since it follows exactly along the lines given previously for a corresponding phenomenon observed in *inactive* absorbing crystals;[5, 6] the principle of superposition must be directly applied and the vibration incident along the singular direction S_1 in Fig. 16, Plate XIII will be propagated with a progressive change in its state of polarisation.

For any direction of propagation lying within the small strip $S_1O_1S_2$ (Fig. 3 *b*, text) the refractive indices of the waves will be equal according to P–*a*, Eq. (13), since for such a direction we have, $2\phi_a = \frac{1}{2}\pi$ from Fig. 4 *a*, text; the absorption coefficients of the waves will however be different according to P–*a*, Eq. (10), tending to equality only as the singular directions are approached. For the remaining points on the hyperbolic branch MO_1M', it is the refractive indices of the two waves which are different, the difference increasing from zero as we proceed outwards from the singular directions; while *the absorption coefficients are equal for this zone of directions* since $2\psi_a = \frac{1}{2}\pi$ from Fig. 4 *b*. Now in all the interference figures observed when the states of the polariser and analyser are crossed, the minima of the ring system should appear perfectly dark only along the zones where the absorption coefficients of the waves are equal [P–IV,[6] Eq. (21)]. Thus Figs. 1–6 and Figs. 9–14 confirm that the absorption coefficients of the waves are equal for points on the rectangular hyperbola one branch of which has been marked MO_1M' (the small strips joining the singular axes being excepted). This is also confirmed by the appearance of Brewster's brushes along the same zones—a feature which is to be theoretically expected from P–IV, Eq. (11) (following the same reasoning as for inactive absorbing crystals[7]), since the sum of the absorption coefficients of the waves may be taken to be constant over the region under consideration according to P–*a*, Eq. (9).

§8. Phenomena with Polariser alone and Analyser alone

In a previous publication[6] it has been explained quite generally that in crystals where the waves propagated along any direction are non-orthogonally polarised, interference rings should be exhibited with a polariser alone in front of the plate (*i.e.*, with no analyser); and also with an analyser alone behind the plate, the incident light being unpolarised. The ' idiophanic rings ' of the former class are exhibited in Figs. 17–20, for various settings of the linear polariser as the latter is turned in a clockwise sense—starting with the setting for which the vibration-direction is along the axial plane, as in

Fig. 17. Similarly, Figs. 21–24 show the idiophanic rings for various settings of a linear analyser as the latter is turned in an *anti*-clockwise sense, starting with the setting of Fig. 21, where the vibration-direction lies along the axial plane. In the observations with a polariser alone it was found that two hyperbolic brushes passing through the optic axes were formed in the setting of Fig. 18, Plate XIII, for which the vibration-direction of the polaroid was parallel to $O'A_2$ in Fig. 1, text; but Fig. 24 obtained with an analyser alone in the same setting is entirely different. So also in observations with an analyser alone, two hyperbolic brushes passing through the axial directions formed in the setting of Fig. 22, Plate XIV, where the vibration-direction of the polaroid was parallel to $O'A_1'$, in Fig. 1, text; but Fig. 20, obtained with a polariser alone in the same setting, is entirely different from Fig. 22.

Thus *the effects presented with a linear polariser alone are, in general, not the same as with a linear analyser alone* in the same setting. This proves that the non-orthogonally polarised states propagated along a general direction *cannot* be of the special type propagated in inactive absorbing crystals (*see* P–IV, §7).

It is physically understandable that the setting of the polaroid at which an optic axial direction, *e.g.*, O_1 appears darkest, differs according as whether the polaroid is set before or after the plate. In the former case the polariser-vibration would have to be parallel to $O'A_2$, *i.e.*, to the vibration-direction of the more heavily absorbed wave propagated along O_1; while in the latter case the analyser-vibration has to be parallel to $O'A_2'$ so that it will be *crossed* with respect to the vibration-direction of the *less* absorbed wave propagated along O_1. It remains to explain why at these settings, we find a whole zone of directions, represented by the hyperbolic brushes in Figs. 18 and 22, which appear as dark as the optic axial directions. For this purpose it must be remembered that the coefficients of linear dichroism as well as the orientations of the principal planes of linear dichroism are taken as constant over the region considered; so that the absorption coefficient of a wave propagated along any direction becomes purely a function of its state of polarisation: more precisely, *the absorption coefficient is purely a function of the angular distance 2ϕ of this state from X_k*, on the Poincaré sphere [P–*a*, Eq. (9)]. For the zone of directions of the rectangular hyperbola, one branch of which is marked $A_2O_1A_2'$ (Fig. 1, text), the state of polarisation of one of the waves is constant—being linearly polarised parallel to $O'A_2$ (§4). Hence when the vibration-direction of the polariser lies along $O'A_2$, the light suffers equal absorption all along this zone of directions, giving rise to hyperbolic brushes of uniform depth as in Fig. 18.

Similarly, consider any direction of propagation such as P′ on the rectangular hyperbola, one branch of which is $A_1O_1A_1'$. For any such direction the absorption coefficient of the more heavily absorbed wave will always be equal to the absorption coefficient (α_2 say) of the more heavily absorbed wave propagated along an optic axis such as O_1; this follows because according to §6, both these states (P_b and A_2) lie on a small circle with X_k as centre, and hence are at the same angular distance from X_k on the Poincaré sphere (Fig. 4 *a*, text). When unpolarised light of unit intensity is incident on a direction such as P′ the two non-orthogonally polarised waves (in states A_1 and P_b) into which it is split will both have initial intensities equal to $\frac{1}{2}\sec^2 \frac{1}{2}A_1'P_b$ (*see* reference 8, §7). When a polaroid is kept behind the plate with its vibration-direction parallel to $O'A_1'$ it completely crosses out the less absorbed wave emerging along the direction P′ since this wave is linearly polarised parallel to $O'A_1$ (§4); a fraction $\cos^2 \frac{1}{2}A_1'P_b$ of the intensity of the more heavily absorbed wave will however be transmitted by the analyser along the direction P′. Thus in the idiophanous figure observed with the analyser-vibration parallel to $O'A_1'$, the intensity of all points such as P′ (lying on the rectangular hyperbola, one branch of which is $A_1O_1A_1'$) will be equal to $\frac{1}{2}\exp(-\alpha_2 d)$, *i.e.*, it will be the same as the intensity of the axial direction in Fig. 18, Plate XIII. This explains the occurrence of the dark brushes in Fig. 22.

It has been shown in P–IV, §7, that the idiophanous figures presented with a polaroid set before or after the plate will not differ *if* the following condition is satisfied; on the Poincaré sphere, the angular distances of the points P_a and P_b (representing the states propagated along any direction) from the point representing the vibration-direction of the polaroid, should be supplements of one another. From the results of P–*a*, §4, it may be seen that this condition will be satisfied in the *particular* cases when the vibration-axis of the polaroid coincides with X_k or Y_k, *i.e.*, with one of the principal planes of linear dichroism $O'X_k$ or $O'Y_k$. This explains why Figs. 17 and 21 appear identical, as also Figs. 19 and 23.

It will be noted from the photographs that the idiophanous figures presented with a linear polariser at a setting of $+\theta$ to the axial plane is similar in some respects to that presented with a linear analyser at the setting $(-\theta)$ to the axial plane—the figures in the two cases being in fact related merely by reflection about the vertical line Y_kY_k' (*Compare* Fig. 18 with Fig. 22, and Fig. 20 with Fig. 24). This may be explained using the results stated at the end of §5 *c*; the intensity at the point P (δ, χ) with the polariser-vibration at $+\theta$ to $O'X_k$ [being given by P–IV, Eq. (6)] may be shown

to be equal to the intensity at P (δ, $-\chi$) with the analyser-vibration at ($-\theta$) to $O'X_k$ [as obtained from P–IV, Eq. (16)].

Finally it may be mentioned that observations with a polariser alone and with an analyser alone readily revealed a characteristic difference in the behaviour of a *left*-rotating sector (occurring in another basal plate). The orientations of the polaroid at which the brush formed in the two cases showed that the azimuth of the linearly polarised states propagated along the optic axes lay in the *positive* quadrant—as is to be expected from theory (P–*a*, §8 *b*).

The author is highly indebted to Prof. Sir C. V. Raman, for his unfailing interest in the present work.

SUMMARY

Using a wavelength (λ 5890) for which the linear dichroism of the amethystine sector is appreciable ($k > |2\rho|$), twenty-four interference figures are reproduced confirming in detail the theory of light propagation in absorbing crystals possessing optical activity.[1] Unlike the behaviour in transparent crystals, the idiophanic interference figures seen with a polariser alone in front of the plate differ in general from those presented with an analyser alone behind the plate in the same setting. The existence of four singular axes, one on either side of each optic axis, is shown: along each singular axis only *one* (elliptically) polarised wave—and not two—can be propagated without change of form.

REFERENCES

1. Pancharatnam, (P–*a*) .. *Proc. Ind. Acad. Sci.*, 1957, **46 A**, 280.
2. ———— .. *Ibid.*, 1956, **44 A**, 247.
3. Johannsen .. *Manual of Petrographic Methods*, McGraw-Hill, 1918, 440.
4. Wooster .. *A Text-book on Crystal Physics*, Cambridge, 1938, 141.
5. Pancharatnam .. *Proc. Ind. Acad. Sci.*, 1957, **46 A**, 86, 235.
6. ————, (P–IV) .. *Ibid.*, 1957, **45 A**, 2.
7. Pockels .. *Lehrbuch der Kristalloptik*, *Teubner*, 1906, 421.
8. Pancharatnam .. *Proc. Ind. Acad. Sci.*, 1956, **44 A**, 398.
9. ———— .. *Ibid.*, 1954, **40 A**, 196.
10. Dove .. *Farbenlehre*, 1853, Seite 251.
11. Liebisch .. *Ber. Berl. Akad.*, 1916, **36**, 870.
12. Leitz and Munchberg .. *Neues Jb. Mineral*, 1956, **10**, 217.

APPENDIX

It was shown in a previous investigation[9] on amethystine quartz that the approximate orientation of the absorption ellipsoid could be derived purely from observations on the pleochroism made at appreciable inclinations to the *c*-axis. As regards the observations in convergent light and their explanation described in that paper, they have no doubt to be supplemented by the account given in the present paper—but this does not alter the conclusions already drawn from them. Thus the present paper establishes rigorously that if we consider the section of the absorption ellipsoid normal to the *c*-axis, then the major semi-axis of the elliptic section coincides with the obtuse-bisectrix—*which in turn coincides with an* a-*axis of quartz.* The method, previously used, of determining the orientations of these principal axes for less intensely coloured areas by observations with a single polaroid* may also be rigorously justified using the results stated at the end of §8. Very significant too is the fact that the intensity of Brewster's brushes (Part I, Fig. 5, Plate IX) appears symmetrical about the plane Y_kY_k' but not about the axial plane. This indicates that the plane Y_kY_k' (normal to the *a*-axis mentioned) is a plane of symmetry of the absorption ellipsoid—though this is not true of the axial plane. This is confirmed by the appearance of Brewster's brushes in white light: the two brushes below the axial plane appear bluish purple towards the border of the figure while those above are of a deeper reddish purple colour. The explanation of this is that there are two colour axes in the symmetry plane Y_kY_k' which lie on either side of the *c*-axis at approximately 45° to it—the colours for vibrations along these axes being blue and deep red respectively.

According to the results of our previous investigation[9] the amethystine material occurring in the quartz can take up one of several discrete optic orientations all consistent with the description given above. An overlap of amethystine material of different optic orientations can be produced by one or more of the following three factors: (1) overlap of sectors associated with different rhombohedral faces, (2) optical twinning in which the different twin members are of opposite handedness, (3) electrical twinning in which the electrical axes of the different twin members are in opposite orientation. The main difficulty of studying the pleochroism of amethyst in any random section plate is that optical twinning of an interpenetrant variety occurs

---

* Brewster's brushes had been referred to in our earlier paper[9] as the idiophanous figure —a term reserved in the present paper for the figure presented with a polariser or analyser alone in conformity with the more prevalent usage.

extensively. Some of the investigations of Dove[10] and Liebisch[11] are of value in interpreting the interference figures in such optically twinned areas, but they do not directly concern the investigations presented in this paper.

Subsequent to our previous publication on the pleochroism of amethyst there has appeared an interesting paper by Lietz and Munchberg[12] dealing with the same problem. The difference between their conclusions and ours certainly appears to raise the interesting possibility of the existence of different species of amethyst with entirely different optical chracteristics.† Nevertheless, it would be difficult to decide how far there is real disagreement between our conclusions and the experimental part of their observations. The existence of pleochroism along the *c*-axis is common ground: and because the subject of refractive index and absorption are closely interlinked by dispersion theory, it follows that the index ellipsoid could not be strictly uniaxial for all wavelengths. In view of this fact their statement that amethyst possesses uniaxial symmetry can only be taken to mean that the index ellipsoid is *very nearly* uniaxial. With this we are in complete agreement, if we restrict ourselves to sectors of moderate colouration such as they have chosen. The mean absorption coefficient of the sector which was used by them for observing the interference figure was about $0 \cdot 75$ cm.$^{-1}$ for wavelengths near the absorption maximum; whereas for the sector used in the present investigation the *difference* k between the absorption coefficients for vibrations parallel to $O'Y_k$ and $O'X_k$ is itself about 15 times that value (*see* §3). Using the same sector as employed in the present investigation the absorption spectrograms for vibrations along the three colour axes had been reproduced in our previous paper: though the actual wavelengths of the absorption maxima were only qualitatively located, the spectrograms clearly showed the difference in intensity and position of the absorption maxima, especially for the two main absorption axes (red and blue). The latter difference would not have been present if there had been electrical twinning. Also—considering the great breadth of the absorption band in amethyst—we do not know whether the shift of the absorption maxima could have been easily detected if the sector had not been so intensely coloured, and if the vibrations had not been polarised exactly along the colour axes. Regarding this point, however (*viz.*, the orientation of the principal axes of the absorption ellipsoid), the conclusions of Leitz and Munchberg differ from ours. This would again appear to point more clearly to a fundamental difference in the nature of the amethystine material investigated in

† The material studied by us were mainly from Hyderabad, but included a few uncut specimens from Uruguay.

...MARA PUBLIC
JAN1965
MADRAS

FIG. 1

FIG. 2

FIG. 3

FIG. 4

FIG. 5

FIG. 6

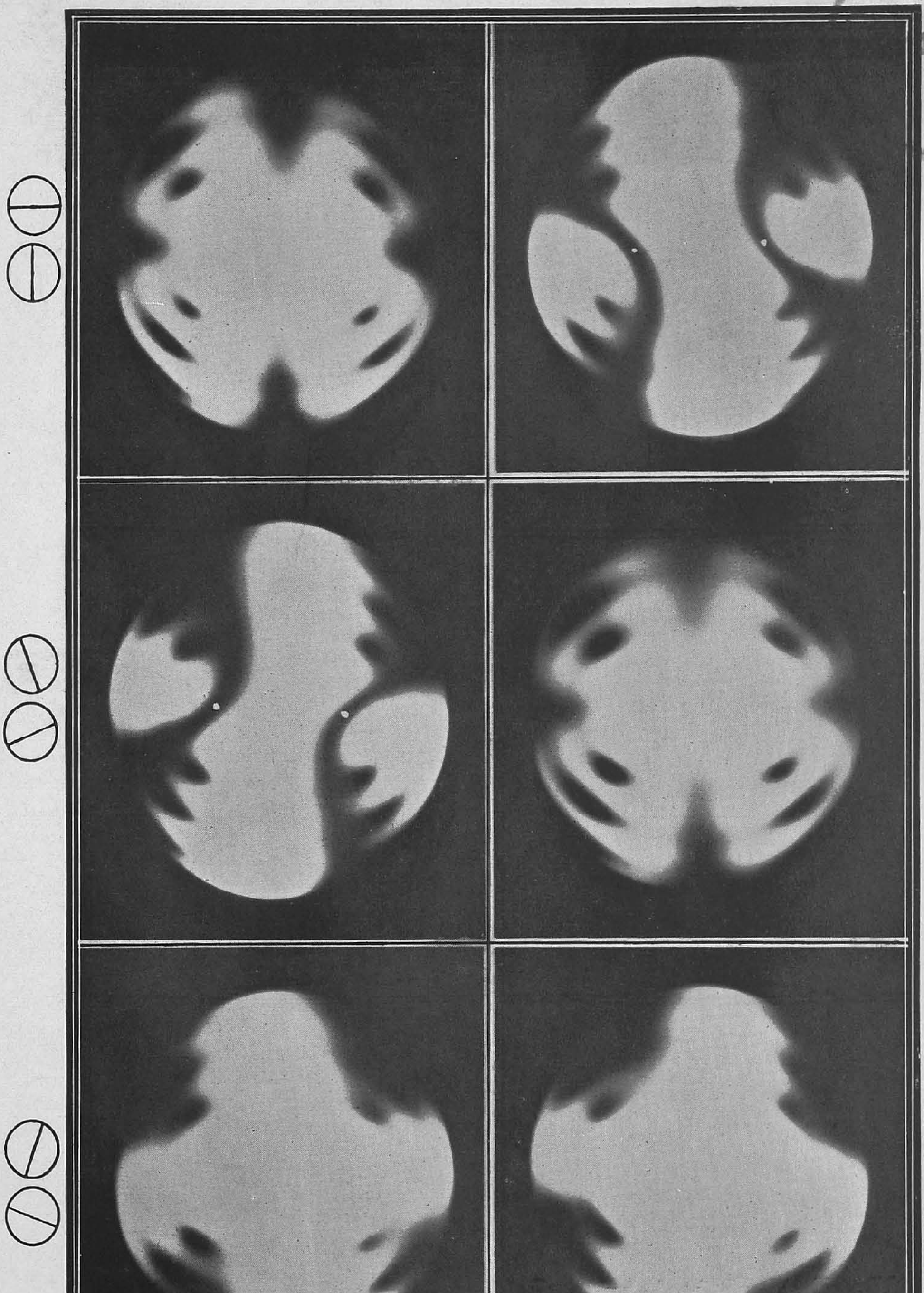

FIGS. 1–6

Interference Figures observed between crossed polaroids.

FIG. 7 FIG. 8

FIG. 9 FIG. 10

G. 11 FIG. 12

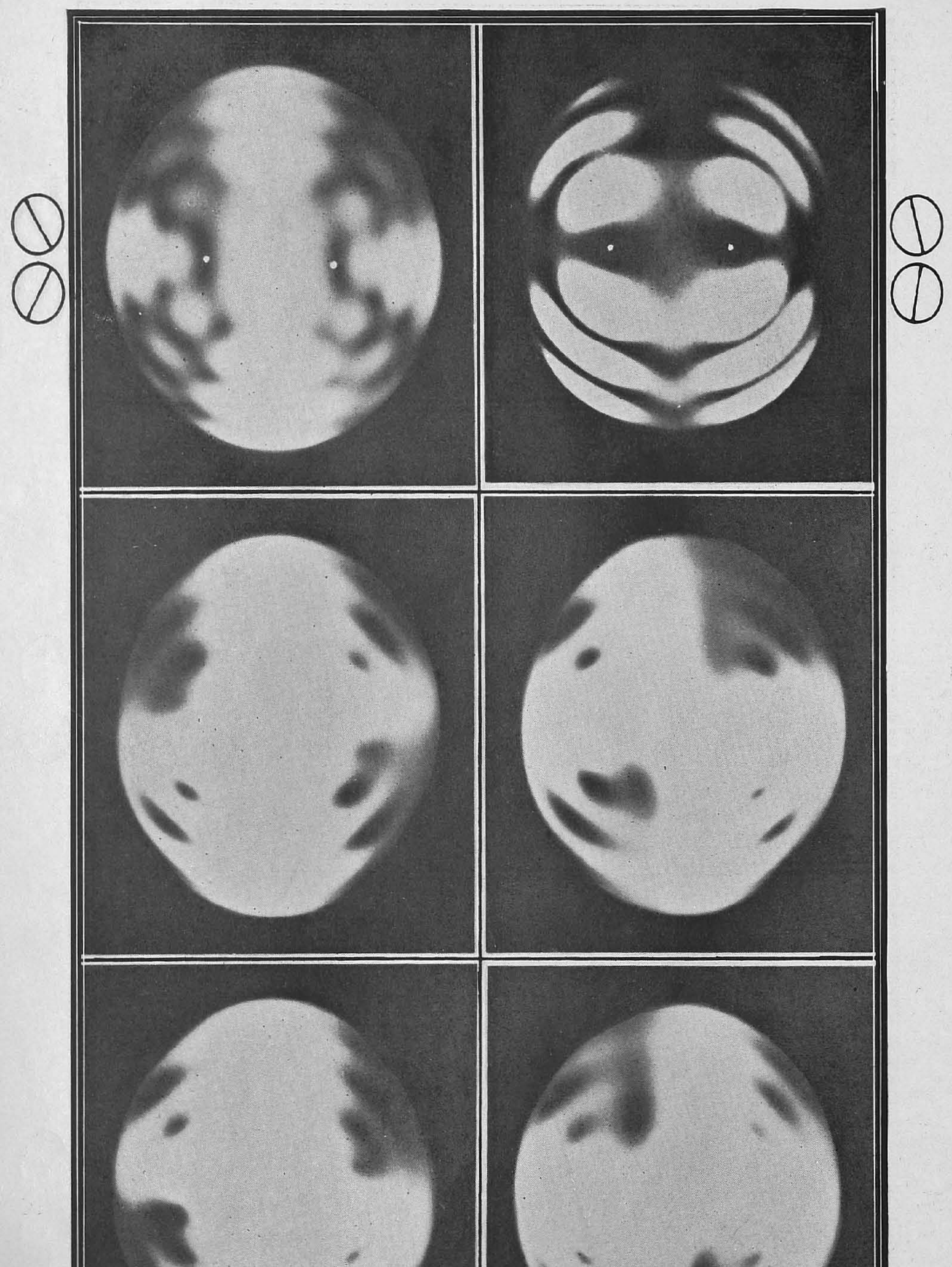

FIGS. 7–12

PUBLIC LIBRARY
4 JAN 1965

FIG. 13

FIG. 14

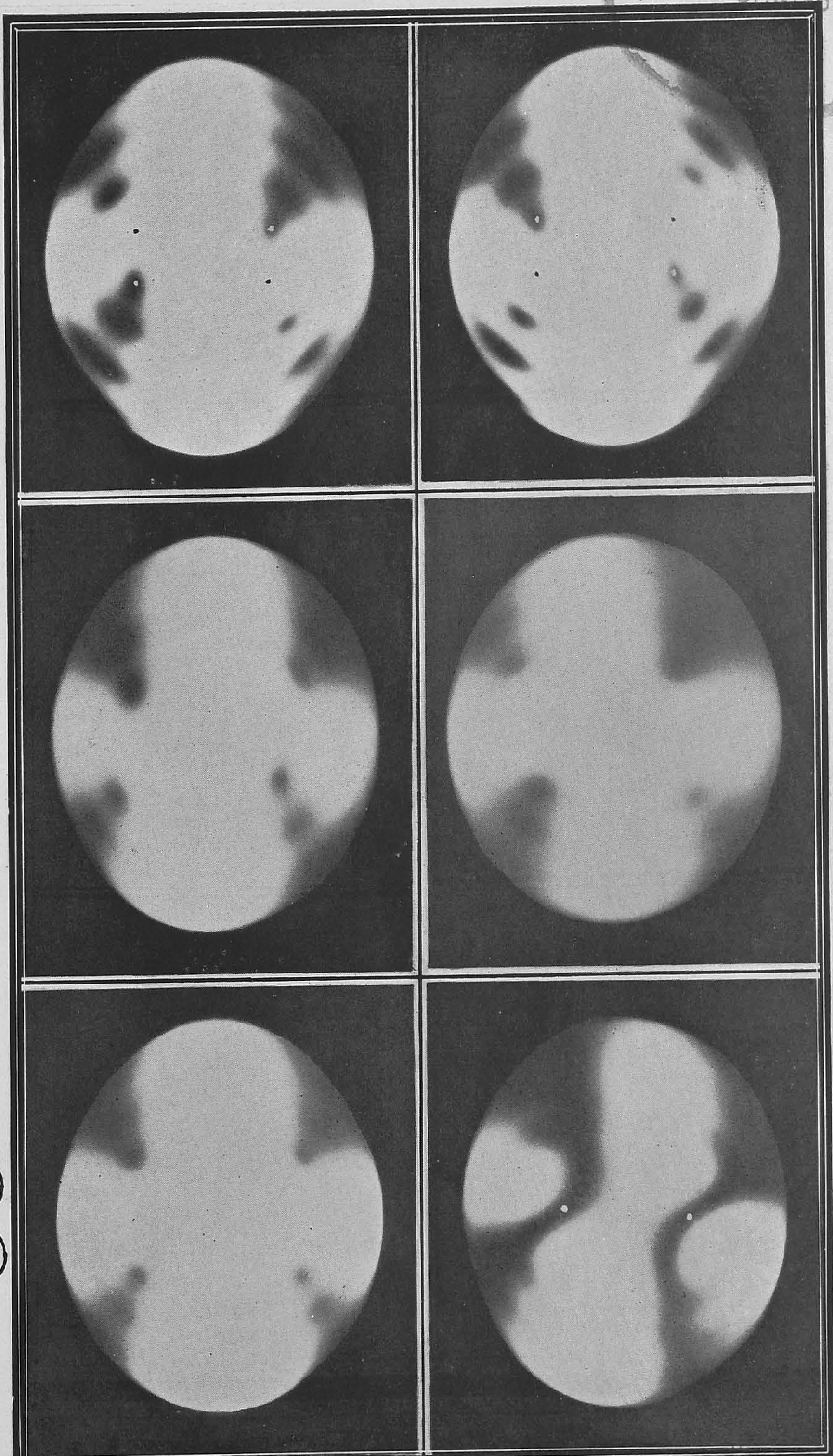

FIG. 15

FIG. 16

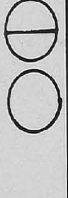

FIG. 17

FIG. 18

FIGS. 13-18

FIG. 19 FIG. 20

FIG. 21 FIG. 22

FIG. 23 FIG. 24

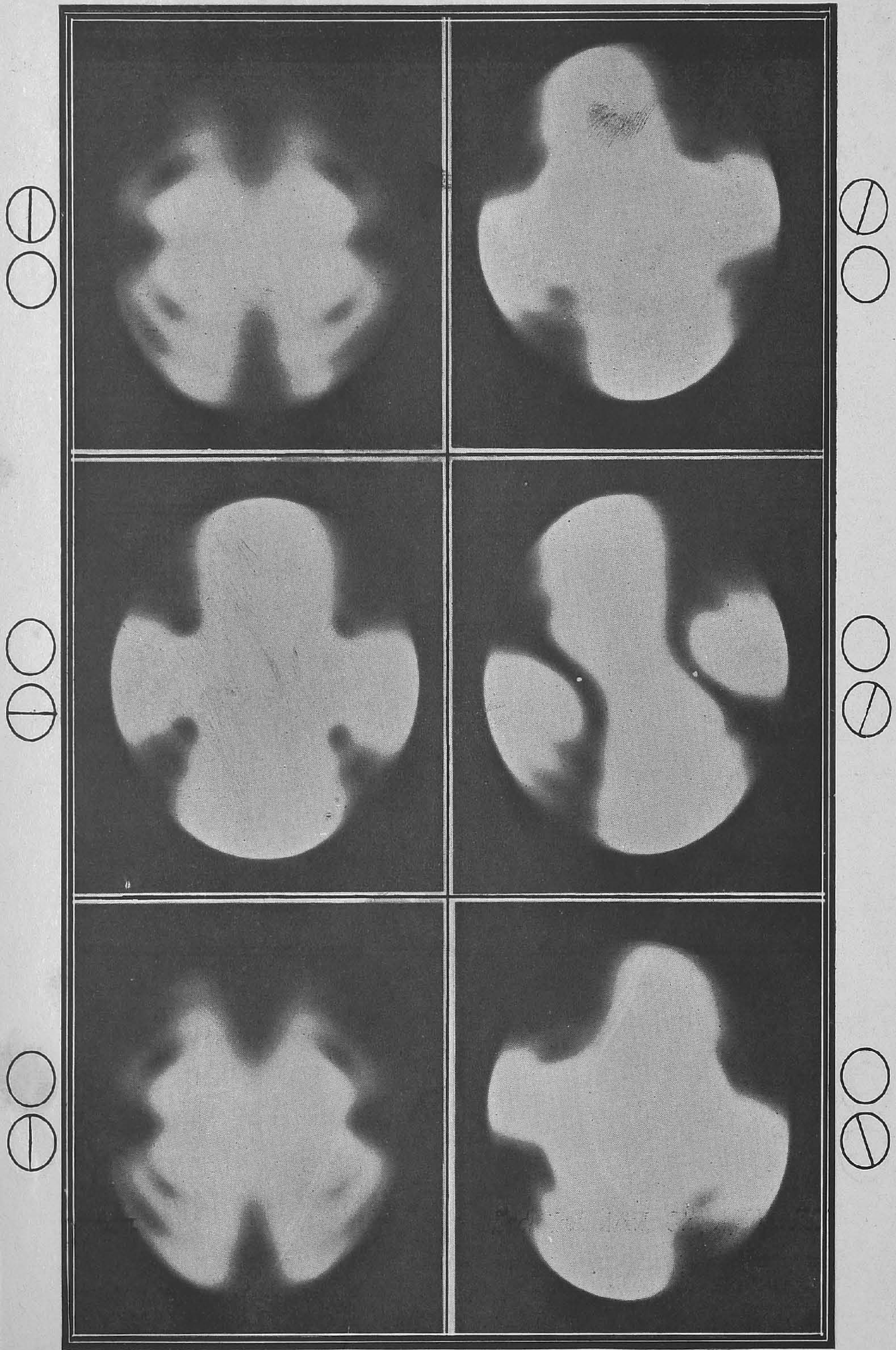

FIGS. 19–24

Phenomena with polariser alone, and analyser alone.

the two cases. But before this can be asserted with any confidence the following fact must also be taken into account: that for finding the orientation of the principal axes of the absorption ellipsoid it is *not* sufficient to measure the absorption for three mutually perpendicular vibrations. This has been done by Leitz and Munchberg by observations through the faces $(10\bar{1}0)$ and $(1\bar{2}10)$. (The observations through the basal section are of course only useful for showing the absence of uniaxial symmetry, unless account is taken theoretically of the presence of optical activity.)

Reprinted from "The Proceedings of the Indian Academy of Sciences",
Vol. XLVII, No. 5, Sec. A, 1958

THE RAMAN SPECTRUM OF QUARTZ AND ITS INTERPRETATION

BY D. KRISHNAMURTI

(*Memoir No.* 108 *from the Raman Research Institute, Bangalore*-6)

Received April 10, 1958
(Communicated by Sir C. V. Raman)

1. INTRODUCTION

QUARTZ is the classic example of a naturally occurring transparent crystalline solid. It was the first crystal in which the existence of an observable diffusion of light as an inherent property of the substance was clearly established. It was naturally therefore also one of the first crystals in which the scattering of monochromatic light was spectroscopically investigated.

The Raman spectrum, the interpretation of which is the main theme of this paper, exhibits several distinctive characters, which have their origin in the special features of the architecture of the crystal. Firstly, the solid itself may be described as a giant molecule, the silicon and oxygen atoms in it being linked together by valence bonds stretching continuously through the crystal. Secondly, the structure of the crystal is based on a three-fold axis of screw symmetry which, as is well known, results in the crystal exhibiting optical activity and other interesting properties. Thirdly, the crystal structure is notably influenced by temperature and undergoes a transformation at 575° C. which results in a change-over of its symmetry from the trigonal class to the hexagonal class. All these circumstances make their influence felt in the Raman spectrum of the crystal and have to be considered in any attempt at its elucidation.

In seeking to interpret or explain the Raman spectra of crystals we have necessarily also to take account of their behaviour in the infra-red region of the spectrum. The absorption and reflection spectra of quartz in that region were the subject of investigations by the pioneers in the field. Several of the characteristic frequencies are however so low that they are only with difficulty accessible to study by infra-red techniques. Some progress has however been made recently in this direction and the new results which have been reported in the literature have been taken into consideration in the present paper.

A detailed experimental study of the Raman spectrum of quartz has been carried out by the author. While in the main the results confirm those reported by earlier workers, a few new features have also been noticed. However, it is in regard to the interpretation of the experimental results that the present investigation is believed to make a distinct advance.

2. The Crystal Structure of Quartz

Quartz belongs to the space group D_3^4 (or D_3^6) of the enantiomorphous hemihedral class of the trigonal system. The unit cell of the quartz structure consists of three SiO_2 groups. The structure possesses the symmetry elements of a three-fold screw axis and three two-fold axes perpendicular thereto and passing through the three silicon atoms of the unit cell. The three SiO_2 groups of the unit cell are rotated with respect to each other by 120°. The three silicons are situated at levels 0, $c/3$ and $2\,c/3$, where c is the lattice constant along the optic axis. The oxygen atoms of each SiO_2 group are symmetrically situated on either side of the silicon above and below it, such that between two silicon planes there intervene two oxygen planes. Thus, the oxygen planes occur at levels $c/9$, $2\,c/9$, $4\,c/9$, $5\,c/9$, $7\,c/9$ and $8\,c/9$. We have described the unit cell here in terms of three SiO_2 groups. The prime characteristic of the structure of quartz is a continuous linking up of the silicons and oxygens so that each silicon atom is tetrahedrally surrounded by four oxygen atoms and each oxygen atom is connected to two silicon atoms. The SiO_4 group in quartz is not a regular tetrahedron, but possesses only the symmetry of a two-fold axis passing through each silicon and perpendicular to the optic axis. The three silicons in the unit cell together with the three other silicons belonging to the adjacent cells form an irregular hexagon possessing only the symmetry of a three-fold axis.

3. The Dynamics of the Quartz Lattice

The problem of the symmetry properties of the normal modes of vibration of the quartz structure was treated by Went (1935) and later in detail by Saksena (1940) on the basis of the assumption that the dynamical behaviour of the system is the same as though it belonged to point group D_3. The point group D_3 possesses the elements of symmetry of a three-fold axis and three two-fold axes perpendicular thereto and all lying in the same plane and inclined with respect to each other at an angle of 120°. The successive operations of this simple three-fold axis thrice is equivalent to the identity operation. On the other hand, three successive operations of a three-fold axis combined with one-third the translation of the lattice each time and parallel to the optic axis result finally in a simple unit translation of the cell

along the optic axis. If it is assumed that an unit translation may be treated as equivalent to the identity operation, the point group D_3 and the space-group D_3^4 (or D_3^6) may be shown to be isomorphous with each other. It is believed that some of the so-called anomalies noticed in the Raman spectrum of quartz may have their origin in the above approximation involved in the theoretical treatment. However, we shall in the present paper try to interpret the main features observed in terms of the theoretical analysis by Saksena.

The character table for point group D_3, the classes into which the vibrations are grouped, their number and selection rules are shown in Table I. The point group D_3 contains three irreducible representations, *viz.*, (1) A: totally symmetric, (2) B: anti-symmetric with respect to the two-fold axes and (3) E: doubly dengenerate.

TABLE I

Character table and selection rules

D_3	E	$2C_3^z$	$3C_2$	Total No. of vibrations	Translations	No. of vibrations	Selection rules	
							Raman Effect	Infra-red
A	1	1	1	4	0	4	$\epsilon_{xx}=\epsilon_{yy}\neq\epsilon_{zz}$; $\epsilon_{ik}=0$	Forbidden
B	1	1	−1	5	1 (T_z)	4	Forbidden	M_z only; $M_x=M_y=0$
E	2	−1	0	9	1 (T_x, T_y)	8	$\epsilon_{xx}=-\epsilon_{yy}=\epsilon_{xy}$; $\epsilon_{xz}=\epsilon_{yz}$; $\epsilon_{zz}=0$	$M_z=0$

4. THE PRINCIPAL FEATURES OF THE RAMAN SPECTRUM

Strongly exposed records of the Raman spectrum of quartz were obtained by the present author using the powerful $\lambda\,2536\cdot5$ resonance radiation of the mercury arc as the exciting radiation. The experimental techniques pertaining to this and other details of the set-up have been described fully in an earlier paper by the author on the Raman spectrum of calcite (1957). The spectra were recorded with the aid of two Hilger instruments, one a medium quartz spectrograph and the other a Littrow quartz spectrograph with greater dispersion and resolution. Using different specimens the spectra were recorded for three different orientations, *viz.*, (1) in which the exciting radiation was incident on a hexagonal face of the crystal and scattering was observed along the optic axis, (2) in which the optic axis was inclined at an angle to the plane of scattering and (3) in which the plane of scattering was perpendicular to the optic axis. With a slit width of 0·05 mm. exposures of the order of 100 hours were given to obtain spectrograms in

which even the faintest features are clearly recorded. From amongst the several spectra recorded we have chosen those corresponding to the first two orientations mentioned above and these are reproduced along with this paper to illustrate the numerous features that manifest themselves in the Raman spectrum of quartz. In addition, a number of microphotometer records on different scales of enlargement were obtained to reveal some of the finer features of the spectrum. Plate XV reproduces the spectra obtained with the Littrow instrument. Figure 1 in Plate XV corresponds to the orientation (1) when the scattering was observed along the optic axis, while Fig. 3 to the case (2) when the optic axis was at an angle to the plane of scattering. Figure 2 is the spectrum of the mercury arc reproduced for comparison. Plate XVI reproduces the microphotometer record (on a scale 1:4) of the spectrum shown in Fig. 3 of Plate XV. Plate XVII reproduces the spectra recorded with the medium spectrograph and Fig. 1 and Fig. 3 of this plate correspond to the same orientations of the crystal as those of Fig. 1 and Fig. 3 of Plate XV. Plate XVIII shows the microphotometer record (on a scale 1:8) of the spectrum in Fig. 3 of Plate XVII.

Fifteen frequency shifts constitute the principal features of the Raman spectrum of quartz. They are: 128 (*v.s.*), 206 (*v.s.*), 265 (*s*), 356 (*s*), 394 (*m*), 404 (*m*), 452 (*w*), 466 (*v.s.*), 696 (*m*), 795 (*m*), 806 (*m*), 1063 (*m*), 1082 (*m*), 1160 (*s*) and 1230 (*w*) cm.$^{-1}$ The intensity of the lines, whether they are very strong, strong or moderate or weak are indicated within brackets. Of all the frequencies the 206 cm.$^{-1}$ shift may be seen (Plate XV) to be extremely broad. The most intense line of the spectrum, *viz.*, the line at 466 cm.$^{-1}$ has to its left and quite close, a rather weak line of frequency shift 452 cm.$^{-1}$ This was first recognized by Cabannes and Bouhet (1937). It is clearly seen in Figs. 1 and 3 in Plate XV. An enlarged microphotometer record of this region of the spectrum reproduced as Fig. 1 in the text below clearly shows the line at 452 cm.$^{-1}$ to the left and on the shoulder of the line at 466 cm.$^{-1}$

A few other interesting features may be noticed in the spectra reproduced in Plates XV and XVII. The components of the doublet at 394–404, as well as those of the other doublet at 795–806, can be seen to exhibit striking variations in their relative intensities with different orientations of the crystal. In addition, the doublet separation of the pair of lines at 795 and 806 changes with the orientation of the crystal; *e.g.*, the separation in Fig. 3 of Plate XV may be clearly seen to be more than in Fig. 1 of the same plate. The frequency shift at 1082 cm.$^{-1}$ also exhibits a remarkable change in its intensity with different orientations of the crystal. While it appears to be almost of vanishingly small intensity in Fig. 1 (of Plates XV and XVII), it is of considerably greater intensity in Fig. 3 (of Plates XV and XVII).

Mathieu (1952) has reported the change in the intensity of the lines at 394, 404 and 1230 cm.$^{-1}$ for different orientations of the crystal, *viz.*, when the optic axis of the crystal is perpendicular to the plane of scattering and the

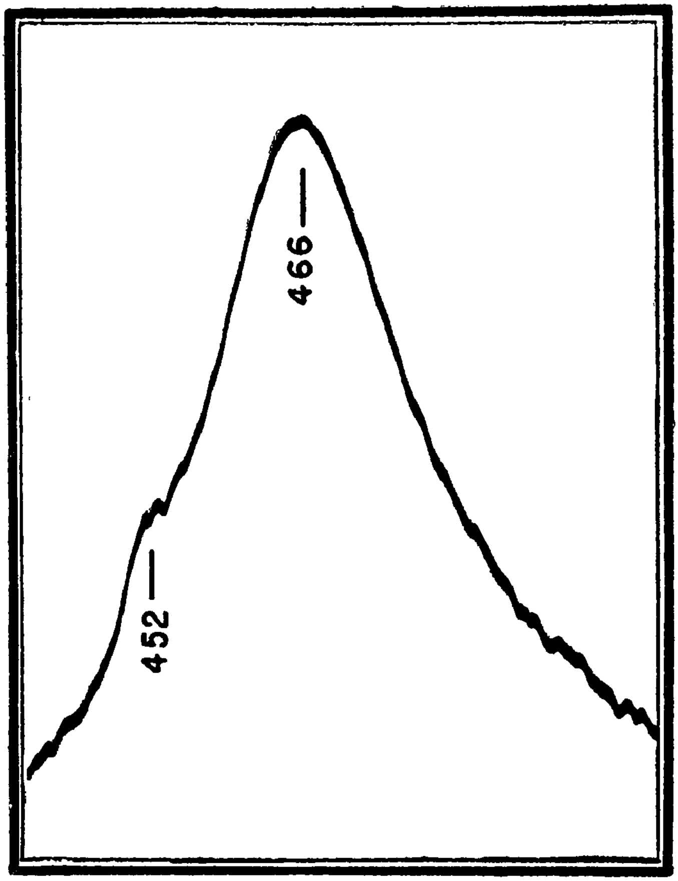

FIG. 1. Enlarged microphotometer record showing the Raman shift 466 cm.$^{-1}$ and the 452 cm.$^{-1}$ shift adjacent to it.

crystal is rotated about the optic axis to different positions. It was also noticed by him that the frequency shifts 404, 806 and 1230 cm.$^{-1}$ differ in their position for different inclinations of the optic axis with respect to the plane of scattering, the differences observed being 2 cm.$^{-1}$ for 404 cm.$^{-1}$, 6 cm.$^{-1}$ for 806 cm.$^{-1}$ and 4 cm.$^{-1}$ for 1230 cm.$^{-1}$

5. SUBSIDIARY FEATURES IN THE SPECTRUM

Numerous lines of low intensity appear in the Raman spectrum of quartz under prolonged exposures, as has already been noticed by Krishnan (1945). The present investigation has revealed a few new features in addition to confirming the majority of the lines already known. The present paper is mainly concerned with the necessity for a revision in the identification of the funda-

mental frequencies themselves. Naturally, these subsidiary features as well need a reinterpretation. A brief description of these features shall therefore be given.

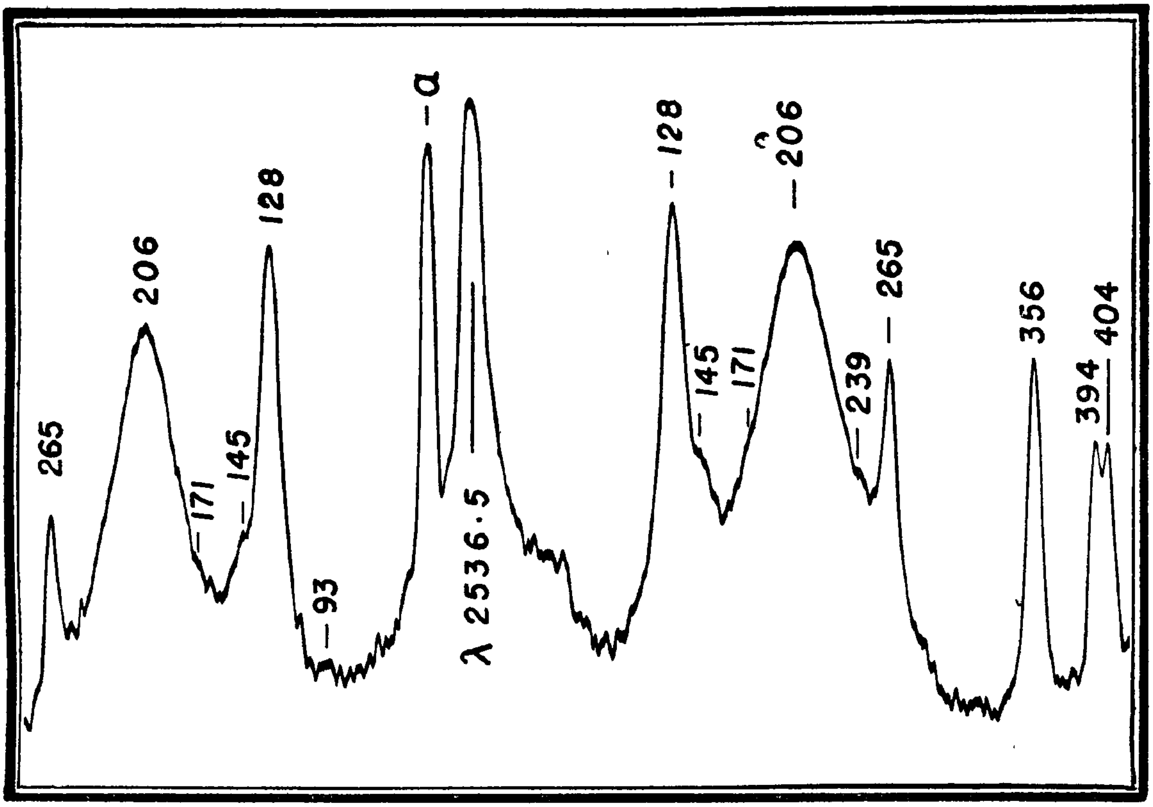

Fig. 2. Enlarged microphotometer record showing the Raman lines observed in the low frequency region.

In all, thirty-three frequency shifts at 93, 145, 171, 239, 435, 490, 509, 520, 541, 584, 728, 780, 828, 846, 867, 894, 903–908, 917, 924, 938, 947–952, 963, 978, 1046, 1269, 1291, 1361, 1381, 1420, 1435–1441, 1456, 1498 and 2129 cm.$^{-1}$ have been observed. The two low-frequencies at 26 and 39 cm.$^{-1}$ reported by Krishnan and Chandrasekharan (1945, 1950) could not be definitely confirmed by us owing to the presence in that region of the wing accompanying the λ 2536·5 radiation.

Several of these lines appear close to the stronger Raman lines, *viz.*, 128, 206, 466, 795, 806 and 1063 cm.$^{-1}$ In particular, the line at 145 cm.$^{-1}$ appears with comparatively considerable strength close to the 128 cm.$^{-1}$ shift as can be seen from Plates XV and XVII and the microphotometer record in Plate XVI. The line at 509 cm.$^{-1}$ is quite clearly seen in Fig. 3 of Plate XVII

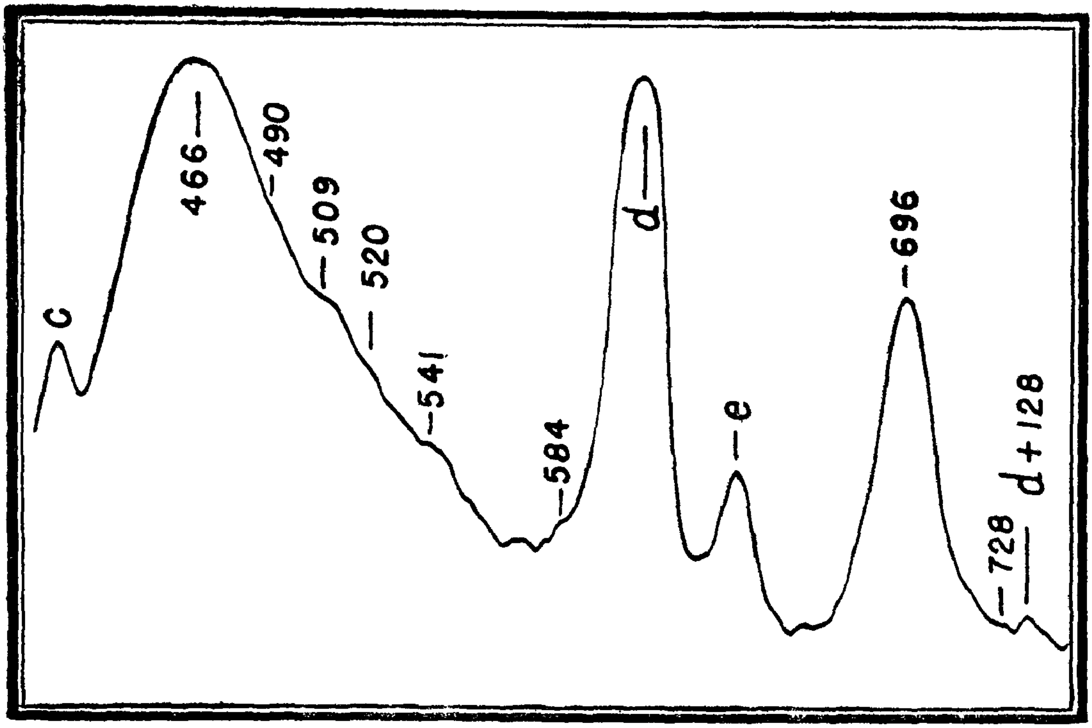

FIG. 3. Enlarged microphotometer record showing the 466 cm.$^{-1}$ Raman line and other subsidiary features.

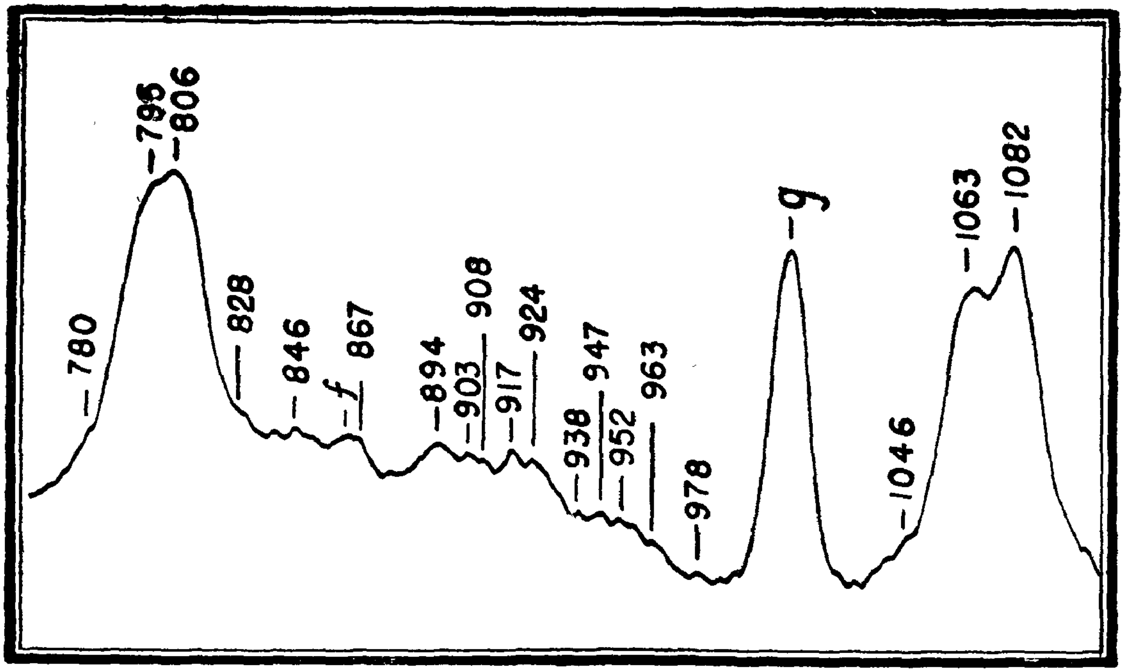

FIG. 4. Enlarged microphotometer record showing the numerous features in the region 50–1100 cm.$^{-1}$

adjacent to and on the long-wavelength side of the intense Raman shift 466 cm.$^{-1}$ The comparatively weaker lines at 780 and 1046 cm.$^{-1}$ close to the doublet 795–806 and 1063 cm.$^{-1}$ shift respectively, are indicated in the microphotometer record of Plate XVI. These and the remaining frequency shifts are clearly indicated in the enlarged microphotometer records appearing as Figs. 2, 3, 4 and 5 in the text and also in the microphotometer records of Plates XVI and XVIII.

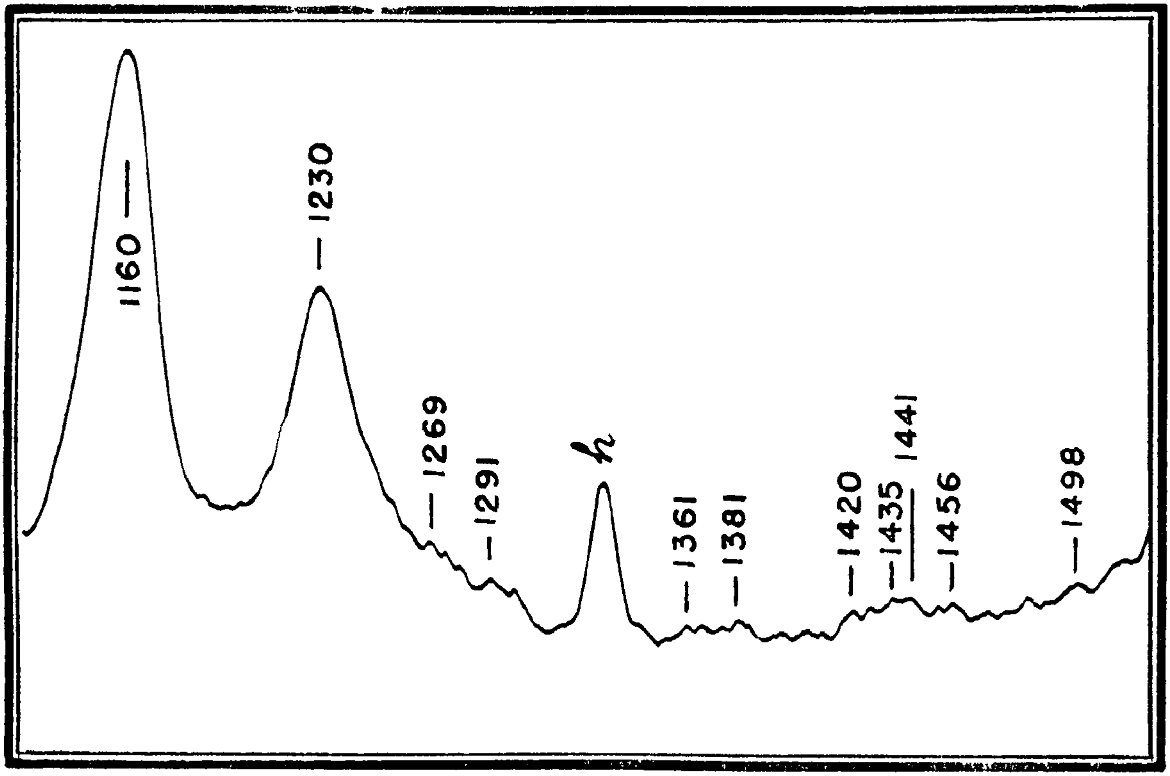

FIG. 5. Enlarged microphotometer record showing the several features observed in the range 1160–1500 cm.$^{-1}$

The lines reported by Krishnan at 1596 and 1630 cm.$^{-1}$ could not be confirmed since the anti-Stokes lines of shift 128 cm.$^{-1}$ excited by the triplet of mercury lines at λ 2652, λ 2653·7 and λ 2655·1, fall in this region. The frequency shifts at 2225 and 2240 cm.$^{-1}$ reported by Krishnan are believed to be respectively (1) the Stokes shift 466 cm.$^{-1}$ excited by λ 2655·1 of the triplet of mercury lines and (2) the anti-Stokes shift of 128 cm.$^{-1}$ excited by the mercury line λ 2698·9. The frequency shift reported by Krishnan at 2420 cm.$^{-1}$ could not be confirmed owing to the presence in the mercury arc exactly at this point a line of wavelength 2702·5 A.U.

6. ANALYSIS OF THE RAMAN SPECTRUM

It may be seen from Table I that the 27 degrees of freedom belonging to the three SiO_2 groups in the unit cell are distributed under the three classes of vibrations A, B and E. Excluding the three translatory movements of the unit cell there are four vibrations each under the classes A and B, and eight under the doubly degenerate class E. We shall proceed straightaway to identify the frequencies appearing under each class.

(1) *Totally symmetric class A*.—The four frequencies under this class which are active only in the Raman effect should always exhibit complete polarisation owing to the vanishing of the transverse components of the polarisability tensor. The early studies of Cabannes and Bouhet (1937) and Michalke (1938) showed that the lines 206, 356 and 466 cm.$^{-1}$ exhibit almost complete polarisation. In these early studies the lines 1063 cm.$^{-1}$ and 1082 cm.$^{-1}$, which are rather close, were unresolved. In addition, the line at 1082 cm.$^{-1}$ appears with very low intensity when the scattering is observed along the optic axis. By orientating the crystal so that the optic axis was perpendicular to the plane of scattering and using unpolarised light, Saksena (1940) found that for the 1082 cm.$^{-1}$ shift, the component parallel to the optic axis appeared strongly whereas the perpendicular component was absent. He also confirmed the findings of the earlier workers with regard to the polarisation of the lines 206, 356 and 466 cm.$^{-1}$

A new experimental method which made use of the optical activity of quartz to reveal the polarisation characters of the Raman lines was found by Chandrasekharan (1948). In this experiment, polarised exciting radiation was incident vertically along the optic axis of the crystal so orientated that its optic axis was parallel to the slit of the spectrograph. The scattered radiation was observed in a direction perpendicular to the optic axis. Due to the high optical rotatory power of quartz the vibration direction of the incident light vector would rotate and be parallel to the direction of observation at several points along the length of the optic axis, *i.e.*, after every 180° of rotation. The Raman lines that are completely polarised would have zero intensity at these points and hence would exhibit a characteristic banding along their length. The frequency shifts 206, 356, 466 cm.$^{-1}$ exhibit this feature. Owing to the vanishingly small intensity of the 1082 cm.$^{-1}$ shift in this orientation of the crystal, no observations could be made for this line by Chandrasekharan. Thus, it has been well established already that the four lines 206, 356, 466 and 1082 cm.$^{-1}$ belong to the totally symmetric class A.

(2) *The doubly degenerate class E*.—Contrary to the behaviour of the four frequencies under class A, the frequencies coming under the doubly

degenerate class E should appear depolarised in the Raman effect. In particular, when the incident electric vector is polarised parallel to the optic axis, the scattered light (of the E class frequency shifts) should have no component parallel to the optic axis since $\epsilon_{zz} = 0$. The detailed polarisation studies undertaken by Saksena (1940) revealed that the lines 128, 265, 394–404 (unresolved), 452, 696, 795–806 (unresolved), 1063, 1160 and 1230 cm.$^{-1}$ exhibit polarisation characters anticipated of lines coming under the doubly degenerate class. In particular, it may be mentioned that Saksena found that the weak line at 452 cm.$^{-1}$ is made much more evident by polarising the incident light or analysing the scattered light and thus diminishing the intensity of the adjacent 466 cm.$^{-1}$ shift. In agreement with the findings of Saksena, no characteristic banding was observed by Chandrasekharan (1948) in the case of the lines 128, 265, 394–404 (unresolved), 696, 795–806 (unresolved), 1063, 1160 and 1230 cm.$^{-1}$ (No banding should be exhibited by lines of the doubly degenerate class since the scattered intensity is the same irrespective of whether the incident light vector be parallel or perpendicular to the direction of observation).

We shall for the present consider in this analysis that the doublet 394–404 and 795–806 arise from single modes which have for some reason suffered a splitting. We identify the frequency shifts at 128, 265, 394–404, 452, 696, 795–806, 1063 and 1160 cm.$^{-1}$ as the eight fundamental vibrations coming under the doubly degenerate class. The polarisation characters of all the lines listed and their considerable intensity (except the 452 cm.$^{-1}$ shift) preclude any other explanation. The identification of the 452 cm.$^{-1}$ shift as a frequency coming under the class E finds additional support in the recent work of Reitzel (1955) on the infra-red reflection spectrum of quartz which reveals a very strong reflection maximum at 455 cm.$^{-1}$ in the ordinary ray. We shall presently consider the question of the explanation of the frequency shift at 1230 cm.$^{-1}$

These frequencies listed above under the degenerate class, being infra-red active in the ordinary ray, have been reported by different investigators. Simon and McMahon (1952) have, from a careful analysis of their data on the infra-red reflection of quartz, reported the frequencies 696, 795–802, 1065 and 1162, in close agreement with the observed Raman shifts. The frequencies 128 and 265 cm.$^{-1}$ were observed by Czerny (1929) and Barnes (1932) in the far infra-red transmission at 77 μ and 38 μ respectively. Liebisch and Rubens have reported a strong restrahlen band in the ordinary ray at 385 cm.$^{-1}$ in agreement with the value for the doublet at 394–404 cm.$^{-1}$

(3) *Anti-symmetric class B.*—According to theory (Table I), the four frequencies belonging to this class are forbidden in the Raman effect, but are infra-red active in the extraordinary ray. The important result of the present investigation is that these frequencies do appear in the Raman spectrum of quartz, though rather weakly. We identify the four frequencies at 145, 509, 780 and 1046 cm.$^{-1}$ listed in Section 5 as the B class frequencies. The basis for this identification as well as the reasons for the appearance of these forbidden frequencies we shall now discuss. Making use of the symmetry co-ordinates derived by him for the vibrations of the A and B classes Saksena (1945) tried to calculate the frequencies under these classes using four force constants respectively due to (1) the changes in the silicon-oxygen bond lengths and (2) changes in the oxygen-oxygen distances and (3), (4) the changes in the bond angles at the oxygen and silicon atoms respectively. These were so chosen as to give a reasonable agreement with the observed frequencies of the A class. The calculated values came out as 195, 310, 508 and 1087 while the observed values are 206, 356, 466 and 1082 cm.$^{-1}$, a not unsatisfactory agreement. Using the same force constants the four B class frequencies were evaluated and came out as 149, 489, 809 and 1160 cm.$^{-1}$

A characteristic feature of the spectrum of quartz is the appearance of the stronger lines of the spectrum in groups in certain frequency ranges. For example, in the low-frequency region, there appear one A class line at 206 cm.$^{-1}$ and two E class lines at 128 and 265 cm.$^{-1}$ We may therefore reasonably expect to find one B class frequency in this region. Saksena's calculated value of 149 cm.$^{-1}$ for the lowest frequency therefore appears reasonable. Hence, the identification of the shift 145 cm.$^{-1}$ appearing in the vicinity of the E class line 128 cm.$^{-1}$ as a B class fundamental is justifiable. Further support for this assignment is forthcoming from the observation by Czerny (1929), Barnes (1932) and Plyler and Acquista (1955) in the infra-red transmission of quartz an absorption at 75 μ with specimens cut parallel and perpendicular to the optic axis, which is in tolerable agreement with the frequencies 128 and 145 cm.$^{-1}$ assigned above for the E and B classes respectively. Some of the earlier investigators had chosen to regard a frequency at 364 cm.$^{-1}$ observed in the restrahlen (extraordinary ray) by Liebisch and Rubens, as the lowest frequency in the B class. This may, however, be explained as arising from a combination of the 145 cm.$^{-1}$ and 206 cm.$^{-1}$ shifts. Such a combination would have the polarisation characters of a B class frequency and would therefore appear in the extraordinary ray.

The 509 cm.$^{-1}$ shift is another well-defined feature in the Raman spectrum of quartz noticed even by the early investigators using the less powerful λ 4358 radiation for the excitation of the Raman effect. The observation by Liebisch and Rubens in the restrahlen extraordinary ray a very strong maximum at 508 cm.$^{-1}$ justifies the identification of this shift at 509 cm.$^{-1}$ as a B class frequency. The observations of Liebisch and Rubens are supported by the recent studies of Reitzel (1955) who reports a strong reflection maximum in the extraordinary ray between 500 and 540 cm.$^{-1}$

The identification of the weak Raman lines observed at 780 and 1046 cm.$^{-1}$ respectively as the fundamental frequencies of the B class is supported by the infra-red data. A strong reflection maximum at 777 cm.$^{-1}$ in the extraordinary ray was reported by Reinkober. Recently also, Simon and McMahon (1952) from a detailed analysis of their reflection data report characteristic frequencies at 780 cm.$^{-1}$ and 1055 cm.$^{-1}$ in the extraordinary ray the accuracy claimed being ± 10 cm.$^{-1}$

The appearance of the frequencies of the B class in violation of the selection rules, admits of two explanations: (1) They become active in the Raman effect by reason of their contiguity to strongly active Raman frequencies and the fact of their thereby gaining dynamic characters analogous to the active Raman frequencies. (2) The selection rules have been derived assuming that all the silicon atoms are of the same mass and hence form an absolutely symmetric trigonal structure. Actually, however, the abundances of the silicon atoms are such that the silicons of atomic weight 28 form a proportion of only 92·3% of the total number, the remaining being 4·7% of Si^{29} and 3·0% of Si^{30}. A random distribution of these silicons of atomic weight 29 and 30 would in reality mean a departure from the trigonal symmetry of the crystal and hence would result in a certain amount of Raman activity for the B class vibrations.

7. Combinations and Overtones

One of the principal features of the Raman spectrum of quartz that we have to explain is the 1230 cm.$^{-1}$ shift which exhibits the polarisation characters of an E class vibration. It is suggested that the frequency shift arises from the combination of the two fundamentals 780 and 452 cm.$^{-1}$ belonging respectively to the B and E classes. Such a combination would have the symmetry properties of the E class and hence would be Raman active, exhibiting the polarisation characters of that class. The intensity with which this combinational frequency shift is recorded is however rather surprising. The same frequency has been observed to be weakly active in the infra-red spectrum (Simon and McMahon, 1952).

The majority of the weak frequency shifts (referred to in Section 5) could be explained as combinations between the several fundamental frequencies. According to theory, all combinations, excepting those between the A and B class frequencies, are permitted to appear in the Raman effect. Also, all first overtones are active in the Raman effect. Table II shows the observed frequency shifts and their suggested origin.

TABLE II

Observed Frequency Shifts in cm.$^{-1}$	Their Suggested Origin	Calculated Values
490	128+356	484
520	128+394–404	522–532
541	145+394–404	539–549
584	128+452	580
728	265+466	731
828	128+696	824
846	394–404+452	846–856
867	394–404+466	860–870
894, 903 and 908	Overtones of 452 and its satellites and	
	394–404+509	903–913
917	452+466	918
924–938	128+795–806	923–934
	and overtones of 466 cm.$^{-1}$ and its satellites	932
947–952	145+795–806	940–951
963	265+696; 452+509	961
978	466+509	975
1230	452+780	1232
1269	206+1063	1269
1291	509+780; 206+1082; 128+1160	1289, 1288
1361	206+1160	1366
1381	?	
1420	265+1160	1425
1435–1441	356+1082	1438
1456	394–404+1063	1457–1467
1498	696+795–806	1491–1502
2129	2×1063	2126

It is rather surprising that the only overtone line observed is that at 2129 cm.$^{-1}$ being the overtone of the 1063 cm.$^{-1}$ shift. It is natural to expect that the intensely Raman active frequencies at 128, 206, 466 and 1160 cm.$^{-1}$ and also the intensely infra-red active frequencies at 452, 509 and 1046 cm.$^{-1}$ would manifest themselves as overtone shifts. But owing to various reasons most of them remain unobserved. The overtone of the 128 cm.$^{-1}$ shift would

fall too close to the Raman line at 265 cm.$^{-1}$ to be detected. Similarly, the overtone of the 206 cm.$^{-1}$ line would be too near the Raman doublet 394–404 to be observed.

The overtones of the frequency shifts at 466 and 452 cm.$^{-1}$ should, however, have been clearly observed but for the fact that this region of the spectrum exhibits numerous combinational shifts. The only relevant feature with regard to these overtones is the presence in the microphotometer records of the spectrum of bands of low intensity at 894, 903, 908 and 924–938 cm.$^{-1}$ The overtones of the Raman shifts 452 and 466 cm.$^{-1}$ and their satellites would appear at precisely this region. The overtone of the B frequency at 509 cm.$^{-1}$ escapes detection owing to the presence of the mercury line λ 2603·2 at about the point of its appearance. The appearance of the overtone of the frequency 1046 cm.$^{-1}$ could not be established owing to its falling in the region where the Raman shifts of 356 and 394–404 cm.$^{-1}$ excited by the triplet of mercury lines appear. The overtones of all other frequencies are presumably too weak to be observed.

In addition to the frequencies listed in Table II, there are others at 93, 171, 239 and 435 cm.$^{-1}$ and those reported by Krishnan and Chandrasekharan at 26 and 39 cm.$^{-1}$ These cannot reasonably be explained as combinational shifts. Their appearance in the vicinity of intensely active Raman lines (excepting those at 26 and 39 cm.$^{-1}$) suggests that they represent the modes of vibration of the super-cell and belong to the 21 *p* class. Though these modes are theoretically forbidden to appear, their close approximation in frequency to strongly active modes and (or), their possessing similar dynamical characters would result in their becoming weakly active in the Raman effect. It is also noteworthy that two bands at 82 and 95 cm.$^{-1}$ were observed by Barnes (1932) in the far infra-red transmission of quartz.

8. Some General Remarks

We shall consider in this section the probable explanation of some of the most striking features observed in the Raman spectrum of quartz.

The frequency shift 466 cm.$^{-1}$ is by far the most intense of all, though the frequency shift 206 cm.$^{-1}$ approximates to it closely: by reason of its diffuseness at ordinary temperatures, its intensity appears less than it would otherwise have been. Both of these frequency shifts belong to the totally symmetric class and hence their great intensity is *prima facie* not surprising. But why they should transcend so greatly in intensity the two other A class frequency shifts 356 and 1082 cm.$^{-1}$ is not so clear. It may be suggested that both of these modes (206 and 466 cm.$^{-1}$) involve large changes of the silicon-

oxygen bond-lengths, but that at the same time their frequencies are rather low by reason of the atomic movements being notably inclined to the directions of these bonds. It may be remarked in this connection that in β-quartz which is the high temperature form, only one vibration of the A class survives. From the observations of Narayanaswami (1948) it would appear that it is the 466 cm.$^{-1}$ shift of α-quartz which is carried over and appears at 453 cm.$^{-1}$ in β-quartz. The enormous broadening of the 206 cm.$^{-1}$ frequency shift with rise of temperature and its ultimate disappearance are clearly attributable to the progressive alteration in structure which precedes the transformation at 575° C.; the extreme diffuseness of the line may be attributed to the anharmonicity of the vibration concerned.

A noteworthy feature of the vibration spectrum of quartz which is emphasized by the present investigation is that all the four B class frequencies appear in close proximity to four out of the eight E class frequencies. It is also noteworthy that the infra-red activities of the vibrations of contiguous frequencies which appear in the extraordinary and ordinary ray are also quite comparable. It appears reasonable to suggest that this feature is in some way connected with the approximately tetrahedral configuration of the four oxygen atoms around the silicon atom to which they are linked.

Finally, mention should be made of the doublets 394–404 and 795–806 cm.$^{-1}$ both of which belong to the E class. Various explanations have been or could be suggested for this doubling and the special features exhibited by the components of the doublet in each case. Comments on these explanations are reserved till the author has had an opportunity of making a fuller examination of the subject.

The author's grateful thanks are due to Professor Sir C. V. Raman for his kind interest in this work.

9. SUMMARY

The Raman spectrum of α-quartz has been re-investigated with a view to obtain the complete spectrum and the results have been correlated with the recent infra-red data. In addition to fifteen principal frequency shifts, thrity-three other subsidiary features of low intensity are observed in heavily exposed spectrograms. These features are illustrated in the paper by microphotometer records on an enlarged scale.

The following Raman shifts are identified as the fundamental frequencies: (1) A class: 206, 356, 466 and 1082; (2) B class: 145, 509, 780 and 1046; (3) E class: 128, 265, 394–404, 452, 696, 795–806, 1063 and 1160 cm.$^{-1}$

CONNEMARA PUBLIC
4 JAN196
MADRAS

FIG. 1 FIG. 2 FIG. 3

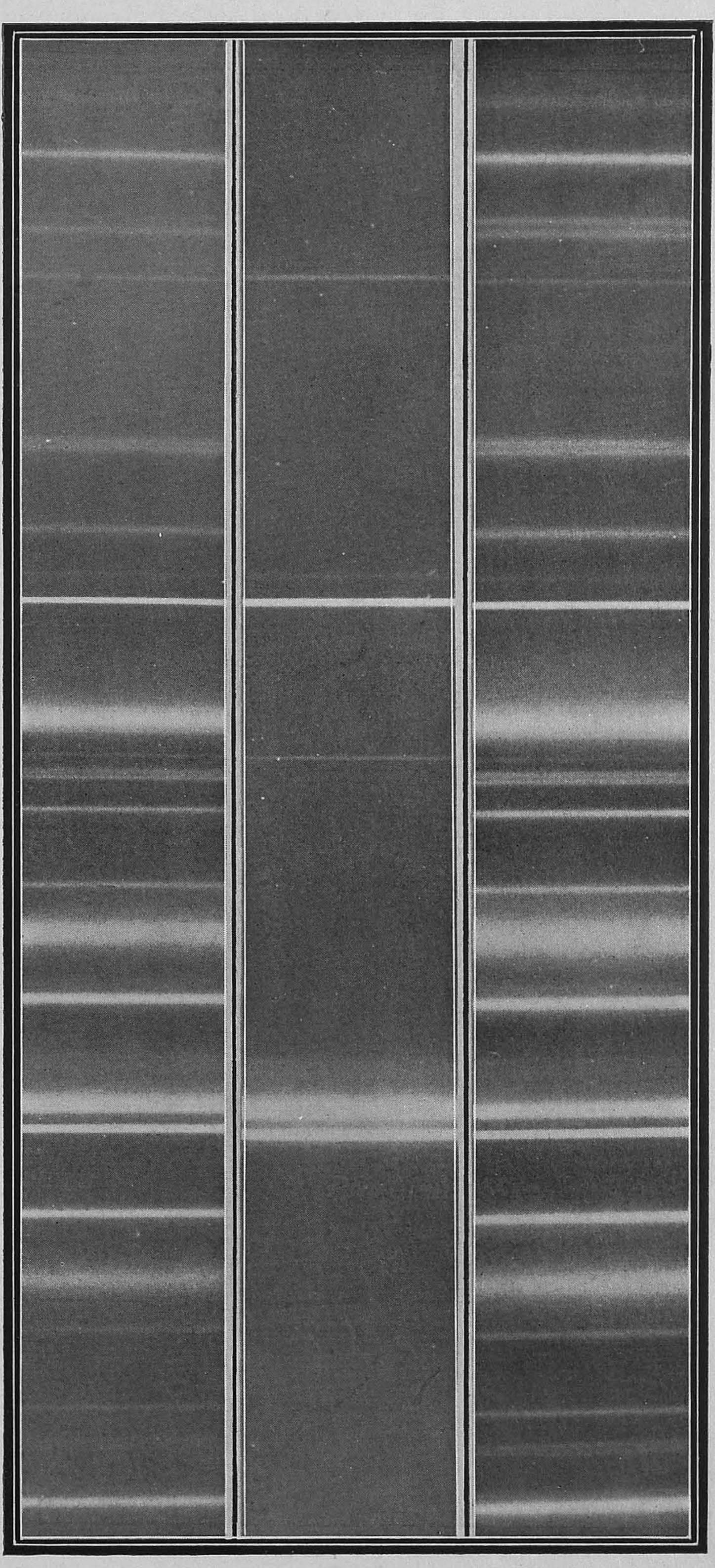

Figs. 1 and 3. The Raman spectrum of quartz recorded with Littrow spectrograph for two different orientations of the crystal.

Fig. 2. Spectrum of the mercury arc.

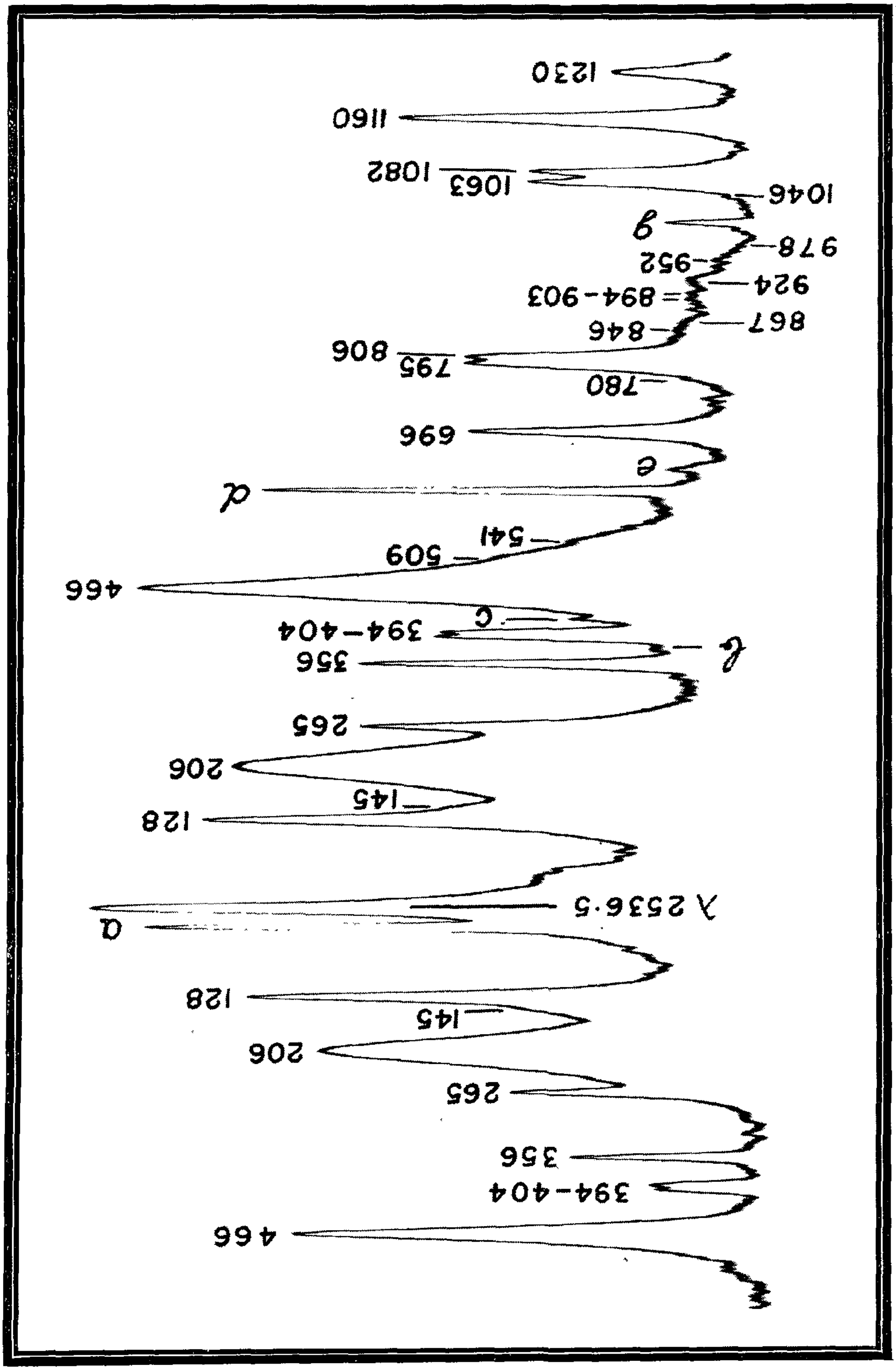

Microphotometer record of the Raman spectrum of quartz recorded with the Littrow spectrograph.

Note.—The numbers denote the Raman shifts in cm.$^{-1}$ while *a*, *b*, *c*, etc., refer to the mercury arc lines.

CONNEMARA PUBLIC
4 JAN1965
MADRAS

FIG. 1 FIG. 2 FIG. 3

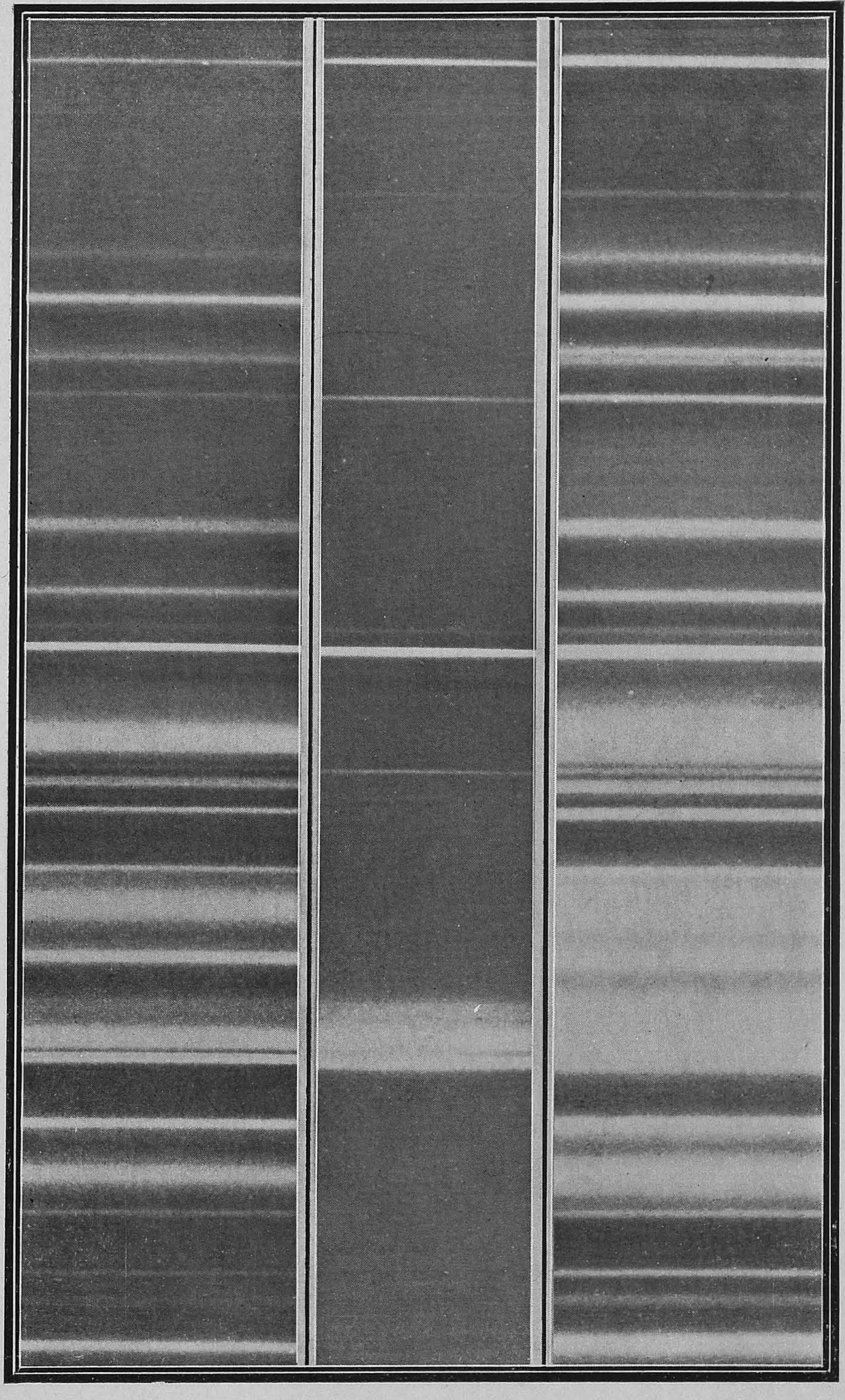

Figs. 1 and 3. The Raman spectrum of quartz recorded with the medium quartz spectrograph for two different orientations of the crystal. Fig. 2. Spectrum of the mercury arc.

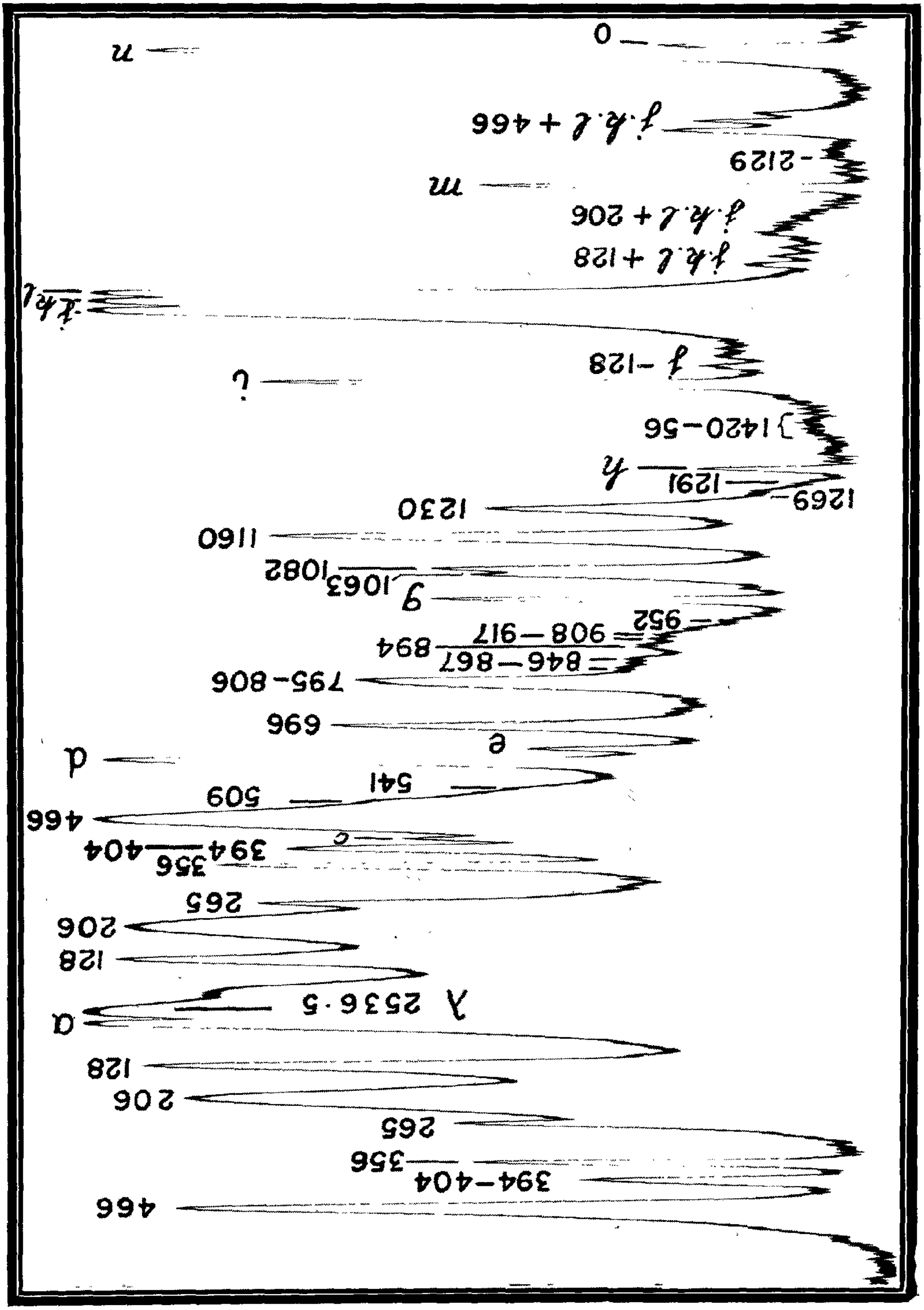

Microphotometer record of the Raman spectrum of quartz recorded with the medium quartz spectrograph.

It is noteworthy that all the four B class fundamentals appear weakly in the Raman effect in violation of the selection rules. The numerous subsidiary features are explained as permissible overtones and combinations of the above fundamental frequencies.

References

Barnes, B. .. *Phys. Rev.*, 1932, **39**, 562.

Cabannes and Bouhet .. *Compt. Rend.*, 1937, **205**, 768.

Chandrasekharan, V. .. *Proc. Ind. Acad. Sci.*, 1948, **28**, 409.

Czerny, M. .. Quoted by Schaefer and Matossi.

Krishnamurti, D. .. *Proc. Ind. Acad. Sci.*, 1957, **46**, 183.

Krishnan, R. S. .. *Ibid.*, 1945, **22**, 329.

Krishnan and Chandrasekharan *Ibid.*, 1950, **31**, 427.

Liebisch and Rubens .. Quoted by Schaefer and Matossi.

Mathieu, J. P. .. *Compt. Rend.*, 1952, **234**, 1961.

Michalke, H. .. *Zeit. f. Phys.*, 1938, **108**, 748.

Narayanaswamy, P. K. .. *Proc. Ind. Acad. Sci.*, 1948, **28**, 417.

Plyler and Acquista .. *J. Opt. Soc. Am.*, 1955, **45**, 900.

Reinkober, O. .. Quoted by Schæfer and Matossi.

Reitzel, J. .. *J. Chem. Phys.*, 1955, **23**, 2407.

Saksena, B D. .. *Proc. Ind. Acad. Sci.*, 1940, **12**, 93.

——— .. *Ibid.*, 1945, **22**, 379.

Schaefer and Matossi .. *Das Ultrarote Spektrum* (Verlag von Julius Springer, Berlin, 1930), pp. 315 *et seq.*

Simon and McMahon .. *J. Chem. Phys.*, 1953, **21**, 23.

Went, J. .. Doctorate Thesis, Utrecht, (1935).

Reprinted from "The Proceedings of the Indian Academy of Sciences", Vol. XLVII, No. 5, Sec. A, 1958

THE DIFFRACTION OF X-RAYS BY DIAMOND: PART I

BY SIR C. V. RAMAN

(*Memoir No.* 109 *of the Raman Research Institute, Bangalore*-6)

Received May 1, 1958

1. INTRODUCTION

BY reason of its remarkable physical properties, diamond stands out uniquely as the crystal which shows us the way to a correct understanding of the fundamental aspects of the physics of the solid state. The atomic vibrations in crystals, the theory of their specific heats and their spectroscopic behaviour may be mentioned in this connection. These topics formed the subject of recent memoirs published in these *Proceedings*, and the experimental results obtained with diamond figured very prominently in them. The present communication deals with the X-ray diffraction effects exhibited by diamond and considers them both from the theoretical and experimental standpoints. It emerges that diamond has a great deal to teach us regarding the fundamental aspects of the subject of X-ray crystallography and indeed compels us to approach the subject from new points of view.

The present investigation stems from a report from the author's laboratory published in the year 1940 under the title " A New X-Ray Effect " (*Current Science*, 1940, **9**, 165–67). That report recorded the discovery of the very striking and indeed surprising features which reveal themselves in strongly exposed X-ray diffraction patterns of diamond. It was very clear that the phenomena stood outside the framework of the classical theory of X-ray diffraction. It was accordingly suggested that they had their origin in the quantum-mechanical excitation of the atomic vibrations in diamond by the monochromatic X-ray beam traversing it, the X-rays being themselves reflected as a result of such excitation with a change of frequency. It was explained in the report why it was possible for reflections of this nature to be observed even when the setting of the crystal was different from that ordinarily required for a reflection of the X-rays by the same lattice planes.

The instrumental equipment available for the research at that time was, unfortunately, not of sufficient power to enable the subject to be explored with any degree of completeness. The investigation had accordingly to be laid aside and the circumstances in which the author found himself did not,

for many years, permit of its being resumed. Happily, however, it has now been possible to take up the work once again, not only with new and more powerful instrumental aid, but also with fresh theoretical ideas derived from the work of the author in the related fields referred to earlier in this introduction. The results are now laid before the reader.

Part I of the paper considers the theory of X-ray diffraction by crystals in general from a fundamentally new standpoint. Part II considers the application of the theory to the particular case of diamond. Part III presents the results of a detailed experimental investigation of the case.

2. THE STRUCTURE OF CRYSTALS

The conventional view of a crystal as an assembly of atoms arranged in a regular three-dimensional array in space is neither useful nor enlightening when we seek to obtain an insight into the behaviour of crystals when traversed by radiation in the different ranges of frequency. It is necessary indeed to lay aside that view and regard a crystal as a system composed of two kinds of charged particles, namely the nucleii and the electrons, their relative numbers being determined by the magnitudes of their charges. Diamond, for example, is an assembly of carbon nuclei and of electrons, the latter being six times as numerous as the former.

The atomic nuclei have enormously larger masses than the electrons and it is this circumstance that determines the manner in which the two sets of particles arrange themselves in space. According to the fundamental notions of the quantum theory, it is not meaningful to regard the electrons as located at any specifiable points in space, while on the other hand, it is permissible to do so in respect of the nuclei. The Coulomb forces exerted by the nuclei on the electrons tend to draw the latter together and hold them in dynamic equilibrium. Accordingly, what may be described as a cloud of negative charge gathers round each nucleus. But when we raise the question as to what determines the position of the nuclei in space, the answer, remarkably enough, is to be found in these very clouds of negative charge which each nucleus gathers around itself. Indeed, it is the electrons which determine the location and ordering in space of the nuclei. Accordingly, it would be appropriate to describe a crystal as consisting of two distinct assemblies, namely an assembly of nuclei whose positions it is possible to specify with some measure of precision, and an assembly of electrons. It is the interaction of these two assemblies with each other that determines the architecture of the crystal and its physical behaviour. This view of crystal structure will be found most illuminating when we proceed to consider the phenomena resulting from the passage of radiation through the crystal.

3. The Response of Crystals to Radiation

The tremendous disparity in the masses of the nuclei and of the electrons justifies us in ignoring any movement of the atomic nuclei which results directly from the action of the electric field of the radiation on the charges carried by the nuclei. What we need consider in every case is the effect of the radiation field on the electronic clouds. But since these are held in place by their interactions with the atomic nuceli, the latter would also tend to be disturbed when the electronic clouds are set in motion by the field. These considerations are valid irrespective of the individual features of the crystal structure and of the frequency or wavelength of the incident radiation. But since the response of the electrons to the field of the incident radiation would depend on these latter factors, the nature and extent of the movements of the atomic nuclei consequent thereon would also be influenced by those factors.

We may illustrate the foregoing remarks by considering first the cases in which the frequency of radiation lies in the infra-red range. Viewing the matter classically, the effect of the radiation on the electronic clouds in this case would be to produce periodic displacements to and fro of the electronic clouds with the same frequency. These displacements would, however, be limited by the binding of the electrons to the nuclei. Even when the frequency of the incident radiation coincides with a natural frequency of vibration of the atomic nuclei about their positions of equilibrium, it would not necessarily follow that such vibration is excited by the field. Indeed, it is well known that in many cases, the field does not excite the vibrations, in other words, the vibrations are not active in the absorption of the infra-red radiation. In order that any given mode of vibration should be excited by the incident radiation field and thereby rendered infra-red active, it is necessary that a certain lack of symmetry in the structure of the crystal or of the particular mode of vibration results in the movements of the nuclei being accompanied by a periodic displacement to and fro of the electronic clouds which hold the nuclei together. The selection rules which define the conditions under which any particular mode of vibration is active in the absorption of infra-red radiation are, indeed, based on considerations of this nature. That they are in agreement with experience demonstrates the validity of the present approach to the subject.

Coming now to the case of visible light, the response of the crystal to the field of the incident radiation would be determined by the relation between the frequencies of the incident radiation and the characteristic frequencies of vibration of the electronic clouds. Further, since the frequency of the radiation

is much higher than the natural frequencies of vibration of the nuclei' the possibility of the incident radiation exciting the latter in the manner considered in the preceding paragraph would not arise at all. There are however possibilities of the nuclear vibrations being excited by the electronic movements in a different way. Considering those electrons which hold together the different nuclei and thus form part of the architecture of the crystal, it is evident that any approach or recession of such nuclei from each other would influence the characteristic frequencies of the electronic clouds attached to them. This is equivalent to stating that the response of the electronic clouds to the field of the incident light would be modified or modulated by the natural frequencies of the nuclear vibrations. That such an effect actually arises is demonstrated by the fact that when monochromatic light traverses a crystal, and the light diffused in its interior is spectroscopically examined, monochromatic radiations are observed in it whose frequencies differ from that of incident light by amounts equal to the characteristic infra-red vibration frequencies. Whether or not any particular mode of vibration of the nuclei thus reveals itself is determined by the circumstances of the case. The selection rules which express these circumstances are naturally different from those that determine the activity in infra-red absorption.

The frequency of X-radiation is very much higher than that of either visible light or of infra-red waves, and the phenomena arising from their passage through crystals would naturally be determined by the high frequencies and correspondingly short wavelengths of the rays. We have, in the first instance, to consider the effect of the radiation field on the electronic clouds. But it is not possible to ignore the fact that the electronic clouds are held in their places by the atomic nuclei and that, consequently, not only the electronic clouds but also the atomic nuclei would tend to be disturbed by the X-radiation. There is every reason therefore to expect that the effects arising from such disturbance of the nuclei would manifest themselves in the X-ray diffraction patterns of the crystal.

The foregoing represents the general point of view which will be developed and discussed in greater detail in the present series of papers. Its consequences will also be compared with the facts of observation. We shall find that it receives the clearest possible support in the phenomena exhibited by diamond in its X-ray diffraction patterns.

4. X-Rays and Crystals

The observational basis of X-ray crystallography is the selective reflection of X-rays by the atomic layers in a crystal at angles of incidence determined by the wavelength of X-rays and the spacing of the layers. The phe

nomenon is clearly analogous to the familiar effect of iridescence exhibited by regularly stratified media on which visible light is incident. Hence it is quite natural to explain the phenomena of X-ray diffraction by crystals on similar lines. We assume the crystal to be a material of which the optical polarisability for X-ray frequencies exhibits space-periodic variations in three dimensions. A determination of the settings of the crystal at which the X-ray reflections for a known wavelength are observed enables us to determine the spacings of the stratifications in various directions as also their relative orientations. A comparative study of the intensities of the various reflections enables us to go further and obtain a measure of the magnitude of the periodic variations of the polarisability for X-ray frequencies appearing in each set of stratifications. The entire procedure is phenomenological in character. In endeavouring to deduce from the experimental results a picture of the ultimate structure of the crystal, various difficulties arise which we shall not discuss here. What we are actually concerned with is the meaning of the phrase " Polarisability for X-Ray Frequencies " employed above in terms of the ultimate structure of the crystal.

In classical optics, where we are concerned with the behaviour of media which can be regarded as continuous, the term polarisability has a simple and definable meaning, namely, the strength of the electric dipole per unit of volume induced by an external electric field of unit strength. Difficulties arise when we endeavour to take over this description into the region of high frequencies and short wavelengths. These difficulties are of two kinds. Firstly, the medium can no longer be regarded as a continuous and structureless substance, since it actually consists of a set of discrete particles arranged in layers. The second difficulty is that these particles are not all similar and similarly circumstanced. In particular, the nuclei and the electrons have very different masses and are oppositely charged; the interactions between them enter fundamentally into the problem of determining the response of the medium to the field of the incident radiation.

A way of escape from the difficulties indicated above may be sought for by regarding the recognisable units in the structure as " diffracting particles " in the sense of classical optics. We find however that such a procedure is not sustainable. For example, the individual electrons in the crystal cannot be assigned the role of " diffracting units". For, as already remarked, an electron does not possess any precisely definable location in space and hence the phase of any radiation that it could diffract would be indeterminate. An even more fundamental difficulty is that if an individual electron does interact with X-rays, the result is a secondary radiation of

altered wavelength, in other words the Compton type of scattering. The alternative approach of regarding the individual *atoms* in the crystal as the 'diffracting units' is also not sustainable. For, in any actual crystal, the atoms are held in their places by the electrons which link them together and these electrons cannot therefore be regarded as the exclusive possession of any particular atom. Taking for instance the case of diamond, only two out of every six electrons can with any measure of justification be considered as attached to an individual carbon nucleus. The remaining four electrons enter into the architecture of the crystal and hence must be considered as held in common with other atoms.

In view of the situation stated above, it is clear that the only logically sustainable approach to the subject of X-ray diffraction is that which proceeds on the following basis: *the X-ray reflections by a crystal are a co-operative effort of the entire structure, meaning thereby all the nuclei and all the electrons included in it.*

5. THE ENERGY LEVELS OF CRYSTALS

The present approach to X-ray diffraction problems differs from that customarily adopted in two respects. In the first place we recognize that the atomic nuclei have a part to play in the phenomena since on the one hand, they hold the electrons in place and on the other hand are themselves held in place by the electrons. Further, what we shall actually concern ourselves with is not the behaviour of the individual electrons or of the individual atoms in the crystal, but the behaviour of the two assemblies consisting of nuclei and of electrons respectively constituting the crystal when it is traversed by the X-radiation. This approach brings the phenomena of X-ray diffraction into the closest relationship with the behaviour of crystals when traversed by ultra-violet, visible or infra-red radiation. In all such cases we are concerned with the changes in the energy levels of a crystal which are or could be induced by the radiations traversing it. As we have two sets of particles which differ greatly in their masses, the possible changes in the energy levels are of two kinds which in the usual language of spectroscopy may be described as changes in the electronic levels and the vibrational levels respectively. The simplest cases are those in which there is no change in either the electronic or vibrational energy states of the crystal when traversed by radiation. This would correspond to a simple undisturbed transmission of the radiation through the crystal in the case of visible or ultra-violet light. In the case of X-radiation, however, the stratifications of optical polarisability in the structure of the crystal can in appropriate circumstances result in geometric reflections of X-rays in various directions. In the language of the

quantum theory, such reflections would be described as the result of an exchange of momentum without an exchange of energy between the radiation and the crystal. Still another possibility has to be recognised, namely, that while the initial and final *electronic* energy states are the same, the radiation induces a change in the *vibrational* energy level which persists. When and in what circumstances such a process can occur as the result of the passage of X-radiation, and what would be the observable results of such a process are the questions which we shall proceed to consider.

The answers to the questions raised above emerge when we consider the effects observed respectively when a crystal is traversed by radiation in the infra-red and in the visible regions of the spectrum. In the former case we are concerned with an actual absorption of the radiation. In the latter case we have a simple transmission accompanied by a diffusion or scattering with shifts of frequency indicating that changes in the vibrational energy levels have been induced by the incident light. It should not be imagined that each and every characteristic mode of vibration can manifest itself in the infra-red absorption spectrum and in the scattering of light as a frequency shift. This is very far indeed from being the case. Whether a particular mode of vibration does or does not so manifest itself is determined by certain selection rules which are different for infra-red absorption and for light-scattering. Why this is so becomes clear when the mechanisms respectively of infra-red absorption and of the scattering of light with change of frequency are examined. The latter effect is explained as arising from the variations of the optical polarisability of the crystal for visible light which accompany changes in its infra-red energy levels. On the other hand, infra-red absorption arises from the displacements of electric charge produced by the incident radiation. The question arises whether effects of the same nature can be induced by X-radiation. It is obvious that any change in the optical polarisability for X-rays produced by the changes in the infra-red energy levels of the crystal would, in view of the very high frequencies of X-radiation, be entirely negligible. On the other hand, the periodic displacements of electric charge associated with vibrational transitions which are active as absorbers of infra-red radiation necessarily involve periodic displacements of the stratifications of optical polarisability which give us the X-ray reflections by the crystal. *It follows that when X-radiations traverse a crystal, they can induce changes in its vibrational energy levels, provided such changes involve displacements of electric charge—in other words, provided that the modes of vibration under reference are active as absorbers of infra-red radiation.*

6. X-RAY REFLECTION WITH CHANGE OF FREQUENCY

We have now to consider what would be the consequences of a change in the vibrational energy levels of crystals induced by X-rays in the circumstances stated above. The question arises whether the observable result of such a process would be a diffusion of the X-rays in various directions or else a reflection similar to that ordinarily observed involving no exchange of erengy. Before this can be answered, we have to ask ourselves: What is the nature of the vibration spectrum of a crystal? This question has already been dealt with by the author in various recent publications and the same ground need not therefore be traversed here once again. As has been shown in the publications referred to, theory and experiment alike indicate that the vibration spectrum of a crystal containing p atomic nuclei in each unit cell consists of a set of $(24p - 3)$ monochromatic frequencies, accompanied by a residue representing the three omitted degrees of freedom which constitutes a continuous spectrum of low frequencies. Amongst the $(24p - 3)$ modes, in $(3p - 3)$ modes which are the only ones with which we are concerned in the present paper, the vibration repeats itself with identical frequency and amplitudes and phases in the successive cells of the crystal structure. It follows from this that the changes in the corresponding vibrational levels induced by the incident X-radiation would extend over the entire volume of the crystal traversed by the incident X-ray beam. As a consequence of this again, the X-rays would be regularly reflected by the stratifications of the crystal; such reflection involves a transfer of energy between the radiation and the crystal equal to the vibrational frequency multiplied by Planck's constant. *Hence, the frequency of the reflected X-rays would differ from that of the incident X-ray beam by the frequency of the vibrational mode excited.* As has been explained in the preceding section, such a process is only possible in respect of the modes of vibration which are active in the absorption of infra-red radiation.

The result stated above has a classical analogue in the reflection of light by a stratified medium which is assumed to execute oscillations of small amplitude normal to its layers. (An oscillation parallel to the layers would obviously be without effect.) It can readily be shown that, the reflected wave of the original frequency A sin $2\pi\nu t$ would be accompanied by *two* additional components which are respectively of diminished and increased frequency, *viz.*,

$$\pi . A . d^*/d . \sin 2\pi(\nu - \nu^*) t$$

and

$$\pi.A.d^*/d.\sin 2\pi (\nu + \nu^*) t$$

d and d^* are respectively the spacing of the stratifications and the amplitude of their oscillation, while ν and ν^* are respectively the frequencies of the incident radiation and of the oscillation of the stratifications. The equality of amplitude of the reflected waves of enhanced and diminished frequency is a natural consequence of our assuming the oscillations of the layers to subsist of themselves. In the quantum theory, on the other hand, the oscillations are *induced* by the incident radiation, and hence the two components would, in general, be of very different intensities; their ratio is determined by thermodynamic considerations and is expressible in terms of the Boltzmann factor $e^{-h\nu^*/kT}$.

The classical analogy referred to above leads to some general inferences regarding the intensity of the X-ray reflections with altered frequency in relation to the intensity of the X-ray reflections of unmodified frequency given by the same set of lattice planes. We notice in the first place that the two are proportional to each other. Hence, if one is absent, the other would also be absent. In other words, the so-called missing reflections familiar to the X-ray crystallographer would also fail to manifest themselves as dynamic reflections. Further, we could normally expect to observe the latter only as accompaniments of the stronger reflections of the ordinary kind. Their relative intensity is determined by the square of the ratio d^*/d, where d^* is the amplitude of oscillation of the stratifications and d is their spacing. Since d^* is a measure of the displacement of electric charge which is responsible for the activity of the mode in the absorption of infra-red radiation, it follows, firstly, that inactive modes would not give rise to dynamic X-ray reflections, and secondly, that the greater the infra-red activity of a mode, the more intense would be the dynamic X-ray reflections associated with it.

7. The Phase-Waves of Dynamic Reflection

The possibility of X-radiation exciting one of the $(3p - 3)$ characteristic modes of nuclear vibration and being itself reflected in the process was deduced above on the assumption that the wavelength of the X-rays, the spacing of the stratifications, and the angle of incidence on them are related to each other in the same manner as that necessary for a reflection of the ordinary kind. In these circumstances, the excited vibration necessarily repeats itself with the same frequency and also with the same amplitudes and phases in every cell of the structure traversed by the X-rays.

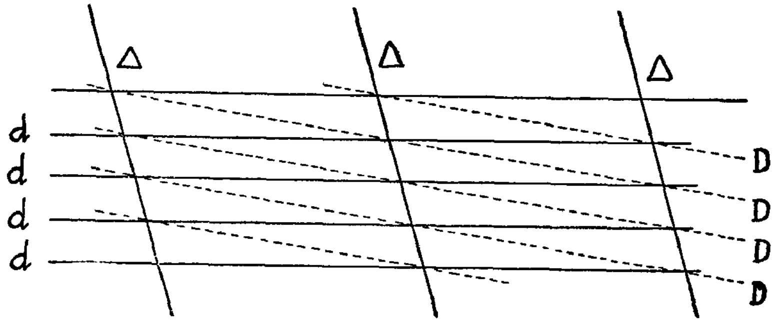

FIG. 1

For X-ray reflections with a change of frequency to be observable at other settings of the crystal, it is necessary that the vibrations excited are everywhere similar, but that the phase of the excited vibration in the individual cells of the structure alters progressively through the crystal in such a manner that the vibrations excited in all the irradiated cells conspire to give a coherent reflection. The condition for this to be possible is most readily stated in the form of a diagram (Fig. 1 in the text). The lines marked *d d d* represent the traces on the plane of the paper of the stratifications in the crystal. The planes marked Δ Δ Δ similarly represent the traces on the plane of the paper of the *phase-waves*, in other words of the planes along which the internal vibrations of the crystal have identical phases. It is evident from the figure that the planes marked D D D cutting across both of them would represent the stratifications which play the same role for the dynamic reflections that *d d d* play for the static ones. The relationship between the spacings D, *d* and Δ is given by the vectorial formula

$$\frac{\vec{1}}{\mathrm{D}} = \frac{\vec{1}}{d} + \frac{\vec{1}}{\Delta} \tag{1}$$

It needs to be explained why the situation indicated in Fig. 1 can arise consistently with the principles of dynamics and of the quantum theory. A vibration in which the frequency as well as the amplitudes and the phases are the same in every cell of the crystal structure is the only possible vibration having the characters of a normal mode. Since, however, the interatomic forces in crystals are essentially short-range forces, it is permissible to regard a crystal as made up of a great number of quasi-independent oscillators which have common modes and frequencies of vibration. Indeed, this is the approach which has necessarily to be adopted in developing the theory of the specific heats of crystals. It leaves out of account the small uncertainties in the frequency of vibration incidental to a limitation in size of the individual oscillators. In our present problem, therefore, it is permissible to consider

modes of internal vibration which are the same everywhere in the crystal but in which the phase of vibration in the individual cells alters progressively as we move through the crystal. If $\triangle$ is large enough compared with *d*, the vibration would be practically indistinguishable from the limiting case in which $\triangle$ is infinite. But as $\triangle$ is diminished, what we have in the crystal is not a normal mode but a *forced* oscillation of which the frequency is different, the more so, the smaller $\triangle$ is. In other words, a dynamic reflection in these circumstances results from a forced oscillation excited by the X-rays with a frequency differing slightly from that of the free oscillations of the structure. Hence, using the language of the quantum theory, we may infer that the probability of such an event happening would diminish rapidly as $\triangle$ becomes smaller. In consequence, we would find that the dynamic reflection has the maximum intensity when the setting of the crystal is that at which the ordinary reflections also appear; the intensity would fall off rapidly as the crystal is moved away from that setting in either direction.

8. The Geometric Law of Dynamic Reflection

The construction shown in Fig. 1 enables us to deduce some general results regarding the geometric behaviour of the dynamic reflections. If the phase wavelength $\triangle$ is infinite, the dynamic stratifications D D D would coincide with the static layers *d d d*. Hence, if the X-rays are incident on the latter at the correct angle for a regular reflection of the ordinary kind, the dynamic reflection would also appear in the same direction superposed on it. In the general case, the direction in which the reflection would appear would be determined by the orientation and the magnitude of the phase-vector. If both of these quantities can vary arbitrarily, then nothing in the nature of a regular reflection would be possible. If, however, the orientation of the phase-vector is precisely defined, a monochromatic X-ray beam incident at a precisely defined angle on the lattice planes of a crystal can result in a dynamic reflection also appearing in a precisely defined direction; but unlike the static reflection in similar circumstances, it would be observable over a wide range of settings of the crystal. The plane of reflection would naturally be the plane of incidence of the X-rays on the dynamic stratifications and the angles of incidence and of reflection with respect to them would also be equal.

Figure 2 exhibits the geometric laws of dynamic reflection of X-rays in a readily comprehensible fashion. The directions of the vectors $\overrightarrow{1/d}$, $\overrightarrow{1/D}$, $\overrightarrow{1/\triangle}$ are represented by points on the surface of a sphere, the X-ray beam

being assumed to traverse the crystal along the polar axis of the sphere. Three meridional circles have been drawn on the sphere passing respectively through those three points. The first circle is evidently the plane of incidence

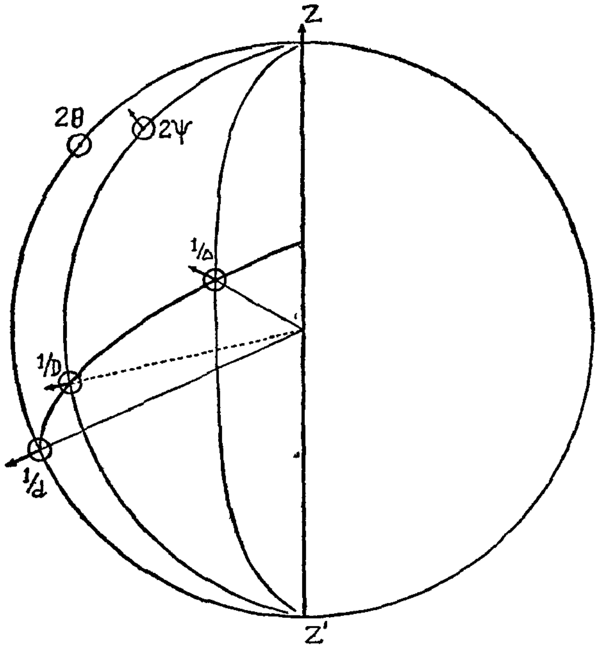

FIG. 2

of the X-rays on the lattice layers whose spacing is d. The second is the plane of incidence of the X-rays on the dynamic stratifications. The third circle is the plane containing the incident X-rays and the normal to the phase-waves. From equation (1) connecting the three vectors $\vec{1/d}$, $\vec{1/D}$ and $\vec{1/\Delta}$, it follows that the point representing $\vec{1/D}$ on our sphere would lie on a great circle drawn through $\vec{1/d}$ and $\vec{1/\Delta}$, its actual position on that circle being determined by the relative values of d and Δ. If θ be the glancing angle of incidence of the X-rays on the lattice layers of the crystal, a reflection would appear in a direction making an angle 2θ with the polar axis of the sphere on the first meridional circle, provided the condition $2d \sin \theta = \lambda$ is satisfied. This would correspond to the case in which the phase wavelength Δ is infinite. In the actual case to which the figure refers, the dynamic reflection would appear in a direction making an angle 2ψ with the polar axis of the sphere, ψ being the glancing angle of the incident X-rays on the dynamic stratifications. It is here assumed that the condition $2\,D \sin \psi = \lambda$ is satisfied. The figure indicates that the dynamic reflection deviates from the direction in which it would appear for an infinite phase wavelength, both along

the meridional circle and transverse to it, to extents determined by the angle between the first and the third meridional circles as also by the angle of incidence of the X-rays on the lattice planes under consideration.

9. Summary

The theory of X-ray diffraction in crystals is discussed and it is shown that the X-ray reflections must be regarded as a co-operative effort of the entire structure in which the nuclei as well as the electrons play their respective roles. It is further shown that the passage of X-rays through a crystal and their reflection by the stratifications of electron density can simultaneously result in vibrational energy transitions, provided that the modes of vibration thus excited involve displacements of electric charge and are therefore active as absorbers of infra-red radiation. Vibrational modes of this kind when excited result in periodic displacements of the stratifications of electron density. Consequently, reflections appear whose frequencies are less (or greater, as the case may be) than the frequency of the incident X-radiation. It is explained why it is possible for such reflections to appear even when the setting of the crystal is different from that required for the usual or unmodified reflections. The geometry of the X-ray reflections which then appear in displaced positions is also discussed.

Reprinted from "The Proceedings of the Indian Academy of Sciences", Vol. XLVII, No. 6, Sec. A, 1958

THE DIFFRACTION OF X-RAYS BY DIAMOND: PART II

BY SIR C. V. RAMAN

(*Memoir No.* 109 *of the Raman Research Institute, Bangalore*-6)

Received May 5, 1958

1. INTRODUCTION

FOR various reasons, diamond is the ideal case for a consideration of the consequences following from the ideas set out in Part I of this series of papers regarding the diffraction of X-rays by crystals. Since diamond is a cubic crystal of relatively simple structure, it is possible to determine and describe in purely geometrical terms the modes of vibration of which that structure is capable and with which we are concerned. It can also be shown that these modes have a high frequency, from which again it follows that they would not be thermally excited to any appreciable extent at ordinary temperatures. For the same reason also, it is permissible to ignore the disturbing effects on the phenomena with which we are concerned, of the thermal agitation in the crystal. It accordingly becomes possible to present a very clear picture of the effects which may be expected to present themselves to observation in strongly exposed X-ray diffraction patterns of diamond, on the basis of the theory developed in Part I.

2. THE STRUCTURE OF DIAMOND

Diamond exhibits in its structure a complete justification of Van't Hoff's hypothesis of the tetrahedral carbon atom. That hypothesis was originally put forward on the basis of the known chemical behaviour of carbon. It implies that the four valences which carbon exhibits in its compounds are tetrahedrally disposed in space and are indistinguishable from each other. Why this is so is one of the fundamental problems of theoretical chemistry. According to the spectroscopist's view of atomic structure, the nucleus of the carbon atom is surrounded by six electrons, two of which are in the inner or K-shell and the other four in the outer or L-shell. The latter four electrons again are assigned to two sub-groups, each containing two electrons. In the first sub-group, the electrons are assumed to be in the $2s$ state, while the two electrons in the other sub-group are in the $2p$ state. This situation of the four outer electrons is not in agreement with that indicated by the facts

of chemistry and hence it becomes necessary to modify the description of their states to bring it into line with the known chemical behaviour of carbon. All the four electrons have indeed to be considered as being in states indistinguishable from each other and so orientated that the resulting structure has perfect tetrahedral symmetry. Such a concept is necessary also to fit the picture of the carbon atom into the known facts concerning the structure of diamond. Having only two atoms in each unit cell, diamond nevertheless exhibits cubic symmetry. This situation requires that the nuclei of the carbon atoms occupy certain special positions in the crystal structure, namely, the points at which the four trigonal axes of cubic symmetry intersect each other.

The theory of hybridised orbitals is one of the best known attempts in the direction of describing the electronic state of the carbon atom in such manner as to bring it into line with the hypothesis of Van't Hoff. As full accounts of that theory are to be found in several recent treatises, it is not necessary here to expound it in detail. It is sufficient to mention that the states of the four electrons are assumed in that theory to be representable as a superposition of four hydrogen-like wave-functions which are so chosen that all the four electrons appear in similar states differing only in their orientations, which again exhibit tetrahedral symmetry. In the wave-functions assumed for the purpose, the $2p$ states preponderate, and hence each of the four electrons is implicitly assumed to possess an orbital angular momentum about an axis which coincides in direction with its directed valence. We may remark that for the shell of valence electrons thus constituted to possess true tetrahedral symmetry, it is necessary that the orbital movements of the four electrons about their respective axes should be described in the same sense, that is to say, either all of them in a right-handed sense, or else all of them in a left-handed sense. We are thus led to recognize that there are two possible descriptions of the carbon atom, namely, a dextro-carbon atom and a lævo-carbon atom, which correspond respectively to the two possible senses of the orbital angular momentum of the electrons about the tetrahedral valence directions.

The considerations set forth above have important consequences in relation to the structure and physical properties of diamond. That crystal is usually described as made up of two non-equivalent sets of carbon atoms each located at the points of a face-centred cubic lattice; the two lattices interpenetrate each other in such manner that every carbon atom in one lattice is tetrahedrally surrounded by four others belonging to the other lattice. Accepting this description, it follows that in a truly homogeneous crystal of

diamond, only one out of four possible situations can exist: (i) both lattices are occupied by dextro-carbon atoms, (ii) both lattices are occupied by lævo-carbon atoms, (iii) one lattice is occupied by dextro-carbon atoms and other by lævo-carbon atoms, or (iv) the first lattice is occupied by lævo- and the second by dextro-carbon atoms. It is entirely possible that two or three or all four of these possible structures may exist simultaneously in different parts of the same crystal. It is sufficient, however, to consider here only the case of truly homogeneous diamonds the structure of which is exclusively one or another of the four categories set out above.

3. The Vibration Spectrum of Diamond

The vibration spectrum of a crystal containing p atomic nuclei in each unit cell consists of $(24p - 3)$ distinct modes with monochromatic frequencies, supplemented by a continuous spectrum which is the residue representing the three omitted degrees of translatory freedom of motion. Since the unit cell of diamond contains 2 atomic nuclei only, we have 45 possible modes of vibration with monochromatic frequencies. The description of these modes and the evaluation of their frequencies have been very fully set out in an earlier memoir published in these *Proceedings*. In two other memoirs again, it has been shown that the heat capacity of diamond over the entire range of temperatures may be quantitatively evaluated in terms of these frequencies. It is therefore unnecessary to traverse the same field again, and indeed in the present paper we are only concerned with the three modes of vibration of highest frequency which may be described as an oscillation of the two lattices of carbon atoms with respect to each other along one or another of the three cubic axes. The free vibrations of the structure in all these three modes have the same frequency, and this is known exactly from spectroscopic studies on the diffusion of monochromatic light in diamond. A sharply defined line with a frequency shift of 1332 $cm.^{-1}$ is recorded in the spectrum of the scattered light, and this frequency is associated with a vibration of the kind described above.

Whether the mode of vibration referred to above would be excited by the passage of X-rays through the crystal depends, as we have seen in Part I, on whether this mode is or is not active in the absorption of infra-red radiation. The circumstances which determine whether a specified mode of vibration in a crystal is active or not in the absorption of infra-red radiation have been considered by various authors and will be found discussed in detail in several recent treatises. It is a well-established rule deduced from theory and confirmed experimentally that if a structure possesses centres of symmetry,

any mode of vibration which manifests itself as a frequency shift in light scattering would be *inactive* in the absorption of infra-red radiation. In the first two sub-species of diamond referred to above, both sets of carbon atoms are dextro-carbon atoms or both lævo-carbon atoms respectively. It is clear that every point midway between a pair of atoms belonging respectively to the two lattices would in these cases be a centre of symmetry. Accordingly, in these two sub-species of diamond, since the mode of vibration with the frequency 1332 cm.$^{-1}$ manifests itself as a frequency in light-scattering, that mode would be *inactive* in infra-red absorption. *Per contra*, in the two other sub-species of diamond where the carbon atoms located at the points of the two lattices are of different species, the points midway between two carbon atoms are *not* centres of symmetry. Hence the rule of mutual exclusion stated above is not applicable in their cases and hence the modes of vibration would be active *both* in the scattering of light and in the absorption of infra-red radiation. In what follows, we shall refer to the first two sub-species of diamond as the Oh I and Oh II types of diamond respectively, and the two other sub-species as Td I and Td II respectively. The use of these symbols has a special significance, *viz.*, that the electronic structure of the first two species of diamond has the full or octahedral symmetry of the cubic cystem, whereas the electronic structure of the two other species has only the lower or tetrahedral symmetry.

We may conclude this section by a categorical statement of the results indicated by the theory. *In diamonds which belong to the two sub-species Oh I and Oh II, the fundamental vibration of the structure with frequency of* 1332 *cm.*$^{-1}$ *would not be active in infra-red absorption and hence the passage of X-rays through the crystal would not excite that vibration and hence would not result in a dynamic reflection.* Per contra, *in diamonds which belong to the two other sub-species Td I and Td II, the said vibration would be active in the absorption of infra-red radiation and hence the passage of X-rays through the crystal would excite those vibrations and give rise to dynamic reflections by the lattice planes in the crystal.*

4. THE PHASE WAVES OF DYNAMIC REFLECTION

We shall proceed to consider the nature of the dynamic reflections which may be expected to manifest themselves in the case of diamonds possessing only the lower or tetrahedral symmetry of electronic structure as the result of the excitation of the infra-red active vibration. As already stated, this vibration is an oscillation of the interpenetrating lattices of carbon atoms (in these cases dissimilar to each other) along one or another of the three cubic axes of the crystal. The atoms belonging to the two lattices appear in distinct but

equidistant layers parallel to the cubic planes. The infra-red activity of the vibration arises from the fact that the electronic structure of the carbon atoms in the alternate layers is not completely identical. Hence, the oscillations of the two lattices with respect to each other results in periodic displacements of electric charge along the direction of vibration. We have three such movements to consider, which are respectively along one or another of the three cubic axes of the crystal. Hence, we have also three sets of phase-waves to consider whose normals are likewise the cubic axes.

The oscillatory movements of electric charge along the cubic axes of the crystal would necessarily also result in periodic movements of the stratifications of electric charge which appear in the crystal in other directions. In considering the question whether these movements would give rise to dynamic reflections by those stratifications, we have to remark that movements *parallel* to any set of stratifications cannot give rise to any dynamic reflections by them; only movements *normal* to the stratifications can give rise to such reflections, and hence if the actual movements are *inclined* to the stratifications, we need consider only the components of the movement along their normals.

Considering for example the (111) planes in a crystal, the three movements respectively along the three cubic axes are equally inclined to those planes, and hence the magnitude of all the three components resolved along the normal to the (111) planes would be diminished to the same extent. Hence, in general, *the* (111) *planes would give three dynamic reflections* which in appropriate circumstances, may be expected to be of comparable intensities. On the other hand, the (220) planes of the crystal contain one cubic axis and are equally inclined to the other two at angles of 45°. The displacements of electric charge parallel to the first axis and hence also parallel to the plane of the stratifications would not give rise to any dynamic reflection. However, movements along the two other cubic axes would result in a displacement of the stratifications in the (220) planes diminished to equal extents by reason of their inclination to those planes. We conclude that *the* (220) *planes would give only two dynamic reflections* which in appropriate circumstances would be of equal intensity. Considering again the (400) planes, these contain two of the cubic axes and are normal to the third, it follows for similar reasons that *the* (400) *planes give only one dynamic reflection.* The fact that the phase-waves are parallel to those planes has a further interesting consequence to which we shall revert later. Finally, we may briefly consider the (311) planes. These planes are equally inclined to two of the cubic axes at small angles and are nearly perpendicular to the third. The dynamic

reflections due to the first two movements may therefore be expected to behave very differently from the third.

5. THE GEOMETRY OF THE DYNAMIC REFLECTIONS

The general method already indicated in Part I enables us to picture the configuration of the dynamic reflections given by the various lattice planes in the crystal. We shall here content ourselves with the consideration of the dynamic reflections associated with the (111), (220), (311) and (400) planes, since these are the four largest spacings in the crystal which also reflect X-rays with notable intensity. The first three cases are represented in Figs. 1, 2 and 3 respectively for settings of the crystal so chosen that the

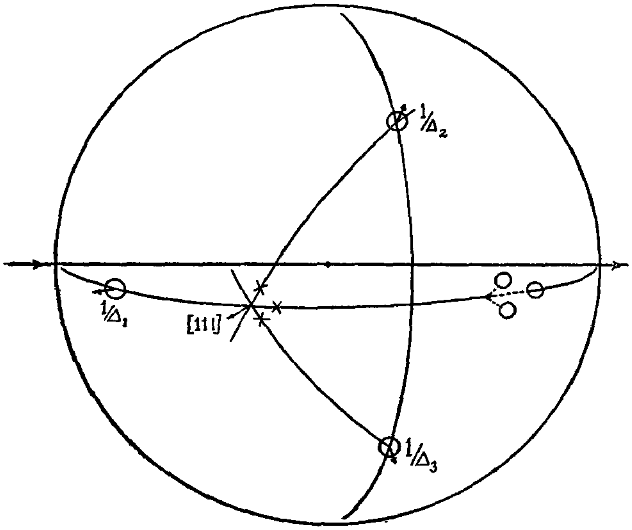

FIG. 1. Dynamic Reflections by the (111) planes.

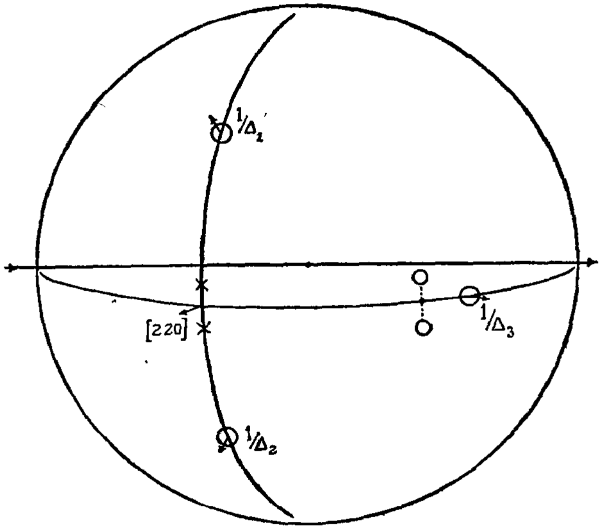

FIG. 2. Dynamic Reflections by the (220) planes.

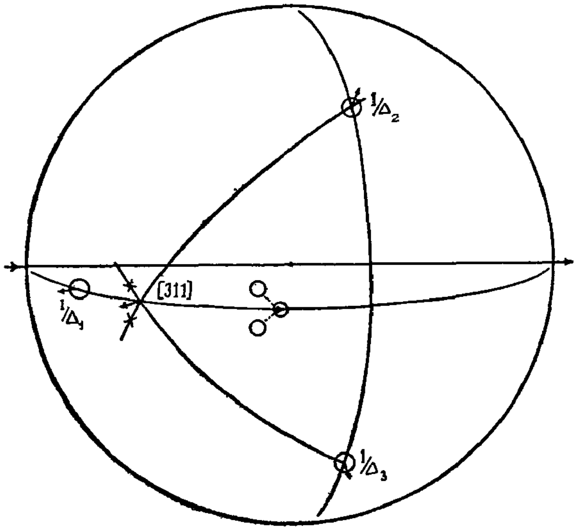

Fig. 3. Dynamic Reflections by the (311) planes.

characteristic features of each case are brought out clearly. The primary X-ray beam is assumed to traverse the crystal horizontally and its direction is indicated by arrows at the points of entry and exit on a sphere. The plane of incidence on the lattice-spacings is also assumed to be horizontal and is indicated by a great circle drawn on the surface of the sphere. The normal to the lattice spacings accordingly appears as a point on the same great circle with an arrow attached to it and directed radially outwards. The three cubic axes of the crystal which are the normals to the phase-waves of dynamic reflection are represented on the sphere in a similar fashion, the points where they appear being determined by the chosen setting of the crystal. Three great circles are also drawn each of which contains one of the phase-wave normals and the normal to the lattice spacings. In each case the setting of the crystal chosen is such that one of the great circles coincides with the plane of incidence. The normals to the three sets of dynamic stratifications would necessarily lie on these three great circles. The positions of the dynamic reflections would be determined by drawing three other great circles, each containing the direction of the incident beam and the normal to the particular dynamic stratification, and marking off on these circles, points such that the angle of reflection is equal to the angle of incidence in the respective planes. The entire procedure is that indicated by the theory of dynamic reflection developed in Part I and contained in the two equations

$$\frac{\vec{1}}{D} = \frac{\vec{1}}{d} + \frac{\vec{1}}{\Delta} \qquad (1)$$

$$2D \sin \psi = \lambda \qquad (2)$$

For a particular X-ray wavelength determined by the lattice spacings and the angle of incidence of the X-rays on them, we would observe the ordinary or unmodified reflection in the plane of incidence. The direction in which this appears is represented in each of the figures as another point on the equatorial circle. For the same X-ray wavelength, the dynamic reflection or reflections permitted would also appear in the same direction superposed on the ordinary or static reflection. For other X-ray wavelengths, the static reflection ceases to appear but the dynamic reflections would persist, their directions being determinable in the manner already explained. The phase wavelength is infinite for the particular case in which the static and dynamic reflections are superposed. With progressively changing X-ray wavelength, $1/\Delta$ would increase in numerical magnitude and the point on the sphere representing the dynamic stratification would move out in one direction or another along the great circle which defines its path. The construction already indicated would then result in giving positions to the dynamic reflections differing from that in which they were originally coincident. In the particular settings of the crystal which have been chosen for drawing the figures, the dynamic reflection which corresponds to the cubic axis in the plane of incidence would—if it exists at all—appear in the plane of incidence, while the other two would swing out of that plane symmetrically in either side.

For reasons already explained, whereas the (111) planes show *three* dynamic reflections in the setting indicated, the (220) planes show only two reflections: these are displaced laterally, one on either side. The third reflection lying in the plane of incidence though *geometrically* permitted is *physically* excluded by reason of the movement of the stratifications being in their own plane. The case of (400) reflection is of special interest. As explained earlier, only one dynamic reflection is possible in this case and since the phase-waves which give that reflection are parallel to the stratifications themselves, the dynamic reflection for all X-ray wavelengths would appear in the same direction, *viz.*, that indicated by the ordinary law of geometric reflection.

6. SUMMARY

Considerations of the physical nature of the directed valences of the tetrahedral carbon atom lead to the conclusion that there are two possible states of the carbon atom, *viz.*, a dextro-state and a lævo-state corresponding respectively to the two possible senses of the orbital angular momentum of the electrons about their tetrahedral valence directions. From this again it follows that a homogeneous diamond crystal may have an electronic structure which has either the highest or octahedral symmetry or else only the lower

or tetrahedral symmetry of the cubic system. In diamonds having octahedral symmetry, the oscillations of the two carbon atoms with respect to each other would be inactive in the absorption of infra-red radiation, whereas in diamonds of which the electronic configuration has tetrahedral symmetry that vibration would be active in such absorption. From this it follows that only with diamonds of the latter type would the X-rays excite the lattice vibrations and exhibit the dynamic reflections consequent thereon. The vibrations excited and their phase-wave-normals are parallel to the three cubic axes of the crystal. It follows that whereas the (111) planes would exhibit *three* dynamic reflections at any one setting of the crystal, the (220) would exhibit only *two* and the (400) planes only *one*.

Reprinted from "The Proceedings of the Indian Academy of Sciences",
Vol. XLVIII, No. 1, Sec. A, 1958

THE DIFFRACTION OF X-RAYS BY DIAMOND: PART III

By Sir C. V. Raman

(*Memoir No.* 109 *of the Raman Research Institute, Bangalore*-6)

Received May 7, 1958

1. Introduction

In the first part of the present memoir, it was shown from theoretical considerations of a very general nature that when X-radiations traverse a crystal, their passage could result in exciting vibrational transitions in the energy levels of the crystal and as a consequence of such excitation lead to a reflection of the incident X-rays by the lattice planes of the crystal with a change of frequency. The theory indicated it as an essential condition for such a process to occur that the vibrational transitions in question are effective as absorbers of infra-red radiation of the appropriate frequency. The phenomenon here envisaged is quantum-mechanical in its nature; in other words, vibrational transitions would be excited and would be accompanied by X-ray reflections of altered frequency even when the frequency of the vibrations is so high that they would not be thermally excited to any appreciable extent. However, considerations of a purely classical nature assist in elucidating the nature of the phenomenon and in deducing its observable features. The infra-red activity of a vibrational mode in a crystal arises because it involves a periodic displacement of the electronic clouds in the crystal with the same frequency; such a displacement would result in an oscillation of the stratifications of electron density which reflect the X-rays traversing the crystal and hence also to dynamic reflections of altered frequency.

Perhaps the most striking feature of the theory expounded in Part I is the connection which it indicates between the behaviour of a crystal in X-ray diffraction and the activity of the modes of its internal vibration in the absorption of infra-red radiation. The particular case of diamond is of special interest in this connection. For, as was shown in Part II of the memoir, theoretical considerations indicate that diamonds should be forthcoming in forms which differ in the inner symmetry of their electronic configuration and hence also in their infra-red behaviour. The detailed discussion showed that the diamonds of which the inner symmetry is octahedral would *not* exhibit dynamic X-ray reflections, whereas those diamonds of which the

symmetry is tetrahedral would exhibit such reflections. In other words, the case of diamond enables us to put the relation between X-ray diffraction and infra-red activity to a direct experimental test. Further, it was also shown in Part II of the memoir that in the case of diamond, we are concerned with three modes of vibration which are respectively parallel to the three cubic axes of crystal and hence variously inclined to the lattice-spacings in it. As a result, the dynamic reflections by these spacings differ both in their number and in their geometric configuration in a highly characteristic fashion. Thus, the application of the general theory to the particular case of diamond furnishes us with abundant material for comparison with the facts of experiment.

2. THE TETRAHEDRAL AND OCTAHEDRAL FORMS OF DIAMOND

Three diamonds employed in the present investigation are represented in Plate I. The first is a cleavage plate parallel to the (111) spacings of the crystal. The second is a flat tabular crystal in its natural form as a hexagonal plate with faces parallel to the (111) planes. The third is a thin facetted plate of diamond with its faces nearly parallel to the (111) planes. All three diamonds are perfectly colourless, without any visible cracks or inclusions in their interior and obviously of the highest quality. Nevertheless, the first two diamonds differ enormously in their physical behaviour from the third, as is apparent from a comparison of the photographs reproduced in the Plate. We proceed to explain how these photographs were obtained.

The photographs on the left-hand side were recorded by placing the diamond against a fluorescent screen. (This was a slab of lithium fluoride crystal impregnated with a little uranium oxide.) The λ 2537 radiation from a water cooled magnet-controlled mercury arc in quartz was isolated by a a monochromator and allowed to fall on the diamond and then on the LiF-UO_2 screen placed behind it, and the fluorescence excited in the latter was photographed from the rear. The photographs on the right-hand side of the Plate were obtained in a very simple manner. The diamond was placed between two crossed polaroids and photographed as seen through them against a bright source of light. It is seen from the photographs reproduced in Plate I that *the cleavage plate and the tabular crystal are both perfectly opaque to the λ 2537 radiations of the mercury arc and that they exhibit not a trace of birefringence, in other words that they are truly and perfectly isotropic crystals.* On the other hand, *the thin facetted plate is completely transparent to the λ 2537 radiations of the mercury arc, but it exhibits a feeble but nevertheless readily observable birefringence pattern with definite geometric features related in their orientation to the structure of the crystal.*

Diamond is, in effect, a giant macro-molecule of carbon. Hence a specimen of it which exhibits no detectable birefringence, in other words, is optically homogeneous, may, *prima facie*, be expected to make a close approach to the ideal state of crystal perfection. *Per contra*, a specimen of diamond—which exhibits over its entire area, a geometric pattern of birefringence however feeble it may be in intensity—must necessarily be regarded as very remote from such ideality. A striking confirmation of the correctness of these remarks is furnished by the results of a simple experimental test in which the diamonds figured in Plate I were used as X-ray spectrometers to resolve the $K\alpha_1$ and $K\alpha_2$ radiations from a copper target. The X-ray beam from the target diverged through a fine slit and fell on the diamond in an appropriate setting placed at a distance of 5 cm. from the slit. The surface reflection of the X-rays by the (111) planes of the crystal was recorded on a photographic film held at a distance of about 100 cm. The spectrograms recorded with the flat tabular diamond and by the facetted plate are reproduced as Fig. 1 (*a*) and 1 (*b*) respectively in Plate II. A very great difference between the two diamonds in regard to the degree of their crystal perfection is indicated by the difference in the two spectrograms. But the actual difference is even greater. For, the width of the $K\alpha_1$ and $K\alpha_2$ lines as recorded in Fig. 1 (*a*) in Plate II represents the natural spectral widths of these radiations and is therefore not a true measure of the crystal perfection of the tabular diamond. To obtain a true measure of that perfection, it is necessary to adopt a spectrographic technique in which two crystals of diamond are employed. The results of that technique are depicted in the series of spectrograms reproduced as Fig. 2 (*a*), (*b*), (*c*) and (*d*) of Plate II and in Figs. 1 (*a*), (*b*) and (*c*) of Plate X. We shall revert to the details of the technique and the significance of the results obtained with it in a subsequent section of the present paper.

Studies on the infra-red absorption spectra of diamond have established the fact that diamonds which are completely transparent to the λ 2537 radiations of the mercury arc in the ultra-violet are also completely transparent to infra-red radiations over the entire range of the characteristic frequencies of vibration of the structure of diamond ranging from 1332 cm.$^{-1}$ downwards to longer wavelengths. *Per contra,* the diamonds which are opaque to the λ 2537 radiations also exhibit a marked absorption over that entire range of infra-red wavelengths. It is thereby established that diamonds of the former kind possess an inner electronic configuration which has the full or octahedral symmetry of the cubic system, whereas the diamonds of the latter kind possess an electronic configuration which possesses the lower or tetrahedral symmetry of that system. The remarkable fact that diamonds with

a lower degree of symmetry are highly perfect crystals, while those with a higher degree of symmetry are highly imperfect receives a natural explanation on the basis of the theory of the structure of diamond expounded in Part II of the memoir. As there explained, the tetrahedral diamonds are those in which each dextro-carbon atom is linked to four lævo-carbon atoms and likewise each lævo-carbon atom is linked to four dextro-carbon atoms. *There is thus no physical difference between the two sub-species Td I and Td II* of the tetrahedral class of diamonds but only an interchange in the description of the two lattices which constitute the structure. On the other hand, the octahedral type of diamonds consists entirely of dextro-carbon atoms or entirely of lævo-carbon atoms; *the two sub-species Oh I and Oh II are therefore physically different.* These circumstances are clearly favourable for the Td diamonds exhibiting a high degree of homogeneity and for the Oh diamonds to be markedly heterogeneous in their texture. But there is another and a deeper consideration which has also to be borne in mind. When a dextro-carbon atom is linked to a lævo-carbon or *vice versa*, the two electrons shared between them describe their orbits about the valence direction in the same sense. On the other hand, when a dextro-carbon atom combines with a dextro-carbon atom or a lævo-carbon atom with a lævo-carbon atom, the shared electrons describe their orbits about the common valence direction in opposite senses. It would seem that a homogeneous structure extending through large volumes would be more likely to appear in the former case than in the latter.

It is appropriate at this stage to remark that it is the perfect diamonds belonging to the tetrahedral class that exhibit the phenomena of dynamic reflection of X-rays, while it is the imperfect diamonds of the octahedral type that do not show those phenomena. This is in agreement with the indications of the theory developed in Part II of the memoir. But it is necessary to demonstrate that the failure of the octahedral diamonds to exhibit dynamic reflections is not ascribable to their imperfection of structure, but is a consequence of their inactivity in infra-red absorption. We shall revert to this presently.

3. DYNAMIC X-RAY REFLECTIONS AND CRYSTAL SYMMETRY

Figure 1 in Plate III is a Laue photograph of a cleavage plate of diamond whose faces are parallel to the (111) planes of the crystal. The crystal was set exactly normal to a fine pencil of X-rays from a copper target. The picture shows perfect trigonal symmetry not only with regard to the ordinary or Laue reflections but equally also with regard to the dynamic reflections appearing in the vicinity of the hexagonal corners of the print adjacent to

the intense (111) Laue spots. Figure 2 in Plate III is a similar photograph taken in similar circumstances with a crystal of diamond which exhibits twinning of the spinel type. It will be seen that this pattern exhibits hexagonal symmetry in all its features, including especially the dynamic reflections which are seen at all the six corners of the hexagonal print. The fact clearly evident from Figs. 1 and 2 in Plate III that the dynamic X-ray reflections of diamond exhibit the symmetry of the crystal in the same manner and to the same extent as the static reflections is obviously of the highest significance. Taken in conjunction with the circumstance that the diamonds which exhibit the dynamic reflections are perfect and indeed—as will appear presently—are ideal crystals, it demonstrates the correctness of the view expressed by the author in the original publication of the year 1940 that these phenomena exhibited by diamond are fundamental in their nature and of the highest importance in relation to the theory of X-ray diffraction in crystals.

As already remarked earlier, the fact that the dynamic reflections are not manifested by the diamonds of octahedral symmetry is a confirmation of the theoretical ideas set out in Part I of the memoir. But the circumstance that these diamonds are imperfect tends to create some doubt in the matter. Very frequently, indeed, diamonds of this class give distorted Laue patterns. Hence a critical observer might be disposed to infer that it is this imperfection rather than the inactivity in infra-red absorption which is responsible for the non-appearance of the dynamic reflections. To dispel such an impression, it is necessary to investigate the matter with carefully selected material. The intensity of the birefringence exhibited by these diamonds is a measure of the imperfections in their structure. It is therefore desirable to select a specimen in which such birefringence is of extremely low intensity. The specimen illustrated in Figs. 3 (*a*) and 3 (*b*) in Plate I was found to be the best available in this respect. Even so, the mosaicity of its structure exhibits itself in a notable enhancement of the intensity of the Laue spots in its diffraction patterns. Such enhancement is particularly striking in the case of spots that are only feebly recorded with diamonds of the tetrahedral class. Even such a weak effect as the diffuse X-ray scattering due to thermal agitation is recorded with greatly enhanced intensity by this specimen. But there is no observable distortion of the Laue spots, and had the dynamic reflections been present, they would have been very striking features in the recorded patterns. Actually, not a trace of them is observable in Figs. 1 (*b*) and 1 (*d*) in Plate VIII which were recorded with this diamond in appropriate settings. For the sake of comparison, the patterns recorded with the tetrahedral diamond in identical settings are reproduced as Fig. 1 (*a*) and 1 (*c*) side by side with them in the same Plate VIII.

4. OBSERVABLE FEATURES OF THE DYNAMIC REFLECTIONS

The following special points are worthy of mention:

I. As the dynamic reflections by diamond are a consequence of the excitation by the incident X-rays of an infra-red vibration of high frequency, variations of temperature within wide limits should be entirely without effect either on the intensity or the sharpness of these reflections.

II. As a result of the crystal perfection of diamond, the ordinary reflections of monochromatic X-rays would demand a very precise setting of the crystal for their observation, on either side of which they would disappear completely. The dynamic reflections would coincide with the static reflections at the correct setting, but would not disappear when the setting is altered. Their intensity would however fall off rapidly as the crystal is moved away from the correct setting in their direction.

III. The dynamics of the excited vibration in diamond demands that the phase-waves which determine the direction in which the dynamic reflections appear are precisely normal to one or another of the cubic axes of the crystal. As a consequence, the reflections would be very sharply defined, being indeed in this respect almost comparable with the static reflections.

IV. By making observations of the directions in which the dynamic reflections appear, it is possible to determine the orientation of the phase-waves. The most suitable arrangement for such determination is to place the crystal so that one of the cubic axes lies in the plane of incidence of the X-rays on the (111) planes, and then to alter the setting in such manner that the plane of incidence does not change. The geometric law of dynamic reflection takes a very simple form in this case and a precise measurement of the orientation of the phase-waves becomes possible.

The various special features referred to above were all fully established by the observations made by the author and his collaborators in the months following the original publication of April 1940. Detailed reports of those studies appeared in the *Proceedings of the Indian Academy of Sciences* in the years 1940 and 1941. It would be superfluous here to traverse the same ground or to comment on the literature of a controversial nature published from other laboratories on the subject then and subsequently. To

make the present memoir complete, however, a series of photographs showing the dynamic reflections by the (111) planes, (220) planes, (311) planes and (400) planes of diamond in various settings are reproduced as Plates IV, V, VI, VII, VIII and IX accompanying the present paper. A comparison of the features noticed in this series of photographs with the theoretical diagrams given in Part II of the memoir will show how complete the agreement is between fact and theory.

5. Spectral Analysis of X-Ray Diffraction

We now return to a detailed description of the technique which enables a spectroscopic analysis to be made of the X-ray diffraction phenomena exhibited by diamond. The general nature of this technique to which a brief reference was made earlier will be evident from Fig. 1, text. A powerful source of X-rays from a copper target passes first through a wide slit and then

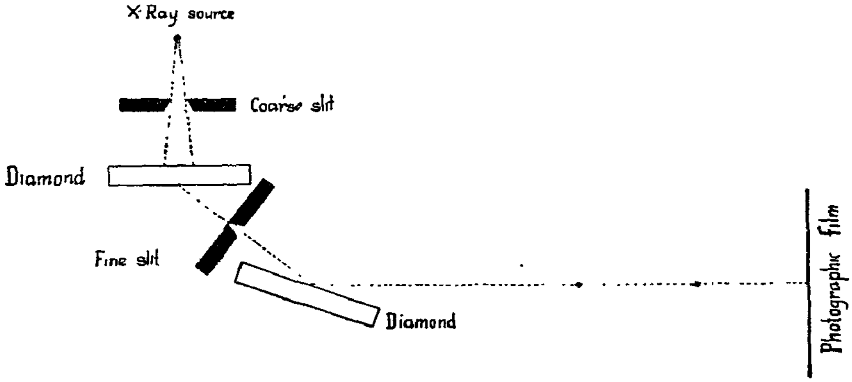

Fig. 1 (Text)

through the diamond under study. The rays *internally* diffracted by the (111) planes of this diamond are restricted by a fine slit through which they pass before they are incident on the surface of a second perfect diamond which functions as a spectrometer. The rays reflected *externally* by the second diamond are received and recorded on a photographic film placed at a distance of 100 cm. The actual technique consists in rotating the first diamond in steps through very small angles over a total range of a few minutes of arc. What is actually recorded on the photographic film is the spectrum of X-radiation in the narrow range between the $K\alpha_1$ and $K\alpha_2$ lines and perhaps a little more on either side of them.

The nature of the results obtained will be evident from a scrutiny of the series of spectrograms reproduced as Figs. 2 (*a*), (*b*), (*c*) and (*d*) in Plate II and the three others which appear as Fig. 1 (*a*), (*b*) and (*c*) in Plate X. The latter three have been enlarged so as to be readily comparable with the single

crystal spectrogram appearing as Fig. 1 (*a*) in Plate II. The most significant feature of the series of spectrograms is the appearance of an extremely sharp line which drifts in its position as the diamond is rotated. The spectral width of this sharp line is not more than about a tenth of the natural width of the $K\alpha_1$ or the $K\alpha_2$ radiations. It represents the super-monochromatic radiation manufactured by the first diamond from the incident white radiation by Laue reflections at the (111) stratifications. Its extreme sharpness reflects the extraordinary perfection of the diamond.

It will be seen that the relative intensities of the $K\alpha_1$ and $K\alpha_2$ lines differ enormously in the different spectrograms. That they persist over the whole range of settings of the diamond clearly shows that they represent the dynamic reflections of the $K\alpha_1$ and the $K\alpha_2$ radiations by the (111) planes of the first diamond. The static reflections of those radiations are recorded only at the precise settings at which those reflections are possible.

6. ACKNOWLEDGEMENT

The Laue patterns reproduced in Plates III, IV, V, VI, VII, VIII and IX, as well as the single crystal and double crystal X-ray spectra reproduced in Plates II and X accompanying this memoir were recorded in the X-ray Laboratory of the Raman Research Institute by the Assistant Director of the Institute, Professor A. Jayaraman, for whose valuable co-operation in the research the author of this memoir is greatly indebted. The gift to the Institute of a rotating target X-ray set by Sir Purushottamdas Thakurdas made the work possible.

7. SUMMARY

Studies on the crystal perfection of diamond by single-crystal and the double-crystal X-ray spectroscopic methods demonstrate that the non-birefringent diamonds which are infra-red active and possess only tetrahedral symmetry in their electronic configuration are extraordinarily perfect and are indeed ideal diamonds. It is these diamonds that exhibit the phenomena of dynamic reflection of X-rays. The detailed studies of the phenomena show that the experimental facts of the subject are completely in agreement with the results of the theory expounded in the first two parts of the memoir. The non-appearance of the dynamic X-ray reflections with the diamonds which have an octahedral symmetry of electronic configuration is shown to be consequential on these diamonds being inactive in the absorption of infra-red radiation.

4 JAN 1965
MADRAS

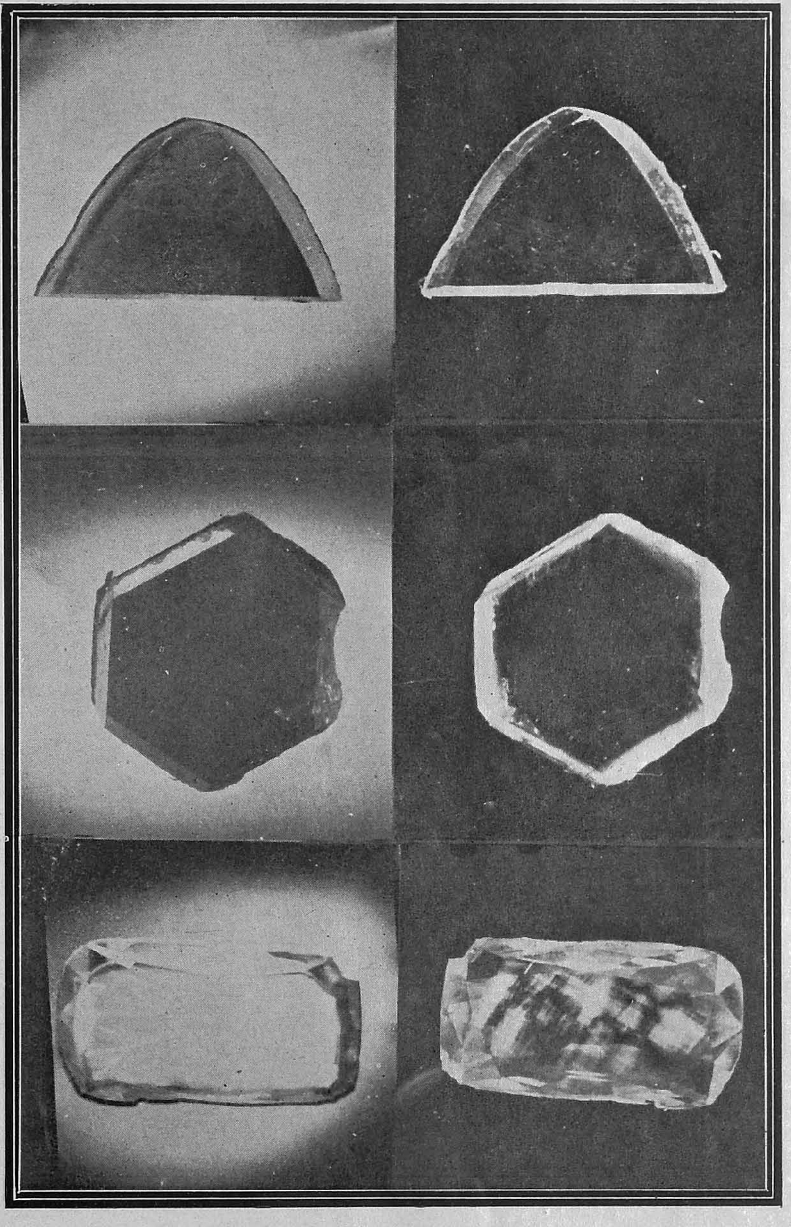

FIG. 1 (*a*) (*b*)

FIG. 2 (*a*) (*b*)

FIG. 3 (*a*) (*b*)

FIG. 1 (*a*) FIG. 1 (*b*)

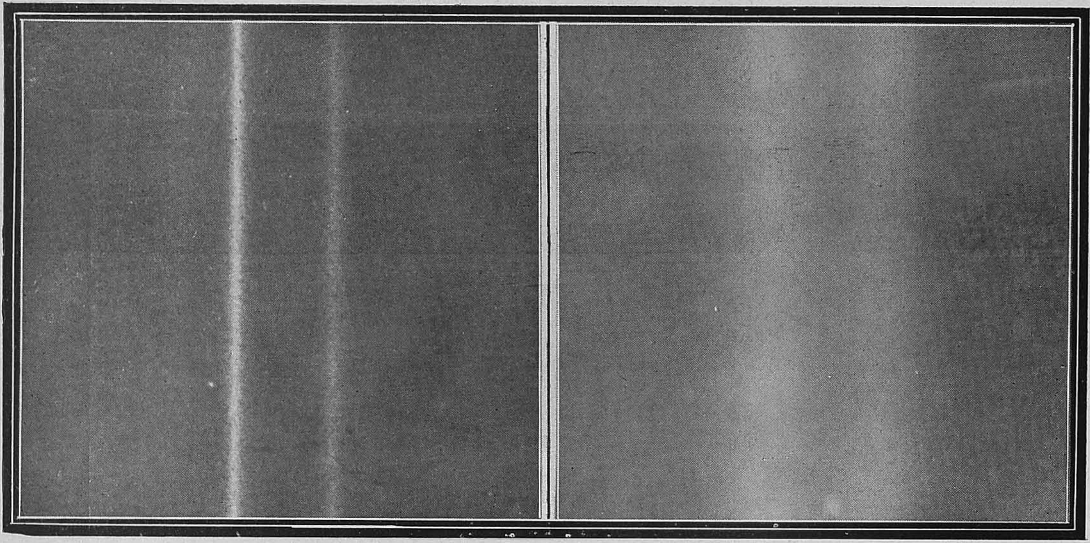

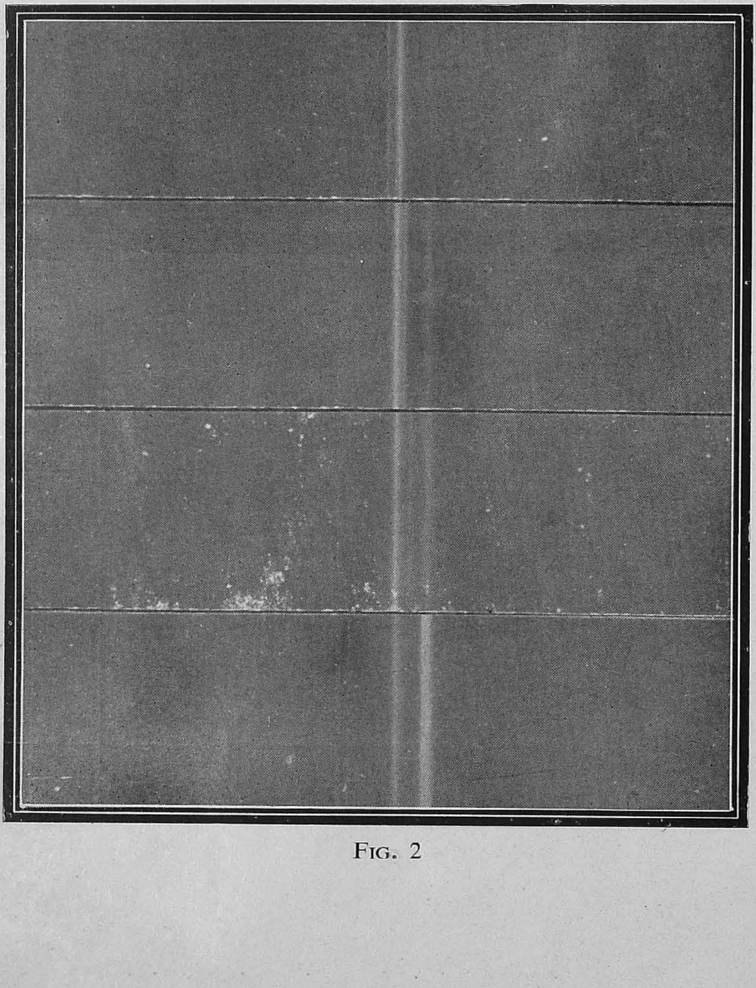

(*a*)

(*b*)

(*c*)

(*d*)

FIG. 2

CONNEMARA PUBLIC LIBRARY
4 JAN 1965

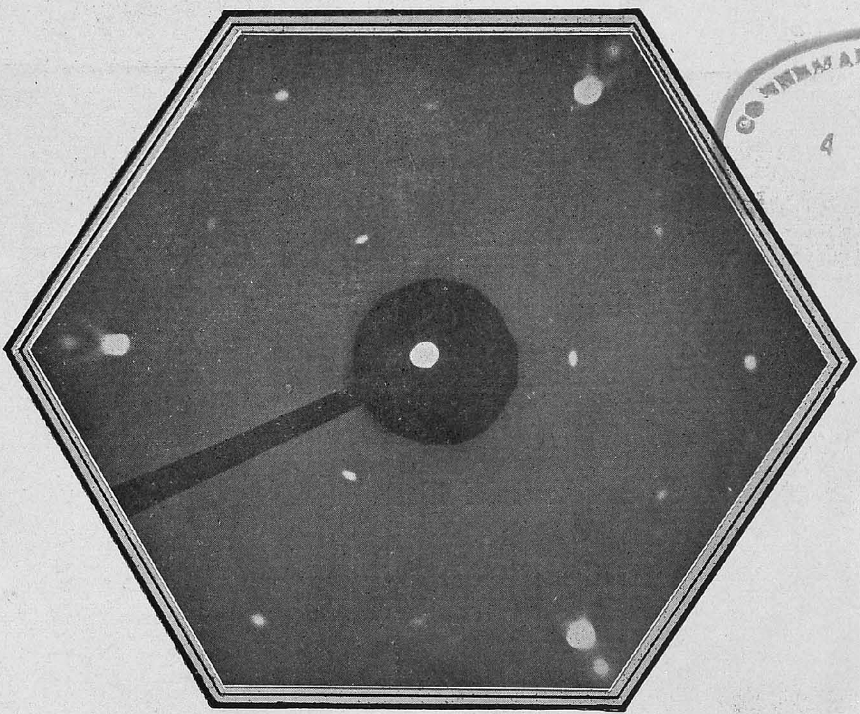

Fig. 1

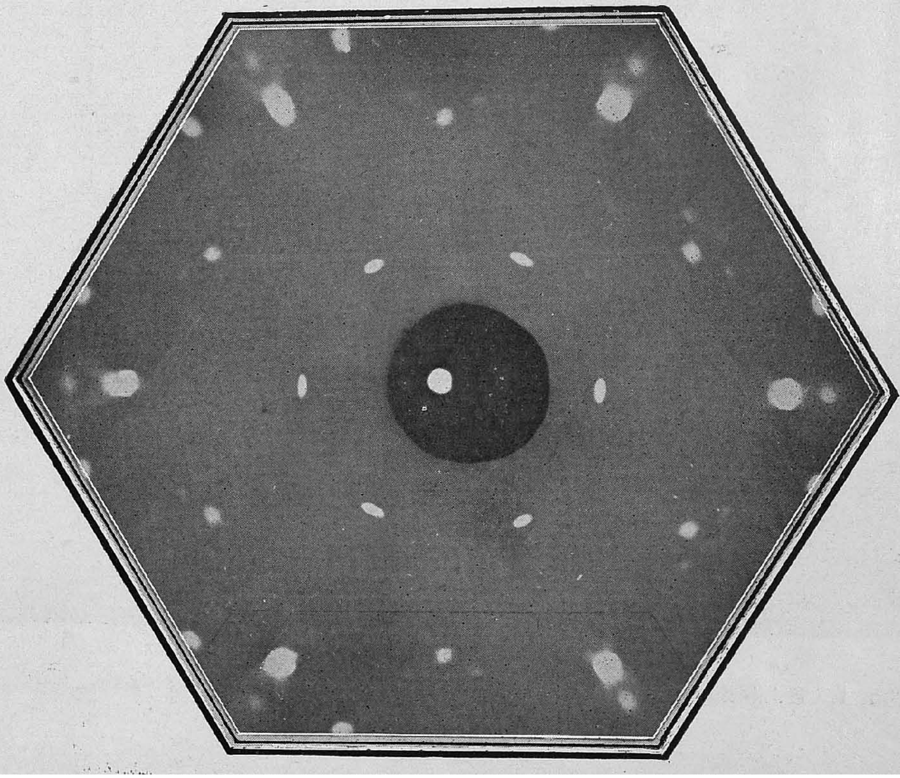

Fig. 2

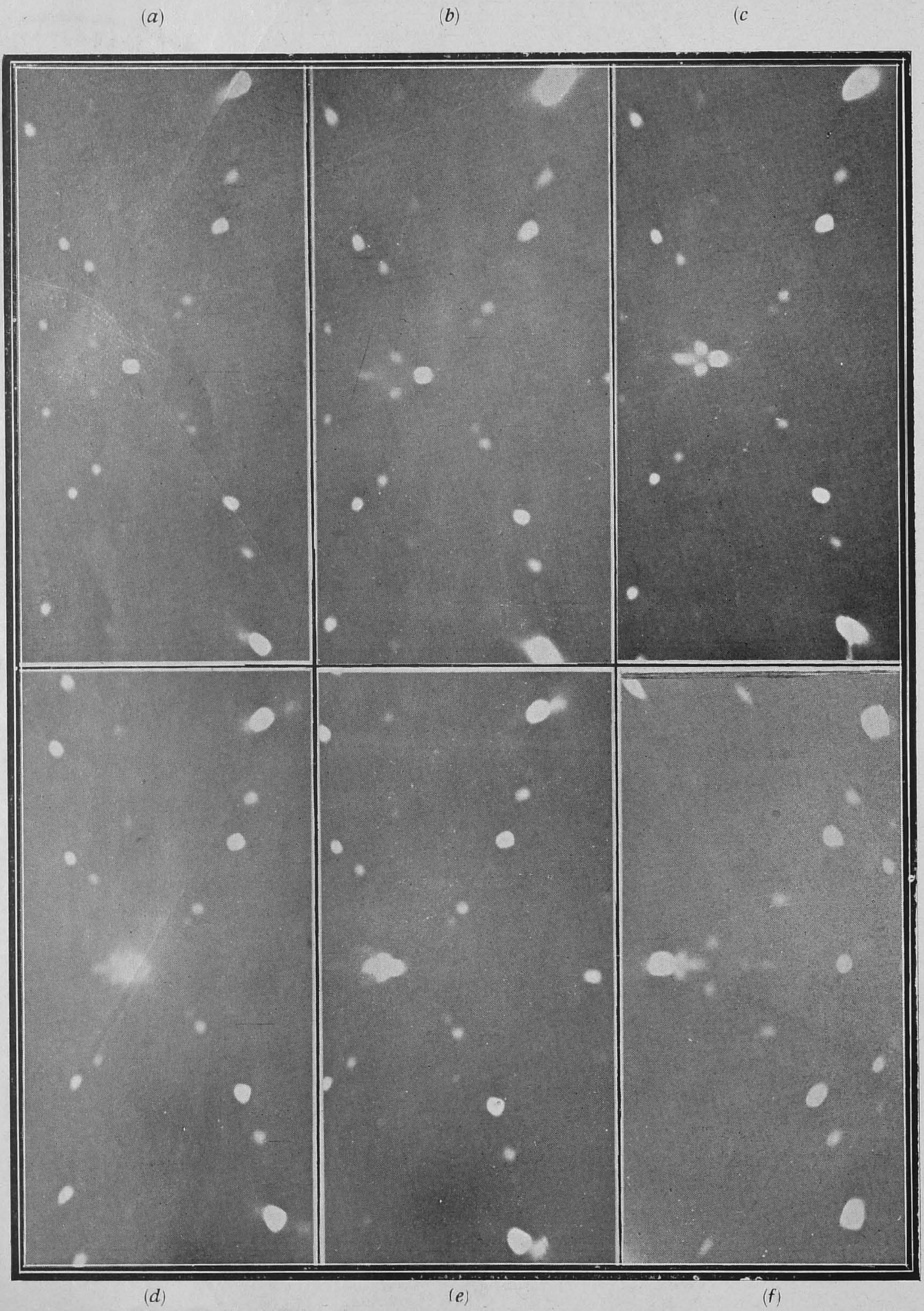

FIG. 1. Exhibiting the dynamic reflections by the (111) planes at various settings.

4 JAN 1965

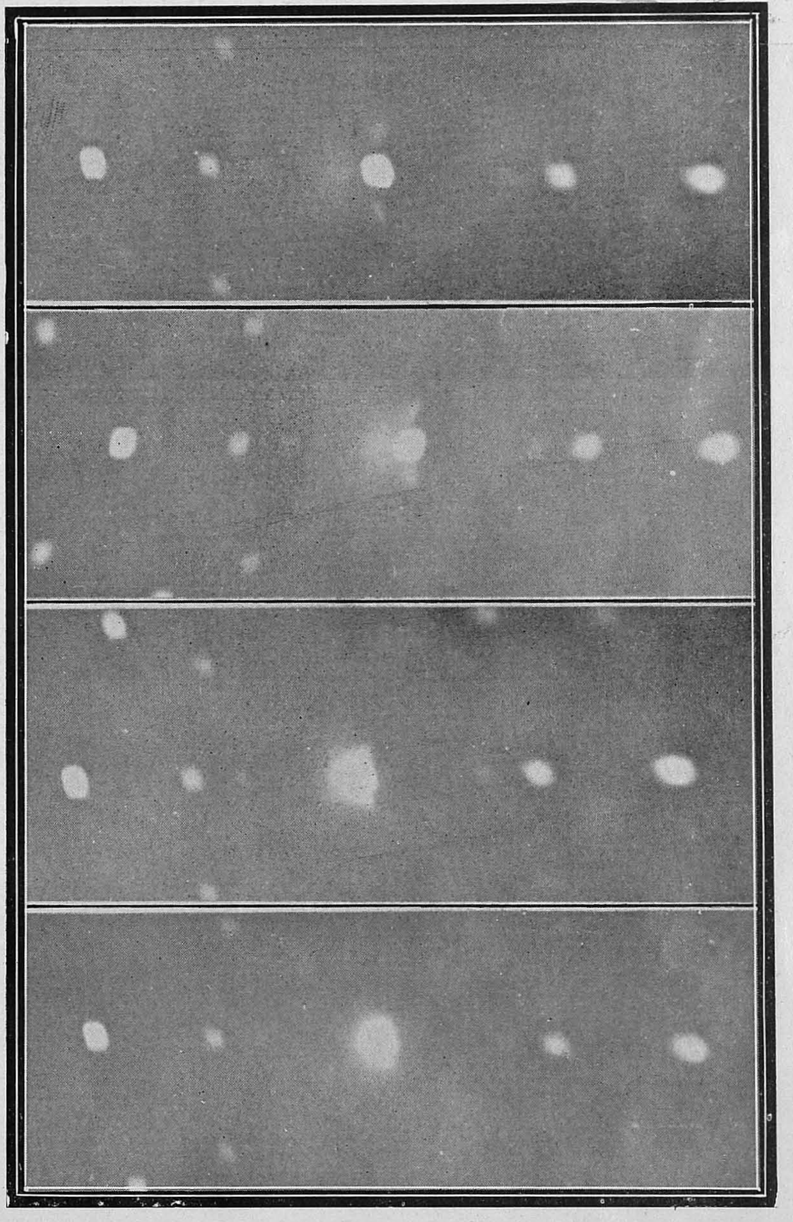

(a)

(b)

(c)

(d)

FIG. 1. Exhibiting the dynamic reflections by the (220) planes at various settings.

(a) (b)

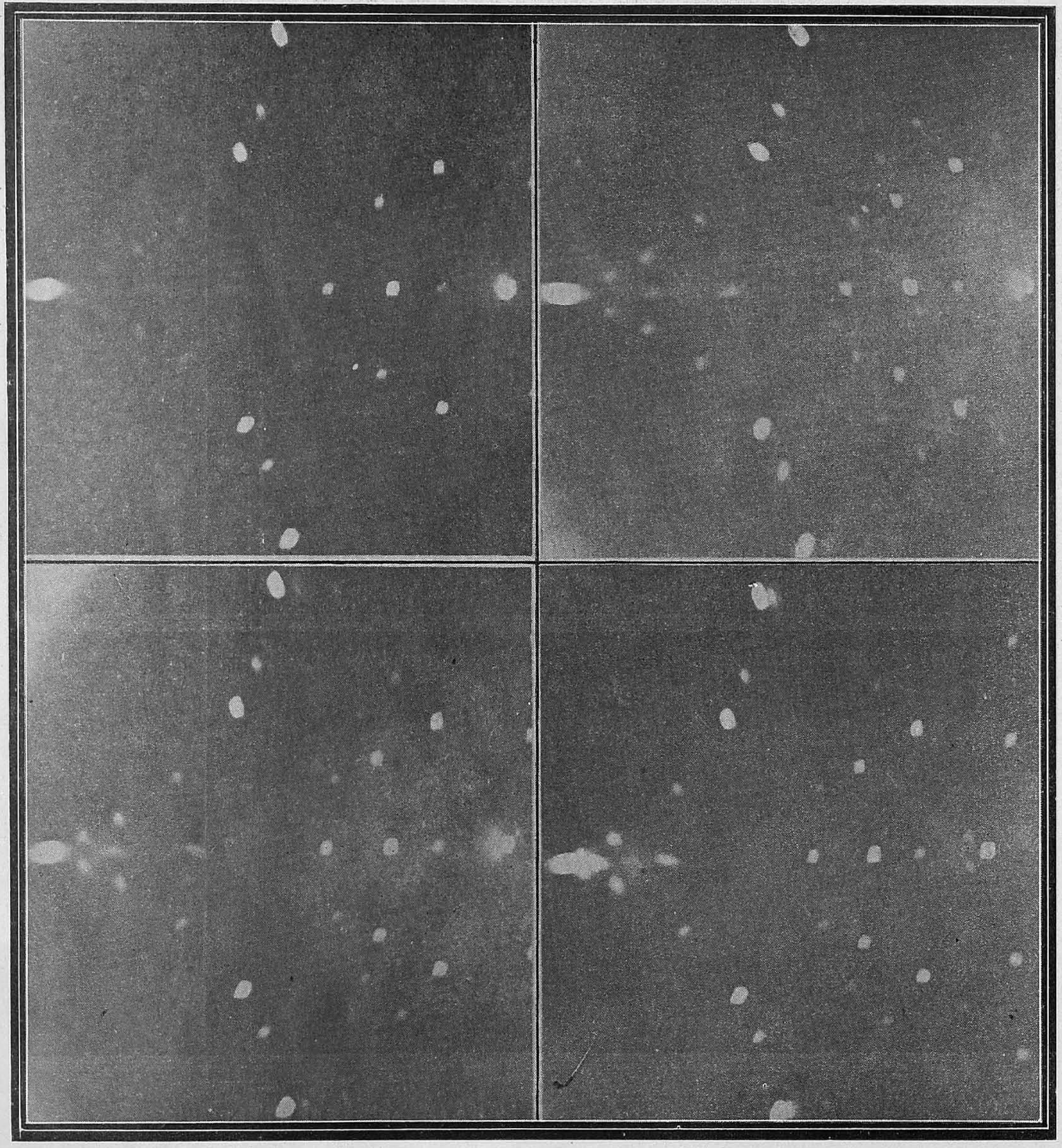

(c) (d)

FIG. 1. Exhibiting the dynamic reflections by the (111) planes at the left and by the (113) planes at the right.

4 JAN 1965

(a) (b)

(c) (d)

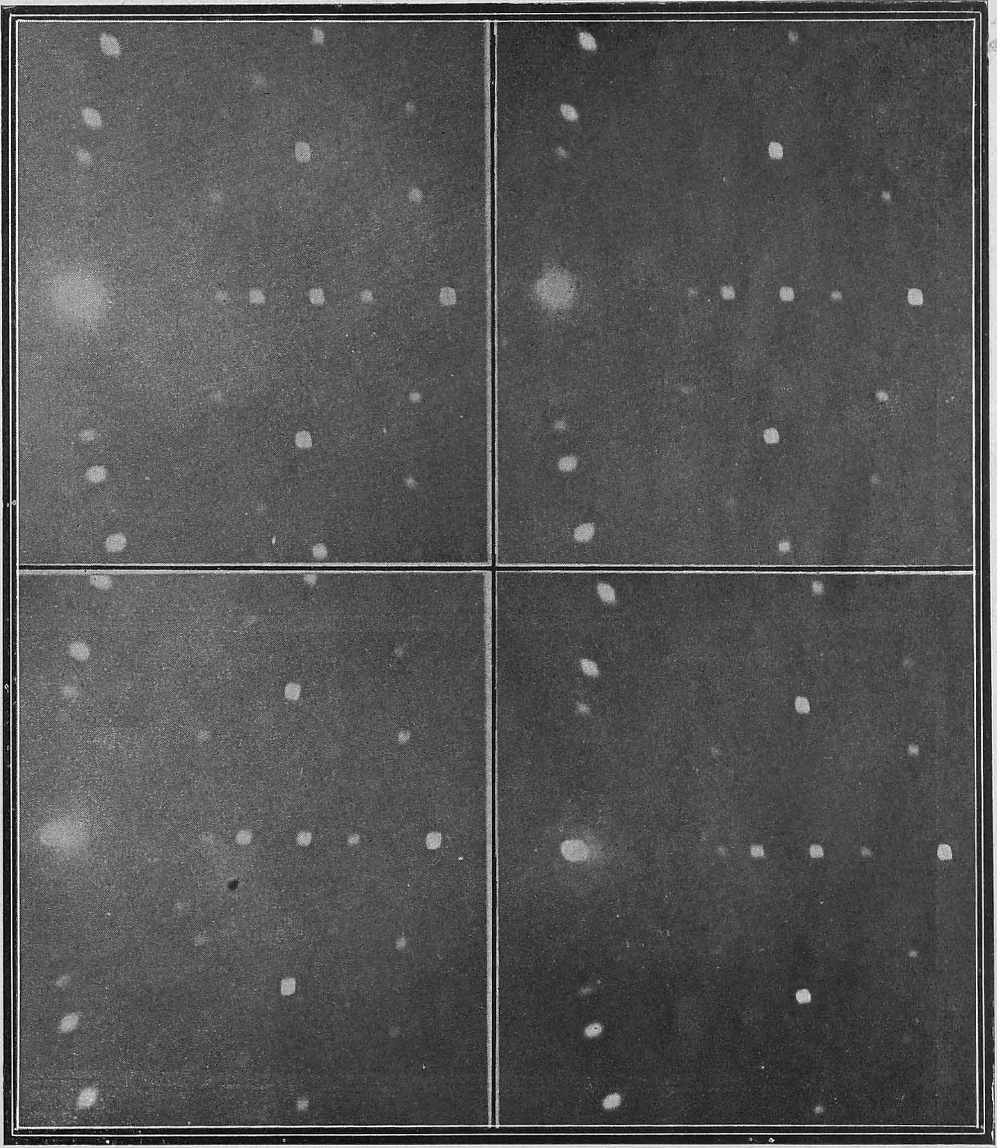

FIG. 1. Exhibiting the dynamic reflections by the (400) planes at the left.

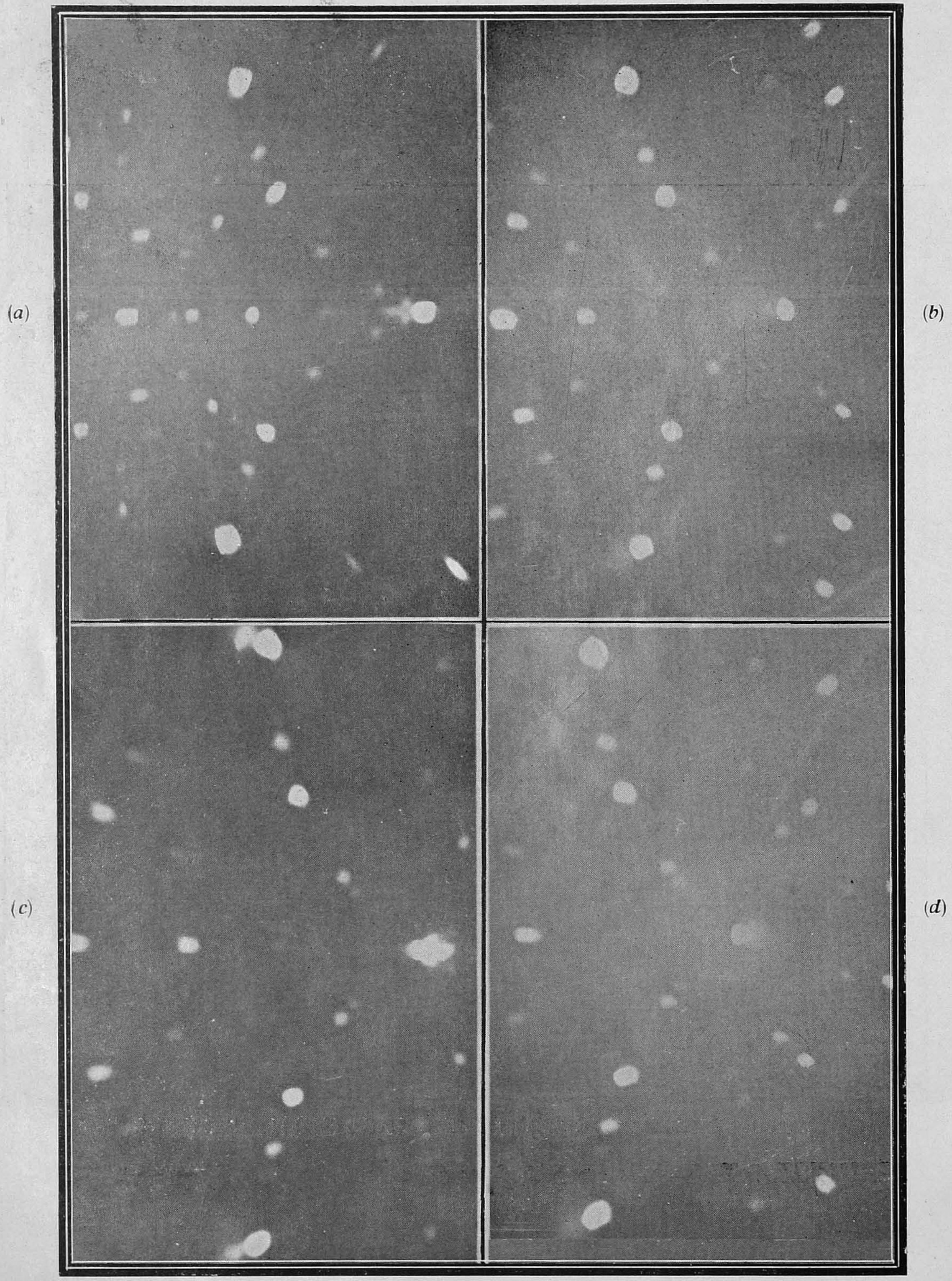

FIG. 1. Exhibiting the dynamic reflections by the (111) planes of tetrahedral diamond on the left and their absence with octahedral diamond on the right.

JAN 1965

(a)

(b)

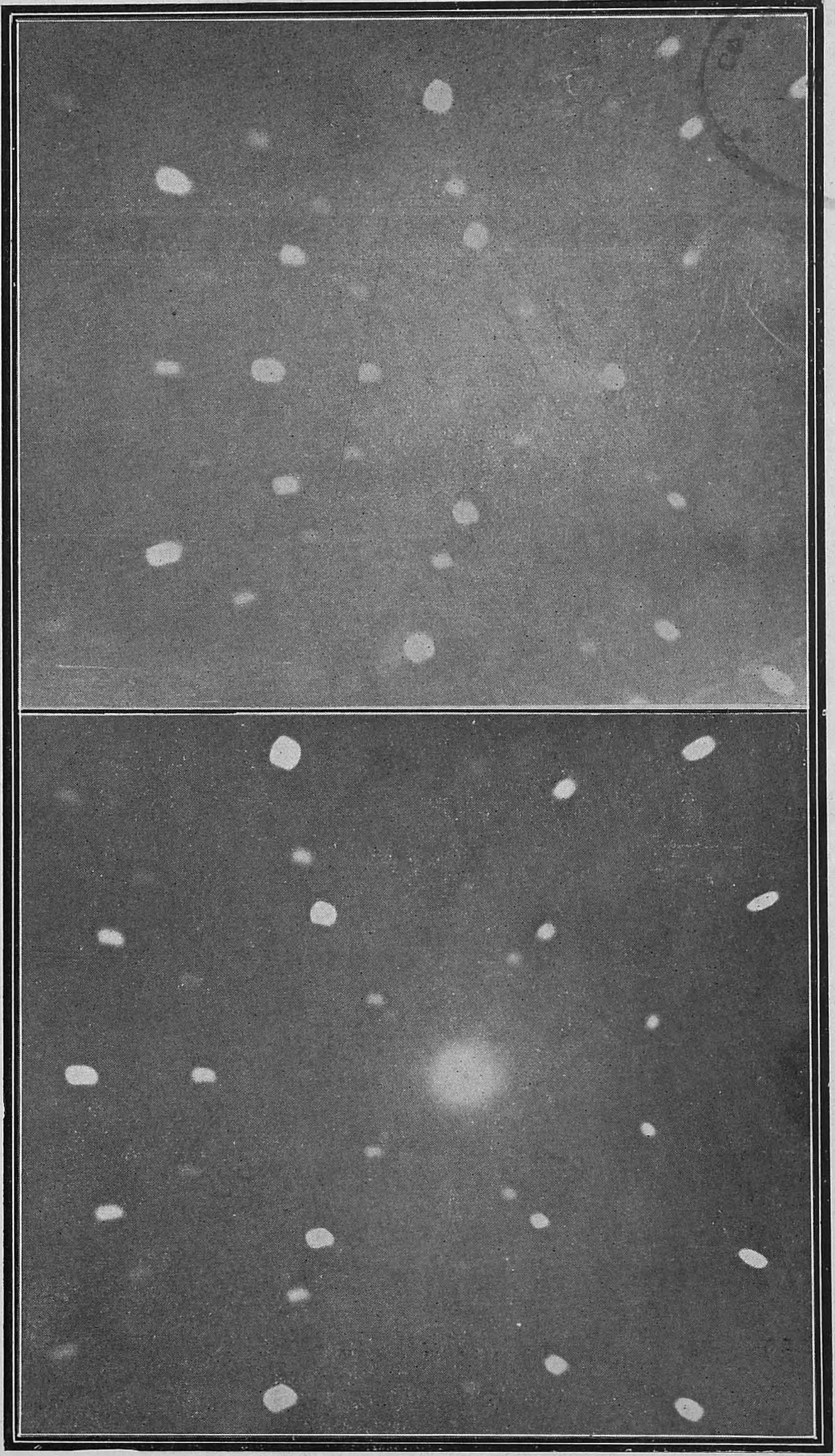

FIG. 1. Laue patterns of octahedral diamond showing intense reflection by the (111) planes at different settings.

4 JAN 196 MADRAS

(a)

(b)

(c)

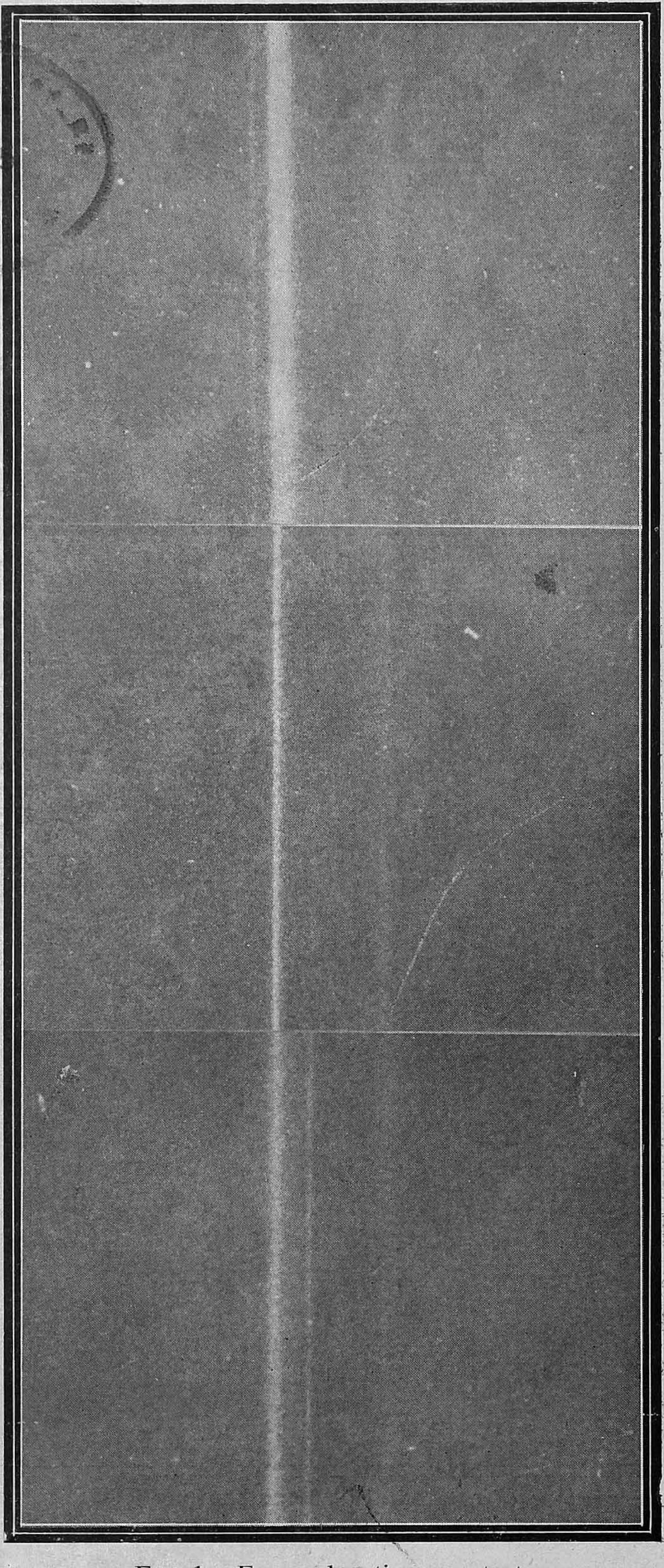

FIG. 1. For explanation, see text.